

School of Doctoral Studies in Biological Sciences
University of South Bohemia in České Budějovice
Faculty of Science

Tick-borne encephalitis - from pathogenesis to therapy

Ph.D. thesis

RNDr. Martin Palus

Supervisor: doc. RNDr. Daniel Růžek, Ph.D.

University of South Bohemia, Faculty of Science
&
Biology Centre of the Academy of Sciences of the Czech Republic,
Institute of Parasitology
&
Veterinary Research Institute

České Budějovice
2016

A mind that is stretched by a new experience
can never go back to its old dimensions.

Oliver Wendell Holmes

To my family and my mentors.

This thesis should be cited as:

Palus, M., 2016: Tick-borne encephalitis - from pathogenesis to therapy. Ph. D. Thesis Series, No. 17. University of South Bohemia, Faculty of Science, School of Doctoral Studies in Biological Sciences, České Budějovice, Czech Republic, 202 pp.

Annotation:

The proposed thesis contributes to the knowledge about tick-borne encephalitis (TBE) and its pathogenesis. The thesis describes pathogenesis and immunopathogenesis of TBE, impact of host's genotype in clinical course determination, immune response of patients with acute TBE, the mechanism of TBEV migration into CNS and virus interaction with cells of neurovascular unit as well as potential medical interventions.

Declaration [in Czech]:

Prohlašuji, že svoji disertační práci jsem vypracoval samostatně pouze s použitím pramenů a literatury uvedených v seznamu citované literatury. Prohlašuji, že v souladu s § 47b zákona č. 111/1998 Sb. v platném znění souhlasím se zveřejněním své disertační práce, a to v úpravě vzniklé vypuštěním vyznačených částí archivovaných Přírodovědeckou fakultou elektronickou cestou ve veřejně přístupné části databáze STAG provozované Jihočeskou univerzitou v Českých Budějovicích na jejích internetových stránkách, a to se zachováním mého autorského práva k odevzdanému textu této kvalifikační práce. Souhlasím dále s tím, aby toutéž elektronickou cestou byly v souladu s uvedeným ustanovením zákona č. 111/1998 Sb. zveřejněny posudky školitele a oponentů práce i záznam o průběhu a výsledku obhajoby kvalifikační práce. Rovněž souhlasím s porovnáním textu mé kvalifikační práce s databází kvalifikačních prací Theses.cz provozovanou Národním registrem vysokoškolských kvalifikačních prací a systémem na odhalování plagiátů.

V Českých Budějovicích, 14. 11. 2016

.....
RNDr. Martin Palus

This thesis originated from a partnership of Faculty of Science, University of South Bohemia, and Institute of Parasitology, Biology Centre of the CAS, supporting doctoral studies in the study programme Infection Biology.



Přírodovědecká
fakulta
Faculty
of Science



Parazitologický ústav
Biologické centrum AV ČR
Institute of Parasitology
Biology Centre CAS

Financial support:

AZVČR NV16-34238A (Czech Health Research Council; Institute of Parasitology, Biology Centre CAS; P.I.: Daniel Růžek) Antiviral therapy of tick-borne encephalitis

GAJU 04-069/2015/P (Grant Agency of University of South Bohemia; P.I.: Martin Palus) Role of the human brain microvascular endothelial cells during tick-borne encephalitisvirus infection in the central nervous system

GAJU 04-127/2014/P (Grant Agency of University of South Bohemia; P.I.: Martin Palus) Role of human non-neural cells in the neuronal injury during tick-borne encephalitis

GAČR GA14-29256S (Grant Agency of the Czech Republic; Veterinary Research Institute; P.I.: Daniel Růžek) Mechanisms of neuronal injury during tick-borne encephalitis virus infection of the CNS.

GAJU 04-155/2013/P (Grant Agency of University of South Bohemia; P.I.: Libor Grubhoffer) Molecular and cell interaction in system vector-pathogen-host

GAČR P502/11/2116 (Grant Agency of the Czech Republic; Institute of Parasitology, Biology Centre CAS; P.I.: Daniel Růžek) Differences in clinical course of tick-borne encephalitis, and their genetic determination.

Acknowledgement:

In first place, I would like to thank my supervisor Assoc. Prof. Daniel Růžek for introducing me to viral research and for his expert guidance through my studies. Thanks to Daniel I had the opportunity to work on interesting topics with space for my own ideas. One of Daniel's qualities, I admire a lot, is his openness for questions and results discussion whenever I needed and despite his growing busyness. Daniel supported me and helped to motivate and re-motivate my mind when the research tasks were not proceeding in right way despite my/our considerable efforts.

I am very grateful to Prof. Libor Grubhoffer and Prof. Jan Kopecký, authorities in tick-borne disease research and heads of laboratories I had opportunity to be part of. I would like to thank to all members of Laboratory of Arbovirology, Laboratory of Molecular Ecology of Vectors and Vector-borne Diseases, Laboratory of Parasite Immunology and whole Budweis tick group and also to Laboratory of Electron Microscopy.

Moreover, I want to express my gratitude to members of laboratory of Emerging Viral Diseases at the Veterinary Research Institute in Brno and collaborative laboratory of Assoc. Prof. Lipoldová, as well to Dr. Žampachová for her collaboration in TBE patient research.

Dr. Lesley Bell-Sakyi and Dr. Sabine Weisheit I want to thank for their kindness and guidance during my internship at The Roslin Institute.

I would like to thank all the co-authors of the papers, for their contribution to our studies.

Namely, I would like to thank and mention Jana Elsterová, Helena Langhansová, Eva Výletová, Václav Hönig, Jana Širmarová, Luděk Eyer, Jiří Salát, Janko Štěrba, Marie Vancová, Jaroslava Lieskovská, Jiří Černý, Honza Erhart, Honza Perner.

Last but not least I would like to thank my parents and my whole family for their love and continuous sincere support, my beloved wife Adélka for her help, love, support and patience and also to our daughter Anička for being such a sunshine.

List of papers and author's contributions

The Ph. D. thesis is based on following papers and manuscripts:

1. Růžek D., Salát J., Palus M., Gritsun T.S., Gould E.A., Dyková I., Skallová A., Jelínek J., Kopecký J., Grubhoffer L. (2009) CD8+ T-cells mediate immunopathology in tick-borne encephalitis. *Virology*. 384:1-6.[IF=3.200]

Martin Palus participated on acquisition of data and data analysis.

2. Palus M., Vojtíšková J., Salát J., Kopecký J., Grubhoffer L., Lipoldová M., Demant P., Růžek D. (2013) Mice with different susceptibility to tick-borne encephalitis virus infection show selective neutralizing antibody response and inflammatory reaction in the central nervous system. *J. Neuroinflamm.* 10:77. [IF=4.667]

Martin Palus participated in performing the experiments, in the design of the experiments and on the draft of the manuscript.

3. Palus M., Žampachová E., Elsterová J., Růžek D. (2014) Serum matrix metalloproteinase-9 and tissue inhibitor of metalloproteinase-1 levels in patients with tick-borne encephalitis. *J. Infect.* 68:165-9.[IF=4.382]

Martin Palus participated on data acquisition, analysis and interpretation, and on the draft of the manuscript.

4. Palus M., Bílý T., Elsterová J., Langhansová H., Salát J., Vancová M., Růžek D. (2014) Infection and injury of human astrocytes by tick-borne encephalitis virus. *J Gen Virol.* 95:2411-26. [IF=3.192]

Martin Palus participated on the concept of the study, data acquisition, analysis and interpretation, and on the draft of the manuscript.

5. Palus M., Formanová P., Salát J., Žampachová E., Elsterová J., Růžek D. (2015) Analysis of serum levels of cytokines, chemokines, growth factors and monoamine neurotransmitters in patients with tick-borne encephalitis: identification of novel inflammatory markers with implications to pathogenesis. *J of Med Virol* 87: 885-892.[IF=1.998]

Martin Palus participated on data acquisition, analysis and interpretation, and on the draft of the manuscript.

6. Bílý T., Palus M., Eyer L., Elsterová J., Vancová M., Růžek D. (2015) Electron tomography analysis of tick-borne encephalitis virus infection in human neurons. *Sci. Rep.* 5: 10745. [IF=5.228]

Martin Palus participated on acquisition of data and analysis of data.

7. Eyer L., Valdés J.J., Gil V.A., Nencka R., Hřebabecký H., Šála M., Salát J., Černý J., Palus M., De Clercq E., Růžek D. (2015) Nucleoside inhibitors of tick-borne encephalitis virus. *Antimicrob Agents Chemother.* 59: 5483-5493. [IF=4.415]

Martin Palus participated on data analysis.

8. Eyer L., Šmídková M., Nencka R., Neča J., Kastl T., Palus M., De Clercq E., Růžek D. (2016) Structure-activity relationships of nucleoside analogues for inhibition of tick-borne encephalitis virus. *Antiviral Res.* 133:119-129. [IF=4.909]

Martin Palus participated on data analysis.

9. Eyer L., Nencka R., Huvarová I., Palus M., Joao Alves M., Gould E.A., De Clercq E., Růžek D. (2016) Nucleoside Inhibitors of Zika Virus. *J Infect Dis.* 214(5):707-11. [IF=6.344]

Martin Palus participated on data analysis.

10. Elsterova J., Palus M., Kopecky J., Niller H. H., Ruzek D. Tick-borne encephalitis virus neutralization by high dose intravenous immunoglobulin (IVIG). *Ticks Tick-Borne Dis.* (accepted)

Martin Palus participated on data acquisition, analysis and interpretation of data and on the draft of the manuscript.

Content

1 Preface	1
2 Introduction	2
2.1 Key background	2
2.2 History	2
2.3 Tick-borne encephalitis	4
2.3.1 Classification	5
2.3.2 Virus particle	5
2.3.3 Ecology and Epidemiology.....	7
2.3.4 Routes of infection	9
2.3.5 Disease development and Clinical features	9
2.3.6 Immuno/Pathology	13
2.3.6.1 Neuronal damage	13
2.3.6.2 Central nervous system.....	13
2.3.6.2a Key players in the protection/defence of the CNS	14
2.3.6.2b Blood brain barrier breakdown	16
2.3.6.3 Humoral immunity	16
2.3.7 Factors affecting disease development	17
2.3.8 Treatment	19
2.3.9 Prevention	20
2.3.10 Summary	21
2.4 References.....	22
2.5 Specific aims.....	30
3 Experimental section	31
CHAPTER I	
CD8+ T-cells mediate immunopathology in tick-borne encephalitis	31
CHAPTER II	
Mice with different susceptibility to tick-borne encephalitis virus infection show selective neutralizing antibody response and inflammatory reaction in the central nervous system.....	41

CHAPTER III	
Electron Tomography Analysis of Tick-Borne Encephalitis Virus Infection in Human Neurons	59
CHAPTER IV	
Infection and injury of human astrocytes by tick-borne encephalitis virus	79
CHAPTER V	
Serum matrix metalloproteinase-9 and tissue inhibitor of metalloproteinase-1 levels in patients with tick-borne encephalitis	99
CHAPTER VI	
Analysis of serum levels of cytokines, chemokines, growth factors, and monoamine neurotransmitters in patients with tick-borne encephalitis: Identification of novel inflammatory markers with implications for pathogenesis	109
CHAPTER VII	
Tick-borne encephalitis virus neutralization by high dose intravenous immunoglobulin	121
CHAPTER VIII	
Nucleoside inhibitors of tick-borne encephalitis virus	145
CHAPTER IX	
Structure-activity relationships of nucleoside analogues for inhibition of tick-borne encephalitis virus	161
Nucleoside Inhibitors of Zika Virus	177
4 Discussion/Summary	183
4.1 Some of proposed future plans	191
4.2 References	193
Curriculum vitae	199

1 Preface

Arthropod-borne flaviviruses represent an immense global health problem. Significant progress was achieved in the understanding of flavivirus structure and replication strategies, and now the complex picture of interactions between the virus and its host cell is being composed. In this thesis, I would like to add some pieces to the imaginary mosaic of tick-borne encephalitis pathogenesis. The more modern molecular technologies are developing the more we are able to find out about this flavivirus infection, which despite its medical importance, lacks effective therapy. Therefore, we have drawn our attention to detailed description of the pathogenesis and immunopathogenesis of tick-borne encephalitis, impact of host's genotype on the clinical course determination, immune response of patients with acute tick-borne encephalitis, the mechanism of tick-borne encephalitis virus migration into central nervous system and virus interaction with cells of neurovascular unit as well as potential medical interventions. The goal of our work is to enhance the knowledge of this disease development that will facilitate an effective medical treatment.

2 Introduction

2.1 Key background

Tick-borne encephalitis (TBE) is caused by tick-borne encephalitis virus (TBEV). In Europe and Northern parts of Asia, TBE represents one of the most serious infection of the central nervous system of humans. Approximately 10–15 thousand of clinical cases of TBE are annually reported, even though this number may be underestimated. Clinical presentations range from meningitis to encephalitis and infection may result in death or long-term neurological sequelae. The risk of infection or disease development can be averted by tick-bite prevention or active vaccination, however, specific medical treatment is not still available.

2.2 History

TBE is a vector-borne disease, that was described in 1937-39 by expeditions organized by Russian ministry of Health to the Far East with purpose to find out the origin of severe infections of central nervous system (CNS) called „Taiga encephalitis“. The expedition successfully identified a tick *Ixodes persulcatus* as the main vector of the virus (Zilber, 1939; Chumakov and Zeitlenok, 1940). The disease was known as „Russian spring–summer encephalitis“, nowadays tick-borne encephalitis. A milder form of the disease was also observed in Western Europe, where the tick *Ixodes ricinus* was found to be the vector responsible for virus transmission (Rampas and Gallia, 1949). In 1943, the TBEV of the western type was isolated for the first time from human patients and from *I. ricinus* ticks by Zilber and collaborators in Belarus (Pogodina *et al.*, 2004a). In Central Europe, the first virus isolation from human patients was achieved in 1948 in Czechoslovakia from a patient hospitalized in Beroun (Gallia *et al.*, 1949) and from another patient hospitalized in Vyškov (Krejci, 1949; 1950). Subsequently, the disease was shown to occur in many European countries and later in northern China and Japan. Based on historical description, TBE has been referred to as Russian spring–summer encephalitis, Far Eastern encephalitis, Taiga encephalitis, Central European encephalitis, Kumlinge disease, Biphasic milk fever,

Czechoslovak encephalitis, Bivandulating meningoencephalitis and “Early summer meningo-encephalitis (in German, Frühsommer-Meningoenzephalitis). Pioneer research work including field studies was conducted mainly in Russia (former USSR), Czechoslovakia and Austria to elucidate the virus cycle in nature (reviewed in Kunz and Heinz, 2003).

During a milk-borne outbreak in Slovakia in 1951, extensive scientific investigations under the supervision of Raška, Bárdoš and Blaškovič were performed, and the etiology and mode of TBE transmission, by goat milk was successfully revealed (Blaskovic, 1954). Transmission of TBE by consumption of milk or milk products (yogurt, cheese) prepared from milk of infected dairy animals was experimentally confirmed by Grešíková (Gresikova, 1958a; 1958b).

2.3 Tick-borne encephalitis

TBEV occurs in three subtypes, the European subtype (previously Central European encephalitis virus; with Neudörfl strain as prototype), the Far Eastern subtype (previously Russian spring–summer encephalitis; prototype strain Sofjin) and the Siberian virus (previously west Siberian virus; prototype strains Zausaev and Vasilchenko). The representatives of each subtype differ in biological properties: strains from the European subtype usually cause mild form of disease, on the other hand strains from Far Eastern subtype are associated with severe encephalitis. TBEV is an arbovirus, virus transmitted by blood-feeding arthropods. In Europe its main vector is tick *Ixodes ricinus*.

The severity of TBE is age-dependent. TBE neurological sequelae appear in one third of patients, often connected with cognitive dysfunctions. The disease is endemic in unevenly distributed focal areas defined by ecological and climatic conditions that determine the suitable environment for arthropod vectors and vertebrate reservoir species. Climate change and the increasing popularity of leisure activities, which may lead to increased human contact with ticks, are contributing to the rising numbers of people infected with TBEV observed during the last decades. Currently, between 10,000 and 15,000 TBE cases per year are reported in Europe and Asia (Bogovic and Strle, 2015). In the Czech Republic, generally 400-800 TBE cases are diagnosed per year (maximum of 1029 cases in 2006). In the years 2006-2014 there were 13 cases of TBE with fatal outcome (EpiDat - Database State Health Institute in Prague). Although TBE represents a considerable public health problem for more than half of a century, our knowledge particularly of its pathogenesis is still incomplete. Especially pathogenesis of the disease remains poorly explored.

Recent research is highlighting the impact of immunopathological reactions during encephalitides caused by flaviviruses, including TBE. Furthermore, it appears that the development of TBE is affected by many factors, including patient specific factors (genotype, immunity etc.).

2.3.1 Classification

TBEV is one of the medically important members of the genus *Flavivirus*, family *Flaviviridae* (Thiel *et al.*, 2005). Members of the genus *Flavivirus* are divided into three groups: the Tick-borne flaviviruses group, the Mosquito-borne flaviviruses group and the No-known vector flaviviruses (Gritsun *et al.*, 2003). Numerous flaviviruses represent important human pathogens, such as dengue virus, Japanese encephalitis virus, West Nile virus, or yellow fever virus.

The Tick-borne flaviviruses group is further divided into two subgroups according to host preference (seabirds and mammals). TBEV belongs to a subset of mammalian flaviviruses (Gaunt *et al.*, 2001).

TBE serocomplex includes Langat virus, Louping-ill virus, Negishi virus, Kyasanur Forest disease virus, Omsk hemorrhagic fever virus, Powassan virus, and others.

2.3.2 Virus particle

TBEV genome consists of a single-stranded RNA of positive polarity. The virion is about 50 nm in diameter. Viral genome of about 11 kb in length contains one open reading frame (ORF) that encodes a polyprotein composed of 3414 amino acids.

This polyprotein is co-translationally and post-translationally cleaved by cellular and viral proteases into three structural proteins (C, M, and E) and seven nonstructural proteins (NS1, NS2a, NS2B, NS3, NS4A, NS4B and NS5) (Lindquist *et al.*, 2008). The ORF is placed between the 5` (about 130 nucleotides) and 3` (350-750 nucleotides) untranslated regions (Fig. 1). RNA in these areas forms secondary structures that have an important role in genome replication, translation and packaging of viral nucleic acid into the virus capsid (Gritsun *et al.*, 1997).

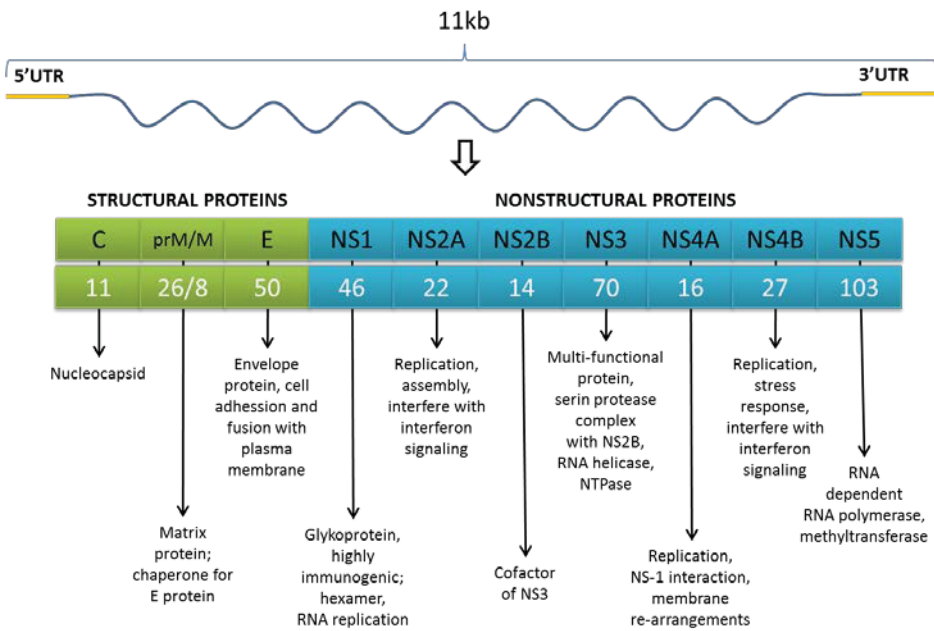


Figure 1: Scheme of the flaviviral genome with the description of the function of the proteins (adapted from Abraham *et al.*, 2001)

Viral nucleocapsid is of icosahedral symmetry and is formed by the viral genome, which is connected with a basic capsid protein C. The nucleocapsid represents an electrodense core. This core is coated with a lipid bilayer, in which two glycoproteins are integrated - protein E (envelope) and protein M (membrane). The M protein is formed by cleavage of immature precursor prM during release of the virion from the host cell. The E protein is the major surface antigen of the viral particle, which interacts with cell receptors and mediates fusion of the virus with the cell membrane. In mammalian cells, this protein also induces formation of virus-neutralizing antibodies, which play an important role in the antiviral immune response (Heinz *et al.*, 1986). The whole process of TBEV replication in the host cell is shown in Figure 2.

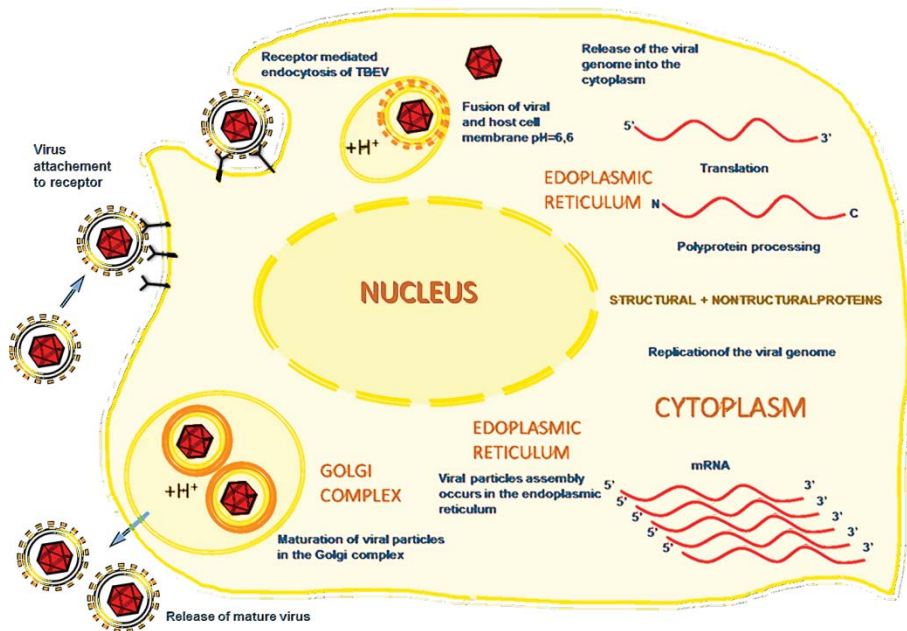


Figure 2: Replication machinery of TBEV in a mammalian cell (adapted from Samuel, 2002)

2.3.3 Ecology and Epidemiology

TBEV is transmitted by ticks of the genus *Ixodes*. Therefore, in natural environment, TBE incidence is closely connected with ecology and biology of the tick, with areas of ticks presence and their period of activity (Nuttal *et al.*, 1994). TBEV vectors are particularly species *I. persulcatus* as a major vector of the Siberian and Far Eastern subtype (Blaskovic *et al.*, 1967) and *I. ricinus* the main vector of representatives of the European subtype (Rampas *et al.*, 1949). As mentioned above, the occurrence of ticks is dependent on a variety of biotic and abiotic conditions (temperature, humidity, vegetation, small rodents presence, etc.). These conditions determine the occurrence of ticks in the environment and define natural foci of TBEV across the Northern hemisphere, from Europe to Japan (Korenberg *et al.*, 1999).

Once infected, the tick remains infected for the rest of its life time. Maintaining of TBEV in environment is facilitated by transstadial (between different developmental stages of a tick) and transovarial transmission (from

infected female to its offspring) (Fig. 3). The transmission of TBEV among ticks is known to be viremic or nonviremic. Nonviremic transmission occurs during co-feeding, when infected and uninfected ticks feed close to each other on small rodents (Labuda *et al.*, 1996). These rodents have a major influence on preservation of the TBEV in environment (Achazi *et al.*, 2011). Man is only a dead-end host, and has no role in the circulation of TBEV in nature.

The ecology of TBEV is still accompanied with many unresolved issues. It is not entirely clear how big a role the nonviremic transmission plays in the TBEV circulation, how important is the transovarial transmission and how multiple virus passages in these transstadial, transovarial and nonviremic transmissions influence biological properties of the virus. In addition, the importance of the long-term and high-level viremia in small rodents for viremic transmission remains unknown. Molecular phylogeography brings a new insight into the virus spreading in space and time (Weidmann *et al.*, 2011; 2013), local microevolution in natural viral outbreaks and possibility of the interaction with different viral variants in the same vector or reservoir remains still unclear.

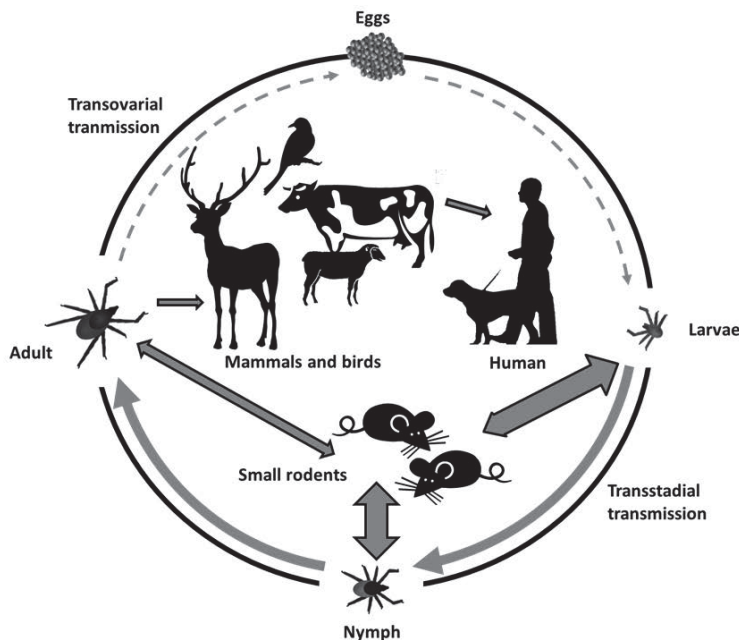


Figure 3: Scheme of TBEV circulation in nature (adapted from Palus and Růžek, 2013)

2.3.4 Routes of infection

The infection of humans with TBEV may not result only from attachment of infected tick. TBE cases after consuming contaminated unpasteurized milk from infected goats, sheep or cows or dairy products also occurs (Gresikova *et al.*, 1958a, 1958b) (Fig. 3, 4). For example, TBE outbreak in Rožňava in Slovakia was reported in 1951. The outbreak was caused by contaminated milk and over 600 people were infected. Recently, smaller local epidemics of alimentary TBE were reported. Retrospective analysis revealed that in years 1997-2008 about 0.9 % of TBE cases in the Czech Republic were of alimentary origin (Kriz *et al.*, 2009). In Slovakia the foodborne origin of TBE is believed to be up to 9 %.

2.3.5 Disease development and Clinical features

Based on serological surveys, it is estimated that up to 70-95 % of TBEV human infections are asymptomatic. In two thirds of the cases, the progress of the disease is biphasic. The host is infected with the virus during tick feeding. The virus replicates then in the subcutaneous tissues (Labuda *et al.*, 1996). Dendritic and Langerhans cells play the major role. These cells spread the virus further to draining lymph nodes, where is the virus multiplied further. After a relatively short incubation period (7-14 days), the first viremic phase of infection takes place (Kaiser, 1999). The virus infects various tissues and organs in the body. The symptoms manifest lasts around 1-8 days after virus entry. Symptoms during the first phase are similar to influenza (fever, fatigue, nausea, malaise, headache and pain of the whole body). There is approximately 7 days symptom-free interval between the first and second phase. During this interval the virus replicates in the peripheral organs, particularly the reticuloendothelial system (Malkova *et al.*, 1959). Subsequent secondary viremia occurs. During the secondary viremia the virus crosses the blood brain barrier (BBB) and enters the central nervous system (CNS).

TBEV is a neurotropic flavivirus (McMinn, 1997), however the mechanisms by which TBEV overcomes BBB and gains access to the CNS is not completely understood. Several hypothetical routes of the CNS invasion exist: by neuronal transport from peripheral nerves; by infection of olfactory neurons; by infection and replication in endothelial cells and virus budding on the parenchymal side; “Trojan horse” mechanism (immune cells infected by TBEV migrate into the CNS); and across the disrupted BBB (Fig. 4) (Ruzek *et al.*, 2010; Dorrbecker *et al.*, 2010). However, the last option seems to be unlikely, since previously published study described that BBB breakdown is rather a result of infection in the CNS and is not necessary for viral entry into the CNS (Ruzek *et al.*, 2011).

This second phase of the disease occurs in about 20-30 % of cases and it is characterized by symptoms of meningitis to severe encephalitis (Mickiene *et al.*, 2002). Pathology in the CNS is to a great extent the result of the inflammatory immune response caused by TBEV infection and associated immunopathological response in the brain tissue.

In general, there are three clinical forms of TBE: fever, meningeal form and meningoencephalitis (Gritsun *et al.*, 2003, Haglund and Gunther, 2003; Ruzek *et al.*, 2010) but also other forms exist: encephalomyelitic, polyradiculoneuritic and chronic form.

Febrile illness occurs in about one third of patients with TBE. Febrile form usually leads to complete recovery of the patient, lack neurological symptoms and any CNS damage. Fever may reach 39 ° C and lasts from several hours to 5 days (Gritsun *et al.*, 2003).

The second and most common form of the infection is meningitis. This form is in the initial symptoms similar to the febrile form, but with more severe symptoms. Patients usually suffer from severe headaches and nausea. Vomiting and increased light sensitivity is frequent. This form usually lasts 7-14 days and recovery is slow (Gritsun *et al.*, 2003).

Encephalomyelitis is a form that occurs with the lowest frequency, however, it is associated with severe damage of CNS tissue. Patients tend to be weak, sleepy, with frequent hallucinations or even fall into a coma. Symptoms include muscle spasm, slow heartbeat, stomach bleeding or paralysis. Some patients subsequently develop epilepsy. Thirty percent of cases of encephalomyelitis is followed by death. Other patients, most frequently the elderly population, may progress to permanent paralysis. Recovery is gradual, accompanied by signs of nervous exhaustion, dizziness and frequent changes of mood (Gritsun *et al.*, 2003).

Moreover, TBE variation may occur not only in the frequency of development of certain disease form, but also in the severity of each form according to the TBEV subtype. Viral strains of the Siberian and Far Eastern TBEV subtypes can be the cause of chronic diseases (Pogodina *et al.*, 2004b). It remains to future studies to find out whether viral or host factors contribute to the pathogenesis of chronic TBEV infections.

In Europe, the mortality following TBE reaches about 1 %. The severity of TBE, the frequency of complications and the number of fatal cases increases with the age of the patient (Lidquist *et al.*, 2008; Mickiene *et al.*, 2002).

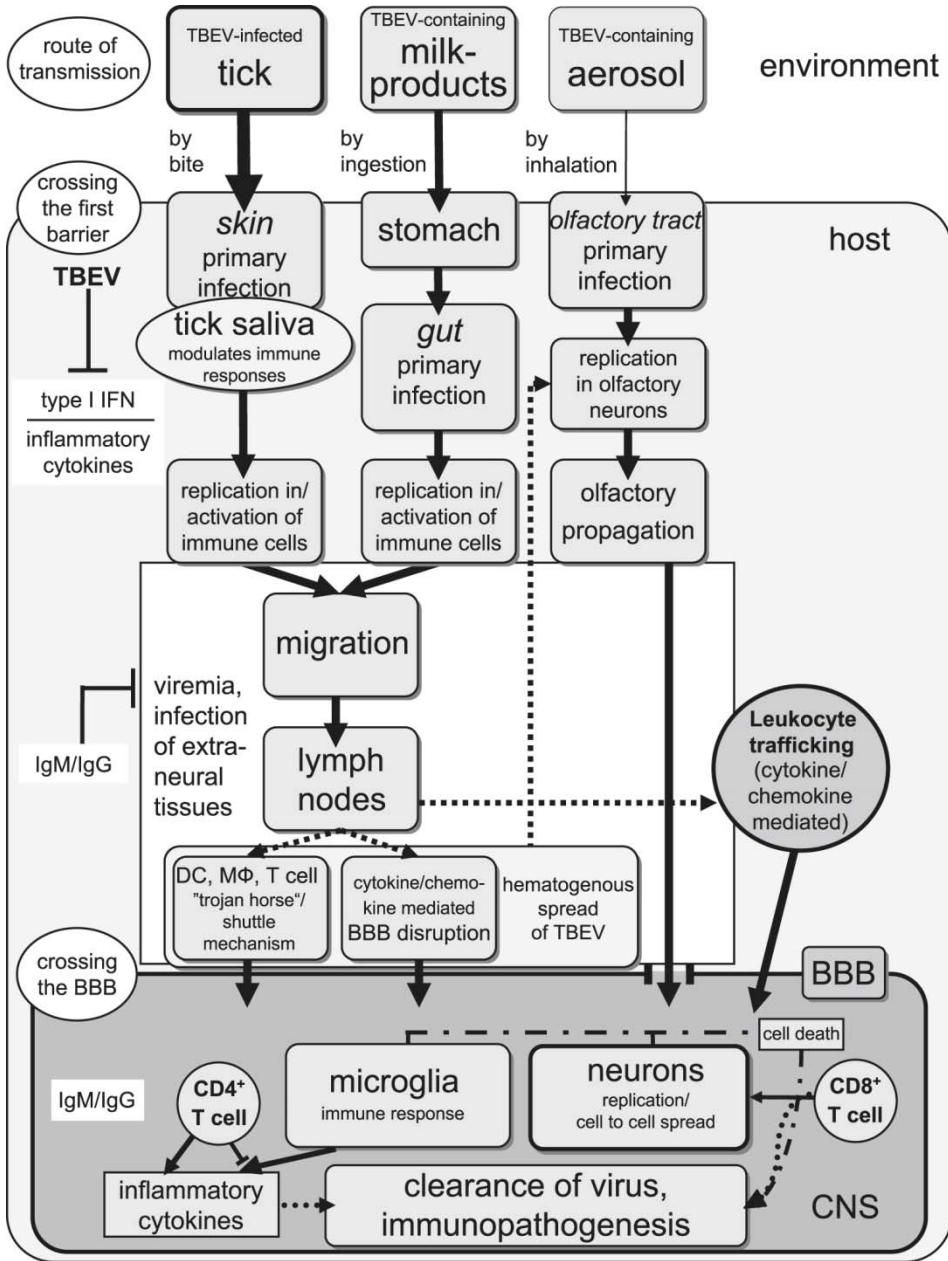


Figure 4: Interaction of TBEV with the mammalian immune system. Abbreviations: TBEV, tick-borne encephalitis virus; LC, Langerhans cell; DC, dendritic cell; MΦ, macrophage; IFN, interferon; IgG/IgM, immunoglobulins G/M; BBB, blood–brain barrier; CNS, central nervous system (Dörrbecker *et al.*, 2010).

2.3.6 Immuno/Pathology

2.3.6.1 Neuronal damage

TBE progress in a host is influenced by many factors at both the virus and the host side. In general, morbidity and mortality of flavivirus encephalitis is directly bound up with neuronal damage. The main mechanisms leading to neuron damage are in case of TBE three: the neuronal damage caused directly by the virus, immunopathological effects of the host immune system, and finally the mutual combination of both factors (Chambers and Diamond, 2003; King *et al.*, 2007; Ruzek *et al.*, 2009; Hayasaka *et al.*, 2009).

2.3.6.2 Central nervous system

The CNS is an immunologically privileged organ, which has, however, a wide range of immune mechanisms that can be activated in the case of infection. The defence response against viral infection involves innate and adaptive immune mechanism. Under certain circumstances, however, the defensive response becomes pathological to the host. Recently, there have been more and more studies that show the importance of immunopathological reactions in the development of flavivirus encephalitis (Klein *et al.*, 2005; Wang *et al.*, 2003; Winter *et al.*, 2004; Olsen *et al.*, 2007; Atrasheuskaya *et al.*, 2003; Lepej *et al.*, 2007; Sui *et al.*, 2006; Palus *et al.*, 2013).

The infection in the CNS leads to activation of various antiviral responses, which include: production of interferon and the expression of other interferon-stimulating genes, complement activation, or NK cell, macrophage and leukocyte infiltration into the CNS (Gupta *et al.*, 2011; Palus *et al.*, 2013; Ruzek *et al.*, 2009). Therefore, the roles of cytokines, chemokines, and growth factors during TBE are the key issues that have not been completely addressed to date. Previous reports characterized an acute immune response to TBEV by profiling certain cytokines and chemokines (e.g., tumor necrosis factor alpha (TNF- α), interleukin (IL)-1 β , IL- 6, CXCL10, CXCL11, CXCL12,

CXCL13) in the sera or cerebrospinal fluid of TBE patients (Kondrusik *et al.*, 2001; Atrasheuskaya *et al.*, 2003; Zajkowska *et al.*, 2011).

2.3.6.2a Key players in the protection/defence of the CNS

Microglia and astrocytes are in general considered to serve as the predominant source of cytokines and chemokines in the CNS, and therefore may act as important processors of neuroinflammation and neurodegeneration (Ramesh *et al.*, 2013; Palus *et al.*, 2014). Microglia represent tissue-specific macrophages in the CNS that have functions similar to monocytes (King *et al.*, 2007). Astrocytes, on the other hand, are recognized as trophic support cells in the CNS. Astrocytes are the most abundant glial cell population in the human brain (Nedergaard *et al.*, 2003) and have various important roles including integration of neuronal functions, neuronal support and regulation of the BBB. Thus, astrocytes present a structural and functional connection between endothelial cells of the BBB and neurons. Together with pericytes, these four cell types represent the 'neurovascular unit' (Fig. 5) (Stanimirovic and Friedman, 2012; Abbot *et al.*, 2010), which regulates blood flow, integrity of the BBB and neuronal activity in response to physiological and pathophysiological changes (Hussmann *et al.*, 2013).

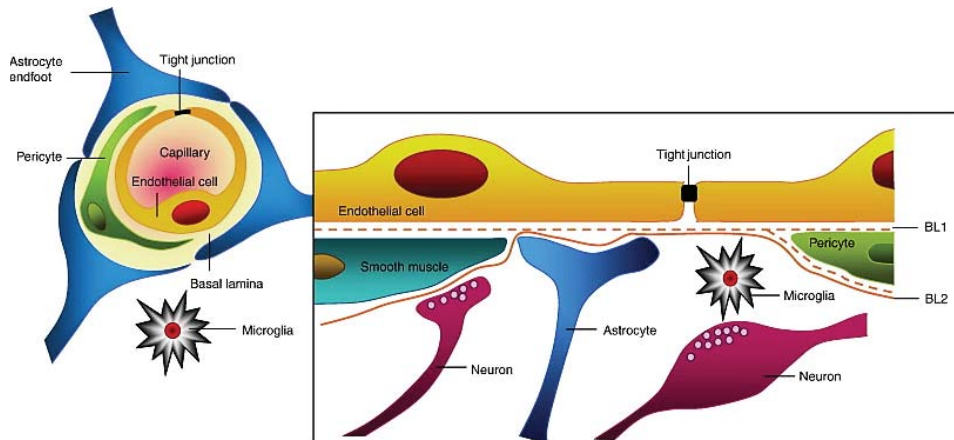


Figure 5: The cell associations at the BBB (Abbot *et al.*, 2010). Basal lamina (BL1, 2) is perivascular extracellular matrix that forms the local basement membrane.

In flavivirus encephalitis, microglia and astrocytes produce a variety of chemokines, which may have, under certain circumstances, immunopathological effects. Such chemokines include, for example, MCP-1 (CCL2) and RANTES (CCL5). These proinflammatory chemokines have no direct immunopathological effects, but can mediate tissue damage by recruiting circulating immune cells or stimulate macrophages and microglia (King *et al.*, 2007).

In addition, another important mediator capable of causing neuronal apoptosis matrix metalloproteinase 9 (MMP-9) is also produced by astrocytes (del Zoppo, 2010). Moreover, MMP-9 is capable of degrading collagen IV, a major component of the basement membrane of the cerebral endothelium (Fig. 5) and the expression of matrix metalloproteinases, especially MMP-9, correlates with BBB disruption during many neuroinflammatory diseases (Leppert *et al.*, 2000).

Infected astrocytes have a key role in the inflammatory response during neural infections caused by flaviviruses, namely Japanese encephalitis (Yang *et al.*, 2012), West Nile encephalitis (Hussmann *et al.*, 2013) and TBE (Palus *et al.*, 2014).

TBEV infected astrocyte also produce significantly higher levels of the chemokine IP-10 (CXCL10) (Palus *et al.*, 2014). Increased production of the chemokine CXCL10 and CXCL11 is connected with the activation and migration of T-lymphocytes. Elevated levels of chemokines have been observed in the cerebrospinal fluid of patients with TBE (Lepej *et al.*, 2007). Cytotoxic T lymphocytes should be primarily targeted to infected neurons. However, these cells are not always observed only at infected neurons. Moreover, there is no apparent topographical correlation between inflammatory infiltrates and virus antigen distribution (Ruzek *et al.*, 2009). A link of cytotoxic T lymphocytes (CD8+) with immunopathology during TBE was confirmed by histopathological studies of brain tissue of deceased patients (Gelphi *et al.*, 2006), but also in experiments carried out on laboratory mouse model (Ruzek *et al.*, 2009).

IP-10 acts not only as T lymphocyte activator, but also as a neurotoxin by itself; it causes apoptosis of neurons (Sui *et al.*, 2006). As shown by experiments on laboratory mice, overexpression of IP-10 (and also MCP-1) in brain tissue directly correlates with severity of TBE (Palus *et al.*, 2013).

2.3.6.2b Blood brain barrier breakdown

The immunopathological effect during TBE can be well presented also on BBB disruption. The integrity of the BBB is necessary for correct transport of nutrients into the CNS, protection against pathogens, toxins and other substances that may be harmful to the cells of the CNS (Hawkins and Davis, 2005). Integrity disruption allows proinflammatory immune cells, which are necessary for removing virus from neural tissue, to enter the CNS (Wang *et al.*, 2003). The conditions leading to BBB disruption and recruitment of inflammatory cells into the CNS are regulated by cytokines /chemokines produced in the affected tissue (Ruzek *et al.*, 2011; Winter *et al.*, 2004). Example of mediators influencing the permeability of BBB are TNF- α or IL-6 (de Vries *et al.*, 1996; Abbot, 2000). Experimental work has revealed that the disruption of BBB during TBE is not a consequence of lymphocyte migration

into the brain tissue, but the disruption occurs due to uncontrolled overproduction of various cytokines/chemokines in the CNS (Ruzek *et al.* 2011).

2.3.6.3 Humoral immunity

It should also be noted that even humoral immune activity, based on virus-neutralizing antibodies, can be detrimental to the host. Antibodies in classes IgM and IgG participate mainly in virus neutralization (Chambers and Diamond, 2003; Konishi *et al.*, 1999). Key role of antibodies in eliminating the infection was documented by a series of experimental studies (Diamond *et al.*, 2003; Palus *et al.*, 2013). On the other hand, the use of specific anti-TBEV immunoglobulins as post-exposure prophylaxis was discontinued in Europe due to the concerns of antibody-dependent enhancement (ADE) of the virus infectivity (Kluger *et al.*, 1995; Waldvogel *et al.*, 1996) as it has been described for secondary dengue virus infection. Nevertheless, specific anti-TBEV immunoglobulins are still used in Russia, with protection on average in 79 % of TBE cases after post-exposure administration of single dose of anti-TBEV immunoglobulin (Pen'evskaia and Rudakov, 2010).

The role of the host immune system in the pathogenesis of TBE is still unclear. The question is: Why is the immune system able to effectively eliminate the infection in some cases, while in others it is harmful to the host rather than to the pathogen itself? Ideal therapy, to the light of the above, should also have immunomodulatory properties leading to suppression of adverse immunopathological reactions.

2.3.7 Factors affecting disease development

As it is known, there are many aspects and factors that can affect a host susceptibility to viral infection and seriousness of the disease. These factors include age, sex, nutritional status, immune status and genetic dispositions.

Factors specific to the virus (virulence, route of transmission, viral load and etc.) play an important role to the same extent as host factors. TBEV is not uniform, its strains range from non-neuroinvasive to highly virulent.

Increased severity and permanent consequences which often significantly affect the patient's life after TBE, correlate with increasing age (> 60 years) (Gritsun *et al.*, 2003). On the other hand, children younger than 4 years of age are rarely affected by severe CNS infection when infected with European TBEV subtype but progression to more severe CNS disease can occur after infection with the Far Eastern subtype (Dumpis *et al.*, 1999).

Similarly, also sex seems to have a role as host factor influencing flaviviral infection. In mice after inoculation with St. Louis encephalitis virus was observed identical susceptibility in female and male at age of two months, however at the age of three and four months female mice showed significant reduction in the susceptibility to infection compared to males (Andersen *et al.*, 1974).

Important factor determining the susceptibility to flavivirus infection is related to 2'-5' oligoadenylate synthetases genes (OAS), whose products participate in activation of RNase L (Samuel *et al.*, 2002). For instance, homozygous dominant mice for gene Flvr (Oas1b) are susceptible to infection with flaviviruses, but infection will not develop in a clinically manifested disease and mice resemble to be resistant against flaviviruses. Additional experiments have shown that Flvr is responsible for resistance to flaviviruses at the intracellular level and without a fully functional immune system the presence of the resistant allele is completely negligible (Brinton and Perelygin, 2003).

There are some studies with TBE based on host genotype (Kindberg *et al.*, 2008; Barkhash *et al.*, 2012). It was demonstrated that a functional gene for Toll-like receptor 3 represents a risk factor for TBE development (Kindberg *et al.*, 2011). Deletions within the CCR5 receptor, which plays an important role in leukocyte transmigration across the BBB is more common in patients with TBE than in patients with aseptic meningitis of different etiology (Kindberg *et*

al., 2008). As already mentioned above, the severity of TBE is also related to the variability within the gene cluster of 2'-5'-oligoadenylate synthetase (Barkhash *et al.*, 2010). Clinical course of TBE is also linked to a single nucleotide polymorphism localized in the promoter sequence of the gene CD209 (Barkhash *et al.*, 2012). From all this evidence, it is apparent that polymorphisms within the series of genes may be associated with the course and severity of infection in patients with TBE.

2.3.8 Treatment

Unavailability of TBE specific treatment and risks associated with the administration of specific hyperimmune globulin as postexposure passive prophylaxis increase the importance of preventing the disease. However, treatment of severe TBE forms by administration of high doses of non-specific immunoglobulin (IVIG) was proposed. The effectivity of IVIG was proven in the case of many other encephalitis (Ruzek *et al.*, 2013). Nevertheless, the experience with this form of therapy for TBE is still missing. Currently the treatment is therefore symptomatic with bed rest, usually within the intensive care unit until fever and neurological symptoms persist. Fluid support, maintenance of electrolyte balance, sufficient caloric intake, and use of analgesics, vitamins and antipyretics are the main pillars of the clinical treatment of patients suffering from TBE. Glucocorticoids (i.v. 5-10 mg / kg / day) have beneficial effect during the TBE acute phase (Dunyewicz *et al.*, 1981).

Alternative approaches in TBE treatment were suggested. Promising results in the treatment of TBE trials were approached using antioxidants, for instance panavir (Litvin *et al.*, 2009), cytoflavin (Skripchenko and Egorova, 2011), or emoxypine (mexidol) (Abramenko, 2011, Udintseva *et al.*, 2012).

Achazi *et al.* (2012) suggest that RNA interference could be a valuable tool for controlling TBE virus infection. In their study, it was demonstrated that small interfering RNAs targeted at the TBEV genome reduce the quantity of infectious TBEV particles, TBEV genome copies, and TBE virus protein *in vitro*

by up to 85 %. RNAi has been demonstrated to be a useful technique for inhibiting the replication of many different viruses (Achazi *et al.*, 2012).

Another comparative *in vitro* study (Krylova and Leonova, 2001) suggested a thymalin (complex of 14 immunomodulators with effect on expression of T lymphocyte receptors) and leukinferon (complex preparation containing alpha-interferon and cytokines) in combination with human leukocytic interferon as possible drugs for immunomodulatory therapy of TBE.

Suppressing effect of tick-borne encephalitis (TBE) virus on expression of lymphocyte subpopulation receptors has been demonstrated *in vitro*.

2.3.9 Prevention

Protection against tick infestation, as use of appropriate clothes and early removal of attached ticks, and active immunization are the most effective preventive measures against TBEV infection (Kunz, 2003; Heinz *et al.*, 2007). Despite availability of active immunization, some endemic countries, including the Czech Republic, have very low vaccination coverage (Heinz *et al.*, 2007). In Europe, there are two available vaccines based on European strains of TBE: FSME-IMMUM from Pfizer (previously Baxter), Austria (strain Neudörf), and Encepur from GSK (previously Novartis Vaccines and Diagnostics), Germany (strain K23). The highly conserved structure of the protein E of TBE then ensures the effectiveness of vaccines against all three virus subtypes (Ruzek *et al.*, 2013). The efficacy of the two vaccines is estimated to be higher than 90%. There is also an age-dependent immune response after vaccination; children show an increased response compare to adults (Girgsdies *et al.*, 1996), while the vaccinated people aged over 60 have usually only weak antibody response (Hainz *et al.*, 2005). Regular booster for people younger than 50 years should be applied after five years (except the first booster after three years), whereas three-year revaccination interval for people aged over 50 years is recommended. Currently, considerable efforts

are made in order to develop a live attenuated vaccines, leading to sufficient immunity after single dose vaccination (Rumyantsev *et al.*, 2013).

2.3.10 Summary

TBE is the disease that undoubtedly deserves our attention. Although many scientific papers have been published about TBE, we still know very little. Every new finding concerning TBE opens new questions. Current research is focused mainly on the pathogenesis of TBE and the role of immune response in it. However, the extent and implications of immunopathological reactions during TBE need to be clarified too. Mode of the virus transition across the BBB; the interaction of TBEV with the cells within the CNS or the patient genetic background task in relation to the severity of the infection belong to the main research priorities. In addition, considerable expertise efforts are devoted to the development of an effective therapy or live attenuated vaccines.

2.4 References

- Abbott, N.J., 2000. Inflammatory mediators and modulation of blood–brain barrier permeability. *Cellular and molecular neurobiology* 20, 131-147.
- Abbott, N.J., Patabendige, A.A., Dolman, D.E., Yusof, S.R., Begley, D.J., 2010. Structure and function of the blood–brain barrier. *Neurobiology of disease* 37, 13-25.
- Abraham, S., Shwetank, G.K., Manjunath, R., 2011. Japanese encephalitis virus: innate and adaptive immunity. *FLAVIVIRUS ENCEPHALITIS*, 339.
- Abramenko, I., 2010. [The assessment of the clinical efficacy, vasoactive and metabolic effects of mexidol in elderly patients with discirculatory encephalopathy]. *Zhurnal nevrologii i psikiatrii imeni SS Korsakova/Ministerstvo zdravookhraneniia i meditsinskoi promyshlennosti Rossiiskoi Federatsii, Vserossiiskoe obshchestvo nevrologov [i] Vserossiiskoe obshchestvo psikiatrov* 111, 35-41.
- Achazi, K., Patel, P., Paliwal, R., Radonic, A., Niedrig, M., Donoso-Mantke, O., 2012. RNA interference inhibits replication of tick-borne encephalitis virus in vitro. *Antiviral research* 93, 94-100.
- Achazi, K., Ruzek, D., Donoso-Mantke, O., Schlegel, M., Ali, H.S., Wenk, M., Schmidt-Chanasit, J., Ohlmeyer, L., Ruhe, F., Vor, T., Kiffner, C., Kallies, R., Ulrich, R.G., Niedrig, M., 2011. Rodents as sentinels for the prevalence of tick-borne encephalitis virus. *Vector borne and zoonotic diseases* 11, 641-647.
- Andersen, A.A., Hanson, R.P., 1974. Influence of sex and age on natural resistance to St. Louis encephalitis virus infection in mice. *Infection and immunity* 9, 1123-1125.
- Atrasheuskaya, A.V., Fredeking, T.M., Ignatyev, G.M., 2003. Changes in immune parameters and their correction in human cases of tick-borne encephalitis. *Clinical and experimental immunology* 131, 148-154.
- Barkhash, A.V., Babenko, V.N., Kobzev, V.F., Romashchenko, A.G., Voevoda, M.I., 2010. [Polymorphism in the human 2'-5'-oligoadenylate synthetase genes (OAS), associated with predisposition to severe forms of tick-borne encephalitis, in populations from North Eurasia]. *Molekuliarnaia biologii* 44, 985-993.
- Barkhash, A.V., Perelygin, A.A., Babenko, V.N., Brinton, M.A., Voevoda, M.I., 2012. Single nucleotide polymorphism in the promoter region of the CD209 gene is associated with human predisposition to severe forms of tick-borne encephalitis. *Antiviral research* 93, 64-68.

- Blaskovic, D., (ed.) 1954. The Epidemic of Encephalitis in Roznava Natural Focus of Infection. Slovak Academy of Sciences, Bratislava.
- Blaskovic, D., 1967. The public health importance of tick-borne encephalitis in Europe. *Bulletin of the World Health Organization* 36 Suppl, 5-13.
- Bogovic, P., Strle, F. 2015. Tick-borne encephalitis: A review of epidemiology, clinical characteristics, and management. *World Journal of Clinical Cases*. 3(5), 430-41.
- Brinton, M.A., Perelygin, A.A., 2003. Genetic resistance to flaviviruses. *Advances in virus research* 60, 43-85.
- de Vries, H.E., Blom-Roosemalen, M.C., van Oosten, M., de Boer, A.G., van Berkel, T.J., Breimer, D.D., Kuiper, J., 1996. The influence of cytokines on the integrity of the blood-brain barrier in vitro. *Journal of neuroimmunology* 64, 37-43.
- Del Zoppo, G.J., 2010. The neurovascular unit, matrix proteases, and innate inflammation. *Annals of the New York Academy of Sciences* 1207, 46-49.
- Diamond, M.S., Shrestha, B., Marri, A., Mahan, D., Engle, M. 2003. B cells and antibody play critical roles in the immediate defense of disseminated infection by West Nile encephalitis virus. *Journal of virology*, 77(4), 2578-2586.
- Dorrbecker, B., Dobler, G., Spiegel, M., Hufert, F.T., 2010. Tick-borne encephalitis virus and the immune response of the mammalian host. *Travel medicine and infectious disease* 8, 213-222.
- Dumpis, U., Crook, D., Oksi, J., 1999. Tick-borne encephalitis. *Clinical infectious diseases: an official publication of the Infectious Diseases Society of America* 28, 882-890.
- Dunyewicz, M., Mertenova, J., Moravcova, E., Kulkova, H., 1981. Corticoids in the therapy of TBE and other viral encephalitides. C. Kunz (Ed.), *Tick-borne encephalitis*, *Facultas-Verlag* . 36-44.
- Gallia, F., Rampas, J., Hollender, J., 1949. Laboratori infekce encefalitickym virem. *Casopis lekaru ceskych* 88, 224-229.
- Gaunt, M.W., Sall, A.A., de Lamballerie, X., Falconar, A.K., Dzhivanian, T.I., Gould, E.A., 2001. Phylogenetic relationships of flaviviruses correlate with their epidemiology, disease association and biogeography. *The Journal of general virology* 82, 1867-1876.
- Gelpi, E., Preusser, M., Laggner, U., Garzuly, F., Holzmann, H., Heinz, F.X., Budka, H., 2006. Inflammatory response in human tick-borne encephalitis: analysis of postmortem brain tissue. *Journal of neurovirology* 12, 322-327.

- Girgsdies, O.E., Rosenkranz, G., 1996. Tick-borne encephalitis: development of a paediatric vaccine. A controlled, randomized, double-blind and multicentre study. *Vaccine* 14, 1421-1428.
- Gresikova, M., 1958a. Excretion of the Tick-Borne Encephalitis Virus in the Milk of Subcutaneously Infected Cows. *Acta virologica* 2, 188-192.
- Gresikova, M., 1958b. Recovery of the tick-borne encephalitis virus from the blood and milk of subcutaneously infected sheep. *Acta virologica* 2, 113-119.
- Gritsun, T.S., Lashkevich, V.A., Gould, E.A., 2003. Tick-borne encephalitis. *Antiviral research* 57, 129-146.
- Gritsun, T.S., Venugopal, K., Zannotto, P.M., Mikhailov, M.V., Sall, A.A., Holmes, E.C., Polkinghorne, I., Frolova, T.V., Pogodina, V.V., Lashkevich, V.A., Gould, E.A., 1997. Complete sequence of two tick-borne flaviviruses isolated from Siberia and the UK: analysis and significance of the 5' and 3'-UTRs. *Virus research* 49, 27-39.
- Gupta, N., Santhosh, S., Babu, J.P., Parida, M., Rao, P.L., 2010. Chemokine profiling of Japanese encephalitis virus-infected mouse neuroblastoma cells by microarray and real-time RT-PCR: implication in neuropathogenesis. *Virus research* 147, 107-112.
- Haglund, M., Gunther, G. 2003. Tick-borne encephalitis—pathogenesis, clinical course and long-term follow-up. *Vaccine*, 21, S11-S18.
- Hainz, U., Jenewein, B., Asch, E., Pfeiffer, K.P., Berger, P., Grubeck-Loebenstien, B., 2005. Insufficient protection for healthy elderly adults by tetanus and TBE vaccines. *Vaccine* 23, 3232-3235.
- Hawkins, B.T., Davis, T.P., 2005. The blood-brain barrier/neurovascular unit in health and disease. *Pharmacological reviews* 57, 173-185.
- Hayasaka, D., Nagata, N., Fujii, Y., Hasegawa, H., Sata, T., Suzuki, R., Gould, E.A., Takashima, I., Koike, S., 2009. Mortality following peripheral infection with tick-borne encephalitis virus results from a combination of central nervous system pathology, systemic inflammatory and stress responses. *Virology* 390, 139-150.
- Heinz, F.X., 1986. Epitope mapping of flavivirus glycoproteins. *Advances in virus research* 31, 103-168.
- Heinz, F.X., Holzmann, H., Essl, A., Kundi, M., 2007. Field effectiveness of vaccination against tick-borne encephalitis. *Vaccine* 25, 7559-7567.
- Hussmann, K.L., Samuel, M.A., Kim, K.S., Diamond, M.S., Fredericksen, B.L., 2013. Differential replication of pathogenic and nonpathogenic strains of West Nile virus within astrocytes. *Journal of virology* 87, 2814-2822.

- Chambers, T.J., Diamond, M.S., 2003. Pathogenesis of flavivirus encephalitis. *Advances in virus research* 60, 273-342.
- Chumakov, M.P., Zeitlenok, N.A., 1940. Tick-borne spring–summer encephalitis in the Ural region. In: *Neuroinfections in the Ural*. Sverdlovsk 23–30. (in Russian).
- Kaiser, R., 1999. The clinical and epidemiological profile of tick-borne encephalitis in southern Germany 1994-98: a prospective study of 656 patients. *Brain : a journal of neurology* 122 (Pt 11), 2067-2078.
- Kindberg, E., Mickiene, A., Ax, C., Akerlind, B., Vene, S., Lindquist, L., Lundkvist, A., Svensson, L., 2008. A deletion in the chemokine receptor 5 (CCR5) gene is associated with tickborne encephalitis. *The Journal of infectious diseases* 197, 266-269.
- Kindberg, E., Vene, S., Mickiene, A., Lundkvist, A., Lindquist, L., Svensson, L., 2011. A functional Toll-like receptor 3 gene (TLR3) may be a risk factor for tick-borne encephalitis virus (TBEV) infection. *The Journal of infectious diseases* 203, 523-528.
- King, N.J., Getts, D.R., Getts, M.T., Rana, S., Shrestha, B., Kesson, A.M., 2007. Immunopathology of flavivirus infections. *Immunology and cell biology* 85, 33-42.
- Klein, R.S., Lin, E., Zhang, B., Luster, A.D., Tollett, J., Samuel, M.A., Engle, M., Diamond, M.S., 2005. Neuronal CXCL10 directs CD8+ T-cell recruitment and control of West Nile virus encephalitis. *Journal of virology* 79, 11457-11466.
- Kluger, G., Schöttler, A., Waldvogel, K., Nadal, D., Hinrichs, W., Wündisch, G., Laub, M., 1995. Tickborne encephalitis despite specific immunoglobulin prophylaxis. *The Lancet* 346, 1502.
- Kondrusik, M., Pancewicz, S., Zajkowska, J., Hermanowska-Szpakowicz, T., 2001. [Tumor necrosis factor alpha and interleukin 1-beta in serum of patients with tick-borne encephalitis]. *Polski merkuriusz lekarski : organ Polskiego Towarzystwa Lekarskiego* 11, 26-28.
- Konishi, E., Yamaoka, M., Kurane, I., Takada, K., Mason, P.W., 1999. The anamnestic neutralizing antibody response is critical for protection of mice from challenge following vaccination with a plasmid encoding the Japanese encephalitis virus premembrane and envelope genes. *Journal of virology* 73, 5527-5534.
- Korenberg, E.I., Kovalevskii, Y.V., 1999. Main features of tick-borne encephalitis eco-epidemiology in Russia. *Zentralblatt fur Bakteriologie : international journal of medical microbiology* 289, 525-539.

- Krejci, J., 1949. Epidemie virusových meningoencefalitid na Vyskovsku. *Lekarske Listy*.
- Krejci, J., 1950. Isolace viru lidske meningoencefalitidy z klistat. *Lekarske Listy*.
- Kriz, B., Benes, C., Daniel, M., 2009. Alimentary transmission of tick-borne encephalitis in the Czech Republic (1997-2008). *Epidemiologie, mikrobiologie, imunologie : casopis Spolecnosti pro epidemiologii a mikrobiologii Ceske lekarske spolecnosti J.E. Purkyne* 58, 98-103.
- Krylova, N.V., Leonova, G.N., 2001. [Comparative in vitro study of the effectiveness of various immunomodulating substances in tick-borne encephalitis]. *Voprosy virusologii* 46, 25-28.
- Kunz, C., 2003. TBE vaccination and the Austrian experience. *Vaccine* 21 Suppl 1, S50-55.
- Kunz, C., Heinz, F.X., 2003. Tick-borne encephalitis. *Vaccine* 21 Suppl 1, S1-2.
- Labuda, M., Austyn, J.M., Zuffova, E., Kozuch, O., Fuchsberger, N., Lysy, J., Nuttall, P.A., 1996. Importance of localized skin infection in tick-borne encephalitis virus transmission. *Virology* 219, 357-366.
- Lepej, S.Z., Misic-Majerus, L., Jeren, T., Rode, O.D., Remenar, A., Sporec, V., Vince, A., 2007. Chemokines CXCL10 and CXCL11 in the cerebrospinal fluid of patients with tick-borne encephalitis. *Acta neurologica Scandinavica* 115, 109-114.
- Leppert, D., Lindberg, R. L., Kappos, L., Leib, S. L. 2001. Matrix metalloproteinases: multifunctional effectors of inflammation in multiple sclerosis and bacterial meningitis. *Brain research reviews*, 36(2), 249-257.
- Lindquist, L., Vapalahti, O., 2008. Tick-borne encephalitis. *Lancet* 371, 1861-1871.
- Litvin, A.A., Ratnikova, L.I., Deriabin, P.G., 2009. [Preclinical and clinical studies of the efficacy of Panavir in therapy for tick-borne encephalitis]. *Voprosy virusologii* 54, 26-32.
- Malkova, D., Frankova, V., 1959. The lymphatic system in the development of experimental tick-borne encephalitis in mice. *Acta virologica* 3, 210-214.
- McMinn, P.C., 1997. The molecular basis of virulence of the encephalitogenic flaviviruses. *Journal of General Virology* 78, 2711-2722.
- Mickiene, A., Laiskonis, A., Gunther, G., Vene, S., Lundkvist, A., Lindquist, L., 2002. Tickborne encephalitis in an area of high endemicity in lithuania: disease severity and long-term prognosis. *Clinical infectious diseases : an official publication of the Infectious Diseases Society of America* 35, 650-658.

- Nedergaard, M., Ransom, B., Goldman, S.A., 2003. New roles for astrocytes: redefining the functional architecture of the brain. *Trends in neurosciences* 26, 523-530.
- Nuttall, P.A., Jones, L.D., Labuda, M., Kaufman, W.R., 1994. Adaptations of arboviruses to ticks. *Journal of medical entomology* 31, 1-9.
- Olsen, A.L., Morrey, J.D., Smee, D.F., Sidwell, R.W., 2007. Correlation between breakdown of the blood–brain barrier and disease outcome of viral encephalitis in mice. *Antiviral research* 75, 104-112.
- Palus, M., Bily, T., Elsterova, J., Langhansova, H., Salat, J., Vancova, M., Ruzek, D., 2014. Infection and injury of human astrocytes by tick-borne encephalitis virus. *The Journal of general virology* 95, 2411-2426.
- Palus, M., Ruzek, D., 2013. Klistova encefalitida–stale vice otazniku nez jasnych odpovedi. *Vakcinologie* 7, 158-164.
- Palus, M., Vojtiskova, J., Salat, J., Kopecky, J., Grubhoffer, L., Lipoldova, M., Demant, P., Ruzek, D., 2013. Mice with different susceptibility to tick-borne encephalitis virus infection show selective neutralizing antibody response and inflammatory reaction in the central nervous system. *Journal of neuroinflammation* 10, 77.
- Pen'evskaia, N.A., Rudakov, N.V., 2010. [Efficiency of use of immunoglobulin preparations for the postexposure prevention of tick-borne encephalitis in Russia (a review of semi-centennial experience)]. *Meditsinskaia parazitologija i parazitarnye bolezni*, 53-59.
- Pogodina, V.V., Bochkova, N.G., Karan, L.S., Frolova, M.P., Trukhina, A.G., Malenko, G.V., Levina, L.S., Platonov, A.E., 2004a. [Comparative analysis of virulence of the Siberian and Far-East subtypes of the tick-born encephalitis virus]. *Voprosy virusologii* 49, 24-30.
- Pogodina, V.V., Bochkova, N.G., Karan, L.S., Trukhina, A.G., Levina, L.S., Malenko, G.V., Druzhinina, T.A., Lukashenko, Z.S., Dul'keit, O.F., Platonov, A.E., 2004b. [The Siberian and Far-Eastern subtypes of tick-borne encephalitis virus registered in Russia's Asian regions: genetic and antigen characteristics of the strains]. *Voprosy virusologii* 49, 20-25.
- Ramesh, G., MacLean, A.G., Philipp, M.T., 2013. Cytokines and chemokines at the crossroads of neuroinflammation, neurodegeneration, and neuropathic pain. *Mediators of inflammation* 2013, 480739.
- Rampas, J., Gallia, F., 1949. Isolation of an Encephalitis Virus from the Tick *Ixodes ricinus*. *Casopis lekaru ceskych* 88, 1179-1180.

- Rumyantsev, A.A., Goncalvez, A.P., Giel-Moloney, M., Catalan, J., Liu, Y., Gao, Q.S., Almond, J., Kleanthous, H., Pugachev, K.V., 2013. Single-dose vaccine against tick-borne encephalitis. *Proceedings of the National Academy of Sciences of the United States of America* 110, 13103-13108.
- Ruzek, D., Dobler, G., Donoso Mantke, O., 2010. Tick-borne encephalitis: pathogenesis and clinical implications. *Travel medicine and infectious disease* 8, 223-232.
- Ruzek, D., Dobler, G., Niller, H.H., 2013. May early intervention with high dose intravenous immunoglobulin pose a potentially successful treatment for severe cases of tick-borne encephalitis? *BMC infectious diseases* 13, 306.
- Ruzek, D., Salat, J., Palus, M., Gritsun, T.S., Gould, E.A., Dykova, I., Skallova, A., Jelinek, J., Kopecky, J., Grubhoffer, L., 2009. CD8+ T-cells mediate immunopathology in tick-borne encephalitis. *Virology* 384, 1-6.
- Ruzek, D., Salat, J., Singh, S.K., Kopecky, J., 2011. Breakdown of the blood-brain barrier during tick-borne encephalitis in mice is not dependent on CD8+ T-cells. *PLoS one* 6, e20472.
- Samuel, C.E., 2002. Host genetic variability and West Nile virus susceptibility. *Proceedings of the National Academy of Sciences* 99, 11555-11557.
- Skripchenko, N., Egorova, E., 2010. [Cytoflavin in the complex treatment of neuroinfections in children]. *Zhurnal nevrologii i psikiatrii imeni SS Korsakova/Ministerstvo zdravookhraneniia i meditsinskoj promyshlennosti Rossijskoj Federatsii, Vserossiiskoe obshchestvo nevrologov [i] Vserossiiskoe obshchestvo psikiatrov* 111, 28-31.
- Stanimirovic, D.B., Friedman, A., 2012. Pathophysiology of the neurovascular unit: disease cause or consequence? *Journal of Cerebral Blood Flow & Metabolism* 32, 1207-1221.
- Sui, Y., Stehno-Bittel, L., Li, S., Loganathan, R., Dhillon, N.K., Pinson, D., Nath, A., Kolson, D., Narayan, O., Buch, S., 2006. CXCL10-induced cell death in neurons: role of calcium dysregulation. *European Journal of Neuroscience* 23, 957-964.
- Thiel, H., Collett, M., Gould, E., Heinz, F., Houghton, M., Meyers, G., Purcell, R., Rice, C., 2005. Family flaviviridae. *Virus Taxonomy: Eight report of the international committee on taxonomy of viruses*, 981-998.
- Udintseva, I.N., Bartfel't, N.N., Zhukova, N.G., Poponina, A.M., 2012. [Mexidol in the complex treatment of patients in the acute period of tick borne encephalitis]. *Zhurnal nevrologii i psikiatrii imeni S.S. Korsakova / Ministerstvo zdravookhraneniia i meditsinskoj promyshlennosti Rossijskoj Federatsii*,

- Vserossiiskoe obshchestvo nevrologov [i] Vserossiiskoe obshchestvo psikhiat 112, 34-38.
- Waldvogel, K., Bossart, W., Huisman, T., Boltshauer, E., Nadal, D., 1996. Severe tick-borne encephalitis following passive immunization. *European journal of pediatrics* 155, 775-779.
- Wang, Y., Lobigs, M., Lee, E., Müllbacher, A., 2003. CD8+ T cells mediate recovery and immunopathology in West Nile virus encephalitis. *Journal of virology* 77, 13323-13334.
- Weidmann, M., Frey, S., Freire, C.C., Essbauer, S., Ruzek, D., Klempa, B., Zubrikova, D., Vogerl, M., Pfeffer, M., Hufert, F.T., Zanotto, P.M., Dobler, G., 2013. Molecular phylogeography of tick-borne encephalitis virus in central Europe. *The Journal of general virology* 94, 2129-2139.
- Weidmann, M., Ruzek, D., Krivanec, K., Zoller, G., Essbauer, S., Pfeffer, M., Zanotto, P.M., Hufert, F.T., Dobler, G., 2011. Relation of genetic phylogeny and geographical distance of tick-borne encephalitis virus in central Europe. *The Journal of general virology* 92, 1906-1916.
- Winter, P.M., Dung, N.M., Loan, H.T., Kneen, R., Wills, B., House, D., White, N.J., Farrar, J.J., Hart, C.A., Solomon, T., 2004. Proinflammatory cytokines and chemokines in humans with Japanese encephalitis. *Journal of Infectious Diseases* 190, 1618-1626.
- Yang, C.M., Lin, C.C., Lee, I.T., Lin, Y.H., Yang, C.M., Chen, W.J., Jou, M.J., Hsiao, L.D., 2012. Japanese encephalitis virus induces matrix metalloproteinase-9 expression via a ROS/c-Src/PDGFR/PI3K/Akt/MAPKs-dependent AP-1 pathway in rat brain astrocytes. *Journal of neuroinflammation* 9, 12.
- Zajkowska, J., Czupryna, P., Pancewicz, S., Adamczyk-Przychodzen, A., Kondrusik, M., Grygorczuk, S., Moniuszko, A., 2011. Fatal outcome of tick-borne encephalitis - a case series. *Neurologia i neurochirurgia polska* 45, 402-406.
- Zilber, L., 1939. Spring (spring-summer) epidemical tick-borne encephalitis. *Arch Biol Nauk* 56, 9-37.
- EpiDat - Database State Health Institute in Prague
<http://www.szu.cz/publikace/data/vybrane-infekcni-nemoci-v-cr-v-letech-2006-2015-absolutne>; <http://www.szu.cz/tema/prevence/klistova-encefalitida>

2.5 Specific aims

- 1) Study of the sensitivity to TBEV-infection in mice differing in their genetic background**
- 2) Study the interaction of TBEV with human primary cells forming the neurovascular unit cells**
- 3) Prepare functional *in vitro* BBB model**
- 4) Analyse cytokine/chemokine, growth factor levels and other inflammatory markers in patients sera with TBE**
- 5) Study potential therapeutical approaches in TBE**

CHAPTER I

CD8+ T-cells mediate immunopathology in tick-borne encephalitis

Daniel Růžek, Jiří Salát, Martin Palus, Tamara S. Gritsun, Ernest A. Gould, Iva Dyková, Anna Skallová, Jiří Jelínek, Jan Kopecký, Libor Grubhoffer

Virology 2009, 384(1), 1-6.

DOI: 10.1016/j.virol.2008.11.023

<http://dx.doi.org/10.1016/j.virol.2008.11.023>

CD8+ T-cells mediate immunopathology in TBE (summary)

Tick-borne encephalitis (TBE), a disease caused by Tick-borne encephalitis virus (TBEV), is an increasing public health problem in northern and central Eurasia, where thousands of human encephalitis cases and numerous deaths are reported annually (Gritsun *et al.*, 2003b). In general, morbidity and mortality of flavivirus encephalitis are directly bound up with neuronal damage. For flavivirus encephalitis, three possible mechanisms of brain tissue damage have been postulated: i) the virus itself causes direct neuronal damage; ii) the neuronal destruction is caused by virus-induced inflammatory response; and finally iii) combination of both, i.e. viral neuronal damage and immunopathology are responsible (Chambers and Diamond, 2003; King *et al.*, 2007). However, the precise mechanism by which viruses in the tick-borne flavivirus group induce encephalitis has not yet been revealed. Our research enhances the current knowledge of antiviral immune response during TBEV infection and the understanding of TBE pathogenesis. We focused on the cellular immune response which in case of flaviviral infections appears to be somewhat double-edged, since there is an apparent necessity for T-cell response, as well as notable evidence of T-cell-mediated immunopathology.

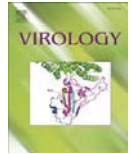
By analyzing the role of specific T-cell subpopulations, CD4⁺ and CD8⁺, in the immunocompetent and immunocompromised mouse models, we provide direct evidence for the immunopathology of TBEV infections.

For instance, mice with severe combined immunodeficiency or CD8^{-/-} knockout mice showed prolonged survival after TBEV infection, when compared with immunocompetent mice or mice with adoptively transferred CD8⁺ T-cells. However, in the absence of an immune response the virus on its own is also capable of causing encephalitis.

Our experiments showing an immunopathological effect of CD8⁺ T-cells and the role of CD4⁺ T-cells in confining the infection, in accordance with some

of the observations on West Nile virus (Wang *et al.*, 2003; Sitati and Diamond, 2006).

Our results imply that tick-borne encephalitis is an immunopathological disease and that the inflammatory reaction significantly contributes to the fatal outcome of the infection. This study provide the basis for a rational therapeutic strategy against this human disease.



Rapid Communication

CD8⁺ T-cells mediate immunopathology in tick-borne encephalitis

Daniel Růžek^{a,b,*}, Jiří Salát^{a,b}, Martin Palus^b, Tamara S. Gritsun^c, Ernest A. Gould^d, Iva Dyková^a, Anna Skallová^{a,b}, Jiří Jelínek^{a,b,1}, Jan Kopecký^{a,b}, Libor Grubhoffer^{a,b}

^a Institute of Parasitology, Biology Centre of the Academy of Sciences of the Czech Republic, Branišovská 31, CZ-37005 České Budějovice, Czech Republic

^b Faculty of Science, University of South Bohemia, Branišovská 31, CZ-37005 České Budějovice, Czech Republic

^c School of Biological Sciences, The University of Reading, Whiteknights, Reading, Berks RG6 6AJ, UK

^d Center for Ecology and Hydrology, Mansfield Road, Oxford OX2 8NN, UK

ARTICLE INFO

Article history:

Received 27 May 2008

Returned to author for revision

18 September 2008

Accepted 13 November 2008

Available online 13 December 2008

Keywords:

Tick-borne encephalitis virus

Immunopathology

CD8⁺ T-cells

CD4⁺ T-cells

SCID mice

ABSTRACT

Epidemics of tick-borne encephalitis involving thousands of humans occur annually in the forested regions of Europe and Asia. Despite the importance of this disease, the underlying basis for the development of encephalitis remains undefined. Here, we prove the key role of CD8⁺ T-cells in the immunopathology of tick-borne encephalitis, as demonstrated by prolonged survival of SCID or CD8^{-/-} mice, following infection, when compared with immunocompetent mice or mice with adoptively transferred CD8⁺ T-cells. The results imply that tick-borne encephalitis is an immunopathological disease and that the inflammatory reaction significantly contributes to the fatal outcome of the infection.

© 2008 Elsevier Inc. All rights reserved.

Introduction

Tick-borne encephalitis (TBE), a disease caused by Tick-borne encephalitis virus (TBEV), is an increasing public health problem in northern and central Eurasia, where thousands of human encephalitis cases and numerous deaths are reported annually (Gritsun et al., 2003a). TBEV is a single-stranded, positive-sense, enveloped RNA virus, a member of the Tick-borne flavivirus (TBFV) group, that together with the Mosquito-borne flavivirus (MBFV) group and the No-known vector (NKV) group comprise the genus *Flavivirus* within the family *Flaviviridae* (Thiel et al., 2005). In humans TBEV may produce a variety of clinical symptoms, including fever and acute or chronic progressive encephalitis (Gritsun et al., 2003a,b), with or without a fatal outcome. As with other viral infections, the virulence of the circulating strain and the immunological status of the infected individual may contribute to the severity of the disease (Růžek et al., 2008). Recent studies on the molecular basis of pathogenesis, mostly performed with the MBFV group, established that apoptosis and immune-mediated tissue damage may determine the outcome of flavivirus infections (reviewed in Chambers and Diamond, 2003; King et al., 2007). However, the mechanism by which viruses in the

TBFV group induce encephalitis is not completely understood. In this study we provide direct evidence for the immunopathology of TBE using different mouse strains to model TBEV infections. We address this issue by analyzing the role of specific T-cell subpopulations, i.e. CD4⁺ and CD8⁺ T-cells, in the recovery and/or immunopathology of TBE in mice.

Results

To assess the contribution of immunopathology in the development of encephalitis, we directly examined the role of two subpopulations of T-cells, i.e. CD4⁺ and CD8⁺, following infection of different strains of mice with TBEV.

Groups of mice with severe combined immunodeficiency (SCID), and control immunocompetent (Balb/c) mice, were inoculated subcutaneously with 100 pfu of the prototype neurovirulent TBEV strain Hypr. Morbidity, mortality, and mean survival times (MST) were then recorded. The clinical signs emerged virtually at the same time in both groups, i.e. approximately on the 8th or 9th day post-infection (p.i.). The mice showed clinical signs of hunching, ruffling of fur and hind-limb paralysis. Mean survival time of the immunocompetent Balb/c mice was 10.4±3.3 days; however, SCID mice survived significantly longer (MST of 13.9±0.8 days, $p < 0.05$; Fig. 1A).

Analogously, CD8^{-/-} knockout mice derived from a C57Bl/6 genetic background, exhibited prolonged mean survival times following TBEV infection (MST of 12.73±2.10 days) when compared with immunocompetent C57Bl/6 mice (7.45±1.37, $p < 0.001$; Fig. 1B).

* Corresponding author. Institute of Parasitology, Biology Centre AS CR, Branišovská 31, CZ-370 05 České Budějovice, Czech Republic. Fax: +420 38 531 0388.

E-mail address: ruzekd@paru.cas.cz (D. Růžek).

¹ Present address: Faculty of Medicine, Masaryk University, Černopolní 9, CZ-66263 Brno, Czech Republic.

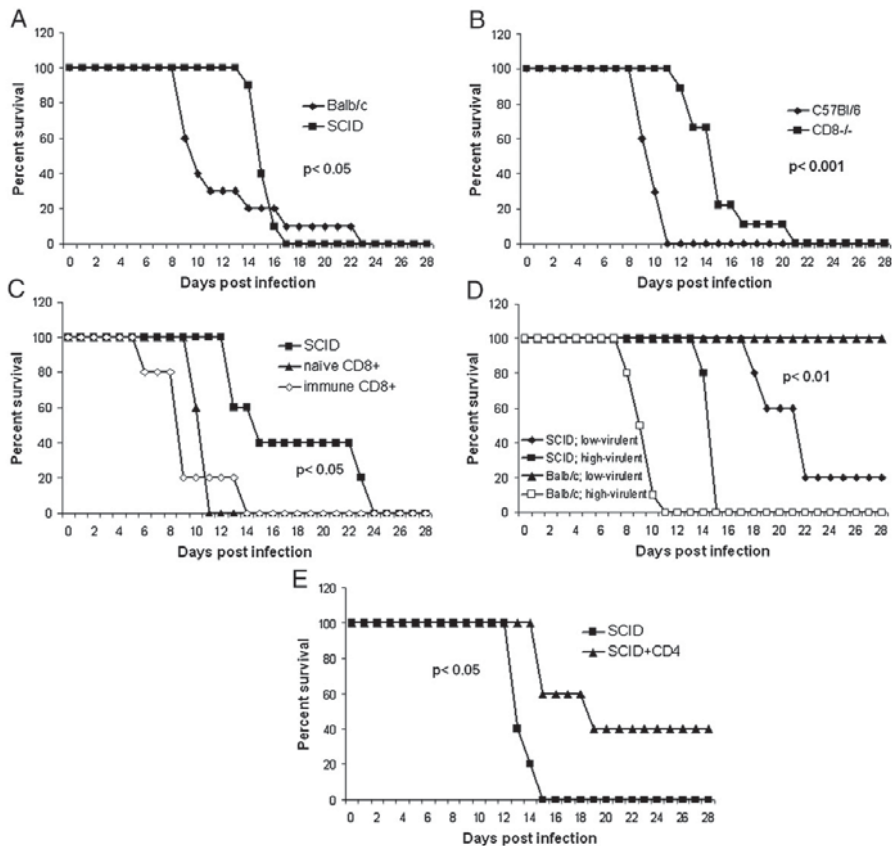


Fig. 1. Survival of mice infected with TBEV. Each animal was inoculated subcutaneously with a 100 pfu of strains Hypr (A–C and E), 263-TR (high-virulent) or 263 (low-virulent) (D). The mouse strains used were Balb/c, SCID, C57Bl/6 and C57Bl/6 $CD8^{-/-}$ as indicated.

To examine the precise role of $CD8^{+}$ T-cells in the pathogenesis of TBE, $CD8^{+}$ T-cells from control immunologically naïve as well as immune Balb/c mice, were isolated and adoptively transferred to SCID mice as described in **Materials and methods**. Adoptive transfer of immune as well as naïve $CD8^{+}$ T-cells led to significantly shorter MST following TBEV infection in comparison with SCID mice (MST of 15.0 ± 3.8 days). Mice that received $CD8^{+}$ T-cells from immunised mice survived slightly shorter (MST of 7.0 ± 2.4 days) than mice receiving $CD8^{+}$ T-cells from naïve mice (MST of 9.3 ± 0.5 days), but the difference was not statistically significant although reproducible.

We compared the infection of SCID and Balb/c mice caused by two TBEV strains (263 and 263-TR) differing in virulence (**Fig. 1D**). Following subcutaneous inoculation, strain 263 is completely non-neuroinvasive in Balb/c mice, whilst 263-TR is highly virulent. Although 263-TR virus causes 100% mortality in both strains of mice, the MST was notably longer in SCID mice. On the other hand, 80% of the SCID mice infected with strain 263 developed lethal encephalitis although their mean survival time was much longer (19.0 ± 2.9 days) compared with mice infected with the neuroinvasive strain (13.4 ± 0.5 days, $p < 0.01$; **Fig. 1D**).

Besides $CD8^{+}$ T-cells, we also evaluated the role of $CD4^{+}$ T-cells in TBEV infection, using the adoptive-transfer approach (**Fig. 1E**). $CD4^{+}$ T-cells negatively selected from spleens of naïve Balb/c mice were adoptively transferred intraperitoneally to SCID mice (2×10^6 cells/

mouse) and after one week, the mice were subcutaneously inoculated with strain Hypr. The adoptive transfer of $CD4^{+}$ T-cells to SCID mice led to a significantly prolonged MST (18.5 ± 4.9 days) and increased survival after infection in comparison with infected SCID mice (13.5 ± 0.7 days; **Fig. 1C**).

We then compared the growth of TBEV in the organs of, Balb/c, C57Bl/6, $CD8^{-/-}$, and SCID mice following subcutaneous inoculation of 100 pfu of the virus. Comparison of the viral load in the blood, spleen and brains of $CD8^{-/-}$, C57Bl/6 and Balb/c mice was not significantly different. However, although SCID mice exhibited prolonged survival following infection, the viral loads in the blood (days 3 and 8 p.i.) and spleen (days 6 and 8 p.i.) were much higher compared with the other strains of mice (**Figs. 2A, B**) and in brain compared to Balb/c mice (day 6 p.i.; **Fig. 2C**). Moreover, in SCID mice, the high viremia increased with time; in contrast, low viremia in all other mouse strains was detected on day 3 p.i. and low titers of virus were also detected in serum on day 8 p.i. in $CD8^{-/-}$ and C57Bl/6 mice (**Fig. 2A**). In brains, there were no statistically significant differences in the viral load in TBEV infected Balb/c, $CD8^{-/-}$ and C57Bl/6 mice (**Fig. 2C**).

To understand the cellular basis for the more rapid progress of the infection in immunocompetent mice in contrast with SCID or $CD8^{-/-}$ mice, we examined brain tissues for histopathological changes. Marked levels of infiltrates were observed in the vicinity of menin-

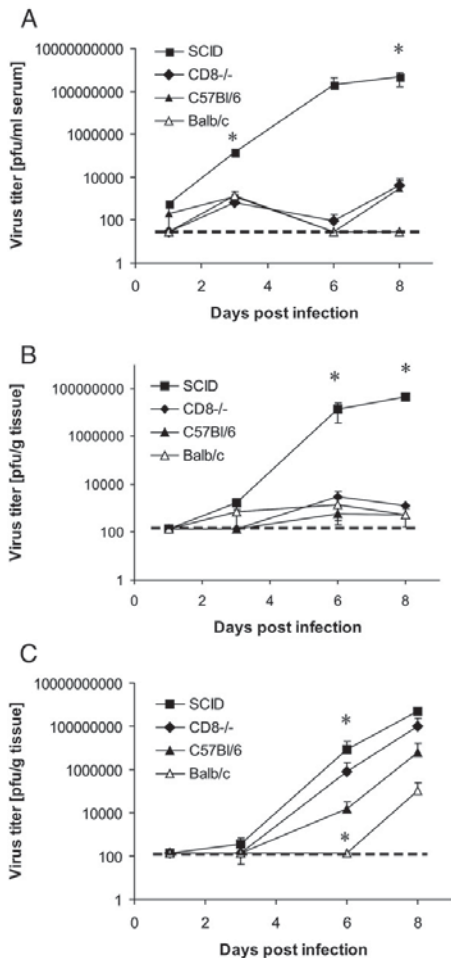


Fig. 2. TBEV burden in serum (A), spleen (B), and brains (C) of SCID, CD8^{-/-}, C57Bl/6, and Balb/c mice subcutaneously inoculated with 100 pfu of TBEV strain Hypr. Tissue and serum specimens were titrated individually by plaque assay on PS cells. For each time point the titers are the average of three mice. The dashed line indicates the limit of sensitivity of the assay. Asterisks indicate the differences that were statistically significant ($p < 0.05$); SCID versus all other mouse strains (A and B), or SCID versus Balb/c (C).

geal vessels in both immunocompetent strains of mice (Balb/c and C57Bl/6) and to a lesser extent also in CD8^{-/-} mice (Fig. 3). In infected Balb/c mice (Fig. 3E), the infiltrates were diffusely distributed and accompanied with signs of oedema. Diffuse/focal microgliosis and neuronal necroses were also seen. Predominantly necrotic lesions were found in the granular layer of the hippocampus (*stratum granulosum*); in this case, partial substitution of the granular layer with necrotic cells containing pyknotic nuclei was observed (Fig. 3K).

In infected C57Bl/6 mice, some of the perivascular infiltrates formed perivascular cuffs containing mononuclear infiltrating cells and histiocytes (Fig. 3F). Diffuse microgliosis, neuronal necrosis (Fig. 3H) and karyorrhexis of glial cells (Fig. 3I) were observed. The alterations observed in stratum granulosum of hippocampus (unicellular necroses) were similar to those observed in TBEV-infected

Balb/c mice. Cell infiltrates were also in the ventricular system (around the plexus chorioideus).

In the case of CD8^{-/-} mice infected with TBEV, histological investigation revealed moderate infiltrates of lymphocytes (Fig. 3G) and isolated hemorrhages (Fig. 3L).

The brain tissue of infected SCID mice was only slightly affected; only occasional isolated hemorrhages or proliferated microglial cells were seen.

There was no difference in the histology of brains of control uninfected Balb/c, C57Bl/6, CD8^{-/-} and SCID mice (Figs. 3A–D).

Immunofluorescence investigation of the brain sections revealed that most of the infiltrating cells were CD8⁺ T-cells (see [Supplementary data](#)). Very few infiltrating CD4⁺ T-cells were detected in the brain sections of infected Balb/c or C57Bl/6 mice and virtually no lymphocytes were detected in brains of uninfected mice. In TBEV infected CD8^{-/-} mice, lymphocytic infiltrates comprised CD4⁺ T-cells. No immunoreactivity was observed in infected and control SCID mice.

Discussion

In flavivirus encephalitis, three possible mechanisms of brain tissue destruction have been postulated. Firstly, the virus itself causes direct neuronal damage; secondly, the neuronal death is caused by virus-induced inflammatory response; and finally, a combination of both, i.e. neuronal damage and immunopathology is responsible (Chambers and Diamond, 2003; King et al., 2007).

Recent data on MBFV indicate that a major cause of encephalitis in mice following infection is the detrimental effect of the host immune response. Transgenic mice lacking functional CD8⁺ T-cells demonstrated extended survival and decreased mortality when infected with West Nile virus (WNV), in comparison with control wild-type mice (Wang et al., 2003). Similarly, for Murray Valley encephalitis virus (MVEV), the lack of perforin or Fas ligand molecules, that mediate effector activity of cytotoxic T-cells, protected mice against the development of encephalitis and fatal infection (Andrews et al., 1999). Generally, the immunopathology in flavivirus encephalitis seems to be mediated primarily by CD8⁺ T-cells. On the other hand, the role of virus specific CD4⁺ T-cells in flavivirus encephalitis is not well understood, although some experimental data indicate a requirement of such cells in protection against acute infection (Chambers and Diamond, 2003). An absence of CD4⁺ T-cells in mice with genetic or acquired deficiency resulted in persistent WNV infection in the CNS, ultimately leading to uniform mortality. Moreover, adoptive transfer of WNV-primed CD4⁺ T-cells significantly improved the survival of CD4^{-/-} mice after WNV infection (Sitati and Diamond, 2006).

No corresponding data in relation to apoptosis or immune-mediated pathology have been reported for TBEV. Therefore, the underlying basis of the development and progress of TBE is still largely undefined.

Here, we addressed the contribution of the host immune system to the development of TBE by a combination of experimental approaches. Prolonged survival of SCID or CD8^{-/-} mice in contrast with immunocompetent Balb/c and C57Bl/6 mice following infection with a neurovirulent TBEV strain indicated the detrimental effect of the host immune response in the development of the disease. Subsequently, we investigated the role of two subpopulations of T-cells, i.e. CD8⁺ and CD4⁺ T-cells, in the immunopathology of TBE using the adoptive transfer approach. The experiments demonstrated that the immunopathology is primarily mediated by CD8⁺ T-cells, whereas CD4⁺ T-cells confine the development of TBE. The helper CD4⁺ T-cells play a protective role although the mechanism for this is not yet clear; it is probably based on CD4⁺-mediated secretion of IFN- γ and other proinflammatory cytokines and/or stimulation of macrophage-like cells. CD4⁺ T-cells are believed to control viral infections through the activation of B- and CD8⁺ T-cell responses, production of inflammatory

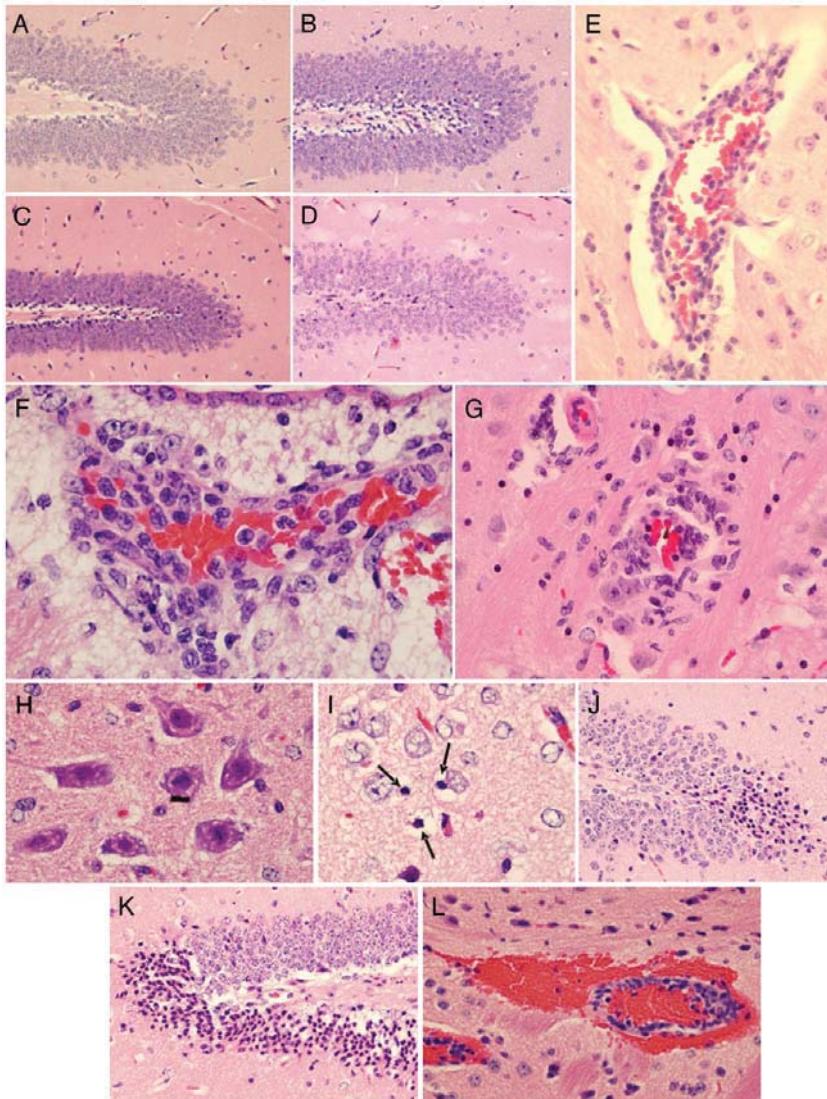


Fig. 3. Histology of TBEV-infected brains in parasagittal sections, hematoxylin-eosin staining. Brain sections of uninfected Balb/c (A), C57Bl/6 (B), CD8^{-/-} (C) and SCID (D) mice. Expanding leukocyte infiltrations in TBEV-infected Balb/c (E), C57Bl/6 (F) and CD8^{-/-} (G) mice. Neuronal necrosis (H) and karyorrhexis of glial cells (arrows) (I) observed in brains of C57Bl/6 mice. Partial substitution of granular layer with necrotic cells containing pyknotic nuclei in C57Bl/6 (J) and Balb/c (K) mice. Hemorrhagia and perivascular cuff in CD8^{-/-} mice (L).

and antiviral cytokines, direct cytotoxic effects on infected cells and promoting memory response (Sitati and Diamond, 2006).

Our results showing an immunopathological effect of CD8⁺ T-cells and the role of CD4⁺ T-cells in confining the infection, correlate with some of the observations on WNV (Wang et al., 2003; Sitati and Diamond, 2006) and confirm the previous suggestions by Gelpi et al. (2006b). These suggestions were based on the observation that prominent inflammatory infiltrates and cytotoxic T-cells were present in close contact with morphologically intact neurons in human post-mortem brain tissues, thus indicating a key role for cytotoxic T-cells in the development of TBE. Similarly, in another study, transferred

splenocytes shortened the incubation period of the disease implying a pathogenic role for the immune system in TBE (Semenov et al., 1975).

We also performed a histopathological investigation of the brains of all mouse strains used in this study. Investigation of moribund Balb/c and C57Bl/6 mouse brains revealed encephalitis associated with inflammatory cell infiltration, in accordance with previously published observations in mice (Osetowska and Wróblewska-Mularczyk, 1966), hamsters (Simon et al., 1966), monkeys (Simon et al., 1967), and humans (Gelpi et al., 2006a,b). Necrotic neurons were also observed. Immunofluorescence staining of CD4⁺ and CD8⁺ T-cells in the brain sections revealed lower levels of CD4⁺ and predominance of

CD8⁺ T-cells in the infected immunocompetent mice. The same result has been reported previously in WNV infections (Liu et al., 1989; Wang et al., 2003), but in brains of TBE infected patients, both CD4⁺ and CD8⁺ T-cells were present (Gelpi et al., 2006b).

Moreover, the comparative data of viral growth in the strains of mice used here, support the concept of a role for immunopathology in the development of TBE. Following infection of mice with 100 pfu of TBEV, viral loads in the blood and spleens were significantly higher in SCID mice compared with the other mice. Although SCID mice exhibited prolonged survival after TBEV infection and only minor histopathological changes in the brains were observed, high viral brain loads were detected in these mice, and they were significantly higher compared with Balb/c mice (day 6 p.i.; Fig. 2C). Therefore, it seems that the viral load did not determine the survival time or the pathology. Interestingly, no substantial differences were seen in the viral load in the blood, spleen and brains of CD8^{-/-} and C57Bl/6 mice, suggesting that the CD8⁺ T-cells have only a little role in TBEV clearance. This contrasts with the data on WNV (Shrestha and Diamond, 2004), where the absence of CD8⁺ T-cells led to higher virus load in the CNS, and increased mortality.

Although we have demonstrated an immunopathological basis for encephalitis caused by TBEV infection, the role of direct damage of neurons or apoptosis remains unknown and these factors also need to be investigated. Apoptosis, as a damaging mechanism of virus-induced neuronal death in experimental mice has been demonstrated for other flaviviruses, e.g. mosquito-borne Yellow fever virus (YFV), Japanese encephalitis virus (JEV) and WNV (Yasui, 2002; Shrestha et al., 2003). However some exceptions have also been reported, for example in the case of MVEV, it was shown that less than 0.1% of mouse neurons develop apoptosis (Andrews et al., 1999). Moreover, ultrastructural investigation of mouse brain neurons indicated that neuronal dysfunction rather than morphological destruction occurs during JEV infection (Hase et al., 1990).

TBEV induces both apoptosis and necrosis in human neuroblastoma and glioblastoma cell lines (Růžek et al., manuscript in preparation) and also in mouse and monkey brain neurons (Isaeva et al., 1998; Kamalov et al., 1998), but prominent signs of neuronal apoptosis were not seen in postmortem brain tissues from human TBE patients, as demonstrated by anti-caspase 3 immunohistochemistry and TUNEL assay (Gelpi et al., 2006b). In addition, TBEV was also isolated from the brains of healthy animals in wild and Syrian hamsters in the laboratory indicating that propagation of TBEV in brain tissue is not necessarily accompanied by apoptosis (reviewed in Gritsun et al., 2003b).

Evidence that direct damage of CNS also occurs in TBEV infected mice was supported by our experiments in which two different TBEV strains differing in neuroinvasiveness were studied. A strain 263 is completely non-neuroinvasive for mice, whereas strain 263-TR is highly neuroinvasive. However, both of these viruses are equally neurovirulent following intracranial inoculation. These differences were attributed to a point mutation in an active centre of the virus serine protease. This mutation delays virus propagation at the site of inoculation, thereby gaining time for adaptive immune responses to develop and limit virus spread into the CNS (Růžek et al., 2008). We compared 263 and 263-TR in SCID and Balb/c mice (Fig. 1D). Although the 263-TR virus causes 100% mortality in both strains of mice, the MST was notably higher in SCID mice supporting the hypothesis of a pathogenic effect due to an immune response (Fig. 1D). However, comparison of 263-mediated infection in Balb/c and SCID mice supports the other hypothesis implying direct damage of the CNS due to virus replication. These observations imply that in the absence of an immune response even the attenuated, less invasive virus, 263 eventually reaches and damages the CNS; this corresponds to the neurovirulent properties of the 263 strain observed following intracranial virus inoculation. Together, these two comparisons indicate that in normal mice, with fully developed immune systems,

both factors, i.e. direct virus damage to the CNS and an immune response contribute to the clinical outcome.

Currently, there is no specific therapy for TBE other than supportive measures. However, the administration of tetracycline hydrochloride, a compound with an anti-inflammatory effect, during experimental TBEV infection in mice led to significantly decreased mortality rates (Atrasheuskaya et al., 2003). Moreover, tetracycline hydrochloride acted as an immunomodulator, which was able to reduce manifestations of inflammation response during TBE infection in humans; this action led to quicker recovery from clinical symptoms and, consequently, to a faster recovery (Atrasheuskaya et al., 2003). Our data, showing the immunopathological features of TBE, provide additional support for immunomodulatory therapy in this disease.

In conclusion, our experiments demonstrate that CD4⁺ T-cells may have some function in the limiting of TBE, whereas CD8⁺ T-cells play a role in the immunopathology of TBE caused by neurovirulent strains. However, in the absence of an immune response the virus on its own is also capable of causing encephalitis. Our study expands the current knowledge of the antiviral immune response during TBEV infection and the understanding of the pathogenesis of TBE and could provide the basis for a rational therapeutic strategy against this dangerous human pathogen.

Materials and methods

Mice

Balb/c and C57Bl/6 mice were originally obtained from Charles River Laboratoires (Sulzfeld, Germany). CD8 α -knockout mice of the C57Bl/6 background (CD8^{-/-}; strain B6.129S2-Cd8a^{tm1Mac}) were obtained from The Jackson Laboratory (Bar Harbor, ME, USA). SCID mice (C.B17/Jcr-scid) of the Balb/c background, originally obtained from Charles River Laboratoires (Sulzfeld, Germany), were housed in plastic cages with sterilized wood-chip bedding situated in flexible film isolators (BEM Znojmo, Czech Republic) with high-efficiency particulate air filters. Sterilized pellet diet and water were supplied *ad libitum*. Balb/c, C57Bl/6 and CD8^{-/-} mice were housed in plastic cages with wood-chip bedding situated in a specific-pathogen free room with a constant temperature of 22 °C and a relative humidity of 65%. Groups of 10 adult mice (6–8-week-old) were used in each experiment.

Viruses

All experiments were performed with representatives of the West-European TBEV subtype. The strain Hypr, a prototype Czech TBEV strain, was originally isolated from the blood of a 10-year-old child diagnosed with tick-borne encephalitis in 1953 in the Czech Republic. A non-neuroinvasive strain 263 was isolated from *Ixodes ricinus* collected by flagging in the Czech Republic in 1987 (Růžek et al., 2008). A highly virulent derivative of the strain 263, designated 263-TR, was obtained after the passage of the original strain in PS cells at 40 °C (Růžek et al., 2008). Low-passage virus strains were used in this study.

Adoptive transfer of CD4⁺ or CD8⁺ T-cells

To produce immune CD8⁺ T-cells, the Balb/c mice, were inoculated intraperitoneally with two doses of 10³ pfu of the non-neuroinvasive strain 263 (Růžek et al., 2008) at two-week intervals. One week after the second dose, spleens from either immune or immunologically naïve Balb/c mice were removed and single-cell suspensions were derived after mechanical disruption of the spleen tissue through a 40- μ m-pore-size filter. Splenocytes were washed three times in RPMI-1640 medium and pure and well-defined populations of CD4⁺ or CD8⁺ T-cells were isolated from whole splenocytes by immunomagnetic separation. For isolation of CD4⁺ T-cells, the Dynal Mouse CD4 Negative Isolation Kit (Invitrogen Dynal AS, Oslo, Norway) was used. CD8⁺ T-cells were isolated from the suspension using the Dynal Mouse CD8 Negative

Isolation Kit (Invitrogen Dynal AS, Oslo, Norway). The purity of lymphocytes was analyzed by flow cytometry. Samples (0.5×10^6 cells) were incubated with specific monoclonal antibodies against surface antigens CD4 (FITC anti-mouse CD4, clone H 129.19, PharMingen, San Diego, CA, USA) and CD8 (PE anti-mouse CD8 α , clone 53-6.7, PharMingen, San Diego, CA, USA). Labeled cell samples were analyzed on an Epics XL Flow Cytometer (Coulter) equipped with a 15-mW argon-ion laser with excitation capabilities at 488 nm. Ten thousand events were measured. The labeled cell population was analyzed using System II software (Coulter). Cell populations with purity >90% were adoptively transferred to SCID mice via intraperitoneal route (2×10^6 cells/mouse). Seven days after the adoptive transfer, mice were infected with 100 pfu of TBEV subcutaneously.

Virus growth in mouse tissues

Groups of adult SCID, CD8 $^{-/-}$, C57Bl/6, and Balb/c mice (females, 6–8-week old) were inoculated subcutaneously with 100 pfu of Hypr strain. At the given time point post-inoculations, 3 mice of each group were anesthetized and humanely killed. Specimens of the blood, spleen, and brain were collected. Organs were individually weighed and homogenized, and prepared as 20% suspensions (w.v $^{-1}$) in L-15 medium containing 3% newborn calf serum. The suspensions were clarified by centrifugation at 10,000 g and the supernatant media were titrated by plaque assay on PS cells.

Histopathological investigation

Brains from control and TBEV-infected Balb/c, C57Bl/6, CD8 $^{-/-}$ and SCID mice were examined for pathological changes. The mice were infected with 100 pfu of the strain Hypr in 200 μ l of L15 medium and control mice were subcutaneously injected with 200 μ l of L15 medium. Brains were collected at the 8th day p.i. (Balb/c, C57Bl/6) or the 11th day p.i. (CD8 $^{-/-}$, SCID), respectively, and were fixed in 10% neutral buffered formalin and embedded in paraffin. 5- μ m parasagittal sections were stained with hematoxylin-eosin.

Immunofluorescence staining

Brain tissues were routinely formalin fixed and paraffin embedded. 5- μ m parasagittal sections were then treated to remove paraffin and antigen retrieval was performed by boiling sections in 10 mM citrate buffer (pH 6.0) for 20 min. After blocking, the sections were incubated with either CD4-specific or CD8-specific monoclonal antibodies (kindly provided by Dr. Imtiaz Khan, Dartmouth Medical School, Hanover, NH) for 1 h at room temperature and then with F(ab) $_2$ goat anti-rat FITC-labeled IgG antibody (Serotec; diluted 1:100) for 1 h at room temperature. The sections were visualized using an Olympus BX60 microscope and photographed using an Olympus DP71 digital camera. Examples of typical infiltrates are submitted as Supplementary data.

Statistical analysis

The significant differences in survival time between groups of infected mice were analyzed by 'Survival Analysis' and the statistical difference in virus burden in mouse organs was determined by ANOVA followed by Fischer LSD Post Hoc test. Data without normal distribution were transformed by use of the $X' = \log(X)$ formula. All analyses were performed using Statistica® 7.1 software (StatSoft CR, Praha, Czech Republic). *p*-values < 0.05 were considered significant.

Acknowledgments

The project was supported by the grants Z60220518, MSM 6007665801 of the Ministry of Education, Youth and Sports of the

Czech Republic, the grant 524/08/1509 from the Grant Agency of the Czech Republic, Research Centre of the Ministry of Education, Youth and Sports of the Czech Republic No. LC 06009 and grant 44/2006/P-BF of the Grant Agency of the University of South Bohemia. Professor Gould and Dr Gritsun are supported by the Sixth Framework grant (VIZIER EU Contract LSHG-CT-2004-511960).

All of the experimental procedures were done in accordance with the national law on the use of experimental animals, safety and use of pathogenic agents.

Appendix A. Supplementary data

Supplementary data associated with this article can be found, in the online version, at [doi:10.1016/j.jvirol.2008.11.023](https://doi.org/10.1016/j.jvirol.2008.11.023).

References

- Andrews, D.M., Matthews, V.B., Samuels, L.M., Carrello, A.C., McMinn, P.C., 1999. The severity of Murray Valley encephalitis in mice is linked to neutrophil infiltration and inducible nitric oxide synthase activity in the central nervous system. *J. Virol.* 73, 8781–8790.
- Atrasheskaya, A.V., Fredeking, T.M., Ignatyev, G.M., 2003. Changes in immune parameters and their correction in human cases of tick-borne encephalitis. *Clin. Exp. Immunol.* 131, 148–154.
- Chambers, T.J., Diamond, M.S., 2003. Pathogenesis of flavivirus encephalitis. *Adv. Virus Res.* 60, 278–342.
- Gelpi, E., Preusser, M., Garzuly, F., Holzmann, H., Heinz, F.X., Budka, H., 2006a. Visualization of Central European tick-borne encephalitis infection in fatal human cases. *J. Neuropathol. Exp. Neurol.* 64, 506–515.
- Gelpi, E., Preusser, M., Lagner, U., Garzuly, F., Holzmann, H., Heinz, F.X., Budka, H., 2006b. Inflammatory response in human tick-borne encephalitis: analysis of postmortem brain tissue. *J. NeuroVirol.* 12, 322–327.
- Gritsun, T.S., Lashkevich, V.A., Gould, E.A., 2003a. Tick-borne encephalitis. *Antivir. Res.* 57, 129–146.
- Gritsun, T.S., Frolova, T.V., Zhankov, A.I., Armesto, M., Turner, S.L., Frolova, M.P., Pogodina, V.V., Lashkevich, V.A., Gould, E.A., 2003b. Characterization of Siberian virus isolated from a patient with progressive chronic tick-borne encephalitis. *J. Virol.* 77, 25–36.
- Hase, T., Summers, P.L., Dubois, D.R., 1990. Ultrastructural changes of mouse brain neurons infected with Japanese encephalitis virus. *Int. J. Exp. Pathol.* 71, 493–505.
- Isaeva, M.P., Leonova, G.N., Kozhemiako, V.B., Borisevich, V.G., Maistrovskaia, O.S., Rasskazov, V.A., 1998. Apoptosis as a mechanism for the cytopathic action of tick-borne encephalitis virus. *Vopr. Virusol.* 43, 182–186.
- Kamalov, N.I., Novozhilova, A.P., Kreichman, G.S., Sokolova, E.D., 1998. The morphological characteristics of cell death in different forms of acute tick-borne encephalitis. *Morfologiya* 114, 54–58.
- King, N.J.C., Getts, D.R., Getts, M.T., Rana, S., Shrestha, B., Kesson, A.M., 2007. Immunopathology in flavivirus infections. *Immunol. Cell. Biol.* 85, 33–42.
- Liu, Y., Blanden, R.V., Müllbacher, A., 1989. Identification of cytolytic lymphocytes in West Nile virus-infected murine central nervous system. *J. Gen. Virol.* 70, 565–573.
- Osetowska, E., Wróblewska-Mularczyk, Z., 1966. Neuropathology of the experimental tick-borne encephalitis. *Polish Med. J.* 5, 1418–1435.
- Růžek, D., Gritsun, T.S., Forrester, N.L., Gould, E.A., Kopecký, J., Golovchenko, M., Rudenko, N., Grubhoffer, L., 2008. Mutations in the NS2B and NS3 genes affect mouse neuroinvasiveness of a Western European field-strain of tick-borne encephalitis virus. *Virology* 374, 249–255.
- Semenov, B.F., Khozinsky, V.V., Vargin, V.V., 1975. The damaging action of cellular immunity in flavivirus infections of mice. *Med. Biol.* 53, 331–336.
- Shrestha, B., Diamond, M.S., 2004. Role of CD8 $^{+}$ T cells in control of West Nile virus infection. *J. Virol.* 78, 8312–8321.
- Shrestha, B., Gottlieb, D., Diamond, D.S., 2003. Infection and injury of neurons by West Nile encephalitis virus. *J. Virol.* 77, 13203–13213.
- Simon, J., Slonim, D., Zavadova, H., 1966. Experimentelle Untersuchungen von klinischen und subklinischen Formen der Zeckencephalitis an unterschiedlich empfänglichen Wirten: Mäusen, Hamstern und Affen. II. Hamster. *Acta Neuropathol.* 7, 89–100.
- Simon, J., Slonim, D., Zavadova, H., 1967. Experimentelle Untersuchungen von klinischen und subklinischen Formen der Zeckencephalitis an unterschiedlich empfänglichen Wirten: Mäusen, Hamstern und Affen. III. Das histologische Bild der Zeckencephalitis bei Affen. *Acta Neuropathol.* 8, 24–34.
- Sitati, E.M., Diamond, M.S., 2006. CD4 $^{+}$ T-cell responses are required for clearance of West Nile virus from the central nervous system. *J. Virol.* 80, 12060–12069.
- Thiel, H.-J., Collett, M.S., Gould, E.A., Heinz, F.X., Houghton, M., Meyers, G., Purcell, R.H., Rice, C., 2005. Family *Flaviviridae*. In: Fauquet, C.M., Mayo, M.A., Maniloff, J., Desselberger, U., Ball, L.A. (Eds.), *Virus Taxonomy: Classification and Nomenclature*, Eighth Report of the International Committee on the Taxonomy of Viruses. Elsevier Academic Press, Amsterdam, Boston, Heidelberg, London, New York, Oxford, pp. 981–998.
- Wang, Y., Lobigs, M., Lee, E., Müllbacher, A., 2003. CD8 $^{+}$ T cells mediate recovery and immunopathology in West Nile virus encephalitis. *J. Virol.* 77, 13323–13334.
- Yasui, K., 2002. Neuropathogenesis of Japanese encephalitis virus. *J. NeuroVirol.* 8 (suppl. 2), 112–114.

CHAPTER II

Mice with different susceptibility to tick-borne encephalitis virus infection show selective neutralizing antibody response and inflammatory reaction in the central nervous system

Martin Palus, Jarmila Vojtíšková, Jiří Salát, Jan Kopecký, Libor Grubhoffer, Marie Lipoldová, Peter Demant and Daniel Růžek

Journal of Neuroinflammation 2013, 10:77

DOI: 10.1186/1742-2094-10-77

<http://jneuroinflammation.biomedcentral.com/articles/10.1186/1742-2094-10-77>

Mice with different susceptibility to tick-borne encephalitis virus infection show selective neutralizing antibody response and inflammatory reaction in the central nervous system

(summary)

The clinical course of TBE ranges from asymptomatic or mild influenza-like infection to severe debilitating encephalitis or encephalomyelitis. Despite the medical importance of this disease, some crucial steps in the development of encephalitis remain poorly understood. In particular, the basis of the disease severity is unknown.

To address this issue we have developed a mouse model for TBEV infection based on BALB/c-c-STS/A (CcS/Dem) recombinant congenic strains showing different levels of TBE severity in relation to the host genetic background. We measured TBEV growth, neutralizing antibody response, key cytokine and chemokine mRNA production and changes in mRNA levels of cell surface markers of immunocompetent cells in brains of mice with different susceptibilities to TBEV infection.

After subcutaneous inoculation of TBEV, BALB/c mice showed medium susceptibility to the infection, STS mice were resistant, and CcS-11 mice were highly susceptible. Our experimental model showed that earlier and greater amounts of neutralizing antibodies could limit neuroinvasion of TBEV and disease progression in less susceptible mice, STS. These resistant mice showed lower and delayed viremia, lower virus production in the brain and low cytokine/chemokine mRNA production, but had a strong neutralizing antibody response. Moreover, we described that resistant STS mice exhibit stronger B-cell infiltration (measured by quantification of changes in mRNA levels of cell surface markers) but lower cytokine/chemokine production in the CNS when compared to the more susceptible mouse strains. The most sensitive strain (CcS-11) failed in production of neutralizing antibodies, but exhibited a strong cytokine/chemokine mRNA response in the brain tissue. After intracerebral inoculation, all mouse strains were sensitive to the infection and had similar virus production in the brain, but STS mice survived significantly longer than

CcS-11 mice. These two strains also differed in the level of expression of key cytokines/chemokines, particularly interferon gamma-induced protein 10 (IP-10/CXCL10) and monocyte chemotactic protein-1 (MCP-1/CCL2) in the brain.

The most susceptible mice had the highest overall cytokine/chemokine production in the CNS, particularly of CCL2/MCP-1 and IP-10, which can elevate the primarily proinflammatory environment in the brain, which could result in brain tissue damage and death of the host through immunopathology.

Taken together, high neutralizing antibody response might be crucial for preventing host fatality, but high expression of various cytokines/chemokines during TBE can mediate immunopathology and be associated with more severe course of the infection and increased fatality. The host immune response based on the genetic background may therefore play a central role in determining the outcome of TBEV infection.

RESEARCH

Open Access

Mice with different susceptibility to tick-borne encephalitis virus infection show selective neutralizing antibody response and inflammatory reaction in the central nervous system

Martin Palus^{1,2}, Jarmila Vojtíšková³, Jiří Salát^{1,4}, Jan Kopecký^{1,2}, Libor Grubhoffer^{1,2}, Marie Lipoldová³, Peter Demant⁵ and Daniel Růžek^{1,4*}

Abstract

Background: The clinical course of tick-borne encephalitis (TBE), a disease caused by TBE virus, ranges from asymptomatic or mild influenza-like infection to severe debilitating encephalitis or encephalomyelitis. Despite the medical importance of this disease, some crucial steps in the development of encephalitis remain poorly understood. In particular, the basis of the disease severity is largely unknown.

Methods: TBE virus growth, neutralizing antibody response, key cytokine and chemokine mRNA production and changes in mRNA levels of cell surface markers of immunocompetent cells in brain were measured in mice with different susceptibilities to TBE virus infection.

Results: An animal model of TBE based on BALB/c-c-STS/A (CcS/Dem) recombinant congenic mouse strains showing different severities of the infection in relation to the host genetic background was developed. After subcutaneous inoculation of TBE virus, BALB/c mice showed medium susceptibility to the infection, STS mice were resistant, and CcS-11 mice were highly susceptible. The resistant STS mice showed lower and delayed viremia, lower virus production in the brain and low cytokine/chemokine mRNA production, but had a strong neutralizing antibody response. The most sensitive strain (CcS-11) failed in production of neutralizing antibodies, but exhibited strong cytokine/chemokine mRNA production in the brain. After intracerebral inoculation, all mouse strains were sensitive to the infection and had similar virus production in the brain, but STS mice survived significantly longer than CcS-11 mice. These two strains also differed in the expression of key cytokines/chemokines, particularly interferon gamma-induced protein 10 (IP-10/CXCL10) and monocyte chemoattractant protein-1 (MCP-1/CCL2) in the brain.

Conclusions: Our data indicate that the genetic control is an important factor influencing the clinical course of TBE. High neutralizing antibody response might be crucial for preventing host fatality, but high expression of various cytokines/chemokines during TBE can mediate immunopathology and be associated with more severe course of the infection and increased fatality.

Keywords: Tick-borne encephalitis, Flavivirus encephalitis, Neuroinflammation, Antibody production

* Correspondence: ruzekd@paru.cas.cz

¹Institute of Parasitology, Biology Centre of the Czech Academy of Sciences, Branišovská 31, České Budějovice CZ-37005, Czech Republic

⁴Department of Virology, Veterinary Research Institute, Hudcova 70, Brno CZ-62100, Czech Republic

Full list of author information is available at the end of the article

Background

Flaviviruses, a group of small, enveloped, positive-sense, single-stranded RNA viruses, include several medically very important pathogens. Especially Japanese encephalitis virus, yellow fever virus, West Nile virus, dengue virus, Murray Valley encephalitis virus and tick-borne encephalitis virus (TBEV) are responsible for large outbreaks of fatal encephalitis or hemorrhagic fevers at diverse geographical regions around the world. Tick-borne encephalitis (TBE), a disease caused by TBEV, represents one of the most important and serious neuroinfections in Europe and northeastern Asia. More than 13,000 clinical cases of TBE, including numerous deaths, are reported annually. Despite the medical importance of this disease, some crucial steps in the development of encephalitis remain poorly understood. In humans, TBEV may produce a variety of clinical symptoms, from an asymptomatic disease (70-90% of cases) to a fever and acute or chronic progressive encephalitis. This is influenced by a variety of factors, e.g., the inoculation dose and virulence of the virus [1], the age, sex and immune status of the host [2], and also susceptibility based on the host's genetic background. Studies of animal models and epidemiological studies in humans have shown that many apparently non-hereditary diseases, including infectious diseases, develop predominantly in genetically predisposed individuals and that this predisposition is caused by multiple genes [3]. In humans, a functional Toll-like receptor 3 gene may be a risk factor for TBEV infection [4]. A deletion within the chemokine receptor CCR5 (CCR5 Δ 32), which plays an important role in leukocyte transmigration across the blood-brain barrier, is significantly more frequent in patients with TBE than in TBE-naïve patients with aseptic meningitis [5]. Moreover, the severity and outcome of TBE is associated with variability in the 2'-5'-oligoadenylate synthetase gene cluster (family members are interferon-induced antiviral proteins that play an important role in the endogenous antiviral pathway) [6] and with the rs2287886 single nucleotide polymorphism located in the promoter region of the human *CD209* gene [7]. This gene encodes dendritic cell-specific ICAM3-grabbing nonintegrin (DC-SIGN), a C-type lectin pathogen-recognition receptor expressed on the surface of dendritic cells and some types of macrophages [7]. Taken together, polymorphism in various genes may largely influence the sensitivity of the host to the infection and determine the severity of this disease.

While in humans involvement of genetic factors in the control of the susceptibility to TBEV infection is quite difficult to investigate, mice provide a useful small animal model for such a kind of study [8]. Mice are suitable animal models of infection with TBEV because they can reproduce symptoms and physiopathological markers as

observed in severe cases in humans. A high susceptibility of most laboratory mouse strains to flavivirus infection has been genetically mapped to a stop codon mutation in the coding region of the 2'-5'-oligoadenylate synthetase gene *Oas 1b* [9].

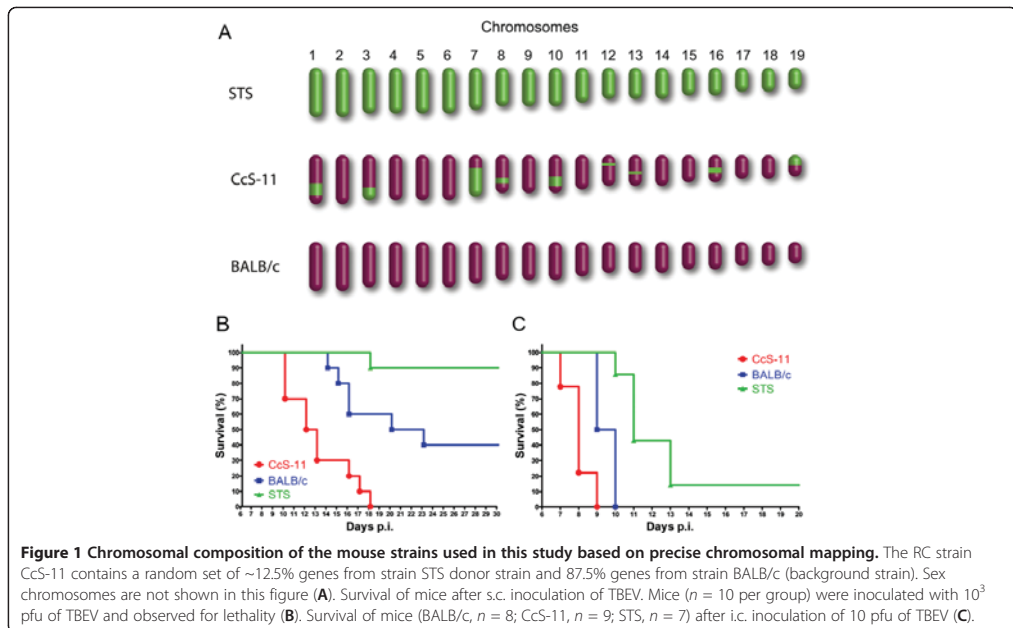
In our study, we developed an animal model of TBE showing several manifestations of the disease in relation to the genetic background, which is not based on the previously published mutation in the *Oas 1b* gene. We analyzed the sensitivity to TBEV in CcS/Dem (CcS) recombinant congenic (RC) strains of mice [10] derived from the background strain BALB/cHeA (BALB/c) and the donor strain STS. Each CcS strain contains a unique random set of about 12.5% genes from the donor strain STS and 87.5% genes from the background strain BALB/c [10]. This system has been very useful in research of bacterial [11] and parasitic [12-18] diseases, as well as in cancer [19-23].

In this study, we identified mouse strains that exhibit high, intermediate and low sensitivity to TBEV infection. Virus growth, key cytokine and chemokine mRNA production in the brain and neutralizing antibody response were measured. Our data suggest that the genetic control represents one of the important factors that influence the clinical course of TBE and that also other genes than the previously described *Oas 1b* are involved in the determination of host susceptibility to the infection. While high neutralizing antibody response might be crucial for preventing host fatality, high local expression of various proinflammatory cytokines/chemokines in the brain during TBE can be associated with a more severe course of the infection and higher fatality. Our data may be instrumental in the development of future therapeutic strategies aimed at treating or preventing TBE neuropathogenesis.

Material and methods

Mice

Specific pathogen-free mice of parental strains BALB/c, STS and ten randomly selected RC strains (see below) were used in the experiments. RC strains were in more than 90 generation of inbreeding and therefore highly homozygous. Genetic composition of the strain CcS-11 is schematically shown in Figure 1A. Sterilized pellet diet and water were supplied ad libitum. In all experiments, female mice aged 12-15 weeks at the time of infection were used. The mice were housed in plastic cages with wood-chip bedding, situated in a specific pathogen-free room with a constant temperature of 22°C and a relative humidity of 65%. The research complied with all relevant European Union guidelines for work with animals and was in accordance with the Czech national law and guidelines on the use of experimental animals and protection of animals against cruelty (Animal Welfare Act no. 246/1992 Coll.). The protocol was approved by the



Committee on the Ethics of Animal Experiments of the Institute of Parasitology and of the Departmental Expert Committee for the Approval of Projects of Experiments on Animals of the Academy of Sciences of the Czech Republic (permit no. 165/2010).

Virus infection

All experiments were performed with European prototypic TBEV strain Neudoerfl (a generous gift from Prof. F.X. Heinz, Medical University of Vienna). The virus was originally isolated from the tick *Ixodes ricinus* in Austria in 1971 and has been extensively characterized including its complete genome sequence and the determination of the three-dimensional structure of its envelope protein [24]. This strain was passaged four times in brains of suckling mice.

Mice were infected either subcutaneously (s.c.) into the scruff of the neck with 10^3 pfu or intracerebrally (i.c.) with 10 pfu of the virus. Mice were scored for mortality for a period of 28 days post-infection (p.i.), and survival curves were established.

Plaque assay

The virus titers were determined by plaque assay on porcine kidney stable cell (PS) monolayers under a carboxymethyl-cellulose overlay, as described previously [25]. Infectivity was expressed as plaque-forming units (pfu) per ml (or g of brain tissue).

Virus growth in mice

At the given time point p.i., three mice of each group were anesthetized and killed by cervical dislocation. Specimens of blood serum and brains were collected. Brains were individually weighed and prepared as 20% suspensions in phosphate-buffered saline (PBS) using TissueLyser II (Qiagen). The homogenate was clarified by centrifugation at $14,000\times g$ for 10 min at $4^{\circ}C$, and supernatant fluids were titrated by plaque assay on PS cells. The detection thresholds were $1.4 \log_{10}$ pfu/ml for serum and $2.1 \log_{10}$ pfu/g for brain suspensions.

Real-time quantitative RT-PCR

Real-time quantitative PCR was performed by the TaqMan Gene Expression Assays (Applied Biosystems) as previously described [26]. RNA was isolated from the brain tissue pellets using RNeasy Mini Kit (Qiagen), according to the recommendations of the manufacturer. cDNA was synthesized using a High Capacity RNA-to-cDNA Kit (Applied Biosystems), according to the manufacturer's protocol. The synthesized cDNAs were used as templates for real-time PCR. In quantitative RT-PCR the following primer probe sets from Applied Biosystems were used: TNF α (Mm00443258_m1), IFN γ (Mm 01168134_m1), CCL2/MCP1 (Mm 00441242_m1), CCL3/MIP1 α (Mm00441258_m1), CCL4/MIP1 β (Mm00-443111_m1), CCL5/RANTES (Mm01302428_m1), CD4 (Mm00442754_m1), CD8b1 (Mm00438116_m1), CD11 β

(Mm00434455_m1), CD19 (Mm00515420_m1), IL1a (Mm00439620_m1), IL1 β (Mm01336189_m1), IL6 (Mm00446190_m1), IL2 (Mm00434256_m1), IL4 (Mm00445259_m1), IL5 (Mm00439646_m1), IL10 (Mm00439614_m1) and IP10/CXCL10 (Mm00445235_m1). Mouse beta actin was used as a housekeeping gene. Amplification conditions were: 2 min at 50°C; 10 min at 95°C; 40 cycles of denaturation at 95°C for 15 s and annealing/extension at 60°C for 1 min.

Quantification of gene expression was performed using the comparative CT method and reported as the fold difference relative to the housekeeping gene. To calculate the fold change, the CT of the housekeeping gene was subtracted from the CT of the target gene to yield the Δ CT. Change in expression of the normalized target gene was expressed as $2^{-\Delta\Delta CT}$ where $\Delta\Delta CT = \Delta CT$ samples - ΔCT controls as previously described [27].

Plaque reduction neutralization test

The titers of neutralizing antibodies against TBEV in mouse sera were determined by the plaque reduction neutralization test (PRNT) as described by Bárdoš [28] with slight modifications. Sera (including positive and negative controls) were diluted 1:4 in L-15 medium (Leibowitz; Sigma) supplemented with 1% antibiotics (penicillin, streptomycin, amphotericin B; Sigma) and 3% inactivated newborn calf serum. After inactivation of the virus and complement in the sera by heating at 56°C for 30 min, two-fold serial dilutions of the samples in L-15 medium were incubated with 10^3 pfu of TBEV (the virus test dose was adjusted so that it caused almost confluent plaques, 90-95% cytolysis) for 90 min at 37°C; 5×10^4 PS cells were added to each well. After 6 days of incubation, the cell supernatant was removed and cells were fixed and stained as described previously [25]. The last dilution of serum that caused an 80-100% reduction in cytolysis of the virus test dose was regarded as the serum titer.

Statistical analysis

The differences in survival time of infected mice were analyzed by survival analysis (log-rank Mantel-Cox test). All other data were analyzed by one-way ANOVA (Newman-Keuls multiple comparison test). Data without normal distribution were transformed by use of the $X' = \ln(X)$ formula. All analyses were performed using GraphPad Prism 5.00 (GraphPad Software, Inc., USA); p -values < 0.05 were considered significant.

Results

CcS/Dem RC mouse strains show diverse susceptibilities to infection with TBEV

To study the susceptibility of mice to TBEV, we infected females of the strains BALB/c, STS and RC strains CcS-3, CcS-7, CcS-9, CcS-11, CcS-15 and CcS-16 s.c. with

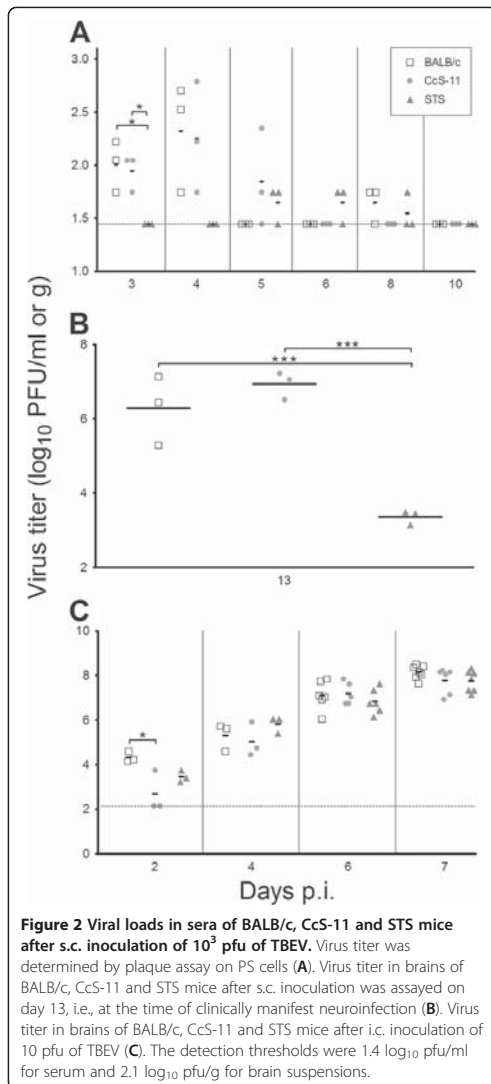
10^4 pfu of TBEV, and survival was recorded. Mice with different genotypes exhibited different susceptibilities to TBEV (Additional file 1: Figure S1). The most striking differences in survival rates and mean survival times were seen in parental strains BALB/c and STS, and RC strain CcS-11 (Figure 1B). CcS-11 mice were shown to be most susceptible, while STS mice are the least susceptible. BALB/c mice exhibited intermediate susceptibility. Mean survival time (MST) of the CcS-11 mice was 13.1 ± 3 days, BALB/c 22.8 ± 7.5 days and STS 29.7 ± 4.1 days ($p < 0.05$). Differences were also found in case of survival rates. While all CcS-11 mice died following the infection, 40% of infected BALB/c and 90% of STS mice survived until the end of the experiment (Figure 1B). STS mice remained free of any clinical signs of the disease during the whole experiment (including that one mouse that died); BALB/c mice exhibited signs of rough fur, hunching or back limb paralysis. Some CcS-11 mice had similar signs as BALB/c mice, but some died without previous appearance of any kind of signs.

In order to test the susceptibility to the TBEV infection if host factors before viral entry of the CNS are avoided, we infected females of the strains BALB/c, STS and RC strains CcS-3, CcS-4, CcS-5, CcS-7, CcS-9, CcS-11, CcS-12, CcS-15, CcS-18 and CcS-20 i.c. with 10^3 pfu of TBEV. In this case, all mouse strains were susceptible to the infection. Most strains died almost at the same time p.i., i.e., between days 10 and 11 p.i. (Additional file 1: Figure S2). However, differences were seen in the MST in case of CcS-11 (MST of 8.0 ± 0.7 days), BALB/c (MST of 9.5 ± 0.5 days) and STS strains (MST of 12.4 ± 2.7 days) ($p < 0.05$; Figure 1C). Therefore, also factors acting directly in the CNS of the infected mice may influence the survival time. For all subsequent experiments, mice of strains CcS-11, BALB/c and STS were selected as representatives of high-, medium- and low-susceptible hosts.

Virus load in serum and brain of TBEV-infected mice

Serum samples of BALB/c, CcS-11 and STS mice were harvested for titration at various time points after s.c. inoculation of TBEV. The virus titers in individual samples were determined by plaque assay on PS cells. While the peak of viremia was observed in BALB/c and CcS-11 mice reaching 2–2.5 \log_{10} pfu/ml at days 3 and 4 p.i., no virus was detected at the same time points in STS mice ($p < 0.05$). STS mice had only traces of the virus in serum (<2 \log_{10} pfu/ml) at later time intervals, i.e. at day 5, 6 and 8 p.i. (Figure 2A).

Virus load in the brain after s.c. inoculation was assayed at day 13 p.i., i.e. at the time point when most of the CcS-11 and BALB/c mice exhibited neurological signs of the infection (Figure 2B). No difference was found in the virus titer in brain of the infected BALB/c



and CcS-11 mice (titer reaching 6–7 \log_{10} pfu/g), but a much lower titer was observed in brains of infected STS mice (approximately 3 \log_{10} pfu/g; $p < 0.005$).

After i.c. inoculation, a dynamics of virus growth in the brain was investigated. Increasing virus titers were seen before mice showed signs of the infection. The virus growth was almost identical in all three mouse strains, reaching its maximum at day 7 (8 \log_{10} pfu/g) (Figure 2C). The only difference was observed at day 2,

when BALB/c mice had slightly higher virus titers in the brain than CcS-11 mice ($p < 0.05$).

Immune cell accumulation in the CNS of TBEV infected mice

Accumulation of immunocompetent cells in the brain of the infected BALB/c, STS and BALB/c mice was quantified as the changes in mRNA levels of cell surface markers of B-cells (CD19), T-helper cells (CD4), cytotoxic T-cells (CD8 β) and macrophage/monocyte/granulocyte/NK cells (CD11b).

In case of s.c. inoculation of TBEV (Figure 3A), the immune cell antigen mRNA accumulation was assayed at day 13 p.i. During our preliminary experiments, mice were also sampled and assayed at days 8 and 10 p.i. (data not shown). However, at these time points only some mice had virus in their CNS, making the results too variable. The day 13 p.i. was the first interval when all mice had virus in their brains. CD4, CD8 β and CD11b mRNA levels in the brains of infected mice at day 13 p.i. became significantly higher than those of normal uninfected mice at day 13 p.i. However, CD19 mRNA levels did not significantly increase in BALB/c and CcS-11 mice, but became elevated in STS mice ($p < 0.05$).

After i.c. inoculation of TBEV (Figure 3B), the dynamics of immune cell accumulation in the CNS was investigated at days 2, 4, 6 and 7 p.i. No significant increase in the CD19 mRNA levels was seen in any of the investigated mouse strain at 4, 6 and 7 days p.i. Levels of CD11b mRNA increased in brains of STS mice as early as at day 2 and 4 p.i., whereas no increase was observed in BALB/c and CcS-11 mice until day 4 p.i. From day 6, a slight but significant increase of CD11b levels was observed in all mice tested; however, there was no difference between the individual mouse strains. CD4 and CD8 β mRNA levels increased remarkably (10–20-fold increase of CD4 mRNA and 100–200-fold increase of CD8 β mRNA compared to negative controls) in all investigated mouse strains from day 6 p.i. Higher levels of CD4 as well as CD8 β mRNA levels were detected in brains of infected STS than BALB/c mice at day 6 p.i. ($p < 0.05$).

Expression of key inflammatory cytokines/chemokines in brains of TBEV infected mice

The levels of mRNA specific for a broad range of cytokines (TNF- α , IFN γ , IL-1 α , IL-1 β , IL-2, IL-4, IL-5, IL-6 and IL-10) and chemokines (CCL2 (chemokine ligand 2)/MCP-1 (monocyte chemotactic protein-1), CCL3/MIP-1 α (macrophage inflammatory protein-1 α), CCL4/MIP-1 β (macrophage inflammatory protein-1 β), CCL5/RANTES (regulated upon activation, normal T-cell expressed and secreted) and interferon- γ -inducible protein-10 (IP-10)/CXCL10) were quantified in brains of TBEV infected BALB/c, CcS-11 and STS mice by real-time RT-PCR, and

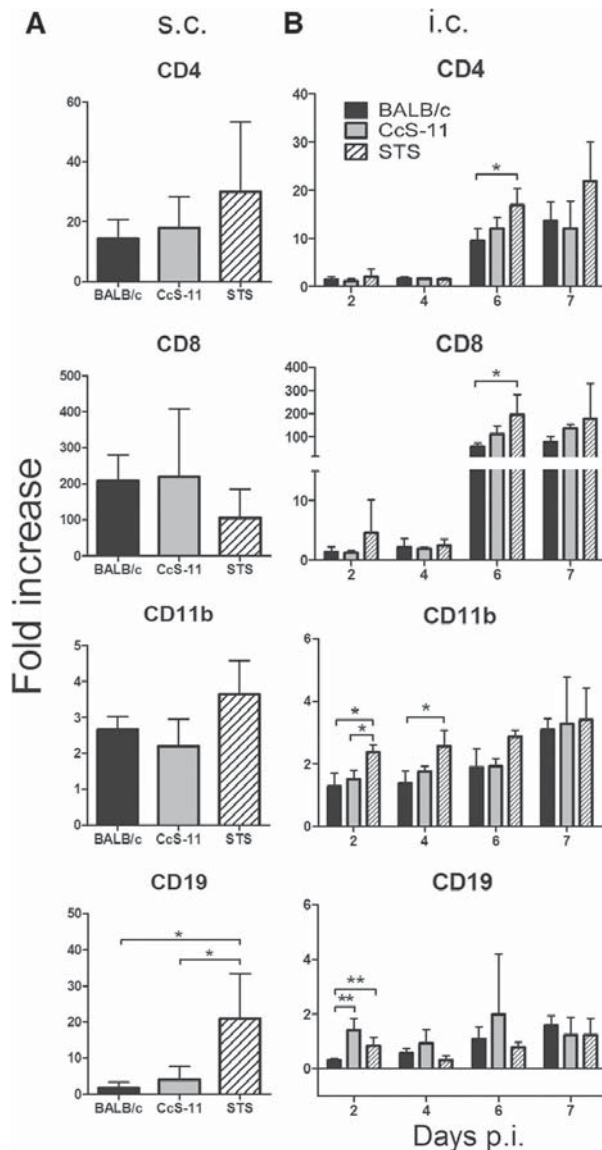


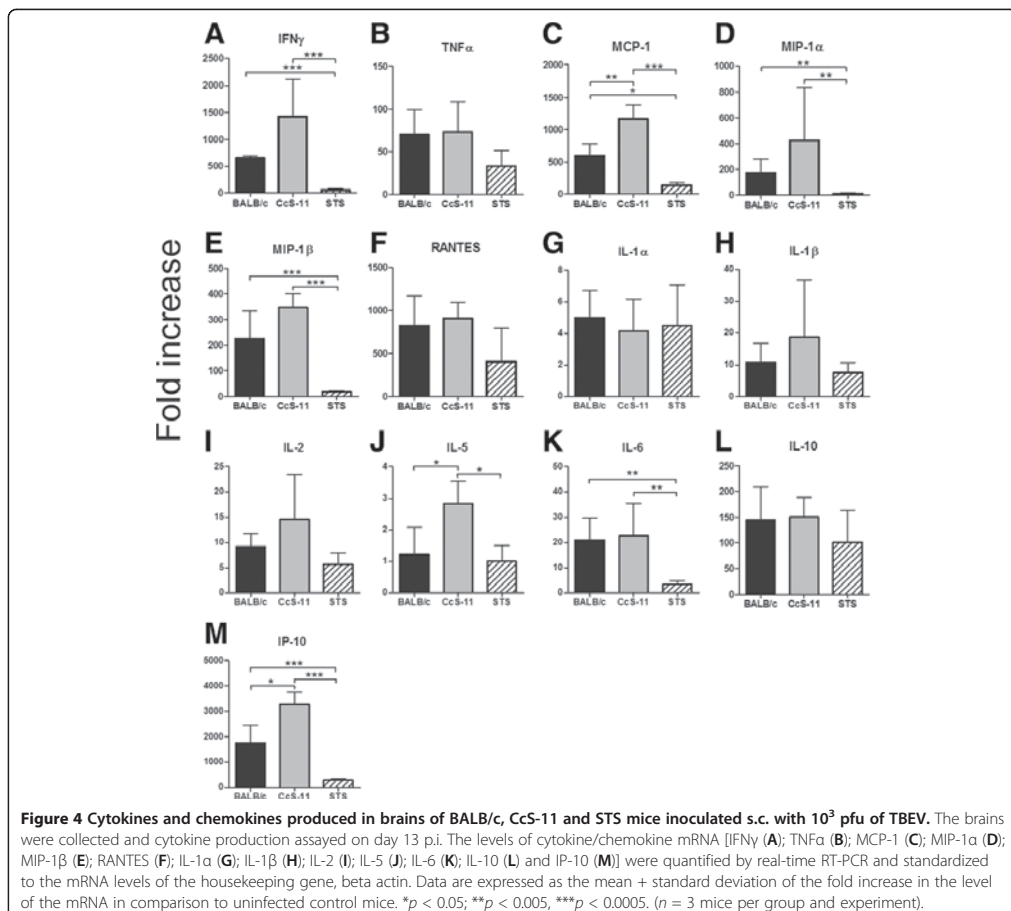
Figure 3 Immune/inflammatory cell accumulation in brains of BALB/c, CcS-11 and STS mice after s.c. (13 day p.i.) (A) or i.c. (B) inoculation of TBEV. Immune cell accumulation in the CNS was quantified as the changes in mRNA levels of cell surface markers of B-cells (CD19), T-helper cells (CD4), cytotoxic T-cells (CD8 β) and macrophage/monocyte/granulocyte/NK cells (CD11b), and normalized to expression of housekeeping gene, mouse beta actin. Data are expressed as the mean + standard deviation of the fold increase in the level of the mRNA in comparison to uninfected control mice. * $p < 0.05$; ** $p < 0.005$ ($n = 3$ mice per group and experiment).

standardized to the levels of the housekeeping gene, beta actin, mRNA (Figures 4 and 5).

After the s.c. inoculation of TBEV (Figure 4), the levels of cytokine/chemokine mRNA were measured on day 13 p.i. During our preliminary experiments, mice were also sampled and assayed at days 8 and 10 p.i. (data not shown). However, at these time points only some mice had virus in their CNS, making the results too variable. The day 13 p.i. was the first interval when all mice had virus in their brains. Significantly increased mRNA levels of TNF- α , IFN γ , IL-1 α , IL-1 β , IL-2, IL-6, IL-10, MCP-1, RANTES and IP-10 were seen in the TBEV-infected mice of all strains when compared to negative uninfected controls at day 13 p.i. In case of CCL3/MIP-1 α (Figure 4D) and CCL4/MIP-1 β (Figure 4E) mRNA, only sensitive

strains BALB/c and CcS-11 exhibited upregulated expression after the TBEV infection, whilst the expression in infected STS mice was not changed. The levels of IL-5 mRNA were increased only in brains of infected CcS-11 mice (Figure 4J), but the infection did not affect the expression of this cytokine in brains of BALB/c and STS mice. The levels of IFN- γ were the highest in brains of infected CcS-11 mice; BALB/c mice exhibited higher levels than STS ($p < 0.0005$; Figure 4A). The levels of upregulation of IL-6 mRNA expression were similar in BALB/c and CcS-11 mice, but both these strains exhibited significantly enhanced expression in comparison to STS mice ($p < 0.005$; Figure 4K).

Major differences in the cytokine mRNA expression among the infected BALB/c, CcS-11 and STS mice were



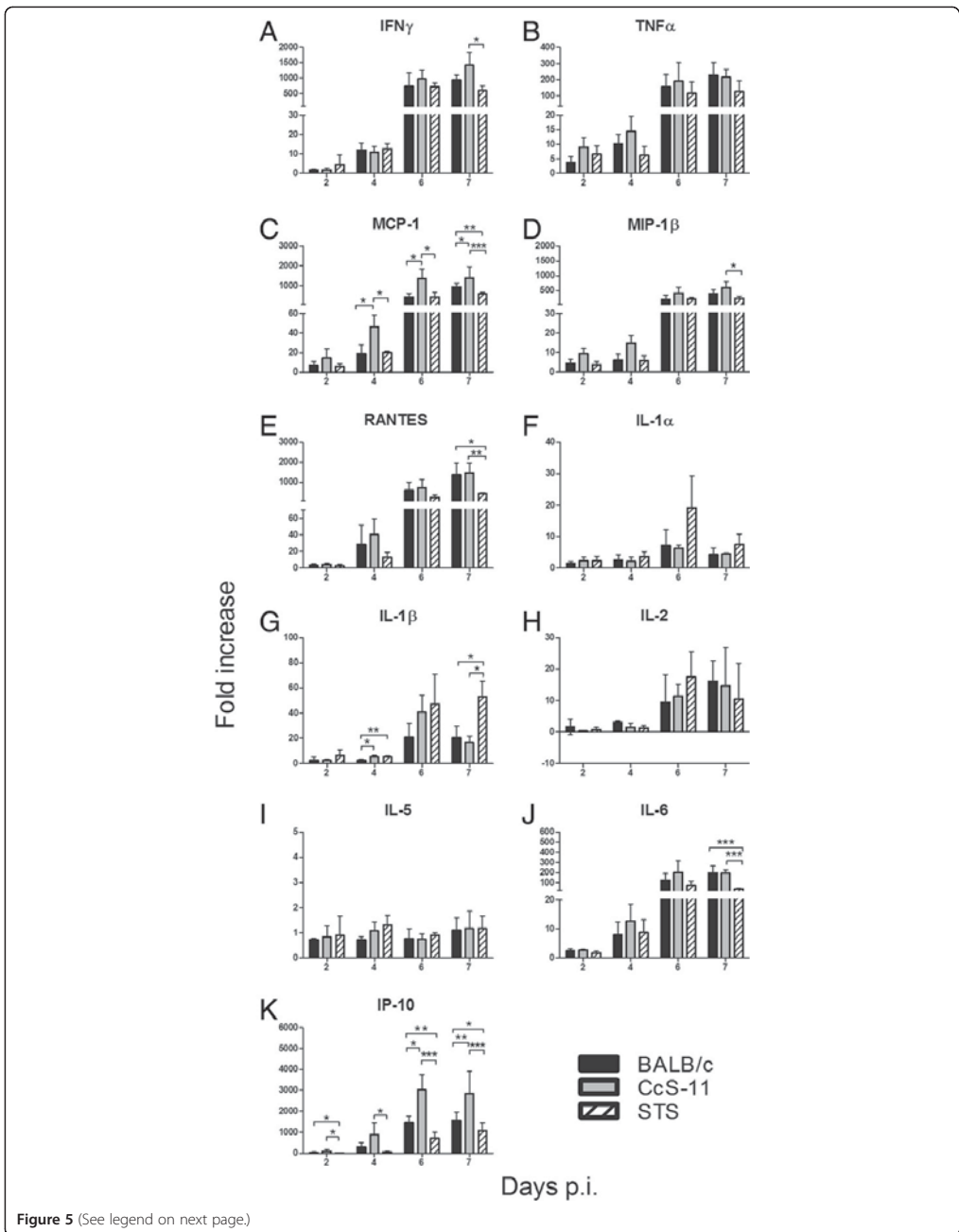


Figure 5 (See legend on next page.)

(See figure on previous page.)

Figure 5 Cytokines and chemokines produced in brains of BALB/c, CcS-11 and STS mice inoculated i.c. with 10 pfu of TBEV. The levels of cytokine/chemokine mRNA [IFN γ (A); TNF α (B); MCP-1 (C); MIP-1 β (D); RANTES (E); IL-1 α (F); IL-1 β (G); IL-2 (H); IL-5 (I); IL-6 (J); and IP-10 (K)] were quantified by real-time RT-PCR and standardized to the mRNA levels of the housekeeping gene, beta actin. Data are expressed as the mean + standard deviation of the fold increase in the level of the mRNA in comparison to uninfected control mice. * $p < 0.05$; ** $p < 0.005$, *** $p < 0.0005$ ($n = 3$ mice per group and experiment).

seen in case of MCP-1 (Figure 4C) and IP-10 (Figure 4M) mRNA. CcS-11 mice had the highest levels of MCP-1 and IP-10 mRNA in brains, while BALB/c had lower levels of MCP-1 and IP-10 mRNA when compared to CcS-11 mice, but higher when compared to STS mice (Figure 4C, M).

The dynamics of the changes in cytokine/chemokine mRNA expression was investigated at days 2, 4, 6 and 7 after i.c. inoculation of TBEV (Figure 5). No changes in the levels of IL-5 mRNA (Figure 5I) were observed in any of the studied mouse strains at any time point. TNF- α (Figure 5B), CCL2/MCP-1 (Figure 5C) and CCL4/MIP-1 β (Figure 5D) mRNA levels increased significantly from day 2 p.i. A significant increase in the level of mRNA for IFN- γ , IL-1 β , IL-2, IL-6 and CCL5/RANTES (Figure 5 A, G, H, J, E) was seen from day 4 p. i. Expression of IL-1 α mRNA was enhanced from the day 6 p.i. (Figure 5F). A large variation in the values of MIP-1 α , IL-10 (data not shown) and IL-2 (Figure 5H) mRNA was observed between the individual mice within the strain each day after the i.c. inoculation of TBEV. IFN- γ mRNA levels were much higher in CcS-11 mice at day 7 p.i. when compared to STS mice ($p < 0.05$). Similarly, the lowest levels of IL-6 ($p < 0.0005$) and CCL5/RANTES (BALB/c vs. STS, $p < 0.05$; CcS-11 vs. STS, $p < 0.005$) mRNA were detected in STS mice versus BALB/c and CcS-11 mice at day 7 p.i. In contrast, STS mice had very enhanced levels of IL-1 β mRNA at day 7 p.i. in comparison to BALB/c and CcS-11 mice ($p < 0.05$). The greatest differences among the infected BALB/c, CcS-11 and STS mice were seen in case of MCP-1 and IP-10 mRNA. CcS-11 mice had the highest levels of MCP-1 mRNA in brains at days 4, 6 ($p < 0.05$) and 7 p.i. (BALB/c vs. STS, $p < 0.005$; CcS-11 vs. BALB/c, $p < 0.05$; CcS-11 vs. STS, $p < 0.0005$). The levels of IP-10 mRNA were the highest in CcS-11 mice at all investigated time points p.i., the highest differences being observed at day 6 p.i. (BALB/c vs. CcS-11 and STS vs. CcS-11, $p < 0.005$) and at day 7 p.i. (BALB/c vs. CcS-11, $p < 0.005$, and STS vs. CcS-11, $p < 0.0005$). BALB/c had lower levels of IP-10 mRNA than CcS-11 mice ($p < 0.05$), but higher than STS mice ($p < 0.05$). A correlation between the IP-10 mRNA levels with the sensitivity of mice to the TBEV infection was observed (Figures 1C, 5K). No changes in the expression of IL-4 mRNA were seen in any mouse strain after either s.c. or i.c. TBEV inoculation (data not shown).

TBEV-specific antibodies elicited in infected mice

In order to compare the host's humoral immune response in the infected BALB/c, CcS-11 and STS mice after s.c. inoculation of TBEV, TBEV-specific antibodies were tested at days 5, 8, 10 and 13 p.i.. The titer of neutralizing antibodies was determined by PRNT (plaque reduction neutralization test) assay. Before day 10, a very low titer of neutralizing antibodies and no difference between the strains were observed (data not shown). At day 10 p.i., very low titers of neutralizing antibodies were found in serum of BALB/c and CcS-11 mice (less than 1:20), but STS mice exhibited neutralizing titers of 1:100 ($p < 0.005$). At day 13 p.i., no increase in the titer of neutralizing antibodies was seen in CcS-11 mice. BALB/c mice exhibited neutralizing titers of 1:100, but STS mice had titers reaching 1:640 ($p < 0.0005$) (Figure 6). No neutralizing activity was detected in sera from control uninfected mice.

Discussion

Host genotype as an important determinant of susceptibility to TBEV infection

Mice provide a useful tool for study of human TBE, since they recapitulate the pathological and pathophysiological processes seen in severe human TBE cases. However, biological and virological markers indicating the severity of TBE in mice as well as in humans remain

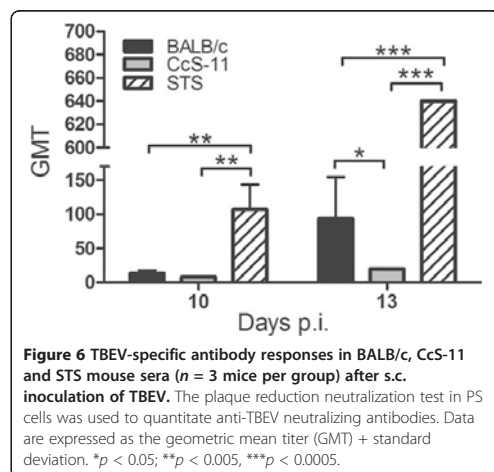


Figure 6 TBEV-specific antibody responses in BALB/c, CcS-11 and STS mouse sera ($n = 3$ mice per group) after s.c. inoculation of TBEV. The plaque reduction neutralization test in PS cells was used to quantitate anti-TBEV neutralizing antibodies. Data are expressed as the geometric mean titer (GMT) + standard deviation. * $p < 0.05$; ** $p < 0.005$, *** $p < 0.0005$.

unclear. The severity of TBE can be influenced by a variety of factors, e.g., the inoculation dose and virulence of the virus [1], the age, sex and immune status of the host [2], and susceptibility based on the host's genetic background. Generally, age of the host is the most common host risk factor identified for severe forms of flavivirus encephalitis [29]. However, genetic host risk factors play an important role in the development of severe flaviviral neurological diseases as well. Several genetic host factors associated with the severe forms of flavivirus encephalitis have been identified. These include polymorphisms in *HLA-A* and *HLA-B*, polymorphism located in the promoter region of the human *CD209* gene [7] and functional Toll-like receptor 3 gene [4], deletion in *CCR5* [5] and variability in 2'-5'-oligoadenylate synthetase gene cluster [6]. In our study, we developed a new mouse model of hosts differing in the susceptibility to TBEV infection based on CcS/Dem RC mouse strains. We observed clearly different patterns in the susceptibility of the CcS/Dem RC strains to s.c. infection with TBEV. Out of the eight strains tested, one (STS) exhibited low susceptibility, five intermediate susceptibility (CcS-3, CcS-7, CcS-9, CcS-16 and BALB/c) and two strains (CcS-11 and CcS-15) high susceptibility (Additional file 1: Figure S1). Differences in MST between the strains CcS-11, BALB/c and STS were also observed after i.c. inoculation of TBEV, i.e., CcS-11 mice had the shortest MST, BALB/c medium MST and STS the longest MST and higher survival (Figure 1C). These differences indicate the presence of TBEV susceptibility genes. Different susceptibility to virus infection in recombinant inbred strains between BALB/c and STS mice was also observed in case of infection with murine coronavirus [30]. After i.c. inoculation of 100 pfu of murine coronavirus, all BALB/c mice were highly susceptible and died; in contrast, STS mice were shown to be partially resistant, with a mortality rate of 30%, longer survival times and lower rates of virus production [30]. In our study, RC strain CcS-11, which contains approximately 12.5% genes of the donor strain STS and 87.5% genes of the background strain BALB/c, was more sensitive to TBEV infection than both parental strains BALB/c and STS. The observations of progeny having a phenotype beyond the range of the phenotype of its parents are not rare in traits controlled by multiple genes [18]. Such an observation may be due to multiple gene-gene interactions of quantitative trait loci, which in new combinations of these genes in RC or chromosomal substitution can lead to the appearance of new phenotypes that exceed their range in parental strains [18]. Another possibility is when some progeny receives predominantly susceptible alleles from both parents. These susceptible alleles are distinct from genes *H2*, *Cd209*, *Tlr3*, *Ccr5* and *Oas1b*, which are involved in genetic control of susceptibility to flavivirus encephalitis (see above), because these genes are in CcS-11

localized on segments derived from the background BALB/c strain [Figure 1A and Mouse Genome Informatics (<http://www.informatics.jax.org/>)]. We also cannot exclude the possibility of a spontaneous mutation appearing during inbreeding and causing the unique phenotype [18]. Similarly to our study, CcS-11 mice were more susceptible to infection with *Leishmania tropica* [18] and to *Trypanosoma brucei brucei* [31] than both parental mouse strains. However, CcS-11 is more resistant to *L. major* than BALB/c [32].

TBEV replication rate in infected mice is not the main factor influencing survival

We attempted to identify biological markers that could be related to differences in survival rates of the highly susceptible (CcS-11), medium susceptible (BALB/c) and lowly susceptible (STS) mice infected with TBEV. STS mice had very low and delayed viremia when compared with BALB/c and CcS-11 mice after s.c. inoculation. All mice showed brain infection, but lower titers were detected in brains of STS mice, while BALB/c and CcS-11 mice showed higher titers for 3–4 log₁₀ pfu. This indicated lower replication rates of the virus in STS mice, but no difference in replication rates in BALB/c and CcS-11 mice. To avoid virus-host interactions before virus neuroinvasion, mice were inoculated i.c., and the dynamics of virus growth in the brain was investigated. Although BALB/c, CcS-11 and STS mice showed different MST after i.c. inoculation, almost the same virus titers were observed in all investigated mouse strains at all intervals p.i. (Figure 2). Virus replication rate is not, therefore, the main factor influencing MST of the host. Similarly, no differences in tissue tropism, viral load or kinetics were observed during acute West Nile virus infection in mouse strains C57BL/6 and C3H/HeN with higher and lower survival rates, respectively [33].

Higher mRNA levels of cell surface marker of B-cells were seen in brains of the mice less susceptible to TBEV infection

Mice differing in susceptibility to TBEV infection exhibited some differences in immune cells accumulation in brains during the development of encephalitis as demonstrated by quantification of mRNA of cell-specific markers by real-time RT-PCR. In our previous work using BALB/c, SCID on the BALB/c background, C57BL/6 and C57BL/6^{CD8^{-/-}} mice we reported that CD8⁺ T-cells have a dual role and mediate recovery, but also immunopathology during TBE [2]. In this study, no differences in the level of CD8 mRNA were seen between the BALB/c, CcS-11 and STS mice after s.c. inoculation. After i.c. inoculation, only STS mice exhibited slightly higher levels of CD8 mRNA (but also CD4 mRNA) than BALB/c mice at day 6 p.i., but no other differences were observed (Figure 3B). The most interesting results

provided quantification of mRNA for CD19, a cell surface marker of B-cells. No increase of CD19 mRNA was observed after i.c. inoculation in all mouse strains. After s.c. inoculation, strains BALB/c and CcS-11 did not increase the levels of CD19 mRNA in their brains, whereas STS mice exhibited a significant increase (Figure 3A). This might indicate stronger B cell infiltration in brains of the less susceptible mice. B cells were also observed in brains in some studies focused on flavivirus encephalitis [34], predominantly found in the perivascular space. The proportion of B and T cells in the brain may vary depending on the infecting flavivirus [35,36]. It is known that TBEV, unlike to Japanese encephalitis and West Nile virus infections, induces CXCL13, a B-cell chemoattractant, in the CNS [37]. Although the antibody reaction is clearly important systemically [38], the importance of B cells infiltrating brain parenchyma in confining of the infection is not clear.

More severe form of TBE associated with higher expression of proinflammatory cytokines/chemokines in the brain

Accumulation of cytokines and chemokines in the CNS may accentuate progression of encephalitis instead of restricting viral replication [37,39-41]. Deregulated or excess release of proinflammatory mediators by the brain may induce tissue damage with different pathology and disease outcome [42]. In this study, we examined the cytokine/chemokine response in brains of the mice differing in susceptibility to TBEV infection (Figures 4 and 5). We showed that a wide range of cytokine and chemokine mRNAs for TNF- α , IFN γ , IL-1 α , IL-1 β , IL-2, IL-6, IL-10, CCL2/MCP-1, CCL5/RANTES, IP-10, MIP-1 α , MIP-1 β and others was produced in response to TBEV infection. There was no clear correlation between the peak of cytokine/chemokine production and the increase of TBEV in the brain. After i.c. inoculation, all mice had comparable virus titers in the CNS (Figure 2C), but the levels of cytokine/chemokine expression differed markedly (Figure 5). STS mice had the highest levels of IL-1 β mRNA after i.c. TBEV inoculation when compared to other strains of mice. In contrast, it is known that higher levels of IL-1 β are associated with more severe cases of chikungunya [43]. Most of other cytokine/chemokine mRNAs tested were on the lowest level in STS mice in comparison to CcS-11 and/or BALB/c mice. The highest levels of proinflammatory cytokines/chemokines (IFN γ , CCL3/MIP-1 α , CCL2/MCP-1, IP-10) (after s.c. and i.c. inoculation) and IL-5 (after s.c. inoculation) were detected in CcS-11 mice, indicating that these cytokines/chemokines can be associated with a more severe form of TBE in our experimental model. On the other hand, the lowest levels of IL-6 and CCL5/RANTES, and also CCL3/MIP-1 α and CCL4/MIP-1 β mRNAs, were demonstrated in STS mice. These data

support the theory that excessive production of proinflammatory mediators could contribute to development of more severe or acute form of TBE. Similarly to our study, higher levels of CCL5/RANTES, CCL3/MIP-1 α , CCL4/MIP-1 β and IP-10 mRNA were found to be associated with a lethal form of West Nile virus infection in comparison with the non-lethal form [41]. CCL2/MCP-1 and IP-10 mRNA levels correlated well with the susceptibility of the mouse strains to TBEV infection, i.e., CcS-11 mice had the highest levels, BALB/c medium and STS the lowest. These data were confirmed in two independent experiments. Both these chemokines can have an important role in immunopathology during TBE. It has been demonstrated that neutralization of CCL2/MCP-1 leads to increased survival rates in West Nile virus-infected mice [44]. Expression of IP-10 mRNA exhibited the biggest differences between the studied mouse strains. The chemokine IP-10, which is IFN- γ inducible and has the ability to attract activated T cells in the CNS, has also been shown to be a potent neurotoxin [45]. In human TBE patients, IP-10 can be detected in serum as well as in cerebrospinal fluid [46,47]. Using genetically deficient mice and antibody neutralization approaches, it was demonstrated that IP-10 is critical for the recruitment of T-cells into the CNS and survival from West Nile virus infection in mice [48]. However, excessively high levels of IP-10 in the CNS can be very harmful to the host. IP-10 levels in the CNS of HIV-1-infected individuals correlate positively with disease progression. There is also evidence that IP-10 participates in the neuropathogenesis of SHIV-infected macaques [49,50] by contributing to the degeneration of neurons possibly through the activation of a calcium-dependent apoptotic pathway [45,51]. Our data strongly suggest that higher levels of IP-10 in the CNS might be associated with more severe forms of TBE. Further studies using mice specifically knocked out for one of the genes identified will determine their contribution to host susceptibility to TBE. Whether the profile of the chemokine production in human cases of TBE will predict the disease outcome requires further study.

Key role of neutralizing antibodies in preventing neuroinvasion and host fatality during TBE

The importance of neutralizing antibodies in the prevention of flaviviral diseases is well accepted. As a rule, the antibodies with relatively high affinity and avidity to the surface proteins of TBEV virions can be detected in neutralization test. Only such antibodies interfere with the interaction of the virus with receptors, preventing it to enter the cell. TBEV infection is associated with breakdown of the host blood-brain barrier [26]; therefore, the antibodies can penetrate into the CNS. In our study, STS mice had a strong neutralizing antibody response, CcS-11

mice failed to produce neutralizing antibodies, and BALB/c mice developed neutralizing antibodies but later and at low titers (Figure 6). Therefore, our data on TBE support the importance of neutralizing antibodies in preventing neuroinvasion and host fatality. Similar data were obtained in experiments with the mouse strains C3H/HeN and DBA/2 with higher and lower susceptibility to the Japanese encephalitis virus, respectively [40]. In human TBE patients, those who fail to produce TBEV neutralizing antibodies usually have a very severe course of the infection [52]. The same is seen in patients who receive vaccination against TBEV and develop antibody response, but their antibodies do not have neutralizing capacity [52].

Conclusions

In summary, our experimental model showed that earlier and greater amounts of neutralizing antibodies could limit neuroinvasion of TBEV and disease progression in less susceptible mice. Moreover, we described that resistant mice exhibit stronger B-cell infiltration (as measured by quantification of changes in mRNA levels of cell surface markers) but lower cytokine/chemokine production in the CNS when compared to the more susceptible mouse strains. The most susceptible mice have the highest overall cytokine/chemokine production in the CNS, particularly of CCL2/MCP-1 and IP-10, which can elevate the primarily proinflammatory environment in the brain, which could result in brain tissue damage and death of the host through immunopathology. This suggests an important role of cytokines and chemokines in the immunopathogenesis of TBE. The host immune response based on the genetic background of the host may therefore play a central role in determining the outcome of TBEV infection.

Additional file

Additional file 1: Figure S1. Differential survival of BALB/c, STS and selected RC strains after subcutaneous inoculation of TBEV. Mice were inoculated with 104 pfu of TBEV and observed for lethality. **Figure S2:** Differential survival of BALB/c, STS and selected RC strains after intracerebral inoculation of TBEV. Mice were inoculated with 10 pfu of TBEV and observed for lethality.

Abbreviations

TBE: Tick-borne encephalitis; TBEV: Tick-borne encephalitis virus; s.c.: Subcutaneous; i.c.: Intracerebral; pfu: Plaque-forming unit; RC: Recombinant congenic; TNF- α : Tumor necrosis factor- α ; IFN γ : Interferon γ ; IL-1 α : Interleukin 1 α ; IL-1 β : Interleukin 1 β ; IL-2: Interleukin 2; IL-4: Interleukin 4; IL-5: Interleukin 5; IL-6: Interleukin 6; IL-10: Interleukin 10; CCL2: (chemokine ligand 2)/MCP-1 (monocyte chemoattractant protein-1); CCL3/MIP-1 α : Macrophage inflammatory protein-1 α ; CCL4/MIP-1 β : Macrophage inflammatory protein-1 β ; CCL5/RANTES: Regulated upon activation normal T-cell expressed and secreted; IP10/CXCL10: Interferon- γ -inducible protein-10.

Competing interests

The authors declare that they have no competing interests.

Authors' contributions

DR conceived and designed the research and wrote the manuscript. MP, JS and JV performed the experiments. MP, JS, JK, LG, ML and PD participated in the design of the experiments and coordination and helped to draft the manuscript. All authors read and approved the final manuscript.

Acknowledgements

The authors acknowledge financial support by the Czechoslovak Foundation project no. P502/11/2116, and grant Z60220518 from the Ministry of Education, Youth and Sports of the Czech Republic, and AdmireVet project no. CZ.1.05/2.1.00/01.006 (ED006/01/01). The founders had no role in the study design, data collection and analysis, decision to publish or preparation of the manuscript.

Author details

¹Institute of Parasitology, Biology Centre of the Czech Academy of Sciences, Branišovská 31, České Budějovice CZ-37005, Czech Republic. ²Faculty of Science, University of South Bohemia, Branišovská 31, České Budějovice CZ-37005, Czech Republic. ³Institute of Molecular Genetics, Academy of Sciences of the Czech Republic, Vídeňská 1083, Prague CZ-14220, Czech Republic. ⁴Department of Virology, Veterinary Research Institute, Hudcova 70, Brno CZ-62100, Czech Republic. ⁵Roswell Park Cancer Institute, Elm and Carlton Streets, Buffalo, New York 14263, USA.

Received: 30 March 2013 Accepted: 11 June 2013

Published: 27 June 2013

References

- Růžek D, Gritsun TS, Forrester NL, Gould EA, Kopecký J, Golovchenko M, Rudenko N, Grubhoffer L: Mutations in the NS2B and NS3 genes affect mouse neuroinvasiveness of a Western European field strain of tick-borne encephalitis virus. *Virology* 2008, **374**:249–255.
- Růžek D, Salát J, Palus M, Gritsun TS, Gould EA, Dyková I, Skallová A, Jelínek J, Kopecký J, Grubhoffer L: CD8+ T-cells mediate immunopathology in tick-borne encephalitis. *Virology* 2009, **384**:1–6.
- Lipoldová M, Demant P: Genetic susceptibility to infectious disease: lessons from mouse models of leishmaniasis. *Nat Rev Genet* 2006, **7**:294–305.
- Kindberg E, Vene S, Mickiene A, Lundkvist Å, Lindquist L, Svensson L: A functional Toll-like receptor 3 gene (TLR3) may be a risk factor for tick-borne encephalitis virus (TBEV) infection. *J Infect Dis* 2011, **203**:523–528.
- Kindberg E, Mickiene A, Ax C, Akerlind B, Vene S, Lindquist L, Lundkvist A, Svensson L: A deletion in the chemokine receptor 5 (CCR5) gene is associated with tickborne encephalitis. *J Infect Dis* 2008, **197**:266–269.
- Barkhash AV, Babenko VN, Kobzev VF, Romashchenko AG, Voevoda MI: Polymorphism in the human 2'-5'-oligoadenylate synthetase genes (OAS), associated with predisposition to severe forms of tick-borne encephalitis, in populations from North Eurasia. *Mol Biol (Mosk)* 2010, **44**:985–993.
- Barkhash AV, Pereygin AA, Babenko VN, Brinton MA, Voevoda MI: Single nucleotide polymorphism in the promoter region of the CD209 gene is associated with human predisposition to severe forms of tick-borne encephalitis. *Antiviral Res* 2012, **93**:64–68.
- Urošević N, Shellam GR: Host genetic resistance to Japanese encephalitis group viruses. *Curr Top Microbiol Immunol* 2002, **267**:153–170.
- Brinton MA, Pereygin AA: Genetic resistance to flaviviruses. *Adv Virus Res* 2003, **60**:43–85.
- Demant P, Hart AA: Recombinant congenic strains—a new tool for analyzing genetic traits determined by more than one gene. *Immunogenetics* 1986, **24**:416–422.
- Banus HA, van Kranen HJ, Mooi FR, Hoebee B, Nagelkerke NJ, Demant P, Kimman TG: Genetic control of *Bordetella pertussis* infection: identification of susceptibility loci using recombinant congenic strains of mice. *Infect Immun* 2005, **73**:741–747.
- Demant P, Lipoldová M, Svobodová M: Resistance to *Leishmania major* in mice. *Science* 1996, **274**:1392.
- Lipoldová M, Svobodová M, Krulová M, Havelková H, Badalová J, Nohýnková E, Holán V, Hart AA, Volf P, Demant P: Susceptibility to *Leishmania major* infection in mice: multiple loci and heterogeneity of immunopathological phenotypes. *Genes Immun* 2000, **1**:200–206.
- Badalová J, Svobodová M, Havelková H, Vladimirov V, Vojtíšková J, Engová J, Pilcik T, Volf P, Demant P, Lipoldová M: Separation and mapping of

- multiple genes that control IgE level in *Leishmania major* infected mice. *Genes Immun* 2002, **3**:187–195.
15. Vladimirov V, Badalová J, Svobodová M, Havelková H, Hart AA, Blazková H, Demant P, Lipoldová M: **Different genetic control of cutaneous and visceral disease after *Leishmania major* infection in mice.** *Infect Immun* 2003, **71**:2041–2046.
 16. Havelková H, Badalová J, Svobodová M, Vojtíšková J, Kurey I, Vladimirov V, Demant P, Lipoldová M: **Genetics of susceptibility to leishmaniasis in mice: four novel loci and functional heterogeneity of gene effects.** *Genes Immun* 2006, **7**:220–233.
 17. Kurey I, Kobets T, Havelková H, Slapničková M, Quan L, Trtková K, Grekov I, Svobodová M, Stassen AP, Hutson A, Demant P, Lipoldová M: **Distinct genetic control of parasite elimination, dissemination, and disease after *Leishmania major* infection.** *Immunogenetics* 2009, **61**:619–633.
 18. Kobets T, Havelková H, Grekov I, Volkova V, Vojtíšková J, Slapničková M, Kurey I, Sohrabi Y, Svobodová M, Demant P, Lipoldová M: **Genetics of host response to *Leishmania tropica* in mice—different control of skin pathology, chemokine reaction, and invasion into spleen and liver.** *PLoS Negl Trop Dis* 2012, **6**:e1667.
 19. Fijneman RJ, de Vries SS, Jansen RC, Demant P: **Complex interactions of new quantitative trait loci, *Sluc1*, *Sluc2*, *Sluc3*, and *Sluc4*, that influence the susceptibility to lung cancer in the mouse.** *Nat Genet* 1996, **14**:465–467.
 20. van Wezel T, Stassen AP, Moen CJ, Hart AA, van der Valk MA, Demant P: **Gene interaction and single gene effects in colon tumour susceptibility in mice.** *Nat Genet* 1996, **14**:468–470.
 21. Ruivenkamp CA, van Wezel T, Zanon C, Stassen AP, Vleck C, Csikós T, Klous AM, Tripodis N, Perrakis A, Boerigter L, Groot PC, Lindeman J, Mooi WJ, Meijer GA, Scholten G, Dauwerse H, Paces V, van Zandwijk N, van Ommen GJ, Demant P: **Ptprj is a candidate for the mouse colon-cancer susceptibility locus *Sccl1* and is frequently deleted in human cancers.** *Nat Genet* 2002, **31**:295–300.
 22. Lipoldová M, Havelková H, Badalová J, Demant P: **Novel loci controlling lymphocyte proliferative response to cytokines and their clustering with loci controlling autoimmune reactions, macrophage function and lung tumor susceptibility.** *Int J Cancer* 2005, **114**:394–399.
 23. Lipoldová M, Havelková H, Badalová J, Vojtíšková J, Quan L, Krulova M, Sohrabi Y, Stassen AP, Demant P: **Loci controlling lymphocyte production of interferon γ after alloantigen stimulation in vitro and their co-localization with genes controlling lymphocyte infiltration of tumors and tumor susceptibility.** *Cancer Immunol Immunother* 2010, **59**:203–213.
 24. Rey FA, Heinz FX, Mandl C, Kunz C, Harrison SC: **The envelope glycoprotein from tick-borne encephalitis virus at 2 Å resolution.** *Nature* 1995, **375**:291–298.
 25. De Madrid AT, Porterfield JS: **A simple micro-culture method for the study of group B arboviruses.** *Bull World Health Organ* 1969, **40**:113–121.
 26. Růžek D, Salát J, Singh SK, Kopecký J: **Breakdown of the blood-brain barrier during tick-borne encephalitis in mice is not dependent on CD8+ T-cells.** *PLoS One* 2011, **6**:e20472.
 27. Livak KJ, Schmittgen TD: **Analysis of relative gene expression data using real-time quantitative PCR and the 2⁻(Delta Delta C(T)) method.** *Methods* 2001, **25**:402–408.
 28. Bárdoš V, Sixl W, Wisidagama CL, Halouzka J, Stünzner D, Hubálek Z, Withalm H: **Prevalence of arbovirus antibodies in sera of animals in Sri Lanka.** *Bull World Health Organ* 1983, **61**:987–990.
 29. Clark DC, Brault AC, Hunsperger E: **The contribution of rodent models to the pathological assessment of flaviviral infections of the central nervous system.** *Arch Virol* 2012, **157**:1423–1440.
 30. Kyuwa S, Yamaguchi K, Toyoda Y, Fujiwara K, Hilgers J: **Acute and late disease induced by murine coronavirus, strain JHM, in a series of recombinant inbred strains between BALB/cHeA and STS/A mice.** *Microb Pathog* 1992, **12**:95–104.
 31. Síma M, Havelková H, Quan L, Svobodová M, Jarosíková T, Vojtíšková J, Stassen AP, Demant P, Lipoldová M: **Genetic control of resistance to *Trypanosoma brucei* infection in mice.** *PLoS Negl Trop Dis* 2011, **5**:e1173.
 32. Lipoldová M, Svobodová M, Havelková H, Krulová M, Badalová J, Nohýnková E, Hart AA, Schlegel D, Volf P, Demant P: **Mouse genetic model for clinical and immunological heterogeneity of leishmaniasis.** *Immunogenetics* 2002, **54**:174–183.
 33. Brown AN, Kent KA, Bennett CJ, Bernard KA: **Tissue tropism and neuroinvasion of West Nile virus do not differ for two mouse strains with different survival rates.** *Virology* 2007, **368**:422–430.
 34. Bréhin AC, Mouriés J, Frenkiel MP, Dadaglio G, Desprès P, Lafon M, Couderc T: **Dynamics of immune cell recruitment during West Nile encephalitis and identification of a new CD19 + B220-BST-2+ leukocyte population.** *J Immunol* 2008, **180**:6760–6767.
 35. Maximova OA, Faucette LJ, Ward JM, Murphy BR, Pletnev AG: **Cellular inflammatory response to flaviviruses in the central nervous system of a primate host.** *J Histochem Cytochem* 2009, **57**:973–989.
 36. King NJC, Van Vreden C, Terry RL, Getts DR, Yeung AWS, Teague Getts M, Davison AM, Deffrasnes C, Munoz Erazo L: **The immunopathogenesis of neurotropic flavivirus infection.** In *Flavivirus Encephalitis*. 1st edition. Edited by Růžek D. Rijeka: Intech; 2011:25–52.
 37. Bardina SV, Lim JK: **The role of chemokines in the pathogenesis of neurotropic flaviviruses.** *Immunol Res* 2012, **54**:121–132.
 38. Diamond MS, Shrestha B, Marri A, Mahan D, Engle M: **B cells and antibody play critical roles in the immediate defense of disseminated infection by West Nile encephalitis virus.** *J Virol* 2003, **77**:2578–2586.
 39. Biswas SM, Kar S, Singh R, Chakraborty D, Vipat V, Raut CG, Mishra AC, Gore MM, Ghosh D: **Immunomodulatory cytokines determine the outcome of Japanese encephalitis virus infection in mice.** *J Med Virol* 2010, **82**:304–310.
 40. Wang K, Deubel V: **Mice with different susceptibility to Japanese encephalitis virus infection show selective neutralizing antibody response and myeloid cell infectivity.** *PLoS One* 2011, **6**:e24744.
 41. Shirato K, Kimura T, Mizutani T, Kariwa H, Takashima I: **Different chemokine expression in lethal and non-lethal murine West Nile virus infection.** *J Med Virol* 2004, **74**:507–513.
 42. Tigabu B, Juelich T, Holbrook MR: **Comparative analysis of immune responses to Russian spring-summer encephalitis and Omsk hemorrhagic fever viruses in mouse models.** *Virology* 2010, **408**:57–63.
 43. Ng LF, Chow A, Sun YJ, Kwek DJ, Lim PL, Dimatatac F, Ng LC, Ooi EE, Choo KH, Her Z, Kourilsky P, Leo YS: **IL-1beta, IL-6, and RANTES as biomarkers of Chikungunya severity.** *PLoS One* 2009, **4**:e4261.
 44. Getts DR, Terry RL, Getts MT, Müller M, Rana S, Shrestha B, Radford J, Van Rooijen N, Campbell IL, King NJ: **Ly6c + “inflammatory monocytes” are microglial precursors recruited in a pathogenic manner in West Nile virus encephalitis.** *J Exp Med* 2008, **205**:2319–2337.
 45. Sui Y, Stehno-Bittel L, Li S, Loganathan R, Dhillon NK, Pinson D, Nath A, Kolson D, Narayan O, Buch S: **CXCL10-induced cell death in neurons: role of calcium dysregulation.** *Eur J Neurosci* 2006, **23**:957–964.
 46. Zajkowska J, Moniuszko-Malinowska A, Pancewicz SA, Muszyńska-Mazur A, Kondrusik M, Grygorczuk S, Swierzyńska-Pijanowska R, Dunaj J, Czupryna P: **Evaluation of CXCL10, CXCL11, CXCL12 and CXCL13 chemokines in serum and cerebrospinal fluid in patients with tick borne encephalitis (TBE).** *Adv Med Sci* 2011, **56**:311–317.
 47. Lepeš S, Misić-Majerus L, Jeren T, Rode OD, Remenar A, Sporec V, Vince A: **Chemokines CXCL10 and CXCL11 in the cerebrospinal fluid of patients with tick-borne encephalitis.** *Acta Neurol Scand* 2007, **115**:109–114.
 48. Klein RS, Lin E, Zhang B, Luster AD, Tollett J, Samuel MA, Engle M, Diamond MS: **Neuronal CXCL10 directs CD8+ T-cell recruitment and control of West Nile virus encephalitis.** *J Virol* 2005, **79**:11457–11466.
 49. Sasseville VG, Smith MM, Mackay CR, Pauley DR, Mansfield KG, Ringle DJ, Lackner AA: **Chemokine expression in simian immunodeficiency virus-induced AIDS encephalitis.** *Am J Pathol* 1996, **149**:1459–1467.
 50. Westmoreland SV, Rottman JB, Williams KC, Lackner AA, Sasseville VG: **Chemokine receptor expression on resident and inflammatory cells in the brain of macaques with simian immunodeficiency virus encephalitis.** *Am J Pathol* 1998, **152**:659–665.
 51. Sui Y, Potula R, Dhillon N, Pinson D, Li S, Nath A, Anderson C, Turchan J, Kolson D, Narayan O, Buch S: **Neuronal apoptosis is mediated by CXCL10 overexpression in simian human immunodeficiency virus encephalitis.** *Am J Pathol* 2004, **164**:1557–1566.
 52. Bender A, Jäger G, Scheuerer W, Feddersen B, Kaiser R, Pfister HW: **Two severe cases of tick-borne encephalitis despite complete active vaccination—the significance of neutralizing antibodies.** *J Neurol* 2004, **251**:353–354.

doi:10.1186/1742-2094-10-77

Cite this article as: Palus et al.: Mice with different susceptibility to tick-borne encephalitis virus infection show selective neutralizing antibody response and inflammatory reaction in the central nervous system.

Journal of Neuroinflammation 2013 **10**:77.

CHAPTER III

Electron Tomography Analysis of Tick-Borne Encephalitis Virus Infection in Human Neurons

Tomáš Bílý, Martin Palus, Luděk Eyer, Jana Elsterová, Marie Vancová, Daniel Růžek

Scientific Reports 2015, 5: 10745

DOI: 10.1038/srep10745

http://www.nature.com/articles/srep10745?WT.ec_id=SREP-631-20150616&spMailingID=48887634&spUserID=ODkwMTM2NjQzMAS2&spJobID=702065282&spReportId=NzAyMDY1MjgyS0

Electron Tomography Analysis of Tick-Borne Encephalitis Virus Infection in Human Neurons

(summary)

Neurons are the primary target cells for TBEV infection, but knowledge about this viral infection and virus-induced neuronal injury is fragmental. Our novel data revealed the neuronal injury caused by TBEV infections, independent of the immune system response.

We have directly examined the pathology following TBEV infection in human primary neurons (HN). We exploited the advantages of advanced high-pressure freezing and freeze-substitution techniques to achieve optimal preservation of infected cell architecture to visualize TBEV infection in primary human neurons in three-dimensional (3D) space at ultrastructural resolution with electron tomography. This study was the first to visualize the architecture of cellular components involved in TBEV replication and transport in human primary neurons and the major ultrastructural changes that occur in response to TBEV infection.

At early time points after infection, virus antigen was detectable in almost the whole body of the neuron. At later time points, antigen accumulation appeared mainly in highly reorganized, proliferated rough endoplasmic reticulum, and only occasionally in dendrites. It was hypothesized that viral protein accumulation in dendrites might affect the distribution and function of host proteins, which in turn, might cause neural dysfunction and cellular degeneration (Hirano *et al.*, 2014).

Electron tomographic (ET) reconstructions produced high-resolution 3D images of the proliferating endoplasmic reticulum, and individual tubule-like structures of diverse diameters in the endoplasmic reticulum cisternae of single cells.

Moreover, ET revealed direct connections between the tubule-like structures and viral particles in the endoplasmic reticulum (ER). Unlike previous studies (Palus *et al.*, 2014a), we frequently observed the presence of tubule-like structures in TBEV-infected neurons. To the best of our

knowledge, this study was the first to demonstrate the simultaneous presence of two sizes of tubule-like structures in the RER of single infected cells. The function of tubule-like structures is not clear. These structures may represent features of replication, aberrant structures, or features of a cellular process that aims to restrict the infection (Offerdahl *et al*, 2012). With confocal microscopy, we observed fibrillary structures composed of viral E protein in cisterns of the ER; these structures suggested that E protein was present in the tubule-like structures. The functional contribution of these tubule-like structures to TBEV replication should be addressed in future research.

Furthermore, based on observations of TBEV-containing vesicles associated with microtubules in HNs connections between cellular microtubules and vacuoles that harbored the TBEV virions in neuronal extensions we hypothesize that vesicles containing TBEV particles are transported in infected neurons. Viral spread in neurons is generally mediated by fast axonal transport, a microtubule-associated transport system. In WNV infections, transneuronal viral spread required axonal release of viral particles. WNV undergoes bidirectional spread in neurons, and axonal transport promoted viral entry into the CNS (Samuel *et al*, 2007).

This study was the first to characterize the 3D topographical organization of membranous whorls and autophagic vacuoles in TBEV-infected human neurons. The functional importance of autophagy during TBEV replication was studied in human neuroblastoma cells. Stimulation of autophagy resulted in significantly increased dose-dependent TBEV production, whereas the inhibition of autophagy showed an intense, dose-dependent decrease of the yield of infectious virus particles.

In conclusion, we directly investigated the morphological changes induced by TBEV infection in HNs with advanced high-pressure freezing, freeze-substitution, and electron tomography techniques to reach optimal preservation of ultrastructure.

These methods enabled clear visualization of connections between microtubules and vacuoles that harbored TBEV virions in neuronal extensions, connections between tubule-like structures and virions, 3D organization of proliferating endoplasmic reticulum membranes, membranous whorls, and the formation of autophagic vacuoles.

These data provided insight into the process of TBEV-induced injury in HNs, and our findings will promote future studies that aim to understand the molecular mechanism of TBEV infection in the human CNS.

SCIENTIFIC REPORTS

OPEN

Electron Tomography Analysis of Tick-Borne Encephalitis Virus Infection in Human Neurons

Received: 09 March 2015
Accepted: 29 April 2015
Published: 15 June 2015

Tomáš Bílý^{1,2,*}, Martin Palus^{1,2,3,*}, Luděk Eyer³, Jana Elsterová^{1,2,3}, Marie Vancová^{1,2} & Daniel Růžek^{1,2,3}

Tick-borne encephalitis virus (TBEV) causes serious, potentially fatal neurological infections that affect humans in endemic regions of Europe and Asia. Neurons are the primary target for TBEV infection in the central nervous system. However, knowledge about this viral infection and virus-induced neuronal injury is fragmental. Here, we directly examined the pathology that occurs after TBEV infection in human primary neurons. We exploited the advantages of advanced high-pressure freezing and freeze-substitution techniques to achieve optimal preservation of infected cell architecture. Electron tomographic (ET) reconstructions elucidated high-resolution 3D images of the proliferating endoplasmic reticulum, and individual tubule-like structures of different diameters in the endoplasmic reticulum cisternae of single cells. ET revealed direct connections between the tubule-like structures and viral particles in the endoplasmic reticulum. Furthermore, ET showed connections between cellular microtubules and vacuoles that harbored the TBEV virions in neuronal extensions. This study was the first to characterize the 3D topographical organization of membranous whorls and autophagic vacuoles in TBEV-infected human neurons. The functional importance of autophagy during TBEV replication was studied in human neuroblastoma cells; stimulation of autophagy resulted in significantly increased dose-dependent TBEV production, whereas the inhibition of autophagy showed a profound, dose-dependent decrease of the yield of infectious virus.

Tick-borne encephalitis virus (TBEV), a member of the *Flaviviridae* family, genus *Flavivirus*, causes tick-borne encephalitis (TBE) in humans, a neuroinfection prevalent in large areas of Europe and North-eastern Asia. Humans develop a febrile illness, and a subset of cases progress to neurological manifestations ranging from mild meningitis to severe encephalomyelitis^{1,2}. Despite the medical importance of TBE, some crucial steps in the development of encephalitis remain poorly understood. TBEV is mainly transmitted to the host when infected ticks feed. Virus replication is first detected in draining lymph nodes; this is followed by development of viremia; during the secondary viremia phase, the virus crosses the blood-brain barrier (BBB) and enters the brain³. Major hallmarks of TBEV neuropathogenesis are neuroinflammation, followed by neuronal death^{4,5}, and disruption of the BBB^{3,6}. Neuronal injury may be directly caused by viral infection, but destruction has also been attributed to infiltrating immunocompetent cells (mainly CD8⁺ T-cells), inflammatory cytokines, and activated microglial cells^{2,7,8}. Tissue culture models of TBEV infections in primary neurons can distinguish between injuries caused by the virus and those caused by the immune response^{9,10}. Various cellular models, including neuronal cell lines, primary cultures of embryonic or neonatal mouse and rat neuronal cells, and neurons derived from embryonic stem cells, have been used to explore infections with various neurotropic viruses (e.g., polio, herpes simplex type 1, varicella-zoster, West Nile, Japanese encephalitis, and rabies)^{10–13}. We previously examined

¹Institute of Parasitology, Biology Centre of the Academy of Sciences of the Czech Republic, Branišovská 31, CZ-37005 České Budějovice, Czech Republic. ²Faculty of Science, University of South Bohemia, Branišovská 31, CZ-37005 České Budějovice, Czech Republic. ³Department of Virology, Veterinary Research Institute, Hudcova 70, CZ-62100 Brno, Czech Republic. *These authors contributed equally to this work. Correspondence and requests for materials should be addressed to D.R. (email: ruzekd@paru.cas.cz)

TBEV infections in human neural (neuroblastoma, glioblastoma, and medulloblastoma) cell lines¹⁴. On the ultrastructural level, the infection caused massive morphological changes in cells, including the proliferation and rearrangement of rough endoplasmic reticulum (RER) and signs of apoptosis or necrosis¹⁴.

Recently, replication features of neurotropic flaviviruses, West Nile virus, Japanese encephalitis virus, and TBEV were compared in primary mouse neuronal cultures. Viral antigen accumulation in neuronal dendrites was induced to a greater extent in a TBEV infection than in infections with the other flaviviruses¹⁵. TBEV replication induced characteristic ultrastructural membrane alterations in neurites, known as laminal membrane structures (LMSs)¹⁵. However, conventional chemical fixation for sample visualization presents obstacles in obtaining sufficient morphological detail¹⁶. Therefore, in the present study, we exploited the advantages of high-pressure freezing and freeze-substitution techniques to improve the preservation of virally modified structures in TBEV-infected neurons.

Here, we visualized TBEV infections in primary human neurons in three-dimensional (3D) space at ultrastructural resolution with electron tomography. To the best of our knowledge, this study was the first to visualize the architecture of cellular components involved in TBEV replication and transport in neurons and the major ultrastructural changes that occur in response to TBEV infections. These novel data revealed the neuronal injury caused by TBEV infections, independent of the immune system response. Our results may facilitate the development of novel strategies for treating this serious human neuroinfection.

Results

Replication of TBEV and distribution of virus antigen in human neurons. We employed a plaque assay to determine TBEV infection and replication kinetics in human neurons (HN; Fig. 1A). The HNs were infected with TBEV, and at 0, 3, 5, 7, and 12 days post infection (p.i.), cell supernatants were collected. Productive TBEV replication was detected in the form of released virions on day 3 p.i. The virus titer in the culture supernatant remained the same until the end of the experiment (Fig. 1A).

Immunofluorescence staining was used to assess viral antigen distribution in HNs. Viral antigen was not detected in mock-infected HNs. Immunofluorescence staining revealed that TBEV antigen was mostly distributed diffusely throughout the entire neuron bodies at early time points after infection (Fig. 1B). However, at later time points, we observed brightly stained aggregates of viral antigen in some cells (Fig. 1B). A co-localization study with protein disulphide isomerase family a, member 3 (PDIA3) antigen (also known as Erp57, Er-60, and GRP58) suggested that the viral antigen was localized primarily in the hypertrophied, rearranged RER. Occasionally, we observed viral antigen accumulation in the dendrites of TBEV-infected HNs (Figs. 1B,2A,B, yellow arrows). Viral antigen also accumulated in association with RER alterations, such as large whorl formations (Fig. 2B, white arrows), or in places that exhibited a local loss of network structure (Fig. 2C). In the latter locations, RER alterations were accompanied by the presence of numerous longitudinal fibers (white arrows) that were positively immunolabeled with anti-viral protein E (Figs. 1B,2C).

TBEV-induced RER alterations and formation of tubule-like structures in HNs. Mock-infected and TBEV-infected HNs were examined with transmission electron microscopy at two time points (3 and 12 days p.i.) to delineate TBEV-induced morphological structures that were associated with early and late phases of the infection. Compared to mock-infected HNs, TBEV-infected cells exhibited a broad range (a complex set) of virus-induced subcellular structural changes at both time points.

At 3 days p.i., HN RER cisternae contained several resident virions (approximately 45 nm in diameter), virus-induced vesicles, and tubule-like structures (Fig. 3). Virus-induced vesicles were often arranged in two tightly apposed cisterns of the RER. Some of these vesicles contained electron-dense material, which represented newly-formed nucleocapsids (Fig. 3C,D). In other parts of the RER compartment, the cisterns accommodated tubule-like structures that ran either in parallel lines or in different directions (Fig. 3C,D, movie S1). The tubule-like structures measured 22 ± 1.3 nm ($N = 51$) in diameter.

The tubule-like structures were frequently observed at both investigated time points in TBEV-infected HNs. In several cases, tubule-like structures with different diameters (e.g., 22 ± 1.3 nm and 43.8 ± 4.3 nm, $N = 7$) were observed separately in the RER cisternae of single cells (Fig. 4A–D, movie S2); typically, virus-induced vesicles and virions were observed in neighboring RER spaces (Fig. 4B–D; Fig. 3C,D).

A prominent morphological change in TBEV-infected HNs was proliferation of the RER membranes that harbored sites of TBEV replication (Fig. 5A,B, movie S3). The proliferative parts of the RER were devoid of ribosomes (Fig. 5A, inset; movie S3, white arrows). At the later time point (12 days p.i.), proliferated RER had rearranged into large whorls (Fig. 5C,D, movie S4). The 3D reconstruction showed complex, lamellar whorls that enclosed a central space containing the cytoplasm of the same structure, and an electron-density as outside, limited by four membranes (Fig. 5D, light blue, movie S5). Numerous flattened ER cisternae were located on the periphery (Fig. 5D, blue). Electron tomography confirmed a continuation/connection of this peripheral part with the RER space, which accommodated TBEV-induced structures (vesicles or tubule-like structures) (Fig. 5D). These observations suggested that the membranous whorls were formed from the peripheral parts of the ER due to extensive ER stress. The large whorls did not contain virions or virus-induced structures. The central part of the whorl had features of an autophagosome, but it did not show signs of degraded content. Finally, we observed a tiny

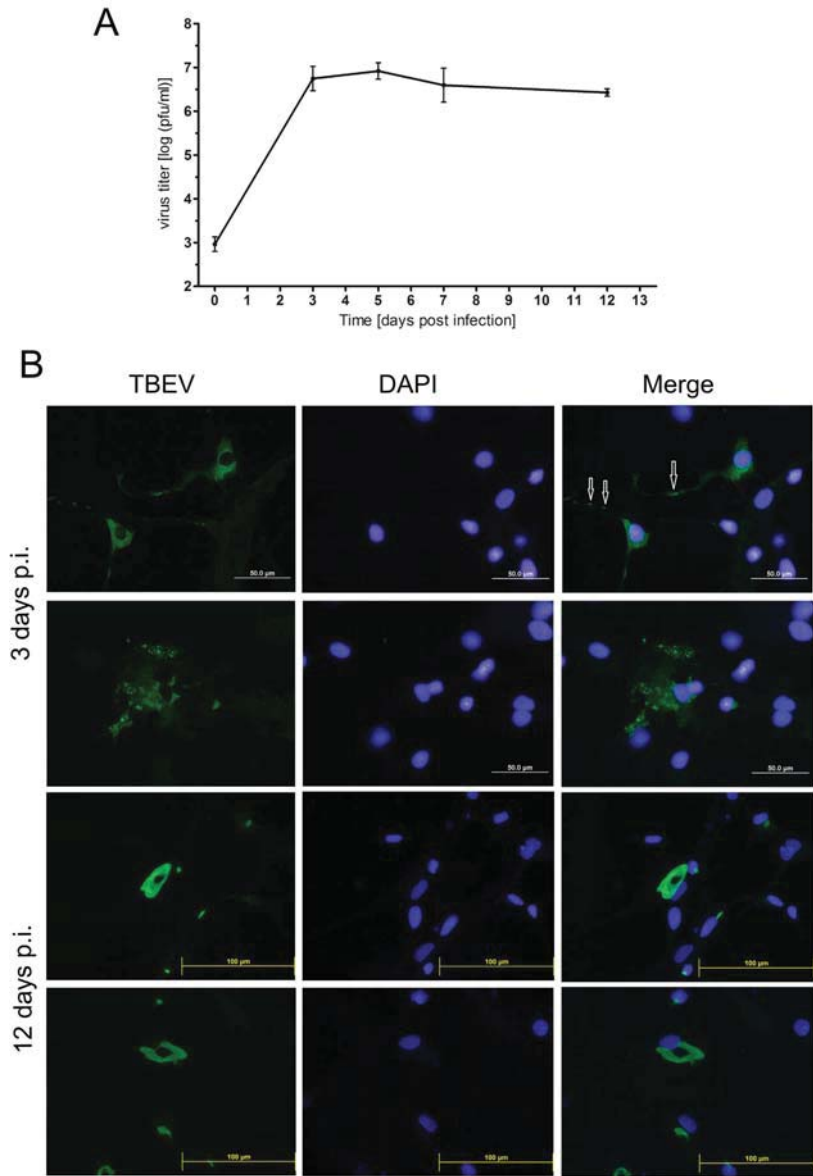


Figure 1. TBEV can infect human neurons. (A) TBEV titers in culture supernatants from HNs collected at 0, 3, 5, 7, and 12 days post-infection (p.i.) were determined in plaque assays with porcine kidney stable cells. Viral titers are expressed as pfu/ml. Data represent means \pm SEM. (B) HNs grown and fixed on slides at days 3 and 12 p.i. were stained with anti-flavivirus envelope antibody (green) and counterstained with DAPI (blue). TBEV-infected HNs immunostained with flavivirus-specific antibody demonstrated virus replication in the cytoplasm at an early time point (3 days p.i.); antigen accumulated into aggregates at later a time point (12 days p.i.). Mock-infected HNs stained with primary and secondary antibodies were used as a negative control, and did not exhibit any TBEV antigen staining (not shown). The arrows indicate accumulation of viral antigen in dendrites of the infected HNs.

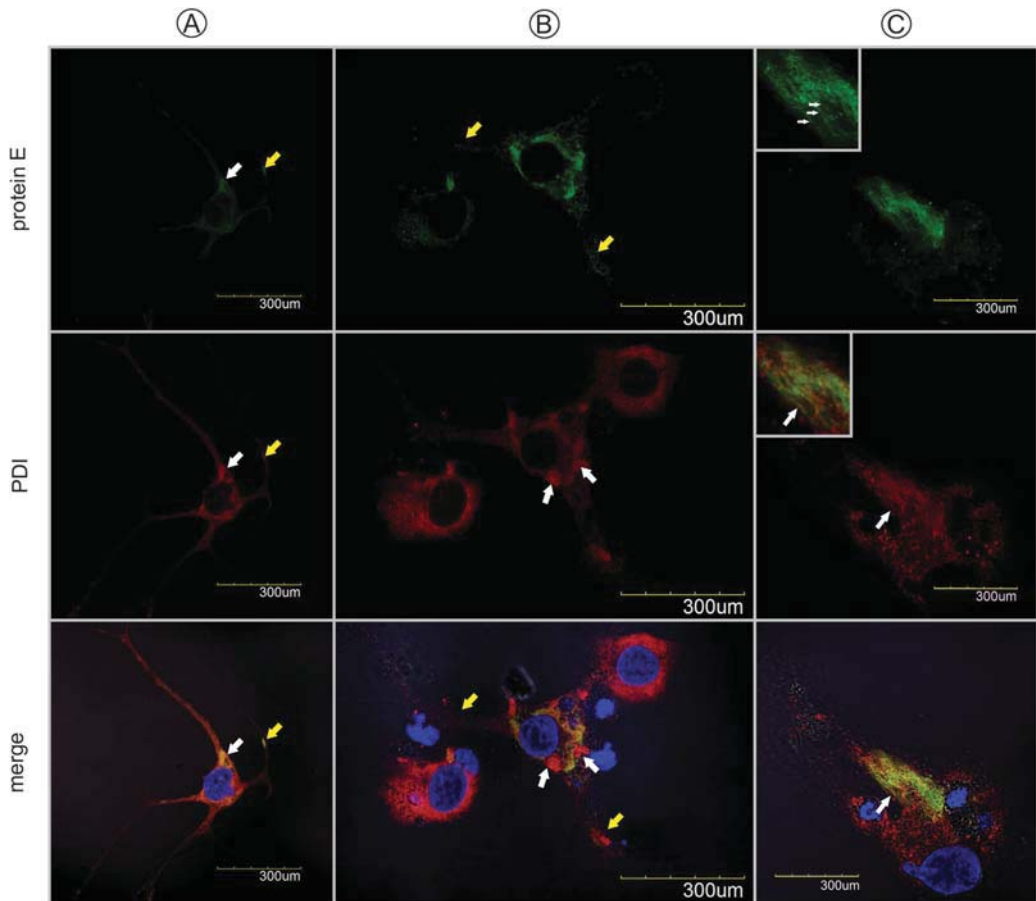


Figure 2. Confocal images of human neurons infected with TBEV. Neurons were fixed at (A,B) 3 days p.i. and (C) 12 days p.i. and double immunolabeled with antibodies against TBEV protein E (green) (*top panels*), PDIA3 (red) (*middle panels*), and (*merge panels*) counterstained with DAPI. (A) Replication complexes were observed in the perikaryon (white arrow) and dendrites (yellow arrow). (B) Infected cells with intact endoplasmic reticulum networks were observed next to infected cells with large whorls (white arrows). (C) Localization of viral protein E in the numerous longitudinal fibers (white arrows) associated with the ER.

connection between two primary virus-induced structures, as shown in detail in a slice of the tomogram (Fig. 5E) and in the 3D model (Fig. 5F; movie S5).

Signs of autophagy observed in TBEV-infected HNs. In several cases, particularly in HN extensions, which represented dendrites, we observed that the TBEV replication space was enclosed by flattened ER cisternae. This suggested the formation of autophagosomes that sequestered cell structures damaged by TBEV. Electron tomography was performed to view the complex architecture of these structures. In most cases, the sequestration was incomplete, as shown in Fig. 6A–E (movie S6 and movie S7), even when the projection images suggested that the structure might be interpreted as an autophagic vacuole (Fig. 6B). The TBEV particles and virus-induced vesicles resided in the RER (Fig. 6A,C,D, black arrows), but the enclosing ER cisternae lacked ribosomes (Fig. 6D, white arrows). Lipid droplets were also found associated with these structures (Fig. 6D,E). No morphologically similar structures were found in the extensions of mock-infected HNs (Fig. 6F). However, in the perikaryon (Fig. 6G), several autophagosomes or autophagolysosomes (with signs of degraded material) were observed. In some TBEV-infected

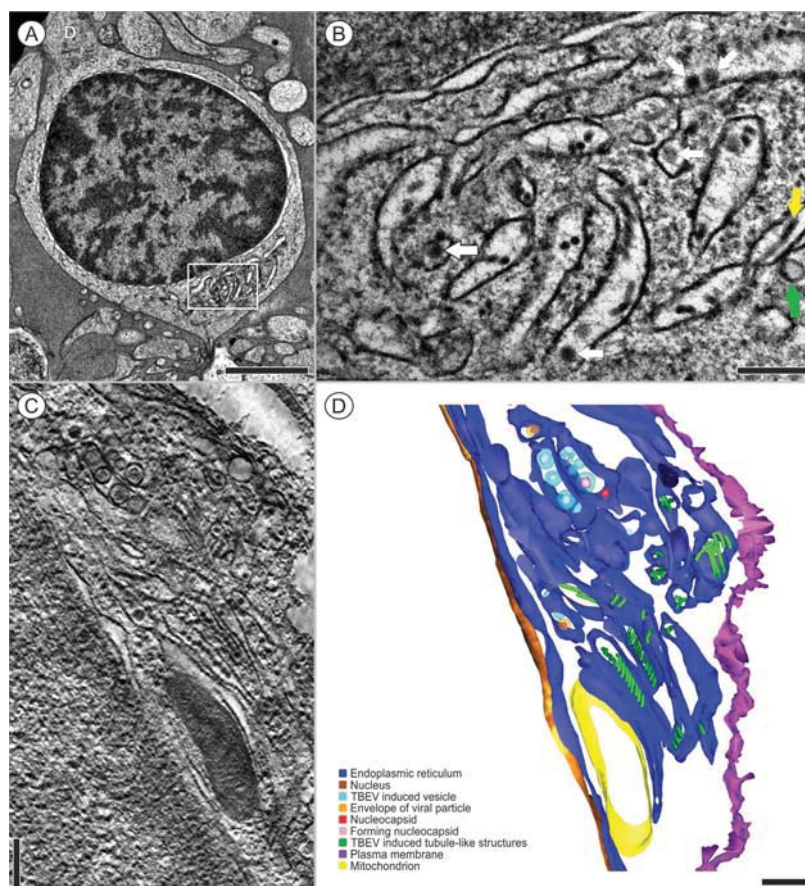


Figure 3. HN_s infected with TBEV for 3 days. (A) A neuron with two cytoplasmic extensions on opposite sides of the cell body. D- Dendrite. (B) Detail of the boxed region in (A) shows the RER, which contains viral particles (44.75 nm, $n = 4$, white arrows), virus-induced vesicles (green arrow), and tubule-like structures (yellow arrow). (C,D) The presence of tubule-like structures (22 ± 1.3 nm, $N = 51$) inside the RER. (C) A slice of the tomogram was rendered as (D) a 3D reconstruction of a single axis of the tomogram. A series of images were collected in a $\pm 65^\circ$ tilt range with 0.65° increments. Pixel resolution: 1.1 nm. This single-axis tomogram is shown in movie S1. Bars: (A) 2 μ m, (B-D) 200 nm. The transmission electron microscope images were acquired with (A,B) a JEOL 1010 80 kV and (C,D) a JEOL F2100 200 kV.

HN extensions, we observed autophagosomes with all the typical morphological features (Fig. 7 and movie S8). These autophagosomes were limited by numerous membranes that did not have ribosomes, but they resembled rearranged, small, membranous ER whorls. In the 3D reconstruction, we have identified numerous membranes that sequestered intact mitochondria, lipid droplets, and vacuoles within the inner space with TBEV particles (Fig. 7B).

Autophagy induction enhances TBEV replication. To study whether autophagy plays a role in TBEV replication, we treated human neuroblastoma cells with rapamycin, an autophagy inducer. The cells were subsequently infected with TBEV at m.o.i. 0.1 pfu per cell. Culture supernatants were harvested after 24, 48, and 72 hours, and viral titers were determined by plaque assay. The viral yields were increased in cells treated with a range of concentrations rapamycin on day 2 and 3 p.i. (Fig. 7C). The induction levels were quite high reaching $1.5 \log_{10}$ pfu/ml higher titers in cells treated either with 0.05 or 0.1 μ M of rapamycin in comparison with the untreated control on day 3 p.i. (Fig. 7C).

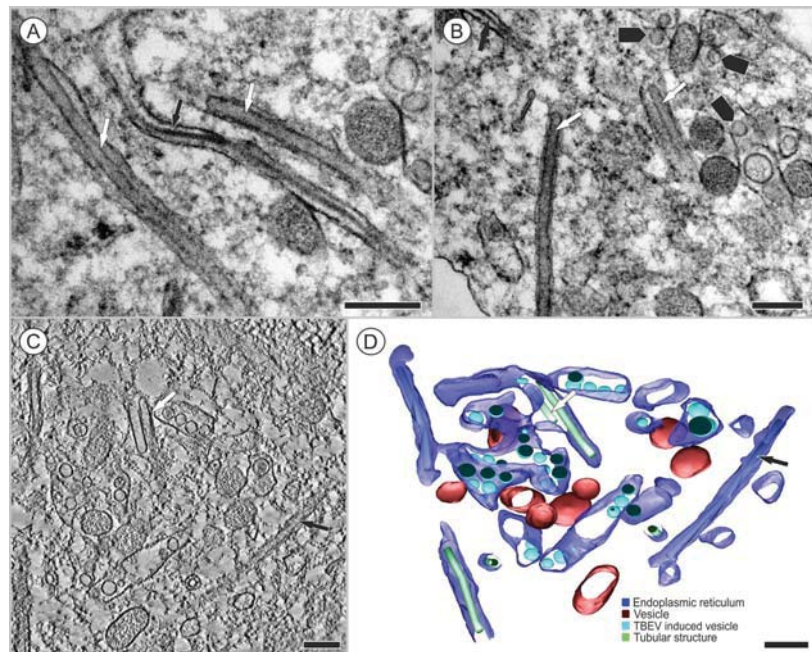


Figure 4. Tubule-like structures of different diameters were localized inside a single neuron infected with TBEV. Transmission electron microscope images were acquired at (A) 3 days p.i. or (B) 12 days p.i. (A) Inside the ER, tubules of 43.8 ± 4.3 nm ($N=7$) in diameter (white arrows) were observed; other cisternae contained tubules of 22 ± 1.3 nm in diameter (black arrow). (B) The TBEV infection induced ER rearrangements (black arrowheads). (C) A slice of the tomogram and (D) a 3D reconstruction of a single axis tomogram. Tilt series images were collected in the $\pm 65^\circ$ tilt range with 1° increments. Pixel resolution: 0.8 nm. This single-axis tomogram is shown in movie S2. Bars: 200 nm. (A–D) The transmission electron microscope images were acquired with a JEOL F2100 200kV.

Suppression of autophagy reduces TBEV replication. To investigate the effect of spautin-1, a compound known to be an effective autophagy inhibitor, on viral replication in the neuronal cells, we tested its effects on TBEV growth in human neuroblastoma cells. The cells pretreated with a range of concentrations of spautin-1 for 30 min, were infected with TBEV at m.o.i. 0.1 pfu per cell, after which the incubation was continued in the presence of the drug. Culture supernatants were harvested after 24, 48, and 72 hours, and viral titers were determined by plaque assay. Treatment with a range of concentrations of spautin-1 showed a profound, dose-dependent inhibition of the yield of infectious virus, with statistically significant drops in TBEV titer of more than two orders of magnitude at the highest spautin-1 concentration ($10 \mu\text{M}$) on day 3 p.i. (Fig. 7D).

Transport of the TBEV in the neuron. One projection image of a 40-nm thick ultrathin section showed that, in the extensions of TBEV-infected HNs, two virions (48.2 nm and 48.9 nm diameters, with nucleocapsids of 30.3 and 30.9 nm diameters, respectively) were located separately inside vacuoles that were directly connected to cellular microtubules (Fig. 8A). The presence of that connection was confirmed by examining a double-axis electron tomography ($\pm 60^\circ$ tilt range with 0.6° increments, pixel resolution: 0.55 nm), and then creating a 3D reconstruction (Fig. 8B, movie S9). Both connections are shown in detail on slices of the tomogram (Fig. 8C,D, arrows). Extensions of mock-infected HNs contained vesicles with electron-dense cores with diameters that ranged from 70 to 90 nm; those vesicles were observed in direct contact with the cytoplasm (Fig. 9A,B). Electron-dense granules (similar to the vacuoles that contained virions in Fig. 8A) were found in close proximity to bunches of microtubules and mitochondria, as seen in the transverse section (Fig. 9A). Other vesicles, 43.8 nm in diameter, but different in structure from virions (for comparison see Fig. 8A), were observed in the control cells (Fig. 9C).

We used nocodazole to assess the effect of microtubule destabilizing agent on virus growth in human neuronal cells. Nocodazole is known to induce depolymerization of actin filaments and microtubules. Human neuroblastoma cells pretreated with a range of non-cytotoxic concentrations of nocodazole

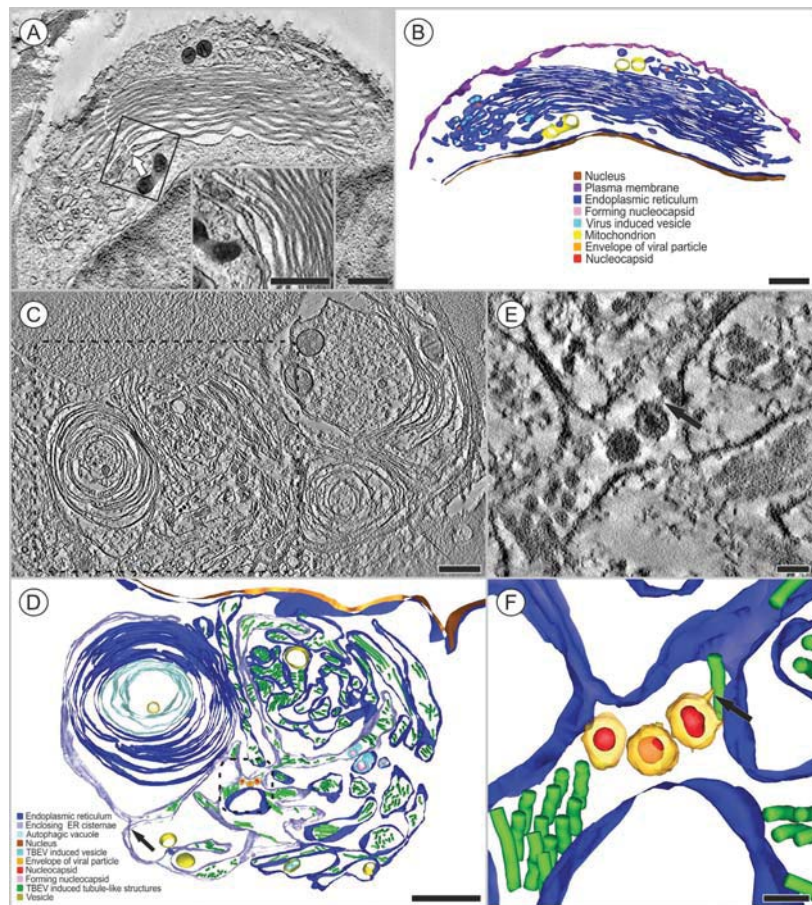


Figure 5. Proliferation of the endoplasmic reticulum observed in HNs infected with TBEV. Transmission electron microscope images were acquired at (A,B) 3 days p.i. and (C–E) 12 days p.i. (A) TBEV particles and TBEV-induced vesicles are located inside the proliferated and reorganized cisterns of the rough endoplasmic reticulum; the boxed region is enlarged in the inset. (B) The image in (A) was rendered as a colored 3D model. (C) Large whorls are clearly observed in abnormal endoplasmic reticulum. (D) The boxed region in (C) is rendered in a 3D model to clarify the different components. (D) The lamellar whorls are surrounded by cisternae (light purple) arising (arrow) from the rough endoplasmic reticulum (blue), which accommodates tubule-like structures (green). The central part of the whorls comprises concentric circles of flattened ER cisternae (light blue). We observed several lipid droplets (yellow) in proximity of the whorls. (E) Detailed image of the boxed region in (D) shows the connection between a TBEV particle and a tubule-like structure (arrow) inside the rough endoplasmic reticulum. (F) The image in (E) was rendered as a colored 3D model. (A) A single axis tomogram, $\pm 65^\circ$ tilt range with 0.65° increments, pixel resolution: 2.2 nm; (C) a single axis tomogram, 2×2 montage, $\pm 65^\circ$ tilt range with 1° increments, pixel resolution: 0.8 nm. Bars: (A–D) 500 nm, (E,F) 50 nm. (A–F) The transmission electron microscope images were acquired with JEOL F2100 200 kV.

for 30 min were infected with TBEV at m.o.i. 0.1 pfu per cell, after which the incubation was continued in the presence of the drug. Culture supernatants were harvested after 24, 48, and 72 hours, and viral titers were determined by plaque assay. Treatment with a range of concentrations of nocodazole showed a profound inhibition of the yield of infectious virus, with statistically significant drops in TBEV titer of more than two orders of magnitude at the all concentrations of nocodazole on days 2 and 3 p.i. (Fig. 8E).

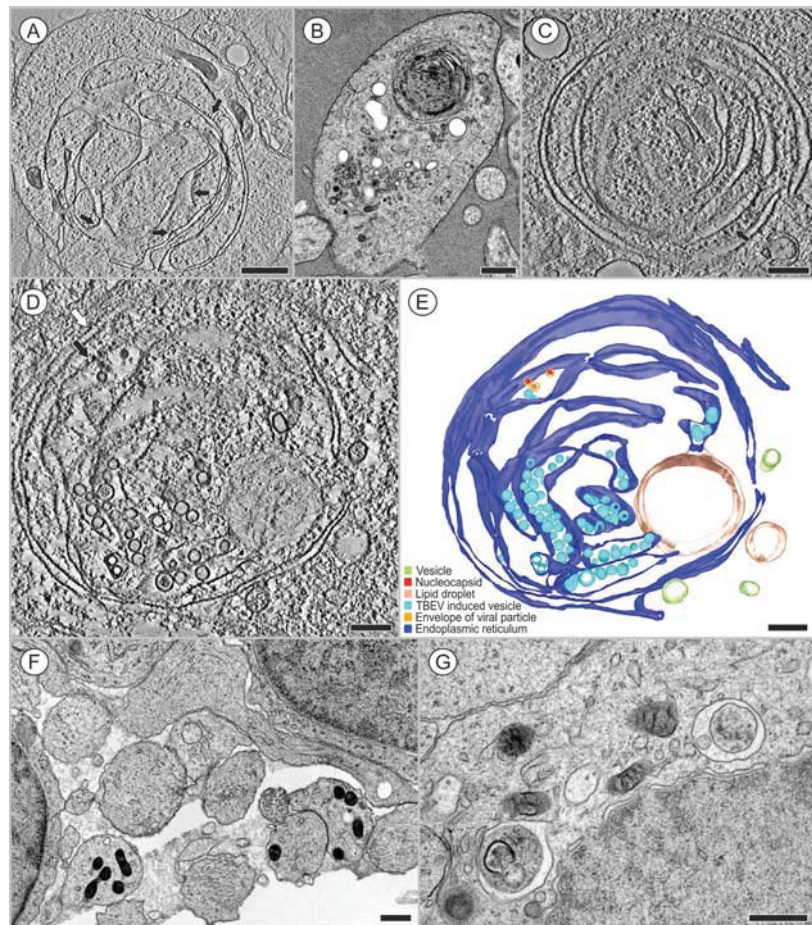


Figure 6. Formation of autophagic vacuoles in HNs infected with TBEV. Transmission electron microscope images were acquired at (A–C) 3 days p.i., (D,E) 12 days p.i., and in (F,G) mock-infected cells. (A,B) The RER (ribosomes are indicated with black arrows), which contain TBEV particles and virus-induced structures, were nearly completely sequestered by peripheral cisterns (see electron tomography in supplement) in neuronal extensions. (C) Detail of (B) shows the coiled RER with TBEV-induced structures. (D) The cisterns of the RER (ribosomes indicated with black arrow) with replicating TBEV particles and virus-induced vesicles are surrounded by one flattened ER cistern that nearly encloses this space, and a lipid droplet. Enclosing cisternae of the ER were devoid of ribosomes (white arrow). (E) 3D model of (D). (F) Similar vacuoles/autophagosomes were not observed in control neuronal extensions. (G) Several vacuoles that sequestered cell parts (debris, fragments of degraded membranes) were found in the cell body of control neurons. Bars: (A,B,F,G) 500 nm, (C–E) 200 nm. (A,C,D) Slices of a single axis tomogram; $\pm 65^\circ$ tilt range with 1° increments, pixel resolution: (A) 1.1 nm, (C) 0.7 nm; (D) 0.8 nm. Transmission electron microscope images were acquired with (A,C–E) JEOL f2100 200 kV and (B,F,G) JEOL 1010 80 kV.

Discussion

We demonstrated that neuronal TBEV infections produced cell-free, infectious virus by using the supernatant from TBEV-infected HNs to infect PS cells and measuring the viral titers with a plaque assay. TBEV replication was detected in the form of released virions on day 3 p.i., and the culture supernatant maintained a virus titer of approximately 10^7 pfu/ml until the end of the experiment (Fig. 1A). This finding suggested that the TBEV-infected HNs had apparently transitioned from an acute to a persistent infection. In a previous study, we compared TBEV growth in human neuroblastoma, glioblastoma,

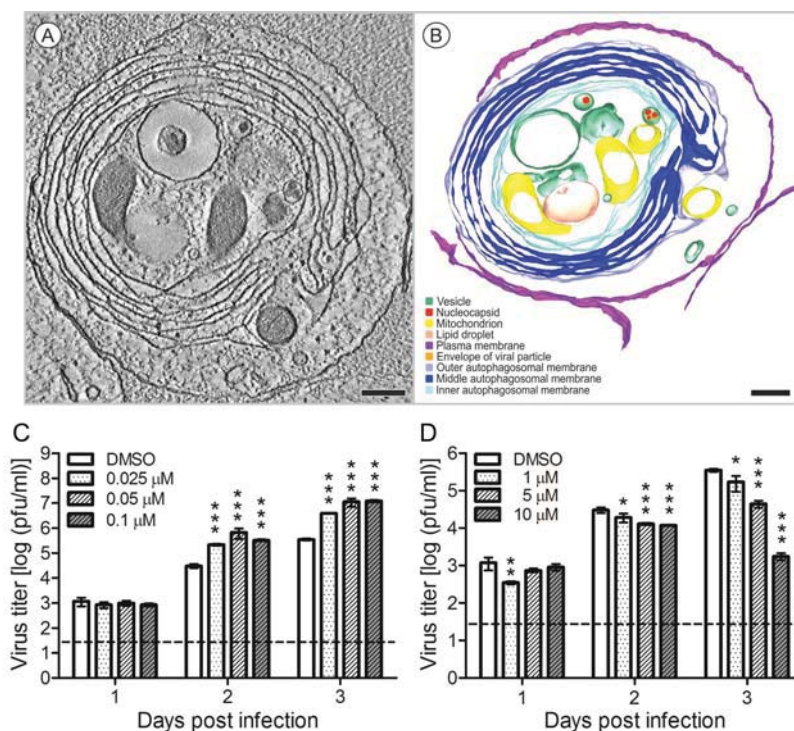


Figure 7. An autophagosome in a neural extension observed 3 days after TBEV infection. The cytoplasm contains mitochondria and TBEV particles in vacuoles, encircled by several double membranous structures, apparently of RER origin (but devoid of ribosomes). (A) A slice of a single axis tomogram; $\pm 65^\circ$ tilt range with 0.6° increments, pixel resolution: 0.8 nm. (B) A 3D model of (A). Bars: 200 nm. (A,B) Transmission electron microscope images were acquired with JEOL F2100 200 kV. (C,D) Autophagy enhanced TBEV production in human neuroblastoma cells. The cells were pretreated with the solvent control (DMSO), rapamycin (0.025, 0.05, or $0.1 \mu\text{M}$) (C), or spautin-1 (1, 5, or $10 \mu\text{M}$) (D) then infected with TBEV at m.o.i. of 0.1 pfu per cell for 24, 48, or 72 hours. The culture supernatants were collected for plaque assay on PS cells. The virus titers (pfu/ml) are shown as the means \pm SEM. The horizontal dashed line indicates the minimum detectable threshold. * $p < 0.05$; ** $p < 0.01$; *** $p < 0.001$.

medulloblastoma, and PS cells. That study showed that virus replication in neural cell lines was more than 100 times more efficient than in the PS cells¹⁴. In the present study, we showed that primary HNs were also highly sensitive to TBEV infection, and they also produced high virus titers.

A previous study in primary mouse neurons showed that TBEV antigen accumulated in the dendrites of infected neurons¹⁵. Viral proteins were synthesized principally in the neuronal cell bodies in the early stages of infection, but they were distributed to dendrites later¹⁵. In the present study, TBEV-infected HNs also showed antigen accumulation in dendrites (Fig. 1B, arrows), but this was not a frequent event. At early time points after infection, virus antigen was present in practically the whole body of the neuron (Figs. 1B,2); at later time points, antigen accumulation appeared mainly in highly reorganized, proliferated RER (demonstrated in the co-localization experiments with the PDIA3 antigen) (Fig. 2), and only occasionally in dendrites. Viral protein accumulation in dendrites may affect neural function¹⁵ and TBEV infections can arrest neurite outgrowth¹⁷. It was hypothesized that viral protein accumulation in dendrites might affect the distribution and function of host proteins, which in turn, might cause neural dysfunction and cellular degeneration¹⁵.

Our results suggested that vesicles containing TBEV particles were transported in infected neurons, based on observations that TBEV-containing vesicles were associated with microtubules in HNs (Fig. 8A–D). In human neuroblastoma cells, non-cytotoxic concentrations of nocodazole, a compound which disrupts microtubules by binding to β -tubulin and preventing formation of one of the two inter-chain disulfide linkages and thus inhibiting microtubules dynamics, resulted in significant reduction

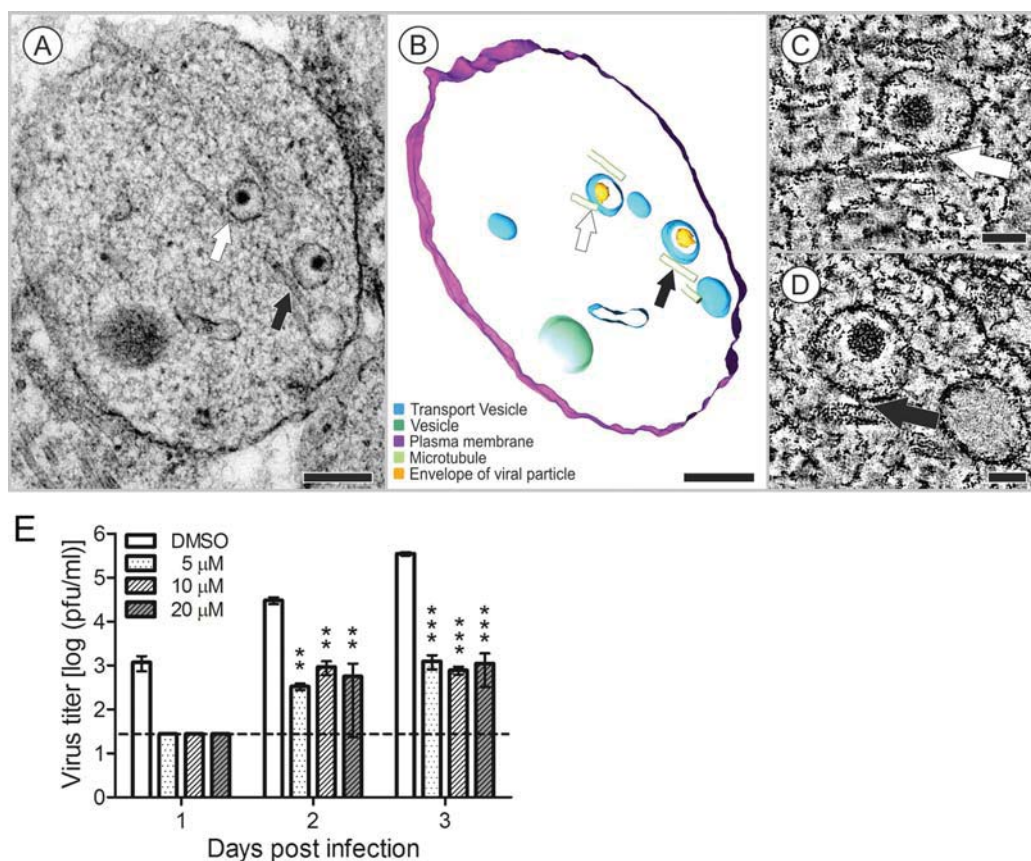


Figure 8. Two vacuoles that accommodated TBEV particles in a neuronal extension at 12 days after infection. (A–D) Arrows indicate connections between vacuoles and microtubules. (A) The projection image and (B) the 3D model. (C,D) Images show slices of a double-axis tomogram acquired with a $\pm 60^\circ$ tilt range in 0.6° increments; pixel resolution: 0.55 nm Bars: (A,B) 200 nm; (C,D) 50 nm. Transmission electron microscope images were acquired with (A) JEOL 1010 80 kV and (C,D) JEOL F2100 200 kV. (E) Nocodazole treatment inhibits TBEV replication in human neuroblastoma cells. The cells were pretreated with the solvent control (DMSO), or nocodazole (5, 10, or 20 μ M) then infected with TBEV at m.o.i. of 0.1 pfu per cell for 24, 48, or 72 hours. The culture supernatants were collected for plaque assay on PS cells. The virus titers (pfu/ml) are shown as the means \pm SEM. The horizontal dashed line indicates the minimum detectable threshold. ** $p < 0.01$; *** $p < 0.001$.

in virus infectivity (Fig. 8E). Viral spread in neurons is generally mediated by fast axonal transport, a microtubule-associated, anterograde and retrograde transport system. In West Nile virus (WNV) infections, transneuronal viral spread required axonal release of viral particles. WNV underwent bidirectional spread in neurons, and axonal transport promoted viral entry into the CNS¹⁸.

Here, we also described the morphology and 3D organization of TBEV-induced, tubule-like structures located in the RER of infected HNs (Figs. 3B,4A–D). Similar structures were previously demonstrated in the RER of other vertebrate or arthropod cells infected with TBEV¹⁹, Langat virus²⁰, and mosquito-borne flaviviruses^{16,21,22}. In a previous study, we observed virus-induced vesicles and viral particles directly attached to tubule-like structures in the RER of TBEV-infected human primary astrocytes¹⁹. The tubule-like structures were only occasionally seen in acutely infected cells, but the number of tubules increased dramatically in persistently infected cells²⁰. Unlike previous studies, we frequently observed the presence of tubule-like structures in TBEV-infected neurons. To the best of our knowledge, this study

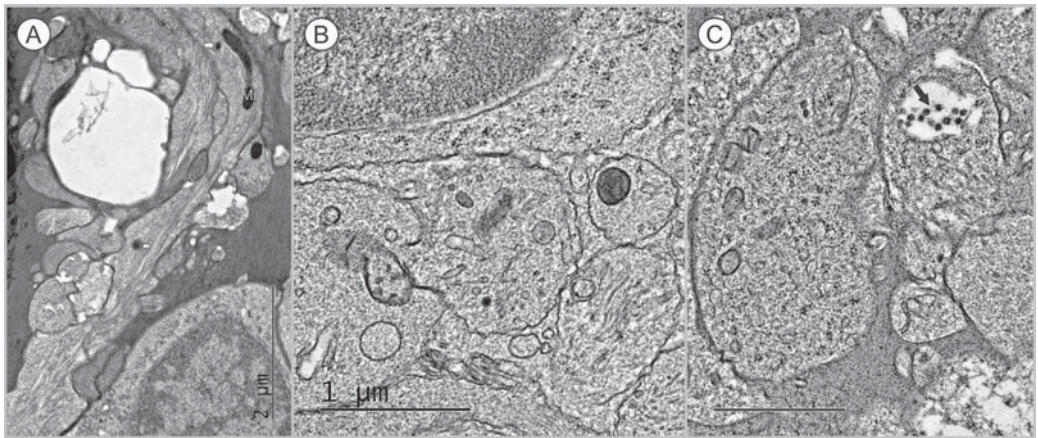


Figure 9. Mock infected HNs examined at 3 days p.i. (A,B) HN extensions contained a few probable secretion granules with electron-dense cores, with diameters of (A) about 70 nm and (B) 90 nm, that were in direct contact with the cytoplasm. (C) Different vesicles of 43.8 nm ($n = 5$) in diameter were located outside the cells (black arrow). Bar 1 μm . (A–C) Transmission electron microscope images were acquired with JEOL 1010 80kV.

was the first to demonstrate the simultaneous presence of two sizes of tubule-like structures in the RER of single infected cells (Fig. 4A–D). Inside the RER, we observed tubules that were 43.8 ± 4.3 nm ($N = 7$) in diameter, and in other cisternae, we observed tubules that were 22 ± 1.3 nm in diameter (Fig. 4A–D). Previous studies reported tubule-like structures that ranged from 50 to 100 nm in diameter and from 100 nm to $3.5 \mu\text{m}$ in length^{20–23}. In TBEV-infected human astrocytes, we previously observed tubule-like structures of 17.9 nm (± 0.2 nm) in diameter¹⁹. The function of tubule-like structures is not clear. These structures may represent features of replication, aberrant structures, or features of a cellular process that aims to restrict the infection²⁰. With immunofluorescence and confocal microscopy, we observed fibrillary structures composed of viral E protein in cisternae of the ER; these structures suggested that E protein was present in the tubule-like structures (Figs. 1B,2). The functional contribution of these tubule-like structures to TBEV replication should be addressed in future studies.

Our detailed 3D ultrastructural analysis clearly demonstrated that the TBEV infection triggered a remarkable alteration in the ER membrane structures of HNs (Fig. 5B,D). Previous studies have shown alterations in ER membranes by flaviviruses, which included formations of vesicle pockets and convoluted structures that represented a platform for viral RNA replication and virion assembly^{15,24,25}. These replication compartments also shielded double-stranded RNA from host cell-intrinsic surveillance mechanisms^{24–26}.

In TBEV-infected mice, Hirano *et al.*¹⁵ described characteristic ultrastructural changes in neurite membranes, called LMSs. They hypothesized that LMSs were formed by membrane reconstitutions triggered by the viral replication, and that the LMS might serve as a platform for dendritic viral replication and virion assembly¹⁵. In the present study, we observed TBEV replication sites in dendrites, but also in perinuclear regions of TBEV-infected HNs. However, our 3D tomography data strongly suggested that, in several cases, the TBEV replication sites were enclosed inside newly formed autophagosomes. Moreover, we observed virions inside autophagosomes that were surrounded by numerous membranes (Figs. 5,6,7) with many typical morphological features. Autophagosome-limiting membranes did not have ribosomes, and they always had two or more limiting membranes²⁷. Additionally, we observed interactions with lipid droplets (LDs)²⁸ in both newly forming autophagosomes and fully-formed autophagosomes of TBEV-infected HNs. A recent report noted the existence of a physical connection between the endoplasmic reticulum and newly forming autophagosomes^{29,30}. We confirmed this observation (Fig. 5C,D and Fig. 6).

Upon autophagy induction, the initial event is the formation of a membranous cistern called the phagophore, or isolation membrane. Autophagy begins with the isolation of double-membrane structures in the cytoplasm. Later, these membrane structures elongate and mature. The elongated double-membranes form autophagosomes (large vesicles with diameters of 500–1500 nm in mammalian cells), which become mature with acidification; then, they fuse with lysosomes to become autolysosomes. The sequestered content is then degraded by lysosomal hydrolases³¹.

There are many proposals for the role of autophagy during virus infection in neurons. In post-mitotic, long-lived cell types, such as neurons, basal and stress-induced autophagy may be particularly important for maintaining cellular health. In addition, it represents an important neuronal antiviral defense mechanism for the sequestration and elimination of viral proteins, viral particles, and viral replication complexes³². Thus, autophagy represents an adaptive, pro-survival process, rather than a maladaptive, pro-death response, during CNS viral infection³². Autophagy has been shown to restrict the replication of several viruses in neurons, including Rift Valley fever virus³³, Sindbis virus³⁴, and herpes simplex virus type 1³⁵. However, the growth of WNV has been shown to be independent of WNV-induced autophagy in neuronal cultures³⁶. Although autophagy is a cellular homeostatic mechanism involved in the antiviral response, it can be also subverted to support viral growth. Virus-induced autophagy promoted the replication of dengue virus^{37,38}, enterovirus 71³¹, poliovirus, and coxsackievirus B4³⁹. Japanese encephalitis virus growth is dependent on autophagy activation during the early stages of infection⁴⁰. Our study was the first to demonstrate that autophagy occurred during TBEV replication in HNs, and is also the first report that autophagy enhances TBEV replication. We treated TBEV-infected neuroblastoma cells with rapamycin (inducer of autophagy, as inhibition of mTOR mimics cellular starvation by blocking signals required for cell growth and proliferation), and spautin-1 (highly specific and potent autophagy inhibitor in mammalian cells, which promotes the degradation of Vps34 PI3 kinase complexes by inhibiting two ubiquitin specific peptidases, USP10 and USP13 that target the Beclin1 subunit of Vps34 complexes) and investigated the effect of the treatment of TBEV growth. The induction of autophagy in human neuroblastoma cells by rapamycin increased TBEV replication (Fig. 7C), whereas the inhibition of autophagy by spautin-1 reduced significantly viral titers (Fig. 7D), indicating that autophagy positively regulates TBEV replication.

As mentioned above, we observed direct interactions between autophagosomes and LDs in TBEV-infected HNs (Fig. 6D,E, Fig. 7). A previous report showed that autophagosomes could target cellular lipid stores (LDs) to generate energy for the cell⁴¹. For example, dengue viral-infection-induced autophagy stimulated the delivery of lipids to lysosomal compartments, which resulted in the release of free fatty acids. These fatty acids underwent β -oxidation in the mitochondria to generate ATP, which produced a metabolically favorable environment for viral replication²⁸. Thus, aside from the many roles of autophagy in regulating cellular homeostasis, its regulation of lipid metabolism can represent a major contributor to robust viral replication⁴¹. The role of autophagy as a provider of free fatty acids as an energy source for RNA replication during viral infection will be a subject of our further studies.

In conclusion, we directly investigated the morphological changes induced by TBEV infections in HNs with advanced high-pressure freezing, freeze-substitution, and electron tomography techniques, with the purpose of achieving optimal preservation of ultrastructure for electron tomography visualization of cellular architecture. These methods enabled clear visualization of connections between microtubules and vacuoles that harbored TBEV virions in neuronal extensions, connections between tubule-like structures and virions, 3D organizations of proliferating endoplasmic reticulum membranes, membranous whorls, and the formation of autophagic vacuoles. These data provided insight into the process of TBEV-induced injury in HNs, and our findings will promote future studies that aim to understand the molecular mechanism of TBEV infection in the human CNS.

Methods

Virus and cells. The virus used in this study was the TBEV strain, Neudoerfl, kindly provided by Professor F. X. Heinz from the Medical University in Vienna. The strain was originally isolated from the tick *Ixodes ricinus* in Austria in 1971. The virus represents a prototype strain of the European subtype of TBEV and was characterized extensively, including its genome sequence and the 3D structure of its envelope protein E⁴². The virus underwent four passages in the brains of suckling mice before use in this study.

Human neurons (HNs) were isolated from the human brain and characterized by immunofluorescence with antibodies specific to neurofilament, microtubule associated protein 2 (MAP2), and β -tubulin III (purchased at passage zero from ScienCell Research Laboratories, Carlsbad, CA). HNs were propagated in Neuronal Medium (ScienCell) with 1% neuronal growth supplement and 1% penicillin/streptomycin (ScienCell) at 37°C and 5% CO₂. In all experiments, cells were used at passage zero.

Human neuroblastoma cells UKF-NB-4¹⁴ were cultured at 37°C and 5% CO₂ in Iscove's modified Dulbecco's medium (IMDM) supplemented with 10% fetal bovine serum (Sigma) and 1% mixture of penicillin and streptomycin (Sigma).

Porcine kidney stable (PS) cells⁴³ were cultured in L-15 medium supplemented with 3% newborn calf serum and 1% penicillin/streptomycin (Sigma-Aldrich) at 37°C.

Viral growth in HNs. HNs were seeded onto gelatin (0.2%) coated wells of 96-well plates at 20,000–25,000 cells/cm². After establishing the culture, cells were inoculated with the virus diluted in culture medium to 5 multiplicity of infection units (MOI). Virus-mediated cytopathic effect (CPE) was investigated with light microscopy. At 0, 3, 5, 7, and 12 days p.i., supernatant medium from appropriate wells was collected and frozen at –70°C. Viral titers were determined by plaque assay.

Plaque assay. PS cells were used to determine virus titers according to a protocol described previously, with minor modifications⁴⁴. Tenfold dilutions of the virus samples were placed in 24-well tissue culture plates, and suspended PS cells were added (5×10^4 cells per well). After incubating for 4 h, the suspension was overlaid with carboxymethylcellulose (1.5% in L-15 medium). After incubating for 5 days at 37 °C, the plates were washed with PBS, and the cells were stained with naphthalene black (Sigma Aldrich). Virus titer was expressed in units of pfu/ml.

Immunofluorescence staining. TBEV-infected and control HNs were grown on slides. Then, cells were fixed in 4% formaldehyde for 1 h at room temperature, rinsed three times in 0.1 M phosphate buffer (PB) with 0.02 M glycine, permeabilized with 0.1% Triton X-100 with 1% normal goat serum in 0.1 M PB for 30 min, and blocked with 5% normal goat serum. Cells were labeled with flavivirus-specific mouse mAb (1:250; Millipore) for 1.5 h at 37 °C. Flavivirus-specific mAb and rabbit anti-PDIA3 antibody (1:250, Sigma-Aldrich) were used for double labeling. After washing with ten-fold diluted blocking solution, the cells were labeled with goat anti-mouse secondary antibody conjugated with FITC (1:500, Sigma-Aldrich) or goat anti-rabbit secondary antibody conjugated with Atto 550 NHS (1:500, Sigma-Aldrich) for 1.5 h at 37 °C. The cells were counterstained with DAPI (1 µg/ml, Sigma-Aldrich) for 10 min at 37 °C, mounted in 2.5% 1,4-diazabicyclo(2.2.2)octane (Sigma-Aldrich), and examined with an Olympus BX-51 fluorescence microscope equipped with an Olympus DP-70 CCD camera. Confocal microscopy was performed with an Olympus FV-1000; serial Z-series images were acquired in blue, red, and green channels.

Transmission electron microscopy and electron tomography. TBEV-infected and control HNs were grown on sapphire discs. At either 3 or 12 days p.i., cells were high-pressure frozen in the presence of 20% BSA diluted in Neuronal Medium with a Leica EM PACT2 high-pressure freezer. Freeze substitution was carried out in 2% osmium tetroxide diluted in 100% acetone, as described previously¹⁹, with a Leica EM AFS2 at −90 °C for 16 h. The samples were then warmed at a rate of 5 °C/h, incubated at −20 °C for 14 h, and finally warmed again at the same rate to a final temperature of 4 °C. The samples were rinsed three times in anhydrous acetone at room temperature and infiltrated stepwise in acetone mixed with SPI-pon resin (SPI) (acetone:SPI ratios of 2:1, 1:1, 1:2, for 1 h at each step). The samples in pure resin were polymerized at 60 °C for 48 h.

Sections were prepared with a Leica Ultracut UCT microtome and collected on 300 mesh copper grids. Staining was performed with alcoholic uranic acetate for 30 min, and then, lead citrate for 20 min. Images were obtained with a JEOL 2100F or JEOL 1010 transmission electron microscope. For electron tomography, protein A-conjugated 10 nm gold nanoparticles (Aurion) were added to both sides of each section as fiducial markers.

Tilt series images were collected in the range of $\pm 60^\circ$ to 65° , with 0.6° to 1° increments. Images were acquired with a 200 kV JEOL 2100F transmission electron microscope equipped with a high-tilt stage and a Gatan camera (Orius SC 1000) and controlled with SerialEM automated acquisition software⁴⁵. Images were aligned based on the fiducial markers. Electron tomograms were reconstructed with the IMOD software package. Manual masking of the area of interest was employed to generate 3D surface models⁴⁶.

Autophagy stimulation and inhibition, and microtubule disruption. Stocks of rapamycin (Sigma-Aldrich) as an autophagy stimulator, spautin-1 (Sigma-Aldrich), an autophagy inhibitor, and nocodazole (Sigma-Aldrich) as a microtubule disruptor, were prepared in DMSO. Monolayers of human neuroblastoma cells in 96-well plates were pretreated with different concentrations of either drug (or DMSO as a negative control) for 30 min at 37 °C and infected with TBEV at a multiplicity of infection of 0.1 pfu per cell. Infection was always performed in triplicate. Supernatants were harvested at 24, 48, and 72 hours p.i. and titers were determined by plaque assay as described above.

Statistical analysis. Statistical analyses were performed using version 5.04 of the GraphPad Prism5 (GraphPad Software, Inc., USA). Data were transformed by use of the $X' = \log(X)$ formula and analyzed using one-way ANOVA (Dunnett's Multiple Comparison Test). p-values < 0.05 were considered significant.

References

- Mansfield, K. L. *et al.* Tick-borne encephalitis virus - a review of an emerging zoonosis. *J. Gen. Virol.* **90**, 1781–94 (2009).
- Růžek, D., Dobler, G., & Donoso Mantke, O. Tick-borne encephalitis: pathogenesis and clinical implications. *Travel Med. Infect. Dis.* **8**, 223–32 (2010).
- Růžek, D., Salát, J., Singh, S. K., & Kopecký, J. Breakdown of the blood-brain barrier during tick-borne encephalitis in mice is not dependent on CD8+ T-cells. *PLoS One* **6**, e20472 (2011).
- Gelpi, E. *et al.* Visualization of Central European tick-borne encephalitis infection in fatal human cases. *J. Neuropathol. Exp. Neurol.* **64**, 506–12 (2005).
- Gelpi, E. *et al.* Inflammatory response in human tick-borne encephalitis: analysis of postmortem brain tissue. *J. Neurovirol.* **12**, 322–7 (2006).
- Palus, M., Zampachová, E., Elsterová, J., & Růžek, D. Serum matrix metalloproteinase-9 and tissue inhibitor of metalloproteinase-1 levels in patients with tick-borne encephalitis. *J. Infect.* **68**, 165–9 (2014).
- Růžek, D. *et al.* CD8+ T-cells mediate immunopathology in tick-borne encephalitis. *Virology* **384**, 1–6 (2009).

8. Hayasaka, D. *et al.* Mortality following peripheral infection with tick-borne encephalitis virus results from a combination of central nervous system pathology, systemic inflammatory and stress responses. *Virology* **390**, 139–50 (2009).
9. Diniz, J. A. *et al.* West Nile virus infection of primary mouse neuronal and neuroglial cells: the role of astrocytes in chronic infection. *Am. J. Trop. Med. Hyg.* **75**, 691–6 (2006).
10. Shrestha, B., Gottlieb, D., & Diamond, M. S. Infection and injury of neurons by West Nile encephalitis virus. *J. Virol.* **77**, 13203–13 (2003).
11. Couderc, T., Guivel-Benhassine, F., Calara, V., Gosselin, A. S., & Blondel, B. An ex vivo murine model to study poliovirus-induced apoptosis in nerve cells. *J. Gen. Virol.* **83**, 1925–30 (2002).
12. Kennedy, P. G., Gairns, J., & MacLean, A. R. Replication of the herpes simplex virus type 1 RL1 mutant 1716 in primary neuronal cell cultures—possible relevance to use as a viral vector. *J. Neurol. Sci.* **179**, 108–14 (2000).
13. Nazmi, A., Dutta, K., & Basu, A. RIG-I mediates innate immune response in mouse neurons following Japanese encephalitis virus infection. *PLoS One* **6**, e21761 (2011).
14. Růžek, D. *et al.* Morphological changes in human neural cells following tick-borne encephalitis virus infection. *J. Gen. Virol.* **90**, 1649–58 (2009).
15. Hirano, M. *et al.* Tick-borne flaviviruses alter membrane structure and replicate in dendrites of primary mouse neuronal cultures. *J. Gen. Virol.* **95**, 849–61 (2014).
16. Junjhon, J. *et al.* Ultrastructural characterization and three-dimensional architecture of replication sites in dengue virus-infected mosquito cells. *J. Virol.* **88**, 4687–97 (2014).
17. Wigerius, M., Melik, W., Elväng, A., & Johansson, M. Rac1 and Scribble are targets for the arrest of neurite outgrowth by TBE virus NS5. *Mol. Cell. Neurosci.* **44**, 260–71 (2010).
18. Samuel, M. A., Wang, H., Siddharthan, V., Morrey, J. D., & Diamond, M. S. Axonal transport mediates West Nile virus entry into the central nervous system and induces acute flaccid paralysis. *Proc. Natl. Acad. Sci. USA* **104**, 17140–5 (2007).
19. Palus, M. *et al.* Infection and injury of human astrocytes by tick-borne encephalitis virus. *J. Gen. Virol.* **95**, 2411–26 (2014).
20. Offerdahl, D. K., Dorward, D. W., Hansen, B. T., & Bloom, M. E. A three-dimensional comparison of tick-borne flavivirus infection in mammalian and tick cell lines. *PLoS One* **7**, e47912 (2012).
21. Welsch, S. *et al.* Composition and three-dimensional architecture of the dengue virus replication and assembly sites. *Cell Host Microbe* **5**, 365–75 (2009).
22. Gillespie, L. K., Hoenen, A., Morgan, G., & Mackenzie, J. M. The endoplasmic reticulum provides the membrane platform for biogenesis of the flavivirus replication complex. *J. Virol.* **84**, 10438–47 (2010).
23. Lorenz, I. C. *et al.* Intracellular assembly and secretion of recombinant subviral particles from tick-borne encephalitis virus. *J. Virol.* **77**, 4370–82 (2003).
24. Miorin, L., Albornoz, A., Baba, M. M., D'Agaro, P., & Marcello, A. Formation of membrane-defined compartments by tick-borne encephalitis virus contributes to the early delay in interferon signaling. *Virus Res.* **163**, 660–6 (2012).
25. Miorin, L. *et al.* Three-dimensional architecture of tick-borne encephalitis virus replication sites and trafficking of the replicated RNA. *J. Virol.* **87**, 6469–81 (2013).
26. Overby, A. K., Popov, V. L., Niedrig, M., & Weber, F. Tick-borne encephalitis virus delays interferon induction and hides its double-stranded RNA in intracellular membrane vesicles. *J. Virol.* **84**, 8470–83 (2010).
27. Eskelinen, E. L. To be or not to be? Examples of incorrect identification of autophagic compartments in conventional transmission electron microscopy of mammalian cells. *Autophagy* **4**, 257–60 (2008).
28. Heaton, N. S., & Randall, G. Dengue virus-induced autophagy regulates lipid metabolism. *Cell Host Microbe* **8**, 422–32 (2010).
29. Hayashi-Nishino, M. *et al.* A subdomain of the endoplasmic reticulum forms a cradle for autophagosome formation. *Nat. Cell Biol.* **11**, 1433–7 (2009).
30. Ylä-Anttila, P., Vihinen, H., Jokitalo, E., & Eskelinen, E. L. 3D tomography reveals connections between the phagophore and endoplasmic reticulum. *Autophagy* **5**, 1180–5 (2009).
31. Huang, S. C., Chang, C. L., Wang, P. S., Tsai, Y., & Liu, H. S. Enterovirus 71-induced autophagy detected *in vitro* and *in vivo* promotes viral replication. *J. Med. Virol.* **81**, 1241–52 (2009).
32. Orvedahl, A., & Levine, B. Autophagy and viral neurovirulence. *Cell. Microbiol.* **10**, 1747–56 (2008).
33. Moy, R. H. *et al.* Antiviral autophagy restricts Rift Valley fever virus infection and is conserved from flies to mammals. *Immunity* **40**, 51–65 (2014).
34. Orvedahl, A. *et al.* Autophagy protects against Sindbis virus infection of the central nervous system. *Cell Host Microbe* **7**, 115–27 (2010).
35. Yordy, B., & Iwasaki, A. Cell type-dependent requirement of autophagy in HSV-1 antiviral defense. *Autophagy* **9**, 236–8 (2013).
36. Beatman, E. *et al.* West Nile virus growth is independent of autophagy activation. *Virology* **433**, 262–72 (2012).
37. Lee, Y. R. *et al.* Autophagic machinery activated by dengue virus enhances virus replication. *Virology* **374**, 240–8 (2008).
38. Mateo, R. *et al.* Inhibition of cellular autophagy deranges dengue virion maturation. *J. Virol.* **87**, 1312–21 (2013).
39. Yoon, S. Y. *et al.* Autophagy in coxsackievirus-infected neurons. *Autophagy* **5**, 388–9 (2009).
40. Li, J. K., Liang, J. J., Liao, C. L., & Lin, Y. L. Autophagy is involved in the early step of Japanese encephalitis virus infection. *Microbes Infect.* **14**, 159–68 (2012).
41. Heaton, N. S., & Randall, G. Dengue virus and autophagy. *Viruses* **3**, 1332–41 (2011).
42. Rey, F. A., Heinz, F. X., Mandl, C., Kunz, C., & Harrison, S. C. The envelope glycoprotein from tick-borne encephalitis virus at 2 Å resolution. *Nature* **375**, 291–8 (1995).
43. Kozuch, O., & Mayer, V. Pig kidney epithelial (PS) cells: a perfect tool for the study of flaviviruses and some other arboviruses. *Acta Virol.* **19**, 498 (1975).
44. De Madrid, A. T., & Porterfield, J. S. A simple micro-culture method for the study of group B arboviruses. *Bull. World Health Organ.* **40**, 113–21 (1969).
45. Mastronarde, D. N. Automated electron microscope tomography using robust prediction of specimen movements. *J. Struct. Biol.* **152**, 36–51 (2005).
46. Kremer, J. R., Mastronarde, D. N., & McIntosh, J. R. Computer visualization of three-dimensional image data using IMOD. *J. Struct. Biol.* **116**, 71–6 (1996).

Acknowledgments

The authors are greatly indebted to Professors Jan Kopecký and Libor Grubhoffer and to Dr. Jana Nebesáfová for general support of our work. This study was supported by the Czech Science Foundation projects Nos. P502/11/2116 and GA14-29256S, the Technology Agency of the Czech Republic (TE 01020118), and by project LO1218, with financial support from the MEYS of the Czech Republic under the NPU I program. The funders played no role in the study design, data collection and analysis, decision to publish, or preparation of the manuscript.

Author Contributions

M.V. and D.R. conceived and designed the experiments and wrote the manuscript. T.B., M.P., L.E., and J.E. performed the experiments and analyzed the data. All authors reviewed the manuscript.

Additional Information

Supplementary information accompanies this paper at <http://www.nature.com/srep>

Competing financial interests: The authors declare no competing financial interests.

How to cite this article: Bily, T. *et al.* Electron tomography analysis of tick-borne encephalitis virus infection in human neurons. *Sci. Rep.* 5, 10745; doi: 10.1038/srep10745 (2015).



This work is licensed under a Creative Commons Attribution 4.0 International License. The images or other third party material in this article are included in the article's Creative Commons license, unless indicated otherwise in the credit line; if the material is not included under the Creative Commons license, users will need to obtain permission from the license holder to reproduce the material. To view a copy of this license, visit <http://creativecommons.org/licenses/by/4.0/>

CHAPTER IV

Infection and injury of human astrocytes by tick-borne encephalitis virus

Martin Palus, Tomáš Bílý, Jana Elsterová, Helena Langhansová, Jiří Salát, Marie Vancová, Daniel Růžek

Journal of General Virology 2014 95: 2411-2426

DOI: 10.1099/vir.0.068411-0

<http://jgv.microbiologyresearch.org/content/journal/jgv/10.1099/vir.0.068411-0>

Infection and injury of human astrocytes by tick-borne encephalitis virus (summary)

Neurons are primary target cells for TBEV (Hirano *et al.*, 2014) in the CNS although other brain cells may also be infected (Potokar *et al.*, 2014). The entry of TBEV into the CNS precedes the breakdown of the BBB (Ruzek *et al.*, 2011). The invasion of TBEV into the CNS brings the virus into close proximity with the second important component of the BBB, astrocytes (Hussmann *et al.*, 2013).

Astrocytes are key players in the inflammatory response during neural infections caused by flaviviruses, namely Japanese encephalitis (Yang *et al.*, 2012) and West Nile encephalitis (Verma *et al.*, 2011; Hussmann *et al.*, 2013). However, their role in the development of TBE remains unstudied. Here, we carried out the experiments to investigate the sensitivity of primary human astrocytes to TBEV infection, virus growth, virus-induced astrocyte activation and cytokine and chemokine production.

We have demonstrated, that TBEV is capable of productive, persistent infection in primary human astrocytes, and that this infection is associated with astrocyte activation and production of various pro-inflammatory cytokines and chemokines.

Thus, infection of non-neuronal cells might play some a role in the entry of the virus into the CNS, development of neuroinflammation and viral persistence in the CNS during chronic infection. A recent report demonstrated that primary rat astrocytes are sensitive to TBEV infection, although the infection did not affect cell viability (Potokar *et al.*, 2014). That was confirmed in our experiments where there was apparent persistent infection without affected the viability of the cells. Therefore, it was suggested that astrocytes might represent an important reservoir of TBEV during chronic brain infection (Potokar *et al.*, 2014; Gritsun *et al.*, 2003b).

The infection induced a marked increase in the expression of glial fibrillary acidic protein (GFAP), a marker of astrocyte activation. GFAP is involved in many important processes in CNS, including cell communication and BBB

function. The activation of glial cells including astrocytes represents one of the major histopathological features of TBE (Környey, 1978; Gelpi *et al.*, 2006). The astrocyte activation leads to a downstream cascade of inflammatory cytokine production that results in the death of neurons (Kumar *et al.*, 2010; Pekny *et al.*, 2014). In our study, GFAP production was higher in TBEV-infected astrocytes than in mock-infected or LPS-stimulated astrocytes.

In addition, expression of matrix metalloproteinase 9 (MMP-9) and several key pro-inflammatory cytokines/chemokines (e.g. tumor necrosis factor α , interferon α , interleukin (IL)-1 β , IL-6, IL-8, interferon γ -induced protein 10, macrophage inflammatory protein, but not monocyte chemoattractant protein 1) was upregulated. Accumulation of cytokines and chemokines in the CNS may accentuate the progression of encephalitis instead of restricting virus replication (Ramesh *et al.*, 2013). Although viral infection is not generally as robust in human glial cells as in neurons, glial cells secrete much higher levels of immune mediators (Verma *et al.*, 2011). Therefore, during the inflammatory response, astrocytes and other glial cells may influence the balance between host protection and neurotoxicity. We reported previously that high expression of various cytokines/chemokines during TBE is able to mediate immunopathology, and might be associated with a more severe course of infection and increased fatality (Palus *et al.*, 2013). Excessively high levels of IP-10 in the CNS can be very harmful to the host (Sasseville *et al.*, 1996; Sui *et al.*, 2006).

In human TBE patients, higher levels of MMP-9, a compound with multiple functions, including disruption of the BBB, have been observed in serum (Palus *et al.*, 2014b) and cerebrospinal fluid (Kang *et al.*, 2013). We observed that TBEV-infected astrocytes produced large quantities of MMP-9, and therefore might represent the main cell population responsible for the increase of BBB permeability during TBE. Moreover, MMP-9 is capable of causing neuronal apoptosis (del Zoppo, 2010).

Moreover, we also used electron tomography to provide important insights into the three-dimensional (3D) morphology of the infected astrocyte cells

using electron tomography. Several novel ultrastructural changes were observed, including the formation of unique tubule-like structures of 17.9 ± 0.15 nm diameter with associated viral particles and/or virus-induced vesicles and located in the rough endoplasmic reticulum of the TBEV-infected cells, that we afterwards identified also in TBEV infected HN cells (Bily *et al.*, 2015), mention above.

Taken together, our findings demonstrate that cultured human primary astrocytes are sensitive to TBEV infection and are a potential source of pro-inflammatory cytokines in TBEV-infected brain cells, which might contribute to TBEV-induced neurotoxicity and/or BBB breakdown during TBE.

Infection and injury of human astrocytes by tick-borne encephalitis virus

Martin Palus,^{1,2,3†} Tomáš Bílý,^{1,2†} Jana Elsterová,^{1,2,3}
Helena Langhansová,^{1,2} Jiří Salát,³ Marie Vancová^{1,2} and Daniel Růžek^{1,2,3}

Correspondence
Daniel Růžek
ruzekd@paru.cas.cz

¹Institute of Parasitology, Biology Centre of the Academy of Sciences of the Czech Republic, Branišovská 31, CZ-37005 České Budějovice, Czech Republic

²Faculty of Science, University of South Bohemia, Branišovská 31, CZ-37005 České Budějovice, Czech Republic

³Department of Virology, Veterinary Research Institute, Hudcova 70, CZ-62100 Brno, Czech Republic

Tick-borne encephalitis (TBE), a disease caused by tick-borne encephalitis virus (TBEV), represents the most important flaviviral neural infection in Europe and north-eastern Asia. In the central nervous system (CNS), neurons are the primary target for TBEV infection; however, infection of non-neuronal CNS cells, such as astrocytes, is not well understood. In this study, we investigated the interaction between TBEV and primary human astrocytes. We report for the first time, to the best of our knowledge, that primary human astrocytes are sensitive to TBEV infection, although the infection did not affect their viability. The infection induced a marked increase in the expression of glial fibrillary acidic protein, a marker of astrocyte activation. In addition, expression of matrix metalloproteinase 9 and several key pro-inflammatory cytokines/chemokines (e.g. tumour necrosis factor α , interferon α , interleukin (IL)-1 β , IL-6, IL-8, interferon γ -induced protein 10, macrophage inflammatory protein, but not monocyte chemoattractant protein 1) was upregulated. Moreover, we present a detailed description of morphological changes in TBEV-infected cells, as investigated using three-dimensional electron tomography. Several novel ultrastructural changes were observed, including the formation of unique tubule-like structures of 17.9 \pm 0.15 nm diameter with associated viral particles and/or virus-induced vesicles and located in the rough endoplasmic reticulum of the TBEV-infected cells. This is the first demonstration that TBEV infection activates primary human astrocytes. The infected astrocytes might be a potential source of pro-inflammatory cytokines in the TBEV-infected brain, and might contribute to the TBEV-induced neurotoxicity and blood–brain barrier breakdown that occurs during TBE. The neuropathological significance of our observations is also discussed.

Received 27 May 2014

Accepted 2 July 2014

INTRODUCTION

Tick-borne encephalitis (TBE) is a serious viral infection of the central nervous system (CNS) caused by tick-borne encephalitis virus (TBEV). TBEV is a single-stranded positive-sense RNA virus belonging to the genus *Flavivirus*, family *Flaviviridae* (Mansfield *et al.*, 2009). More than 13 000 clinical cases of TBE, including numerous deaths, are reported annually in Europe and north-eastern Asia (Mansfield *et al.*, 2009). Despite the medical importance of this disease, some crucial steps in the development of encephalitis remain poorly understood. In humans, TBEV may produce a variety of clinical symptoms. The clinical spectrum of acute TBE ranges from

symptoms of undifferentiated febrile illness or mild meningitis to severe meningoencephalitis with or without myelitis (Haglund & Günther, 2003; Růžek *et al.*, 2010). Chronic TBE occurs less frequently and has been reported only in some regions of Russia, mainly in Siberia and the Far East, where this form comprises 1–3% of all TBE cases (Gritsun *et al.*, 2003).

Major hallmarks of TBEV neuropathogenesis are neuro-inflammation followed by neuronal death and disruption of the blood–brain barrier (BBB) (Růžek *et al.*, 2009a, 2011; Palus *et al.*, 2013, 2014). The response of TBEV infection in the brain is characterized by massive inflammatory events, including the production of cytokines (e.g. IFN- γ , TNF- α , and IL-1 β , IL-6 and IL-10) and chemokines [e.g. monocyte chemoattractant protein (MCP)-1/CCL2, IFN- γ -induced protein 10 (IP-10)/CXCL10, macrophage inflammatory

†These authors contributed equally to this study.

A supplementary movie is available with the online version of this paper.

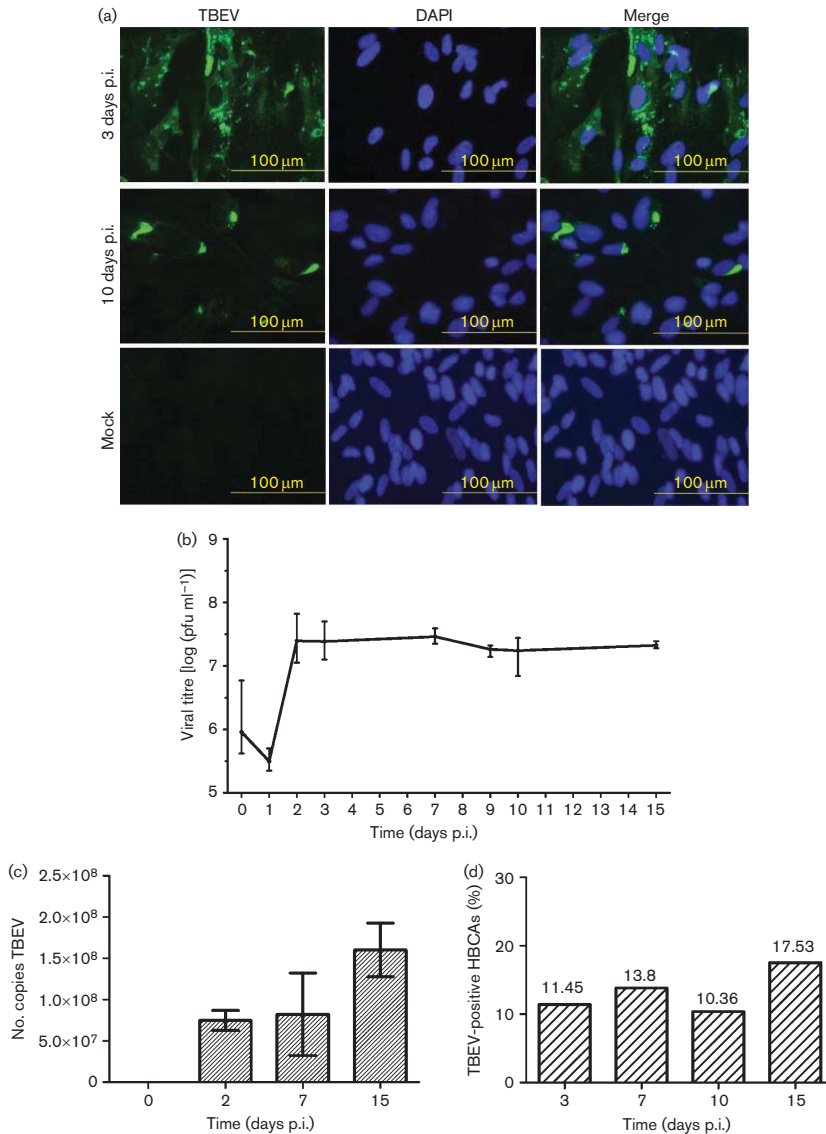


Fig. 1. TBEV can infect human primary astrocytes. (a) HBCAs grown and fixed on slides at days 3 and 10 post-infection (p.i.) were stained with anti-flavivirus envelope antibody (green) and counterstained with DAPI (blue). TBEV-infected HBCAs immunostained with flavivirus-specific antibody demonstrated virus replication in the cytoplasm, with antigen aggregates forming at day 3 p.i. At later time points (10 days p.i.), only the brightly stained aggregates of viral antigen were observed. Mock-infected HBCAs stained with primary and secondary antibodies were used as a negative control, and did not exhibit any TBEV antigen staining. (b) TBEV titres in culture supernatant from HBCAs collected at 0, 1, 2, 3, 7, 9 and 15 days p.i. were determined by plaque assay using porcine kidney stable cells. Viral titres are expressed as p.f.u. ml^{-1} . Data represent means \pm SEM. (c) Total RNA extracted from HBCA cell lysates at 0, 2, 7, and 15 days p.i. was used to determine the number of

intracellular TBEV RNA copies by quantitative RT-PCR. Values represent means \pm SEM. (d) The percentage of HBCAs that were positive for TBEV antigen in culture at 3, 7, 10 and 15 days p.i. was determined. Data were obtained based on a total of 23 000 cells counted in at least seven independent fields.

protein (MIP)-1 α and RANTES] (Palus *et al.*, 2013). Microglia and astrocytes are classically believed to serve as the predominant source of these cytokines and chemokines in the CNS, and therefore may act as important processors of neuroinflammation and neurodegeneration (Ramesh *et al.*, 2013). The pro-inflammatory chemokines attract immunocompetent cells to the CNS (Réaux-Le Goazigo *et al.*, 2013), including CD8⁺ T-cells, which may mediate immunopathology during TBE (Růžek *et al.*, 2009a). Moreover, the pro-inflammatory molecules can further activate downstream apoptotic signalling pathways in neurons, resulting in neuronal death (Kumar *et al.*, 2010) or inducing breakdown of the BBB (Růžek *et al.*, 2011; Erickson *et al.*, 2012; Palus *et al.*, 2014). We used a rodent model to demonstrate that TBEV infection is associated with the dramatic BBB breakdown that occurs during the later stages of infection. The BBB breakdown most likely represents a bystander effect of virus-induced cytokine/chemokine overproduction in the brain (Růžek *et al.*, 2011). However, the specific cell types that express these cytokines and chemokines have not been characterized.

Although neurons are primary targets after TBEV enters the CNS (Hirano *et al.*, 2014), other brain cells may also be infected (Potokar *et al.*, 2014). Infection of non-neuronal CNS cells including astrocytes has, albeit infrequently, been reported in cases of flavivirus encephalitis (Desai *et al.*, 1995; Nogueira *et al.*, 2002; German *et al.*, 2006; Balsitis *et al.*, 2009; de Araújo *et al.*, 2009; Sips *et al.*, 2012). It was shown recently that TBEV infects cultured primary rat astrocytes without affecting their viability. Therefore, it was suggested that astrocytes might represent an important reservoir of TBEV in brain during the infection (Potokar *et al.*, 2014). Astrocytes are the most abundant glial cell population in the human brain (Nedergaard *et al.*, 2003) and have various leading roles in the brain, including integrating neuronal functions, neuronal support and regulation of the BBB. Thus, astrocytes serve as a structural and functional bridge between endothelial cells of the BBB and neurons; together, they form the 'neurovascular unit' (Stanimirovic & Friedman, 2012), which regulates blood flow, the integrity of the BBB and neuronal activity in response to physiological and pathophysiological changes (Husmann *et al.*, 2013).

Astrocytes are key players in the inflammatory response during neural infections caused by flaviviruses, namely Japanese encephalitis (Bhowmick *et al.*, 2007; Yang *et al.*, 2012) and West Nile encephalitis (Diniz *et al.*, 2006; Verma *et al.*, 2011; Husmann *et al.*, 2013); however, their role in the development of TBE remains largely unstudied. Here, we aimed to investigate the sensitivity of primary human astrocytes to TBEV infection, virus growth, virus-induced astrocyte activation, and cytokine and chemokine production.

We demonstrate here for the first time, to the best of our knowledge, that TBEV is capable of productive, persistent infection in primary human astrocytes, and that this infection is associated with astrocyte activation and the production of various pro-inflammatory cytokines and chemokines.

On the ultrastructural level, the infection causes massive morphological changes that include the proliferation and rearrangement of the rough endoplasmic reticulum (RER) and lead to the formation of new compartments with an optimal microenvironment that provides functional sites for protein synthesis, processing and RNA replication, whilst providing protection against the host immune system (Welsch *et al.*, 2009; Gillespie *et al.*, 2010; Offerdahl *et al.*, 2012; Miorin *et al.*, 2013). These newly transformed compartments are represented by vesicles or vesicle packets that contain a pore opening to the cytosol (Offerdahl *et al.*, 2012; Miorin *et al.*, 2013) and convoluted membranes with a putative polyprotein processing function (Welsch *et al.*, 2009). A number of other functions have been ascribed to the proliferation of this membrane network, including the concentration of virus replication machinery, the provision of a solid-state platform for viral protein synthesis and replication, and the sequestration of viral dsRNA (the replicative form) from innate immune sensors (Overby *et al.*, 2010; Offerdahl *et al.*, 2012).

We also used electron tomography to provide important insights into the three-dimensional (3D) morphology of the infected cells, and, to the best of our knowledge, this is the first description of the 3D architecture of the tubule-like structures found in the RER of TBEV-infected human astrocytes. Taken together, our findings suggest that astrocytes can significantly contribute to the development of inflammation in the CNS during TBE. This information may facilitate novel strategies for treating this important neural infection.

RESULTS

TBEV can infect and replicate in human astrocytes

We employed a plaque assay and immunofluorescence staining for viral antigen to determine TBEV infection and replication kinetics in primary human brain cortex astrocytes (HBCAs) (Fig. 1). Viral antigen was not detected in mock-infected HBCAs (Fig. 1a) or in cells stained with secondary antibody alone. Based on a total of 23 000 cells counted in at least seven independent fields, approximately 11 % of HBCAs were infected with TBEV at day 3, 14 % at day 7, 10 % at day 10 and 18 % at day 15 post-infection (p.i.) (Fig. 1d).

TBEV replication was quantified using a plaque assay in TBEV-infected cell supernatants collected daily from days 0

to 3 and then at 7, 9, 10 and 15 days p.i. Productive TBEV replication in the form of release of virions was first detected at day 2 after infection, and day 2 also represented the limit of virus production (Fig. 1b). Intracellular TBEV replication assessed by quantitative real-time reverse transcription (RT)-PCR also confirmed virus replication for the first 15 days p.i., and the number of TBEV RNA copies increased in a time-dependent manner (Fig. 1c). We also used phase-contrast microscopy to examine TBEV-infected astrocytes for cytopathogenic effect (CPE) and cell death; neither was observed at any time point (data not shown).

Immunofluorescence staining revealed that the TBEV antigen was distributed mostly diffusely throughout the entire body of the astrocyte at early time points after infection (Fig. 1a). However, at later time points (as early as day 3 after infection), we observed brightly staining aggregates of viral antigen. A co-localization study with protein disulfide isomerase family A, member 3 (PDIA3) antigen (also known as Erp57, Er-60 and GRP58) suggested that the antigen was localized primarily in extremely hypertrophied and rearranged endoplasmic reticulum of the cells as early as day 3 p.i. (Fig. 2).

TBEV induces the expression of multiple pro-inflammatory cytokines/chemokines in human astrocytes

Pro-inflammatory cytokines, such as IL-1 β and TNF- α , play an important role in mediating neuronal death and

neuroinflammation in various diseases. Therefore, we investigated the effect of TBEV infection on the mRNA expression of key pro-inflammatory cytokines, such as IL-1 β , IL-6, IL-8, IFN- α and TNF- α . We also measured the expression of MCP-1/CCL2, MIP-1 β /CCL4 and IP-10/CXCL10 mRNAs in infected and control astrocytes (Figs 3 and 4). On day 1 p.i., we observed no significant increase in the mRNA expression of any cytokine/chemokine.

The expression of CCL2/MCP-1 mRNA did not change significantly at any time point (Fig. 3f). Robust upregulation of TNF- α mRNA was detected at 3 and 4 days p.i.; however, the expression was decreased at 15 days p.i. (Fig. 3a). IFN- α mRNA expression was slightly upregulated only at day 4 p.i. (Fig. 3b). Although the expression of IL-1 β , IL-6 and IL-8 mRNAs increased from day 3 to 4, no upregulation was observed at day 15 p.i. (Fig. 3c–e, respectively). We observed strong increases of CCL4/MIP-1 β and CXCL10/IP-10 mRNA expression from 3 to 4 days p.i.; however, at day 15, the expression level for these molecules was similar in infected cells and control cells (Fig. 4a, c).

We used ELISA to investigate the release of secreted MIP-1 β /CCL4 and IP-10/CXCL10 cytokines/chemokines in the culture medium of TBEV-infected and control cells. The amount of soluble MIP-1 β /CCL4 did not increase until day 4 p.i. At day 5 p.i., the amount of soluble MIP-1 β /CCL4 was significantly increased (Fig. 4d). Basal levels of IP-10/CXCL10 in culture media were very low. Starting on day 2

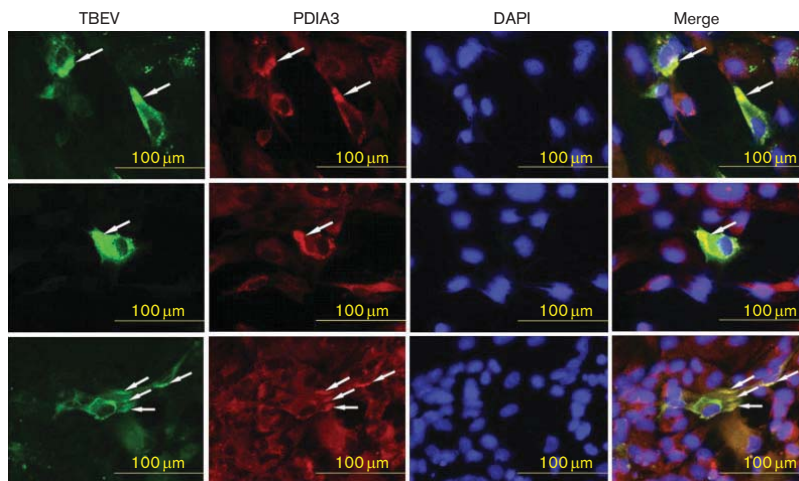


Fig. 2. TBEV antigen is co-localized with PDIA3 antigen in infected HBCAs at later times p.i. HBCAs grown and fixed at day 3 p.i. were stained with anti-flavivirus envelope antibody (green) and anti-PDIA3 antibody (red), and counterstained with DAPI (blue). Co-localization of TBEV and PDIA3 antigens was observed at all investigated time points p.i. Three representative examples are shown. Mock-infected HBCAs stained with primary anti-flavivirus and secondary antibodies (or cells stained with secondary antibodies only) were used as negative controls and did not exhibit any TBEV or PDIA3 antigen staining (not shown).

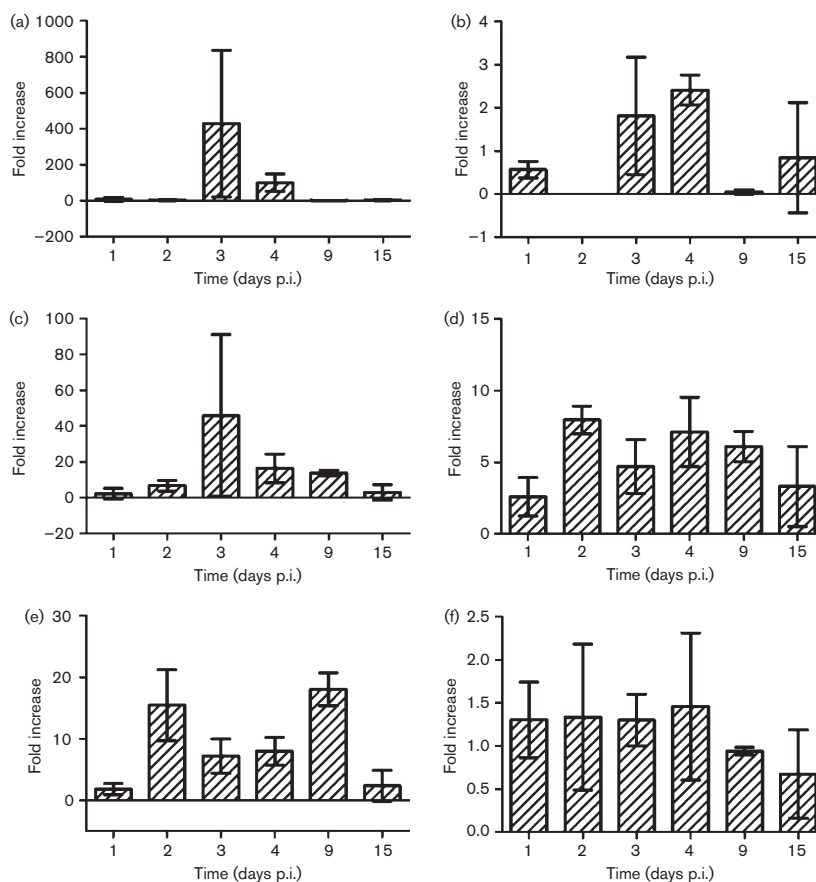


Fig. 3. TBEV differentially modulates the expression of pro-inflammatory cytokines and chemokines in HBCAs. Total RNA from mock-infected and TBEV-infected HBCAs at days 1–4, 9 and 15 p.i. were used to determine the fold change of TNF- α (a), IFN- α (b), IL-1 β (c), IL-6 (d), IL-8 (e) and MCP-1/CCL2 (f) mRNAs with quantitative RT-PCR. Changes in cytokine and chemokine levels were first normalized to the expression of housekeeping genes (human β -actin and glyceraldehyde 3-phosphate dehydrogenase) and the fold change in the infected cells was calculated compared with the corresponding controls. Data are expressed as means \pm SEM.

p.i., the amount of soluble IP-10/CXCL10 increased substantially ($P < 0.001$; Fig. 4b).

TBEV infection induces the production of matrix metalloproteinase 9 by astrocytes

The expression of matrix metalloproteinases (MMPs), especially MMP-9, correlates with BBB disruption during many neuroinflammatory diseases. Therefore, we investigated the effect of TBEV infection on the production of MMP-9 by astrocytes. The release of soluble MMP-9 into the culture medium of mock- and TBEV-infected

astrocytes was detected using ELISA. Starting at day 2 after infection, the amounts of soluble MMP-9 increased continuously until the end of the experiment, with a dramatic increase at day 7 (Fig. 5).

TBEV infection is associated with the activation of infected astrocytes, as demonstrated by increased glial fibrillary acidic protein (GFAP) expression

To provide additional evidence that TBEV infection per se causes astrocyte activation, we measured the production of

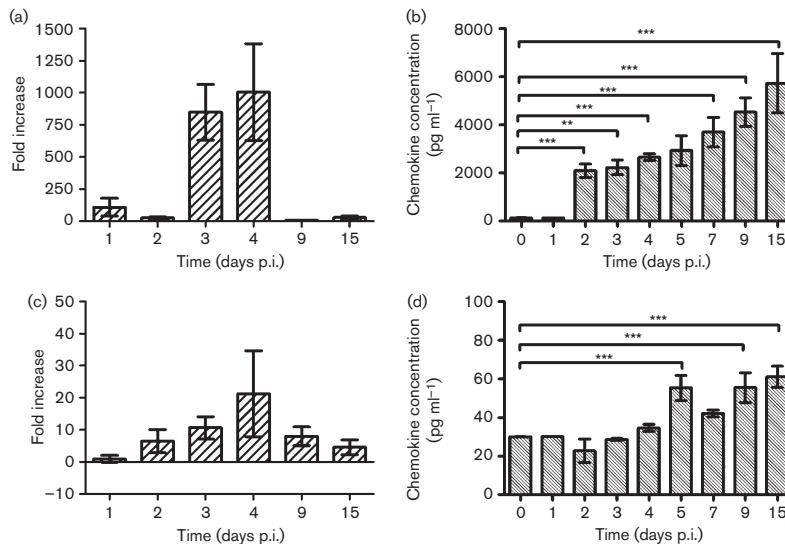


Fig. 4. TBEV increases the production of IP-10/CXCL10 and MIP-1 β /CCL4 in infected HBCAs. (a, c) Total RNA from mock-infected and TBEV-infected HBCAs at 1–4, 9 and 15 days p.i. was used to determine the fold change of IP-10/CXCL10 (a) and MIP-1 β /CCL4 (c) mRNAs with quantitative RT-PCR. Changes in the cytokine and chemokine mRNA levels were first normalized to the expression of housekeeping genes (human β -actin and glyceraldehyde 3-phosphate dehydrogenase) and the fold change in the infected cells was calculated compared with corresponding controls. Data are expressed as means \pm SEM. (b, d) Levels of IP-10/CXCL10 (b) and MIP-1 β /CCL-4 (d) in culture supernatants were determined using ELISA at 0–7, 9 and 15 days p.i. Data represent mean concentrations \pm SEM. ** P <0.01; *** P <0.001.

GFAP, a marker of astrocyte activation, in mock-infected and TBEV-infected astrocytes, as well as in cells treated with lipopolysaccharide (LPS) at various times p.i. Flow cytometry indicated that the intensity of GFAP production increased significantly in TBEV-infected HBCAs at 3, 7 and 15 days p.i. compared with mock-infected and LPS-treated

cells, clearly demonstrating astrocyte activation (Fig. 6a, b). The intensity of GFAP production in the TBEV- and mock-infected cells was also visualized with fluorescence microscopy using a specific anti-GFAP antibody (Fig. 6c).

TBEV causes dramatic ultrastructural morphological changes in infected astrocytes

We used transmission electron microscopy and electron tomography to investigate ultrastructural changes in mock- and TBEV-infected HBCAs at 3 and 9 days p.i. At 3 days p.i., we observed rearranged cisterns of the RER with typical virus-induced vesicles and viral particles, as described elsewhere (Fig. 7a) (Růžek *et al.*, 2009b). Next, we observed that many enveloped TBEVs were crowded into the Golgi complex (Figs 7b and 8b). In contrast, at 9 days p.i., we observed a lower number of viral particles in the cisterns of the RER (Fig. 7c) and in vacuoles close to the Golgi complex (Fig. 7d). At 9 days p.i., we observed intra-mitochondrial electron-dense granules that formed annular structures in the mitochondrial matrix (Fig. 7c). Moreover, these cells contained both swollen mitochondria with mitochondrial cristae located in the periphery, and mitochondria that apparently lacked any alteration in morphology (Fig. 7e). Furthermore, some infected cells displayed other

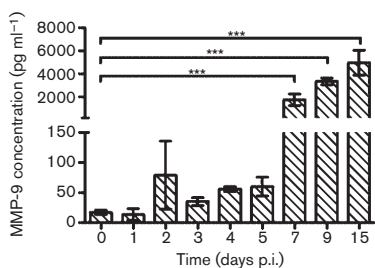


Fig. 5. TBEV-infected HBCAs release large quantities of MMP-9. Levels of MMP-9 in culture supernatants were determined using ELISA at 0–7, 9 and 15 days p.i. Data represent mean concentrations \pm SEM. *** P <0.001.

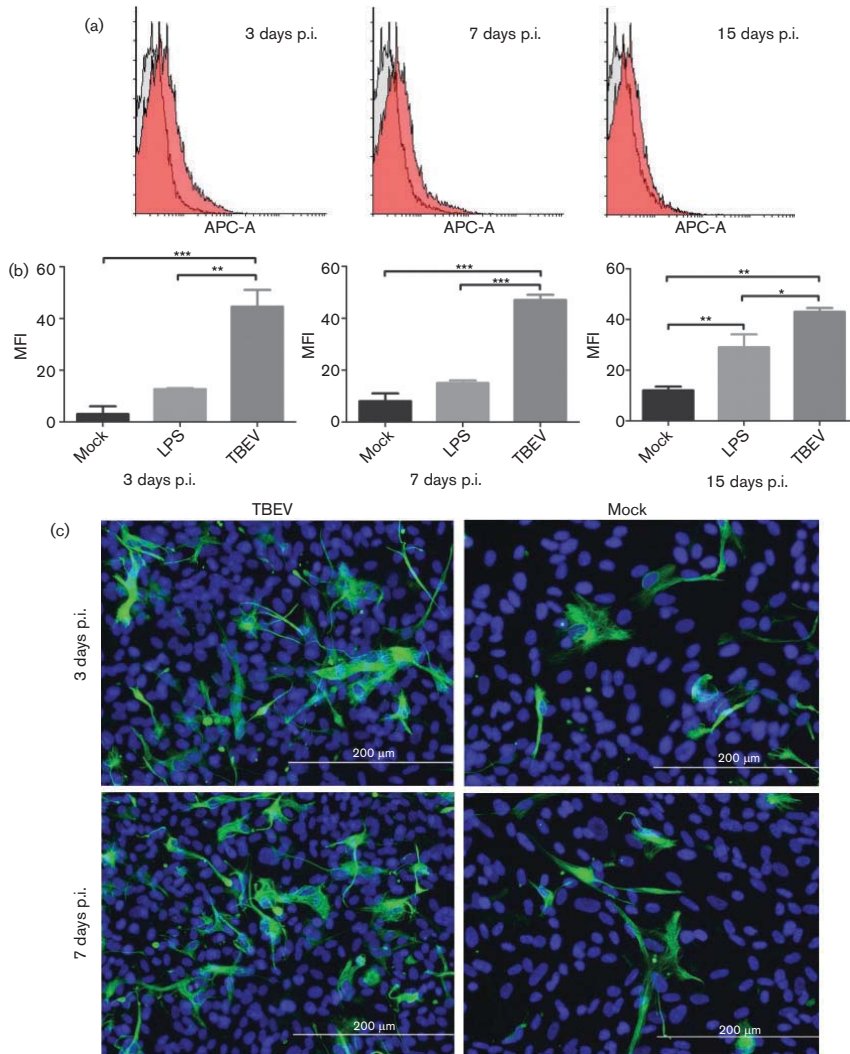


Fig. 6. TBEV infection activates HBCAs, as demonstrated by increased GFAP production. (a) Flow cytometry analysis of GFAP production in mock-infected and TBEV-infected HBCAs at 3, 7 and 15 days p.i. is shown as overlapping histograms of relative fluorescence intensity of the analysed cells. (b) The mean fluorescence intensity (MFI) of GFAP-positive cells in culture after mock infection or TBEV infection and LPS treatment at 3, 7 and 15 days p.i. was determined by flow cytometry; it was significantly increased in TBEV-infected HBCAs at all time points investigated. (c) HBCAs grown and fixed at days 3 and 7 p.i. were stained with anti-GFAP antibody (green) and counterstained with DAPI (blue). HBCAs stained with secondary antibody alone were used as a negative control and did not exhibit any GFAP antigen staining (not shown). * $P < 0.05$; ** $P < 0.01$; *** $P < 0.001$.

morphological features of cells undergoing necrotic cell death, such as chromatin aggregates in the nuclear periphery, irregularly shaped cells and surface blebs, and enlarged

cisternal space in the endoplasmic reticulum (Fig. 7c–e). In contrast, neither virus replication nor ultrastructural alterations were evident in several other cells from the same

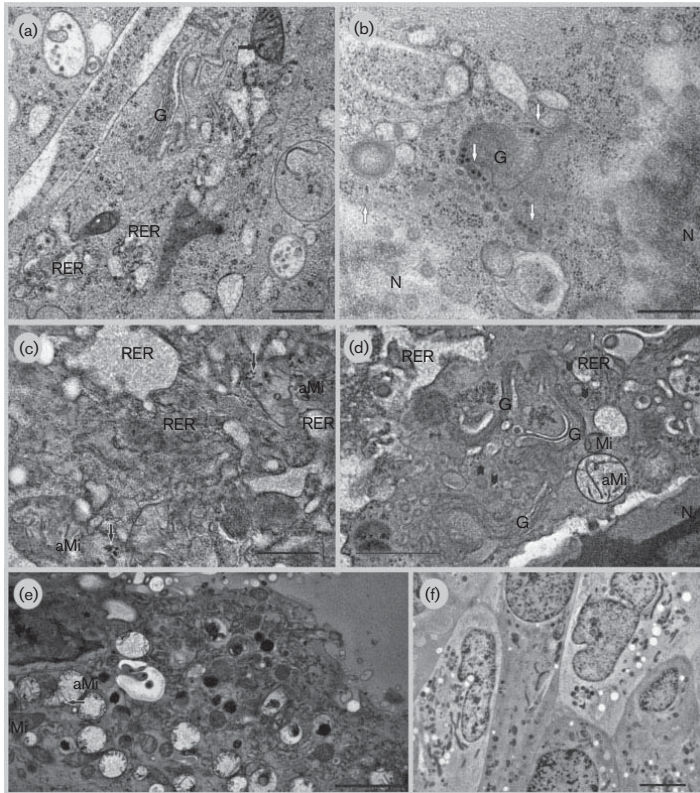


Fig. 7. Morphological changes in TBEV-infected HBCAs at 3 (a, b) and 9 (c–f) days p.i. (a) TBEV particles located inside the remodelled RER and the Golgi complex (G). In particular, note the mitochondrion with the electron-dense granules (black arrow). (b) Viral particles (white arrows) accumulated in the periphery of the Golgi stack (G). N, nucleus. (c–e) Ultrastructural alterations were observed in infected cells at 9 days p.i.: enlarged cisternae of the RER, rearranged RER membranes, swollen mitochondria (aMi) with annularly arranged granules (black arrows) and mitochondria without structural changes (Mi), as well as viral particles inside vacuoles (arrowheads). (f) Transmission electron microscopy did not reveal any ultrastructural abnormalities in several HBCAs at 9 days p.i. Bars: 500 nm (a, b), 100 nm (c); 1 μ m (d); 2 μ m (e); 5 μ m (f).

culture and the same time interval (Fig. 7f), which is in accordance with immunofluorescence staining for viral antigen. The ultrastructure of these cells was similar to that of the mock-infected HBCAs (Fig. 8a). Morphological changes induced by TBEV infection involved almost all cell compartments (RER, Golgi complex, mitochondria and phagosomes) as visible on the 3D model of the infected cells (Fig. 8b).

TBEV induces the formation of tubule-like structures in the endoplasmic reticulum of some infected astrocytes

We observed tubule-like structures, which were located inside the RER cisternal space of only a very few of the

infected astrocytes (Fig. 9 and Movie S1, available in the online Supplementary Material). The tubule-like structures were laid out in many parallel groupings of bundle-like fascicles. The electron density of these tubule-like structures was consistent throughout their shape (Fig. 10a–c), and they were 17.9 nm (± 0.2 nm; $n=101$) in diameter. In contrast, when viewed using the electron microscope, cellular microtubules outside the ER appeared to be less electron-dense on the inside and were bordered on the outside by two dense lines; the diameter of these microtubules was 20.3 nm (microtubules in Fig. 10d–f). All enveloped viral particles were observed in the lumen of the RER, and most were directly connected to the tubule-like structures (Fig. 11a–d). The diameter of the enveloped

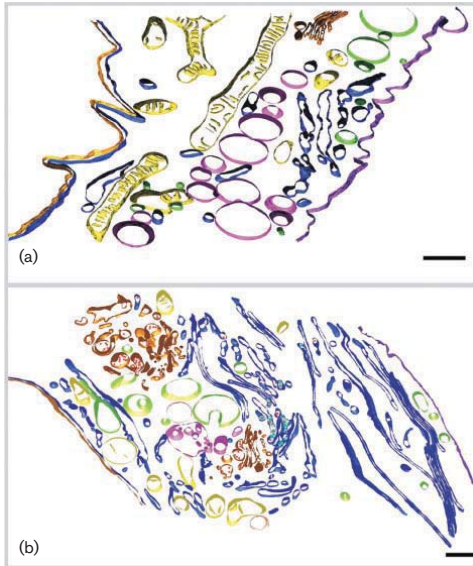


Fig. 8. 3D models of mock-infected (a) and TBEV-infected HBCAs (b) at 3 days p.i. TBEV infection causes extensive morphological changes, including membrane reorganization of the RER; differences are evident in the Golgi complex, mitochondria and phagosomes. 3D reconstructions of single axis tomograms are shown. Tilt series images were collected with either $\pm 60^\circ$ tilt range in 0.65° increments (a) or $\pm 65^\circ$ tilt range in 1° increments (b). The final 3D reconstructed thicknesses are 52 nm (a) and 56 nm (b). Pixel resolution: 1.66 nm (a), 2.16 nm (b). Orange, the Golgi complex; red, TBEV particles; light blue, TBEV-induced structures; dark blue, RER; yellow, mitochondria; green, vacuole; pink, phagosome/endosome; violet, cell membrane; brown, nuclear membrane. Bars, 500 nm.

viral particles was 42.5 nm (± 0.7 nm; $n=12$), and the diameter of the nucleocapsid was 26.1 nm (± 0.7 nm; $n=12$). Several TBEV-induced vesicles that were nearly spherical and ranged from 60 to 90 nm in diameter were observed in close proximity to viral enveloped particles. Some TBEV-induced vesicles were connected in a manner identical to that described regarding the tubule-like structures (Fig. 11e–h). We also noted the presence of a subviral particle enclosed in a vesicle in close proximity to the tubule-like structures. The presence of subviral particles (Fig. 11i, j) indicated defective virus assembly.

DISCUSSION

Although TBEV is a significant cause of encephalitis in humans, relatively little attention has been given to TBEV infection of cells in the human CNS. Neurons are primary

targets for TBEV (Hirano *et al.*, 2014) in the CNS, and other brain cells may also be infected (Potokar *et al.*, 2014). Although TBEV antigen was not detected in astrocytes in a study investigating brains from fatal human TBE cases (Gelpi *et al.*, 2005), data from other studies indicate that non-neuronal CNS cells including astrocytes are also, albeit infrequently, infected in cases of flavivirus encephalitis (Desai *et al.*, 1995; Nogueira *et al.*, 2002; German *et al.*, 2006; Balsitis *et al.*, 2009; de Araújo *et al.*, 2009; Sips *et al.*, 2012). Infection of non-neuronal cells might play some role in the entry of the virus into the CNS, development of neuroinflammation and viral persistence in the CNS during chronic infection. A recent report demonstrated that primary rat astrocytes are sensitive to TBEV infection, although the infection did not affect cell viability (Potokar *et al.*, 2014). Therefore, it was suggested that astrocytes might represent an important reservoir of dormant TBEV during chronic brain infection (Potokar *et al.*, 2014), for example in cases of chronic TBEV infections reported in humans in Siberia and the Far East (Gritsun *et al.*, 2003). Moreover, an increasing number of studies have demonstrated the important role of astrocytes during encephalitis caused by other flaviviruses, such as West Nile virus and Japanese encephalitis virus (Chen *et al.*, 2000, 2004; Diniz *et al.*, 2006; Kumar *et al.*, 2010; Verma *et al.*, 2011; Yang *et al.*, 2012; Hussmann *et al.*, 2013; Hussmann & Fredericksen, 2014). However, cultured astrocytes were not sensitive to infection with dengue virus (Imbert *et al.*, 1994). In this study, we showed that primary human astrocytes could be infected with TBEV and produce relatively high virus titres (Fig. 1). The viability of the infected cells was not altered during the monitored time interval after infection (15 days), which is in accordance with the findings of a study on primary rat astrocytes (Potokar *et al.*, 2014). In agreement with other authors (Potokar *et al.*, 2014), we can conclude that primary human astrocytes are much more resilient to TBEV infection than other cell types, such as human neuroblastoma, glioblastoma and medulloblastoma cells (Růžek *et al.*, 2009b). However, the number of infected cells in the culture did not exceed 20% during the entire investigated period, suggesting that only a fraction of the cells is sensitive to infection, whilst the rest remain resistant. It remains unknown exactly what renders some cells sensitive to the infection and others resistant.

TBEV infection in the brain is associated with the induction of several cytokines and chemokines. Accumulation of cytokines and chemokines in the CNS may accentuate the progression of encephalitis instead of restricting virus replication (Ramesh *et al.*, 2013). Although viral infection is not generally as robust in human glial cells as in neurons, they secrete much higher levels of immune mediators, such as cytokines and chemokines (Verma *et al.*, 2011). Therefore, during the inflammatory response, astrocytes and other glial cells may influence the balance between host protection and neurotoxicity. We reported previously in a mouse study

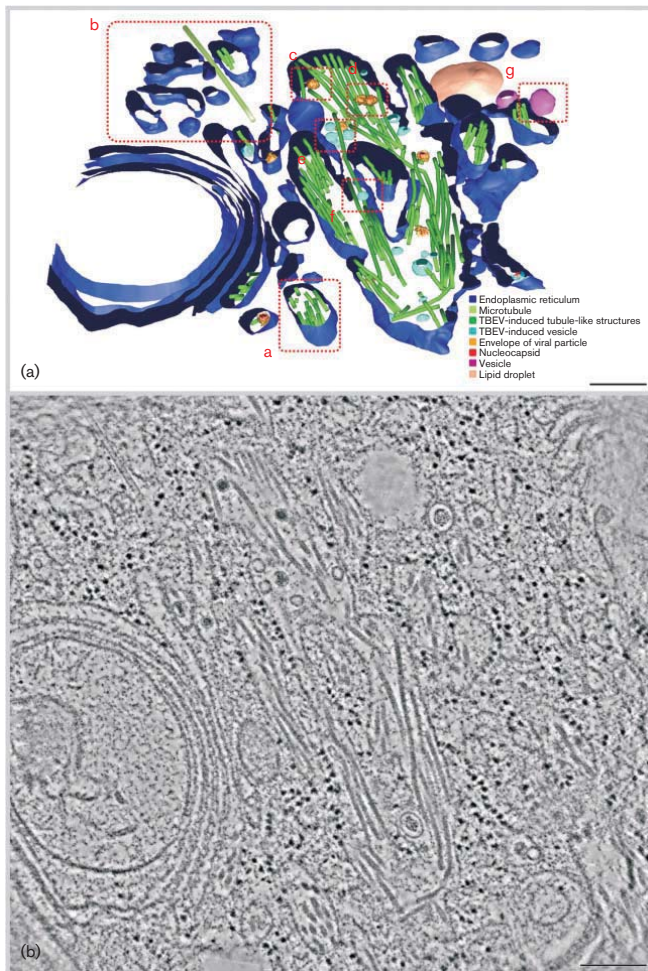


Fig. 9. Tubule-like structures observed in TBEV-infected HBCAs at 3 days p.i. This is a 3D reconstruction of a dual axis tomogram (a) and a slice of the tomogram (b). Tilt series images were collected in the range $\pm 65^\circ$ in 0.65° increments. The final reconstructed section thickness was approximately 60 nm, which was divided into 75 slices. Pixel resolution: 0.81 nm. Bars, 200 nm. This tomogram is shown in Movie S1.

that high expression of various cytokines/chemokines during TBE is able to mediate immunopathology, and might be associated with a more severe course of infection and increased fatality (Palus *et al.*, 2013). In the present study, we observed that TBEV infection of astrocytes is associated with the dramatically increased production of various pro-inflammatory cytokines and chemokines. In particular, quantitative real-time RT-PCR and ELISA indicated that the expression/production of IL-1 β , IL-6, IL-8, IFN- α , TNF- α , IP-10/CXCL10 and MIP-1 β /CCL4 was significantly elevated in TBEV-infected astrocytes (Figs 3 and 4), which is consistent with other studies describing cytokine/chemokine production by flavivirus-infected astrocytes (Verma *et al.*, 2011; Yang *et al.*, 2012; Hussmann & Fredericksen, 2014). The greatest increase

in cytokine/chemokine production was observed between days 2 and 3 p.i. (Figs 3 and 4). This finding was consistent with the time of peak virus production in HBCAs (Fig. 1b).

Cytokines such as TNF- α and IL-1 β have been reported as potent inducers of neuronal injury (Brabers & Nottet, 2006; Ghoshal *et al.*, 2007; McColl *et al.*, 2008; Kumar *et al.*, 2010; Verma *et al.*, 2011). IL-1 β , IL-6 and IL-8 are endogenous pyrogens that exert multiple downstream inflammatory signalling pathways (Verma *et al.*, 2011). These cytokines are elevated during various CNS infections, including TBE (Palus *et al.*, 2013). Increased concentrations of pro-inflammatory cytokines, including TNF- α and IL-6, were detected in sera from TBE patients, and their elevated levels corresponded with the acute phase

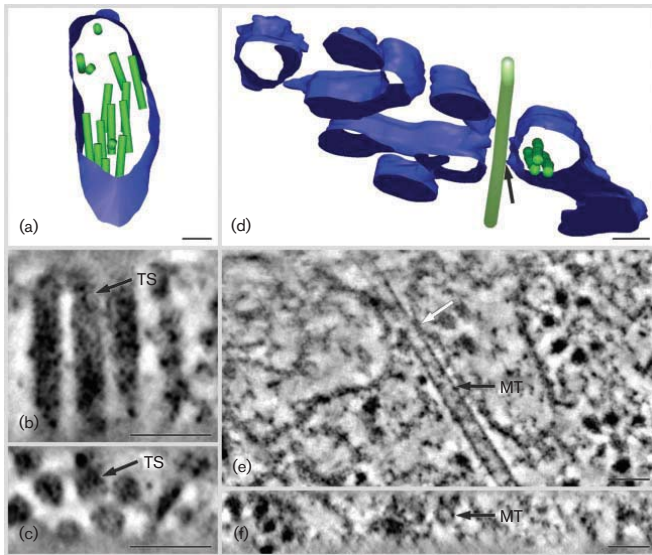


Fig. 10. Comparison of the ultrastructure of tubule-like structures (a–c) and a microtubule (d, e) in TBEV-infected HBCAs. (a–c) Detail of tubule-like structures from Fig. 9(a), area a. The model is shown in (a), a slice of a dual axis tomogram in (b) and the side view in (c). (d–f) Detail of microtubule from Fig. 9(a), area b. The model is shown in (d), a slice of a dual axis tomogram in (e) and the side view in (f). The white arrow in (e) indicates a connection between the microtubule and the membrane of the RER. Tilt series images were collected in the range $\pm 65^\circ$ in 0.65° increments. The final reconstructed section thickness was approximately 60 nm, which was divided into 75 slices. Pixel resolution: 0.81 nm. Bars, 50 nm.

of the disease (Atrasheuskaya *et al.*, 2003). The chemokine IP-10 has the ability to attract activated T-cells in the CNS (Klein *et al.*, 2005). Excessively high levels of IP-10 in the CNS can be very harmful to the host (Sasseville *et al.*, 1996; Westmoreland *et al.*, 1998; Sui *et al.*, 2006), possibly by activating a calcium-dependent apoptotic pathway (Sui *et al.*, 2004). In human TBE patients, higher levels of IP-10 can be detected in serum, as well as in cerebrospinal fluid (Lepej *et al.*, 2007; Zajkowska *et al.*, 2011). The attraction of CD8⁺ T-cells to the CNS by IP-10 can have important consequences for viral clearance, as well as for immunopathological reactions observed during TBE (Růžek *et al.*, 2009a). Similar to our study, astrocytes have been described as a predominant source of IP-10 in Japanese encephalitis (Bhowmick *et al.*, 2007). The expression of MCP-1/CCL2, a compound that is able to disrupt the integrity of the BBB and modulate the progression of neuroinflammation (Yao & Tsirka, 2014), is highly upregulated in TBEV-infected brain tissue (Palus *et al.*, 2013). However, its expression was not increased in astrocytes after TBEV infection in the present study, suggesting that astrocytes are not responsible for the production of this cytokine in the CNS during TBE. Together, TBEV-infected astrocytes produce a variety of cytokines that can mediate a diverse range of neurodegenerative functions, including disruption of the BBB, chemoattraction of peripheral immune cells into the CNS and neuronal damage.

We reported previously that TBE is associated with the disruption of BBB integrity, which is most likely caused by cytokine/chemokine overproduction in the brain (Růžek *et al.*, 2011). In human TBE patients, higher levels of

MMP-9 (a compound with multiple functions, including disruption of the BBB) have been observed in serum (Palus *et al.*, 2014) and cerebrospinal fluid (Kang *et al.*, 2013). However, it was not clear which cells were involved in MMP-9 production and BBB disruption. In the present study, we observed that TBEV-infected astrocytes produced large quantities of MMP-9 (Fig. 5), and therefore might represent the main cell population responsible for the increase of BBB permeability during TBE. The entry of TBEV into the CNS precedes the breakdown of the BBB (Růžek *et al.*, 2011). The invasion of TBEV into the CNS brings the virus into close proximity with the second component of the BBB, astrocytes (Hussmann *et al.*, 2013). TBEV-activated astrocytes then produce MMP-9, which might cause the BBB breakdown. Moreover, MMP-9 is capable of causing neuronal apoptosis (del Zoppo, 2010).

Additional evidence of astrocyte activation by TBEV was demonstrated by the increased production of GFAP (Fig. 6). GFAP is involved in many important CNS processes, including cell communication and BBB function. Increased GFAP expression/production as a marker of astrocyte activation has been documented in many studies (Brodie *et al.*, 1997; Zhou *et al.*, 2004; Pozner *et al.*, 2008; Watanabe *et al.*, 2008; Kumar *et al.*, 2010; Fan *et al.*, 2011; Ojeda *et al.*, 2014), represents one of the earliest responses to CNS injury and is a distinguishing feature of reactive astrogliosis (Montgomery, 1994). The activation of glial cells including astrocytes represents one of the major histopathological features of TBE (Környey, 1978; Gelpi *et al.*, 2006). The astrocyte activation leads to a downstream cascade of inflammatory cytokine production that results in the death of neurons (Kumar *et al.*, 2010; Pekny *et al.*, 2014). In our

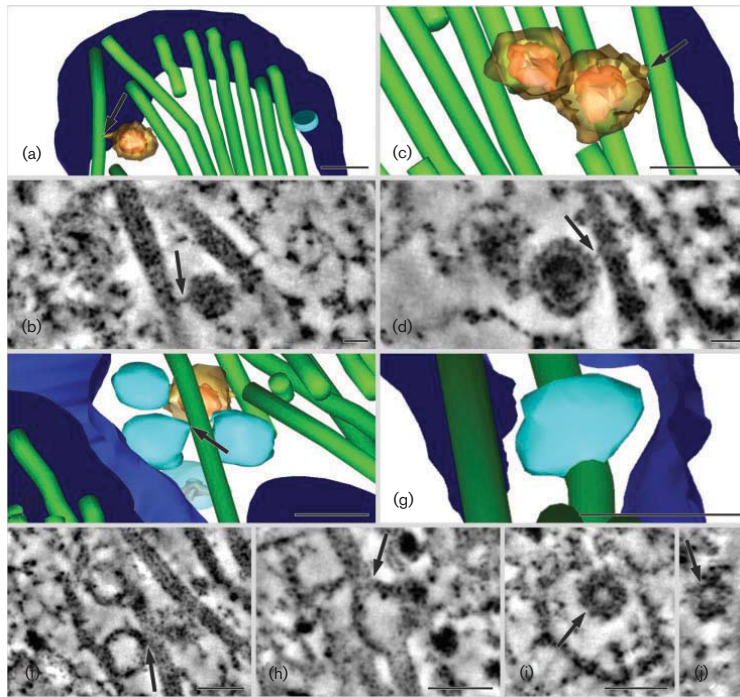


Fig. 11. 3D architecture of tubule-like structures observed in TBEV-infected HBCAs. The connection (arrow) between tubule-like structures and enveloped virions in the model (a, c, e, g) and in a slice of a dual axis tomogram (b, d, f, h). Enlargement of Fig. 9(a), areas c (a, b), d (c, d), e (e, f) and f (g, h) is shown. Supposed subviral particle enclosed in the vesicle outside the RER, detail from Fig. 9(a), area g, is shown in the tomogram top view (i) and side view (j). Tilt series images were collected in the range $\pm 65^\circ$ in 0.65° increments. The final reconstructed section thickness was approximately 60 nm, which was divided into 75 slices. Pixel resolution, 0.81 nm. Bars, 50 nm.

study, GFAP production was higher in TBEV-infected astrocytes than in mock-infected or LPS-stimulated astrocytes. Treatment with LPS had no effect on GFAP production at 3 and 7 days after treatment, which is in accordance with a previous study that demonstrated that LPS downregulates the expression of GFAP mRNA (Letournel-Boulland *et al.*, 1994). However, on day 15 post-treatment, LPS treatment increased GFAP production in astrocytes compared with controls, although at a lower level than in TBEV-infected cells (Fig. 6a, b).

We demonstrated previously that TBEV infection of human neural cells (neuroblastoma, medulloblastoma and glioblastoma cells) is associated with a number of morphological changes. The infection of medulloblastoma and glioblastoma cells led to proliferation of the RER and extensive rearrangement of cytoskeletal structures (Růžek *et al.*, 2009b). With the exception of typical remodelling of the RER (Figs 7 and 8), here we have described the morphology and 3D organization of TBEV-induced

structures, called tubule-like structures, located in the RER of infected HBCAs (Figs 9–11). Tubular structures (also called elongated vesicles or rod-like particles) of sizes ranging from 50 to 100 nm in diameter and 100 nm to 3.5 μm in length have been reported previously inside the RER of other cells infected with either tick-borne flaviviruses (Lorenz *et al.*, 2003; Offerdahl *et al.*, 2012) or mosquito-borne flaviviruses (Welsch *et al.*, 2009). Tubules with closed ends and without pores or connections to other tubules or other structures have been observed in the RER of ISE-6 tick cells persistently infected with Langat virus (Offerdahl *et al.*, 2012). Tubular structures measuring 50 nm in diameter have been found in mammalian COS-1 cells expressing proteins prM and E of TBEV (Lorenz *et al.*, 2003). We supposed that enveloped virus particles were also connected to tubule-like structures in TBEV-infected neuroblastoma cells (Růžek *et al.*, 2009b; Fig. 5). However, the tubular structures that we observed in TBEV-infected astrocytes differed from those reported previously with

respect to diameter and the appearance of the inner part of the structure. The presence of these tubule-like structures solely in the RER and their small diameter dispute their microtubular origin. Although the function and origin of the tubule-like structures remain unexplained, these structures appear to be a feature of persistent infection (Lorenz *et al.*, 2003; Offerdahl *et al.*, 2012). We propose that viral activity leads to the production of tubule-like structures, either directly as a result of defective virus assembly, or due to disruption of the host's cellular metabolism.

In TBEV-infected HBCAs at 9 days p.i., we observed the presence of swollen mitochondria next to mitochondria without any ultrastructural alterations. This finding might indicate irreversible injury of some astrocytic mitochondria that is connected with the permeability of mitochondrial membranes and the uptake of water from the cytosol. The remaining mitochondria inside astrocytes may help maintain the energy balance, supporting cell survival and thus contributing (as the glial cells) to neuronal protection. The absence of TBEV particles and lack of ultrastructural alteration in other HBCAs in the culture is in accordance with immunofluorescence staining and the observation of Potokar *et al.* (2014) regarding the resistance of astrocytes to TBEV-mediated cell death. In contrast to previous observations of TBEV infections of neural cells, we did not observe any signs of apoptosis (Růžek *et al.*, 2009b) or the formation of structures described recently as laminal membrane structures in neurons (Hirano *et al.*, 2014).

In summary, these results demonstrate for the first time, to the best of our knowledge, that cultured human primary astrocytes are sensitive to TBEV infection and are a potential source of pro-inflammatory cytokines in TBEV-infected brain cells, which might contribute to TBEV-induced neurotoxicity and/or BBB breakdown during TBE.

METHODS

Virus and cells. The TBEV strain Neudoerfl, a prototype strain of the European subtype, kindly provided by Professor F. X. Heinz from the Medical University of Vienna, was used in all experiments. The virus was originally isolated from the tick *Ixodes ricinus* in Austria in 1971. The virus has been characterized extensively, including its genome sequence (GenBank accession no. U17495) and the 3D structure of its envelope protein, E (Rey *et al.*, 1995). The virus was passaged four times by infecting suckling mice intracranially before its use in the present study.

HBCAs were purchased from ScienCell at passage 1 and propagated in CSC Complete Medium with 10% serum (ACBR) at 37 °C and 5% CO₂. In all experiments, low-passage-number cells were used. Porcine kidney stable (PS) cells (Kožuch & Mayer, 1975) were grown at 37 °C in L-15 medium supplemented with 3% newborn calf serum and a 1% antibiotic mixture of penicillin and streptomycin (Sigma).

Viral growth in HBCAs. Monolayer HBCA cultures grown in 96-well plates were inoculated with virus diluted in the culture medium to an m.o.i. of 5. Virus-mediated CPE was investigated using light microscopy. At 0, 1, 2, 3, 5, 7, 9 and 15 days p.i., supernatant medium from

appropriate wells was collected and frozen at -70 °C. Titres were determined by plaque assay.

Plaque assay. Virus titres were assayed on PS cell monolayers, as described previously (De Madrid & Porterfield, 1969). Briefly, 10-fold dilutions of the virus sample were placed in 24-well tissue culture plates and PS cells were added in suspension (0.6×10^5 – 1.5×10^5 cells per well). After incubation for 4 h, the suspension was overlaid with carboxymethylcellulose (1.5% in L-15 medium). After incubation for 5 days at 37 °C, the plates were washed with PBS, and the cell monolayers were stained with naphthalene black. Infectivity was expressed as p.f.u. ml⁻¹.

Immunofluorescence staining. Infected and non-infected cells on slides were subjected to cold acetone:methanol (1:1) fixation for 10 min, rinsed in PBS and blocked with 10% FBS. Cells were labelled with flavivirus-specific mAb (1:250; Sigma-Aldrich) or with anti-GFAP antibody conjugated with Alexa Fluor 488 (1:200, eBioscience) for 1 h at 37 °C. Flavivirus-specific, mouse mAb and anti-PDIA3 rabbit antibody (1:250; Sigma-Aldrich) were used for double labelling. After washing with Tween 20 (0.05%, v/v) in PBS, the cells were labelled with anti-mouse, goat secondary antibody conjugated with FITC (1:500; Sigma-Aldrich) or anti-rabbit, goat secondary antibody conjugated with Atto 550 NHS (1:500, Sigma-Aldrich) for 1 h at 37 °C. The cells were counterstained with DAPI (1 µg ml⁻¹; Sigma) for 30 min at 37 °C, mounted in 2.5% 1,4-diazabicyclo(2.2.2)octane (Sigma) and examined with an Olympus BX-51 fluorescence microscope equipped with an Olympus DP-70 CCD camera.

Flow cytometry. HBCAs were cultured in a 96-well plate at a concentration of 5×10^4 cells ml⁻¹ and infected with the TBEV strain Neudoerfl (m.o.i. of 5) 1 day after seeding. Mock-infected or LPS-treated (at a final concentration of 100 ng ml⁻¹) cells were used as controls. Cells were harvested at 3, 7 and 15 days p.i. Astrocytes were fixed with a Foxp3/Transcription Factor Staining Buffer Set (eBioscience). Briefly, the cultured cells were washed twice with Dulbecco's PBS (Sigma-Aldrich), trypsinized, inactivated with FCS and centrifuged at 160 g for 5 min at 4 °C. Harvested cells were fixed and permeabilized for 45 min according to the manufacturer's protocol. An anti-flavivirus group antigen antibody (1:500; Merck-Millipore) and a secondary FITC-conjugated anti-mouse polyvalent antibody (1:500; Sigma-Aldrich) were used to stain the TBEV-positive cells. An anti-GFAP antibody (1:100, Santa Cruz) conjugated to Alexa Fluor 488, was used to stain GFAP-positive cells. The cells were washed with 1 × permeabilization buffer after each staining and centrifuged at 300 g for 5 min at room temperature. Finally, the cells were resuspended in 1% FCS and used for flow cytometry analysis on a BD FACS Canto II with BDFACS Diva software. Obtained data were analysed using Flowing Software 2, version 2.5.1 (Perttu Terho, University of Turku, Finland).

Quantitative real-time RT-PCR. Total RNA was extracted from TBEV-infected HBCAs and control cells and cDNA was synthesized by reverse transcription using an Ambion Cells-to-CT kit (Applied Biosystems) according to the manufacturer's instructions. The synthesized cDNAs were used as templates for quantitative real-time PCR. The PCR was performed using pre-developed TaqMan Assay Reagents [Assay IDs: IL-6 (Hs00985639_m1), IL-1β (Hs01555410_m1), IL-8 (Hs00174103_m1), IFN-α (Hs00819693_sH), TNF-α (Hs00174128_m1), MIP-1β/CCL4 (Hs99999148_m1), MCP-1/CCL2 (Hs00234140_m1) and IP-10 (Hs01124251_g1)] and TaqMan Gene Expression Master Mix (Applied Biosystems) on a Rotor Gene-3000 (Corbett Research). Human β-actin (Hs99999903_m1) and glyceraldehyde 3-phosphate dehydrogenase (Hs03929097_g1) were used as housekeeping genes. The amplification conditions were as follows: 2 min at 50 °C (to allow UNG to destroy any contaminating templates); 10 min at 95 °C (to denature UNG and activate the

enzymes); 40 cycles of denaturation at 95 °C for 15 s and annealing/extension at 60 °C for 1 min.

To calculate the fold change in gene expression, the cycle threshold (C_t) of the housekeeping genes was subtracted from the C_t of the target gene to yield ΔC_t . Change in expression of the normalized target gene was expressed as $2^{-\Delta\Delta C_t}$, where $\Delta\Delta C_t = \Delta C_{t\text{sample}} - \Delta C_{t\text{control}}$ as described previously (Livak & Schmittgen, 2001).

Viral RNA was quantified in cells grown in 96-well plates at 0, 2, 7 and 15 days p.i. with TBEV strain Neudoerfl (m.o.i. of 5). The cells were lysed using an Ambion Cells-to-CT kit and subsequently subjected to RNA purification with a QIAamp Viral RNA Mini kit (Qiagen) according to the manufacturer's instructions. Viral RNA was quantified using a TBEV Real-time RT-PCR kit (Liferiver) on a Rotor Gene-3000 (Corbett Research) following the manufacturer's instructions.

ELISA. We used human ELISA kits (Invitrogen) to measure the effect of TBEV exposure on cytokine/chemokine and MMP-9 expression in HBCAs. Mock-infected and TBEV-infected HBCAs were plated in 96-well plates at a density of 2×10^4 cells per well and infected 24 h later. The cells were infected with TBEV (m.o.i. of 5) and mock infected with the same dilution of brain suspension without virus. At 0, 1, 2, 3, 4, 5, 9 and 15 days p.i., supernatant medium from appropriate wells was collected and frozen at -70 °C. Cell supernatants were then assayed for CXCL10/IP10 (Human ELISA kit, KAC2361; Invitrogen), MIP-1 β (Human ELISA kit, KAC2291; Invitrogen) and MMP-9 (Human ELISA kit, KHC3061; Invitrogen) according to the manufacturer's instructions.

Transmission electron microscopy and electron tomography. TBEV-infected and control HBCAs that had been grown on sapphire discs were high-pressure frozen at either 3 or 9 days p.i. in the presence of 20% BSA diluted in growing medium using a Leica EM PACT2 high-pressure freezer. Freeze substitution (Leica EM AFS2) was carried out in 2% osmium tetroxide diluted in 100% acetone at -90 °C for 16 h, and then warmed up at a rate of 5 °C h^{-1} to remain at -20 °C for 14 h, and finally warmed up again at the same rate to a final temperature of 4 °C. Samples were rinsed three times in anhydrous acetone at room temperature and infiltrated stepwise in acetone mixed with SPI-pon resin (SPI) (acetone:SPI ratios of 2:1, 1:1 and 1:2, for 1 h at each step). The samples, now in pure resin, were polymerized at 60 °C for 48 h.

Sections were prepared using a Leica Ultracut UCT microtome (Leica Microsystems) and collected on 300 mesh copper grids. Staining was performed using alcoholic uranic acetate for 30 min and in lead citrate for 20 min. Images were obtained using a JEOL 2100F or JEOL 1010 transmission electron microscope. For electron tomography, protein A-conjugated 10 nm gold nanoparticles (Aurion) were added to both sides of each section as fiducial markers.

Tilt series images were collected in the range of $\pm 65^\circ$ with 0.65° increments using a 200 kV JEOL 2100F transmission electron microscope equipped with a high-tilt stage and Gatan camera (Orion SC 1000) and controlled by SerialEM automated acquisition software (Mastrorade, 2005). Images were aligned using the fiducial markers. Electron tomograms were reconstructed using the IMOD software package. Manual masking of the area of interest was employed to generate a 3D surface model (Kremer *et al.*, 1996).

Statistical analysis. Data were analysed using version 5.04 of the GraphPad Prism5 software program (GraphPad Software). ELISA measurements of increased chemokine and cytokine production were analysed using one-way ANOVA (Tukey's multiple comparison test). All other data were analysed using one-way ANOVA (Newman-Keuls

multiple comparison test). Differences of $P < 0.05$ were considered statistically significant.

ACKNOWLEDGEMENTS

The authors are indebted to Professors Jan Kopecký and Libor Grubhoffer and Dr Jana Nebesařová for general support of our work. This work was supported by the Academy of Sciences of the Czech Republic (Z60220518), Czech Science Foundation (projects nos P502/11/2116, P302/12/2490 and GA14-29256S), the MEYS of the Czech Republic (project LO1218) under the NPU I programme, Grant Agency of the University of South Bohemia (127/2014/P), and Technology Agency of the Czech Republic (TE 01020118). The founders had no role in the study design, data collection and analysis, decision to publish or preparation of the manuscript.

REFERENCES

- Atirasheuskaya, A. V., Fredeking, T. M. & Ignatyev, G. M. (2003). Changes in immune parameters and their correction in human cases of tick-borne encephalitis. *Clin Exp Immunol* **131**, 148–154.
- Balsitis, S. J., Coloma, J., Castro, G., Alava, A., Flores, D., McKerrow, J. H., Beatty, P. R. & Harris, E. (2009). Tropism of dengue virus in mice and humans defined by viral nonstructural protein 3-specific immunostaining. *Am J Trop Med Hyg* **80**, 416–424.
- Bhowmick, S., Duseja, R., Das, S., Appiahgiri, M. B., Vрати, S. & Basu, A. (2007). Induction of IP-10 (CXCL10) in astrocytes following Japanese encephalitis. *Neurosci Lett* **414**, 45–50.
- Brabers, N. A. & Nottet, H. S. (2006). Role of the pro-inflammatory cytokines TNF- α and IL-1 β in HIV-associated dementia. *Eur J Clin Invest* **36**, 447–458.
- Brodie, C., Weizman, N., Katzoff, A., Lustig, S. & Kobiler, D. (1997). Astrocyte activation by Sindbis virus: expression of GFAP, cytokines, and adhesion molecules. *Glia* **19**, 275–285.
- Chen, C. J., Liao, S. L., Kuo, M. D. & Wang, Y. M. (2000). Astrocytic alteration induced by Japanese encephalitis virus infection. *Neuroreport* **11**, 1933–1937.
- Chen, C. J., Chen, J. H., Chen, S. Y., Liao, S. L. & Raung, S. L. (2004). Upregulation of RANTES gene expression in neuroglia by Japanese encephalitis virus infection. *J Virol* **78**, 12107–12119.
- de Araújo, J. M., Schatzmayr, H. G., de Filippis, A. M., Dos Santos, F. B., Cardoso, M. A., Britto, C., Coelho, J. M. & Nogueira, R. M. (2009). A retrospective survey of dengue virus infection in fatal cases from an epidemic in Brazil. *J Virol Methods* **155**, 34–38.
- De Madrid, A. T. & Porterfield, J. S. (1969). A simple micro-culture method for the study of group B arboviruses. *Bull World Health Organ* **40**, 113–121.
- del Zoppo, G. J. (2010). The neurovascular unit, matrix proteases, and innate inflammation. *Ann N Y Acad Sci* **1207**, 46–49.
- Desai, A., Shankar, S. K., Ravi, V., Chandramuki, A. & Gourie-Devi, M. (1995). Japanese encephalitis virus antigen in the human brain and its topographic distribution. *Acta Neuropathol* **89**, 368–373.
- Diniz, J. A., Da Rosa, A. P., Guzman, H., Xu, F., Xiao, S. Y., Popov, V. L., Vasconcelos, P. F. & Tesh, R. B. (2006). West Nile virus infection of primary mouse neuronal and neuroglial cells: the role of astrocytes in chronic infection. *Am J Trop Med Hyg* **75**, 691–696.
- Erickson, M. A., Dohi, K. & Banks, W. A. (2012). Neuroinflammation: a common pathway in CNS diseases as mediated at the blood–brain barrier. *Neuroimmunomodulation* **19**, 121–130.

- Fan, Y., Zou, W., Green, L. A., Kim, B. O. & He, J. J. (2011). Activation of Egr-1 expression in astrocytes by HIV-1 Tat: new insights into astrocyte-mediated Tat neurotoxicity. *J Neuroimmune Pharmacol* **6**, 121–129.
- Gelpi, E., Preusser, M., Garzuly, F., Holzmann, H., Heinz, F. X. & Budka, H. (2005). Visualization of Central European tick-borne encephalitis infection in fatal human cases. *J Neuropathol Exp Neurol* **64**, 506–512.
- Gelpi, E., Preusser, M., Laggner, U., Garzuly, F., Holzmann, H., Heinz, F. X. & Budka, H. (2006). Inflammatory response in human tick-borne encephalitis: analysis of postmortem brain tissue. *J Neurovirol* **12**, 322–327.
- German, A. C., Myint, K. S., Mai, N. T., Pomeroy, I., Phu, N. H., Tzartos, J., Winter, P., Collett, J., Farrar, J. & other authors (2006). A preliminary neuropathological study of Japanese encephalitis in humans and a mouse model. *Trans R Soc Trop Med Hyg* **100**, 1135–1145.
- Ghoshal, A., Das, S., Ghosh, S., Mishra, M. K., Sharma, V., Koli, P., Sen, E. & Basu, A. (2007). Proinflammatory mediators released by activated microglia induces neuronal death in Japanese encephalitis. *Glia* **55**, 483–496.
- Gillespie, L. K., Hoenen, A., Morgan, G. & Mackenzie, J. M. (2010). The endoplasmic reticulum provides the membrane platform for biogenesis of the flavivirus replication complex. *J Virol* **84**, 10438–10447.
- Gritsun, T. S., Frolova, T. V., Zhankov, A. I., Arnesto, M., Turner, S. L., Frolova, M. P., Pogodina, V. V., Lashkevich, V. A. & Gould, E. A. (2003). Characterization of a Siberian virus isolated from a patient with progressive chronic tick-borne encephalitis. *J Virol* **77**, 25–36.
- Haglund, M. & Günther, G. (2003). Tick-borne encephalitis–pathogenesis, clinical course and long-term follow-up. *Vaccine* **21** (Suppl. 1), S11–S18.
- Hirano, M., Yoshii, K., Sakai, M., Hasebe, R., Ichii, O. & Kariwa, H. (2014). Tick-borne flaviviruses alter membrane structure and replicate in dendrites of primary mouse neuronal cultures. *J Gen Virol* **95**, 849–861.
- Hussmann, K. L. & Fredericksen, B. L. (2014). Differential induction of CCL5 by pathogenic and non-pathogenic strains of West Nile virus in brain endothelial cells and astrocytes. *J Gen Virol* **95**, 862–867.
- Hussmann, K. L., Samuel, M. A., Kim, K. S., Diamond, M. S. & Fredericksen, B. L. (2013). Differential replication of pathogenic and nonpathogenic strains of West Nile virus within astrocytes. *J Virol* **87**, 2814–2822.
- Imbert, J. L., Guevara, P., Ramos-Castañeda, J., Ramos, C. & Sotelo, J. (1994). Dengue virus infects mouse cultured neurons but not astrocytes. *J Med Virol* **42**, 228–233.
- Kang, X., Li, Y., Wei, J., Zhang, Y., Bian, C., Wang, K., Wu, X., Hu, Y., Li, J. & Yang, Y. (2013). Elevation of matrix metalloproteinase-9 level in cerebrospinal fluid of tick-borne encephalitis patients is associated with IgG extravasation and disease severity. *PLoS ONE* **8**, e77427.
- Klein, R. S., Lin, E., Zhang, B., Luster, A. D., Tollett, J., Samuel, M. A., Engle, M. & Diamond, M. S. (2005). Neuronal CXCL10 directs CD8⁺ T-cell recruitment and control of West Nile virus encephalitis. *J Virol* **79**, 11457–11466.
- Környey, S. (1978). Contribution to the histology of tick-borne encephalitis. *Acta Neuropathol* **43**, 179–183.
- Kožuch, O. & Mayer, V. (1975). Pig kidney epithelial (PS) cells: a perfect tool for the study of flaviviruses and some other arboviruses. *Acta Virol* **19**, 498.
- Kremer, J. R., Mastronarde, D. N. & McIntosh, J. R. (1996). Computer visualization of three-dimensional image data using IMOD. *J Struct Biol* **116**, 71–76.
- Kumar, M., Verma, S. & Nerurkar, V. R. (2010). Pro-inflammatory cytokines derived from West Nile virus (WNV)-infected SK-N-SH cells mediate neuroinflammatory markers and neuronal death. *J Neuroinflammation* **7**, 73.
- Lepej, S. Z., Misić-Majerus, L., Jeren, T., Rode, O. D., Remenar, A., Sporec, V. & Vince, A. (2007). Chemokines CXCL10 and CXCL11 in the cerebrospinal fluid of patients with tick-borne encephalitis. *Acta Neurol Scand* **115**, 109–114.
- Letournel-Boulland, M. L., Fages, C., Rolland, B. & Tardy, M. (1994). Lipopolysaccharides (LPS), up-regulate the IL-1-mRNA and down-regulate the glial fibrillary acidic protein (GFAP) and glutamine synthetase (GS)-mRNAs in astroglial primary cultures. *Eur Cytokine Netw* **5**, 51–56.
- Livak, K. J. & Schmittgen, T. D. (2001). Analysis of relative gene expression data using real-time quantitative PCR and the 2^{-ΔΔCT} method. *Methods* **25**, 402–408.
- Lorenz, I. C., Kartenbeck, J., Mezzacasa, A., Allison, S. L., Heinz, F. X. & Helenius, A. (2003). Intracellular assembly and secretion of recombinant subviral particles from tick-borne encephalitis virus. *J Virol* **77**, 4370–4382.
- Mansfield, K. L., Johnson, N., Phipps, L. P., Stephenson, J. R., Fooks, A. R. & Solomon, T. (2009). Tick-borne encephalitis virus – a review of an emerging zoonosis. *J Gen Virol* **90**, 1781–1794.
- Mastronarde, D. N. (2005). Automated electron microscope tomography using robust prediction of specimen movements. *J Struct Biol* **152**, 36–51.
- McColl, B. W., Rothwell, N. J. & Allan, S. M. (2008). Systemic inflammation alters the kinetics of cerebrovascular tight junction disruption after experimental stroke in mice. *J Neurosci* **28**, 9451–9462.
- Miorin, L., Romero-Brey, I., Maiuri, P., Hoppe, S., Krijnse-Locker, J., Bartenschlager, R. & Marcello, A. (2013). Three-dimensional architecture of tick-borne encephalitis virus replication sites and trafficking of the replicated RNA. *J Gen Virol* **94**, 6469–6481.
- Montgomery, D. L. (1994). Astrocytes: form, functions, and roles in disease. *Vet Pathol* **31**, 145–167.
- Nedergaard, M., Ransom, B. & Goldman, S. A. (2003). New roles for astrocytes: redefining the functional architecture of the brain. *Trends Neurosci* **26**, 523–530.
- Nogueira, R. M., Filippis, A. M., Coelho, J. M., Sequeira, P. C., Schatzmayr, H. G., Paiva, F. G., Ramos, A. M. & Miagostovich, M. P. (2002). Dengue virus infection of the central nervous system (CNS): a case report from Brazil. *Southeast Asian J Trop Med Public Health* **33**, 68–71.
- Offerdahl, D. K., Dorward, D. W., Hansen, B. T. & Bloom, M. E. (2012). A three-dimensional comparison of tick-borne flavivirus infection in mammalian and tick cell lines. *PLoS ONE* **7**, e47912.
- Ojeda, D., López-Costa, J. J., Sede, M., López, E. M., Berria, M. I. & Quarleri, J. (2014). Increased in vitro glial fibrillary acidic protein expression, telomerase activity, and telomere length after productive human immunodeficiency virus-1 infection in murine astrocytes. *J Neurosci Res* **92**, 267–274.
- Overby, A. K., Popov, V. L., Niedrig, M. & Weber, F. (2010). Tick-borne encephalitis virus delays interferon induction and hides its double-stranded RNA in intracellular membrane vesicles. *J Virol* **84**, 8470–8483.
- Palus, M., Vojtišková, J., Salát, J., Kopecký, J., Grubhoffer, L., Lipoldová, M., Demant, P. & Růžek, D. (2013). Mice with different susceptibility to tick-borne encephalitis virus infection show selective neutralizing antibody response and inflammatory reaction in the central nervous system. *J Neuroinflammation* **10**, 77.

- Palus, M., Zampachová, E., Elsterová, J. & Růžek, D. (2014). Serum matrix metalloproteinase-9 and tissue inhibitor of metalloproteinase-1 levels in patients with tick-borne encephalitis. *J Infect* **68**, 165–169.
- Pekny, M., Wilhelmsson, U. & Pekna, M. (2014). The dual role of astrocyte activation and reactive gliosis. *Neurosci Lett* **565**, 30–38.
- Potokar, M., Korva, M., Jorgačevski, J., Avšič-Županc, T. & Zorec, R. (2014). Tick-borne encephalitis virus infects rat astrocytes but does not affect their viability. *PLoS ONE* **9**, e86219.
- Pozner, R. G., Collado, S., Jaquenod de Giusti, C., Ure, A. E., Biedma, M. E., Romanowski, V., Schattner, M. & Gómez, R. M. (2008). Astrocyte response to Junin virus infection. *Neurosci Lett* **445**, 31–35.
- Ramesh, G., MacLean, A. G. & Philipp, M. T. (2013). Cytokines and chemokines at the crossroads of neuroinflammation, neurodegeneration, and neuropathic pain. *Mediators Inflamm* **2013**, 480739.
- Réaux-Le Goazigo, A., Van Steenwinckel, J., Rostène, W. & Mélik Parsadaniantz, S. (2013). Current status of chemokines in the adult CNS. *Prog Neurobiol* **104**, 67–92.
- Rey, F. A., Heinz, F. X., Mandl, C., Kunz, C. & Harrison, S. C. (1995). The envelope glycoprotein from tick-borne encephalitis virus at 2 Å resolution. *Nature* **375**, 291–298.
- Růžek, D., Salát, J., Palus, M., Gritsun, T. S., Gould, E. A., Dyková, I., Skallová, A., Jelínek, J., Kopecký, J. & Grubhoffer, L. (2009a). CD8⁺ T-cells mediate immunopathology in tick-borne encephalitis. *Virology* **384**, 1–6.
- Růžek, D., Vancová, M., Tesarová, M., Ahantarig, A., Kopecký, J. & Grubhoffer, L. (2009b). Morphological changes in human neural cells following tick-borne encephalitis virus infection. *J Gen Virol* **90**, 1649–1658.
- Růžek, D., Dobler, G. & Donoso Mantke, O. (2010). Tick-borne encephalitis: pathogenesis and clinical implications. *Travel Med Infect Dis* **8**, 223–232.
- Růžek, D., Salát, J., Singh, S. K. & Kopecký, J. (2011). Breakdown of the blood-brain barrier during tick-borne encephalitis in mice is not dependent on CD8⁺ T-cells. *PLoS ONE* **6**, e20472.
- Sasseville, V. G., Smith, M. M., Mackay, C. R., Pauley, D. R., Mansfield, K. G., Ringler, D. J. & Lackner, A. A. (1996). Chemokine expression in simian immunodeficiency virus-induced AIDS encephalitis. *Am J Pathol* **149**, 1459–1467.
- Sips, G. J., Wilschut, J. & Smit, J. M. (2012). Neuroinvasive flavivirus infections. *Rev Med Virol* **22**, 69–87.
- Stanimirovic, D. B. & Friedman, A. (2012). Pathophysiology of the neurovascular unit: disease cause or consequence? *J Cereb Blood Flow Metab* **32**, 1207–1221.
- Sui, Y., Potula, R., Dhillon, N., Pinson, D., Li, S., Nath, A., Anderson, C., Turchan, J., Kolson, D. & other authors (2004). Neuronal apoptosis is mediated by CXCL10 overexpression in simian human immunodeficiency virus encephalitis. *Am J Pathol* **164**, 1557–1566.
- Sui, Y., Stehno-Bittel, L., Li, S., Loganathan, R., Dhillon, N. K., Pinson, D., Nath, A., Kolson, D., Narayan, O. & Buch, S. (2006). CXCL10-induced cell death in neurons: role of calcium dysregulation. *Eur J Neurosci* **23**, 957–964.
- Verma, S., Kumar, M. & Nerurkar, V. R. (2011). Cyclooxygenase-2 inhibitor blocks the production of West Nile virus-induced neuro-inflammatory markers in astrocytes. *J Gen Virol* **92**, 507–515.
- Watanabe, C., Kawashima, H., Takekuma, K., Hoshika, A. & Watanabe, Y. (2008). Increased nitric oxide production and GFAP expression in the brains of influenza A/NWS virus infected mice. *Neurochem Res* **33**, 1017–1023.
- Welsch, S., Miller, S., Romero-Brey, I., Merz, A., Bleck, C. K., Walther, P., Fuller, S. D., Antony, C., Krijnse-Locker, J. & Bartenschlager, R. (2009). Composition and three-dimensional architecture of the dengue virus replication and assembly sites. *Cell Host Microbe* **5**, 365–375.
- Westmoreland, S. V., Rottman, J. B., Williams, K. C., Lackner, A. A. & Sasseville, V. G. (1998). Chemokine receptor expression on resident and inflammatory cells in the brain of macaques with simian immunodeficiency virus encephalitis. *Am J Pathol* **152**, 659–665.
- Yang, C. M., Lin, C. C., Lee, I. T., Lin, Y. H., Yang, C. M., Chen, W. J., Jou, M. J. & Hsiao, L. D. (2012). Japanese encephalitis virus induces matrix metalloproteinase-9 expression via a ROS/c-Src/PDGFR/P13K/Akt/MAPKs-dependent AP-1 pathway in rat brain astrocytes. *J Neuroinflammation* **9**, 12.
- Yao, Y. & Tsirka, S. E. (2014). Monocyte chemoattractant protein-1 and the blood-brain barrier. *Cell Mol Life Sci* **71**, 683–697.
- Zajkowska, J., Moniuszko-Malinowska, A., Pancewicz, S. A., Muszyńska-Mazur, A., Kondrusik, M., Grygorczuk, S., Swierzbńska-Pijanowska, R., Dunaj, J. & Czupryna, P. (2011). Evaluation of CXCL10, CXCL11, CXCL12 and CXCL13 chemokines in serum and cerebrospinal fluid in patients with tick borne encephalitis (TBE). *Adv Med Sci* **56**, 311–317.
- Zhou, B. Y., Liu, Y., Kim, Bo., Xiao, Y. & He, J. J. (2004). Astrocyte activation and dysfunction and neuron death by HIV-1 Tat expression in astrocytes. *Mol Cell Neurosci* **27**, 296–305.

CHAPTER V

Serum matrix metalloproteinase-9 and tissue inhibitor of metalloproteinase-1 levels in patients with tick-borne encephalitis

Martin Palus, Eva Žampachová, Jana Elsterová, Daniel Růžek

Journal of Infection 2014, 68: 165-169

DOI: 10.1016/j.jinf.2013.09.028

<http://dx.doi.org/10.1016/j.jinf.2013.09.028>

Serum matrix metalloproteinase-9 and tissue inhibitor of metalloproteinase-1 levels in patients with tick-borne encephalitis
(summary)

MMP-9 and tissue inhibitor of metalloproteinase-1 (TIMP-1) play important roles in the function of the BBB. To investigate the mechanism influencing function of the BBB during TBE, the levels of MMP-9 and its common tissue inhibitor, TIMP-1, were measured in serum from patients with acute phase of TBE.

Various experimental studies demonstrated that MMP-9 might be a potential mediator for the disruption of BBB (Ruzek *et al.*, 2011; Paul *et al.*, 1998). Matrix metalloproteinases (MMPs) represent a family of enzymes that are responsible for the degradation of extracellular matrix proteins. MMPs play important roles in normal and pathological processes, including inflammation. MMP-9 is capable of degrading a major component of the basement membrane of the cerebral endothelium, collagen IV, and promotes the migration of cells through tissue or across the BBB (Ichiyama *et al.*, 2007; 2008). The activity of MMPs is controlled by specific tissue inhibitors of metalloproteinases (TIMPs). TIMP-1 has a high affinity for MMP-9 (Ichiyama *et al.*, 2007). The levels of and the ratio between MMP-9 and TIMP-1 proteins were extensively studied in various diseases of the central nervous system, including subacute sclerosing panencephalitis (Ichiyama *et al.*, 2007 and 2008), infectious HIV-associated neurological diseases (Liuzzi *et al.*, 2000) herpes simplex virus encephalitis (Martínez-Torres *et al.*, 2004) and other neurological diseases.

In our study, serum MMP-9 levels and MMP-9/TIMP-1 ratios of TBE patients were significantly higher than controls. There is no specific therapy for TBE, but it was demonstrated that corticoids have a positive effect during the acute stage of this disease (Dunyewicz *et al.*, 1981). It can be speculated that the effect of corticoids in TBE may be explained by the down-regulation of MMP-9 activity, since corticosteroids improve capillary functions by reducing activity of MMP-9 and increasing levels of TIMPs (Rosenberg *et al.*, 1996).

Moreover, during WNV infection it was demonstrated that MMP-9 facilitates virus entry into the brain by enhancing BBB permeability (Wang *et al.*, 2008). On the other hand, the role of MMP-9 in TBEV entry into the CNS and subsequent neuropathogenesis remains unknown and requires further study.

There were no significant differences in serum TIMP-1 levels between TBE patients and controls. Serum MMP-9 and TIMP-1 levels and MMP-9/TIMP-1 ratios were not associated with age of the patients. However, TBE-positive males with TBE had higher levels of MMP-9 than TBE-positive females ($p < 0.05$).

Our data indicate that increased serum level of MMP-9 and MMP-9/TIMP-1 ratios may play an important role in the BBB breakdown and brain damage development and can serve as an indicator of inflammatory brain damage during TBE.



ELSEVIER

BIAA
British Infection Association

www.elsevierhealth.com/journals/jinf



Serum matrix metalloproteinase-9 and tissue inhibitor of metalloproteinase-1 levels in patients with tick-borne encephalitis

Martin Palus^{a,b}, Eva Žampachová^c, Jana Elsterová^{a,b},
Daniel Růžek^{a,d,*}

^aInstitute of Parasitology, Biology Centre of the Academy of Sciences of the Czech Republic, Branišovská 31, CZ-37005 České Budějovice, Czech Republic

^bFaculty of Science, University of South Bohemia, Branišovská 31, CZ-37005 České Budějovice, Czech Republic

^cDepartment of Virology, Hospital České Budějovice, Boženy Němcové 585/54, CZ-37001 České Budějovice, Czech Republic

^dDepartment of Virology, Veterinary Research Institute, Hudcova 70, CZ-62100 Brno, Czech Republic

Accepted 24 September 2013
Available online 1 October 2013

KEYWORDS

Tick-borne encephalitis;
Matrix metalloproteinase-9;
Tissue inhibitor of metalloproteinase-1;
Blood–brain barrier

Summary Objectives: Matrix metalloproteinase-9 (MMP-9) and tissue inhibitor of metalloproteinase-1 (TIMP-1) play important roles in the function of the blood–brain barrier (BBB). To investigate the function of the BBB during tick-borne encephalitis (TBE), the levels of MMP-9 and its common tissue inhibitor, TIMP-1, were measured in serum from patients with acute phase of TBE.

Methods: Serum MMP-9 and TIMP-1 levels were measured in 147 patients with TBE and 153 controls by ELISA.

Results: Serum MMP-9 levels and MMP-9/TIMP-1 ratios of TBE patients were significantly higher than controls ($p < 0.0001$ and $p < 0.005$, respectively). There were no significant differences in serum TIMP-1 levels between TBE patients and controls. Serum MMP-9 and TIMP-1 levels and MMP-9/TIMP-1 ratios were not associated with age of the patients. However, TBE-positive males with TBE had higher levels of MMP-9 than TBE-positive females ($p < 0.05$).

Conclusions: Our results suggest that the increased serum level of MMP-9 and MMP-9/TIMP-1 ratio is associated with the pathogenesis of TBE. Serum MMP-9 can serve as an indicator of breakdown of the BBB and inflammatory brain damage during TBE.

© 2013 The British Infection Association. Published by Elsevier Ltd. All rights reserved.

* Corresponding author. Department of Virology, Veterinary Research Institute, Hudcova 70, CZ-62100 Brno, Czech Republic. Tel.: +420 5 3333 1101; fax: +420 5 4121 1229.

E-mail address: ruzekd@paru.cas.cz (D. Růžek).

Introduction

Tick-borne encephalitis (TBE) is considered an important health problem in Europe and Russia because of protracted course and in some cases severe illness resulting in long-lasting cognitive dysfunction and even persisting pareses of spinal nerves. Although mortality in Europe is relatively low (<1%), rates as high as 20% have been observed in Asia.¹ TBE is endemic in regions of 27 European countries, and new risk areas are discovered every year. In the 30 years between 1974 and 2003, a continuous increase in TBE morbidity reaching up to 400%, was observed in Europe.² From 2004 to 2006, another considerable increase was seen in some TBE countries, notably the Czech Republic, Germany, Poland, Slovenia, and Switzerland.³ The etiologic agent, tick-borne encephalitis virus (TBEV), a member of the family *Flaviviridae*, genus *Flavivirus*, is an arbovirus that is transmitted to humans by infected ixodid tick vectors.

The pathophysiology of the development of encephalitis is unclear.⁴ In particular, very little is known about the role of the blood–brain barrier (BBB) in the neuropathogenesis of TBE.⁵ In this study, the function of the BBB during TBE was investigated by measurements the levels of matrix metalloproteinase-9 (MMP-9) and its common tissue inhibitor (TIMP-1) in serum from patients with acute phase of TBE. Various experimental studies demonstrated that MMP-9 might be a potential mediator for the disruption of BBB.^{6–8} Matrix metalloproteinases (MMPs) represent a family of enzymes that are responsible for the degradation of extracellular matrix proteins. MMPs play important roles in normal and pathological processes, including inflammation.⁹ MMP-9 is capable of degrading collagen IV, a major component of the basement membrane of the cerebral endothelium, and promotes the migration of cells through tissue or across the BBB.^{9,10} The activity of MMPs is controlled by specific tissue inhibitors of metalloproteinases (TIMPs). TIMP-1 has a high affinity for MMP-9.^{9,11} The levels of MMP-9, TIMP-1 and the ratio between these two proteins were extensively studied in various diseases of the central nervous system, including subacute sclerosing panencephalitis,^{9,10} fungal or tuberculous meningoencephalitis,¹² HIV-associated neurological diseases,¹³ herpes simplex virus encephalitis,¹⁴ and influenza-associated encephalopathy.¹⁵

Here, we demonstrate that the development of TBE is associated with increase of MMP-9 levels and MMP-9/TIMP-1 ratio in serum. Our results suggest that the increased serum level of MMP-9 and MMP-9/TIMP-1 ratio is associated with the pathogenesis of TBE, and serum MMP-9 can serve as an indicator of inflammatory damage to the brain during TBE.

Patients and methods

Serum samples were obtained from 147 patients (78 males and 69 females, aged from 5 to 91 years; median, 46 years) with serologically confirmed acute TBE (detection of specific anti-TBEV IgM and IgG antibodies by ELISA). The samples were collected in years 2011 and 2012. Patients (or their parents) signed an informed consent before sample collection. Then the samples were investigated

anonymously. The study was approved by Institutional Ethical Committee (PARU ASCR No. 01/11).

The control subjects for the serum levels of MMP-9 were 239 and TIMP-1 were 153 healthy individuals of a corresponding age group (115 males and 124 females; aged from 4 to 83 years; median, 40 years).

The serum concentrations of MMP-9 and TIMP-1 were determined by sandwich-type ELISA kits (Human TIMP-1 and Human MMP-9, Invitrogen Corporation CA, USA). Assays were performed following the instructions of the manufacturer. The detection limits were 0.0235 ng/ml for MMP-9, and 1.56 ng/ml for TIMP-1.

The statistical differences in MMP-9 and TIMP-1 concentration in sera between groups were analyzed using the Mann–Whitney test. Differences with $p < 0.05$ were considered significant. Correlations were analyzed using Pearson's coefficient correlation. Analyses and calculations were performed using GraphPad Prism 5.04 (GraphPad Software, Inc., USA).

Results

The geometric means of serum MMP-9 and TIMP-1 levels, and MMP-9/TIMP-1 ratios of the controls were 251.8 ng/ml (range, 58.8–342.5 ng/ml), 742.8 ng/ml (range, 153.4–3635.7 ng/ml), and 0.5400 (range, 0.0004–2.1804), respectively. The geometric means of serum MMP-9 and TIMP-1 levels, and MMP-9/TIMP-1 ratios of the TBE patients were 403.1 ng/ml (range, 93.9–599.3 ng/ml), 749.3 ng/ml (range, 188.1–3384.1 ng/ml), and 0.6801 (range, 0.0302–2.0236), respectively (Fig. 1). Serum MMP-9 levels and MMP-9/TIMP-1 ratios of TBE patients were significantly higher than the controls ($p < 0.0001$ and $p < 0.005$, respectively). There were no significant differences in serum TIMP-1 levels between TBE patients and controls ($p = 0.7964$).

When patients and control subjects divided into two groups according to their age (<50 and ≥ 50 years), there were no statistical differences between the groups (Fig. 2). The geometric means of serum MMP-9, TIMP-1 levels, and MMP-9/TIMP-1 ratios of the TBE patients <50 years-old were 350.8 ng/ml (range, 65.62–599.26 ng/ml), 758.90 ng/ml (range, 202.00–3384.13 ng/ml), and 0.6766 (range, 0.0302–1.8104), respectively. The geometric means of serum MMP-9, TIMP-1 levels, and MMP-9/TIMP-1 ratios of the TBE patients ≥ 50 years-old were 359.40 ng/ml (range, 74.88–588.28 ng/ml), 736.00 ng/ml (range, 188.11–1902.71 ng/ml), and 0.6848 (range, 0.0532–2.0237), respectively. There was no correlation of serum MMP-9 and TIMP-1 levels and MMP-9/TIMP-1 ratios with age of the TBE patients as well as controls (Fig. 3).

The geometric means of serum MMP-9, TIMP-1 levels, and MMP-9/TIMP-1 ratios of the male TBE patients were 372.80 ng/ml (range, 74.88–599.26 ng/ml), 763.9 ng/ml (range, 188.1–3384.1 ng/ml), and 0.709 (range, 0.532–2.024), respectively. The geometric means of serum MMP-9, TIMP-1 levels, and MMP-9/TIMP-1 ratios of the female TBE patients were 333.8 ng/ml (range, 65.6–567.3 ng/ml), 732.70 ng/ml (range, 199.67–2751.42 ng/ml), and 0.65 (range, 0.03–1.81), respectively. In case of controls, no difference in serum MMP-9 and TIMP-1 levels, and MMP-9/TIMP-1 ratios was seen between males and females. Males

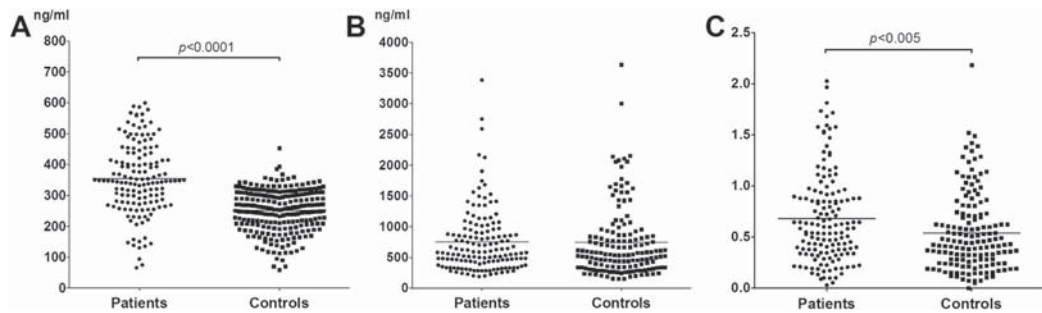


Figure 1 Serum concentrations of MMP-9 (A) and TIMP-1 (B) and MMP-9/TIMP-1 (C) ratio in TBE patients and in controls. The horizontal lines indicate mean values.

with TBE had significantly higher levels of MMP-9 than females with TBE ($p < 0.05$). There were no significant differences in serum TIMP-1 levels and MMP-9/TIMP-1 ratios between male and female patients with TBE ($p = 0.5181$) (Fig. 4).

Discussion

The BBB is a critical component of the CNS in that it limits the flow of material between the general circulation, either lymphatic or circulatory, and the CNS.¹⁶ In human patients with severe forms of TBE, BBB breakdown has been suggested based on the increased level of neurospecific proteins, such as α -1 brain globulin (α 1BG) or neuron-specific enolase (NSE), in serum.¹⁷ The kinetic serum profiles of α 1BG and NSE in severe TBE followed the general time courses of specific clinical manifestations.¹⁷ Similarly, increased sICAM-1 concentrations in CSF of TBE patients suggested BBB disturbances occurring during early phase of the disease.¹⁸ In TBEV infected mice, breakdown of the BBB was demonstrated at later times post-infection. This breakdown was, however, not necessary for virus entry in the CNS, was independent on migration of CD8⁺ T-cells into brain parenchyma, and more likely represented a

bystander effect of virus-induced cytokine/chemokine overproduction in the brain.⁵ Here we present further evidence that the BBB injury occurs during TBE by measurement of serum MMP-9 and TIMP-1 levels, and MMP-9/TIMP-1 ratio. It is well documented that elevated levels of MMP-9 in the serum/plasma and brain are associated with BBB disruption, leading to an exacerbation of neurodegenerative diseases.¹⁹ MMP-2, MMP-3 and MMP-9 increase the permeability of the BBB and inhibitors of MMPs can reduce damage to the BBB.²⁰ Whenever the BBB is affected, MMP-9 is a key factor in the injury process. MMP-9 is produced in the cells constituting the BBB, including brain microvascular endothelial cells²¹ and astrocytes²² under pathological conditions. The changed levels of MMP-9, its inhibitor TIMP-1, and the ratio between these two proteins were shown to play important role in pathological processes associated with BBB breakdown in various diseases of the central nervous system, including subacute sclerosing panencephalitis,^{9,10} fungal or tuberculous meningoencephalitis,¹² HIV-associated neurological diseases,¹³ herpes simplex virus encephalitis,¹⁴ and influenza-associated encephalopathy.¹⁵

The present study is the first to demonstrate that serum MMP-9 levels and MMP-9/TIMP-1 ratios are markedly higher

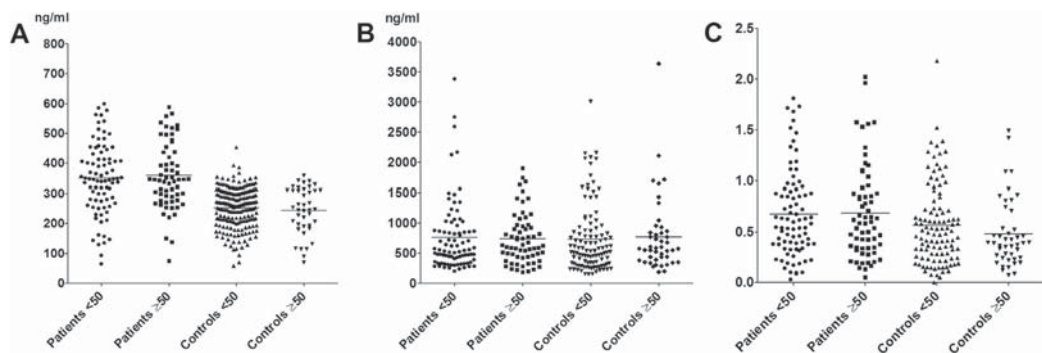


Figure 2 Serum concentrations of MMP-9 (A) and TIMP-1 (B) and MMP-9/TIMP-1 (C) ratio in TBE patients and in controls aged <50 and ≥ 50 years. The horizontal lines indicate mean values.

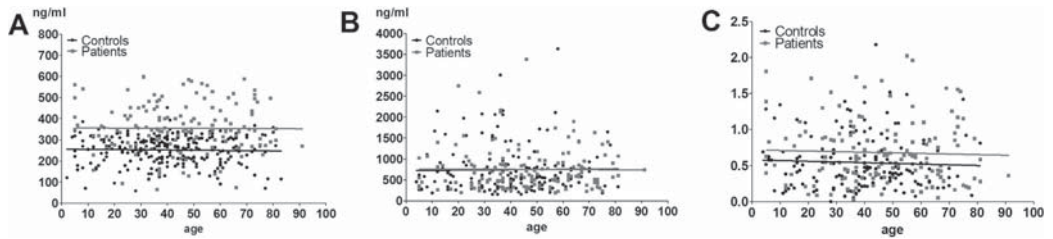


Figure 3 Correlation of the serum concentrations of MMP-9 (A) and TIMP-1 (B) and MMP-9/TIMP-1 (C) ratio in TBE patients and in controls with age of the individuals.

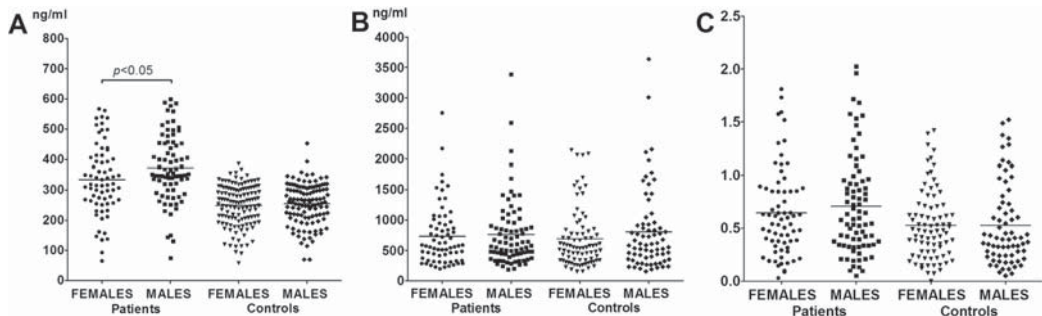


Figure 4 Serum concentrations of MMP-9 (A) and TIMP-1 (B) and MMP-9/TIMP-1 (C) ratio in male and female TBE patients and in controls. The horizontal lines indicate mean values.

in TBE patients compared to controls (Fig. 1). There is no specific therapy for TBE, but it was demonstrated that corticoids (5–10 mg/kg/day intravenously) have favourable effect during the acute stage of this disease.²³ Since corticosteroid is known to improve capillary functions by reducing activity of MMP-9 and increasing levels of TIMPs,²⁴ it can be speculated that the effect of corticoids in TBE may be explained at least in part by the down-regulation of MMP-9 activity, similarly as it was suggested for fungal and tuberculous meningoencephalitis.¹² In West Nile virus infection, it was demonstrated that MMP-9 facilitates virus entry into the brain by enhancing BBB permeability.²⁵ However, the role of MMP-9 in TBEV entry into the CNS and subsequent neuropathogenesis remains unknown and requires further study.

The incidence and severity of TBE are highest in people aged ≥ 50 years. Generally, patients above the age of 50 years experience significantly more sequelae and a higher case fatality rate.²⁶ It was also demonstrated that serum levels of interleukin 6 (IL-6) correlate positively with age of TBE patients.^{27,28} IL-6 and also IL-8 act as stimulators of MMPs, which comes along with our results. However, in our study we did not find any differences in serum levels of MMP-9, TIMP-1 and MMP-9/TIMP-1 ratios in patients below and above the age of 50 years (Fig. 2) and there was also no correlation of the serum levels of MMP-9, TIMP-1 and MMP-9/TIMP-1 ratios with increasing age (Fig. 3). This indicates that the MMP-9 activity during TBE is not dependent on the age of the patient. The fact that

there is no correlation between the MMP-9 levels and age, while IL-6 titers correlate with age,²⁷ suggests a more complicated mechanism.

Higher serum levels of MMP-9 were detected in male than female TBE patients. Sex-specific incidence of TBE is higher in men than in women in the Czech Republic (men to women ratio 1.5:1),²⁹ but there are no data if there are differences in sequelae and case fatality rates between males and females.

In conclusion, we have shown that serum MMP-9 levels and MMP-9/TIMP-1 ratios were higher in TBE patients than in controls. The increased levels of MMP-9 and MMP-9/TIMP-1 ratios in serum were not dependent on age of the patients, but TBE-positive males had higher levels of serum MMP-9 than TBE-positive females. Our data in the present study indicate that MMP-9 may play an important role in the BBB breakdown and development of brain damage during TBE.

Acknowledgements

We thank to Veronika Slavíková for excellent technical assistance, Dr Jiří Salát for critical reading of the manuscript and Prof Jan Kopecký for general support. The authors acknowledge financial support by the Czech Science Foundation project No. P502/11/2116, and grant Z60220518 from the Ministry of Education, Youth, and Sports of the Czech Republic, and the AdmireVet project

No. CZ.1.05./2.1.00/01.006 (ED006/01/01). The founders had no role in study design, data collection and analysis, decision to publish, or preparation of the manuscript.

References

- Růžek D, Dobler G, Donoso Mantke O. Tick-borne encephalitis: pathogenesis and clinical implications. *Travel Med Infect Dis* 2010;**8**(4):223–32.
- Süss J. Increasing prevalence of early summer meningoencephalitis in Europe. *Dtsch Med Wochenschr* 2005;**130**(22):1397–400.
- Süss J. Tick-borne encephalitis in Europe and beyond – the epidemiological situation as of 2007. *Euro Surveill* 2008;**19**(12): pii: 18916.
- Günther G, Haglund M. Tick-borne encephalopathies: epidemiology, diagnosis, treatment and prevention. *CNS Drugs* 2005;**19**(12):1009–32.
- Růžek D, Salát J, Singh SK, Kopecký J. Breakdown of the blood–brain barrier during tick-borne encephalitis in mice is not dependent on CD8+ T-cells. *PLoS One* 2011;**6**(5):e20472.
- Paul R, Lorenzl S, Koedel U, Sporer B, Vogel U, Frosch M, et al. Matrix metalloproteinases contribute to the blood–brain barrier disruption during bacterial meningitis. *Ann Neurol* 1998;**44**(4):592–600.
- Rosenberg GA, Kornfeld M, Estrada E, Kelley RO, Liotta LA, Stetler-Stevenson WG. TIMP-2 reduces proteolytic opening of blood–brain barrier by type IV collagenase. *Brain Res* 1992;**576**(2):203–7.
- Roe K, Kumar M, Lum S, Orillo B, Nerurkar VR, Verma S. West Nile virus-induced disruption of the blood–brain barrier in mice is characterized by the degradation of the junctional complex proteins and increase in multiple matrix metalloproteinases. *J Gen Virol* 2012;**93**(Pt 6):1193–203.
- Ichiyama T, Siba P, Suarkia D, Takasu T, Miki K, Kira R, et al. Serum levels of matrix metalloproteinase-9 and tissue inhibitors of metalloproteinases 1 in subacute sclerosing panencephalitis. *J Neurol Sci* 2007;**252**(1):45–8.
- Ichiyama T, Matsushige T, Siba P, Suarkia D, Takasu T, Miki K, et al. Cerebrospinal fluid levels of matrix metalloproteinase-9 and tissue inhibitor of metalloproteinase-1 in subacute sclerosing panencephalitis. *J Infect* 2008;**56**(5):376–80.
- Lacraz S, Nicod LP, Chicheportiche R, Welgus HG, Dayer JM. IL-10 inhibits metalloproteinase and stimulates TIMP-1 production in human mononuclear phagocytes. *J Clin Invest* 1995;**96**(5):2304–10.
- Matsuura E, Umehara F, Hashiguchi T, Fujimoto N, Okada Y, Osame M. Marked increase of matrix metalloproteinase 9 in cerebrospinal fluid of patients with fungal or tuberculous meningoencephalitis. *J Neurol Sci* 2000;**173**(1):45–52.
- Liuzzi GM, Mastroianni CM, Santacroce MP, Fanelli M, D'Agostino C, Vullo V, et al. Increased activity of matrix metalloproteinases in the cerebrospinal fluid of patients with HIV-associated neurological diseases. *J Neuroviral* 2000;**6**(2):156–63.
- Martínez-Torres FJ, Wagner S, Haas J, Kehm R, Sellner J, Hacke W, et al. Increased presence of matrix metalloproteinases 2 and 9 in short- and long-term experimental herpes simplex virus encephalitis. *Neurosci Lett* 2004;**368**(3):274–8.
- Ichiyama T, Morishima T, Kajimoto M, Matsushige T, Matsubara T, Furukawa S. Matrix metalloproteinase-9 and tissue inhibitors of metalloproteinases 1 in influenza-associated encephalopathy. *Pediatr Infect Dis J* 2007;**26**(6):542–4.
- Tigabu B, de Kok-Mercado F, Holbrook MR. Neuroviral infections and immunity. In: Singh SK, Růžek D, editors. *Neuroviral infections: general principles and DNA viruses*. CRC Press; 2013. p. 21–61.
- Chekhonin VP, Zhirkov YA, Belyaeva IA, Ryabukhin IA, Gurina OI, Dmitriyeva TB. Serum time course of two brain-specific proteins, alpha(1) brain globulin and neuron-specific enolase, in tick-borne encephalitis and Lyme disease. *Clin Chim Acta* 2002;**320**(1–2):117–25.
- Moniuszko A, Pancewicz S, Czupryna P, Grygorczuk S, Świerzbńska R, Kondrusik M, et al. ssiCAM-1, IL-21 and IL-23 in patients with tick borne encephalitis and neuroborreliosis. *Cytokine* 2012;**60**(2):468–72.
- Rosenberg GA. Matrix metalloproteinases and their multiple roles in neurodegenerative diseases. *Lancet Neurol* 2009;**8**(2):205–16.
- Gasche Y, Copin JC, Sugawara T, Fujimura M, Chan PH. Matrix metalloproteinase inhibition prevents oxidative stress-associated blood–brain barrier disruption after transient focal cerebral ischemia. *J Cereb Blood Flow Metab* 2001;**21**(12):1393–400.
- Kolev K, Skopál J, Simon L, Csonka E, Machovich R, Nagy Z. Matrix metalloproteinase-9 expression in post-hypoxic human brain capillary endothelial cells: H2O2 as a trigger and NF-kappaB as a signal transducer. *Thromb Haemost* 2003;**90**(3):528–37.
- Hsieh HL, Wu CY, Yang CM. Bradykinin induces matrix metalloproteinase-9 expression and cell migration through a PKC-delta-dependent ERK/Elk-1 pathway in astrocytes. *Glia* 2008;**56**(6):619–32.
- Dunyewicz M, Mertenová J, Moravcová E, Kulková H. Corticoids in the therapy of TBE and other viral encephalitides. In: Kunz C, editor. *Tick-borne encephalitis*. Facultas-Verlag; 1981. p. 36–44.
- Rosenberg GA, Dencoff JE, Correa Jr N, Reiners M, Ford CC. Effect of steroids on CSF matrix metalloproteinases in multiple sclerosis: relation to blood–brain barrier injury. *Neurology* 1996;**46**(6):1626–32.
- Wang P, Dai J, Bai F, Kong KF, Wong SJ, Montgomery RR, et al. Matrix metalloproteinase 9 facilitates West Nile virus entry into the brain. *J Virol* 2008;**82**(18):8978–85.
- Haglund M, Forsgren M, Lindh G, Lindquist L. A 10-year follow-up study of tick-borne encephalitis in the Stockholm area and a review of the literature: need for a vaccination strategy. *Scand J Infect Dis* 1996;**28**(3):217–24.
- Toporkova MG, Aleshin SE, Ozherelkov SV, Nadezhkina MV, Stephenson JR, Timofeev AV. Serum levels of interleukin 6 in recently hospitalized tick-borne encephalitis patients correlate with age, but not with disease outcome. *Clin Exp Immunol* 2008;**152**(3):517–21.
- Atrasheuskaya AV, Fredeking TM, Ignatyev GM. Changes in immune parameters and their correction in human cases of tick-borne encephalitis. *Clin Exp Immunol* 2003;**131**(1):148–54.
- Kříž B, Benes C, Danielová V, Daniel M. Socio-economic conditions and other anthropogenic factors influencing tick-borne encephalitis incidence in the Czech Republic. *Int J Med Microbiol* 2004;**293**(Suppl. 37):63–8.

CHAPTER VI

Analysis of serum levels of cytokines, chemokines, growth factors, and monoamine neurotransmitters in patients with tick-borne encephalitis: Identification of novel inflammatory markers with implications for pathogenesis

Martin Palus, Petra Formanová, Jiří Salát, Eva Žampachová, Jana Elsterová, Daniel Růžek

Journal of Medical Virology 2015, 87:885–892.

DOI: 10.1002/jmv.24140

<http://onlinelibrary.wiley.com/doi/10.1002/jmv.24140/full>

Analysis of serum levels of cytokines, chemokines, growth factors, and monoamine neurotransmitters in patients with tick-borne encephalitis: Identification of novel inflammatory markers with implications for pathogenesis
(summary)

Acute immune response to TBEV was characterized by measuring cytokines, chemokines, and growth factors, including molecules that have been never or rarely studied in TBE patients in order to enhance knowledge about pathophysiology of TBE. Increased knowledge of these mediators may provide a basis for the design and development of new pharmacological approaches to treat this important neuroinfection.

The levels of 30 cytokines, chemokines, and growth factors were measured in serum samples from 87 patients with clinically and serologically confirmed acute TBE and from 32 control subjects using the Cytokine Human Magnetic 30-Plex Panel for the Luminex platform, the method employed a fluorescent beadbased technology in a multiplex array system.

Moreover, the serum levels of monoamine neurotransmitters were measured in TBE patients and in control subjects via enzyme-linked immunosorbent assay, since it was suggested that decreased levels of monoamine neurotransmitters such as serotonin might be consistent with TBE severity (Sumlivaya *et al.*, 2013). Serum levels of the monoamine neurotransmitters serotonin, dopamine, and noradrenaline as well as levels of catecholamines (dopamine and noradrenaline) were significantly lower in TBE patients than in the control group. The lower levels of monoamine neurotransmitters detected in sera from TBE patients may be association with neuropsychological complications observed frequently during or after TBE (Juchnowicz *et al.*, 2002; Schmolck *et al.*, 2005).

TBE virus infection elicited increased levels of the pro-inflammatory cytokines interleukin (IL)-6, IL-8, and IL-12. TBE patients had higher IL-12:IL-4 and IL-12:IL-10 ratios than control patients, reflecting the global proinflammatory cytokine balance.

Most interestingly, increased levels of hepatocyte growth factor (HGF) and vascular endothelial growth factor (VEGF) were observed in TBE patients. These proteins may be novel and functionally important inflammatory biomarkers of TBE. The growth factors HGF and VEGF represent new inflammatory biomarkers of TBE with potentially important biological functions, findings worthy of further investigation.

HGF, also known as hepatopoietin A, serves as a mitogen (stimulating growth and enhancing the cell motility of various epithelial cells) and as a morphogen (Matsumoto and Nakamura, 1991; Ozden *et al.*, 2004). Increased amounts of HGF have been observed in sera from patients after acute injuries, in organs, where HGF serves as a regeneration factor. HGF is produced by mesenchymal cells in response to injuries of distant organs (Kono *et al.*, 1992). Increased levels of HGF were reported in the cerebrospinal fluid of patients with various diseases affecting brain tissue (Yamada *et al.*, 1994; Tsuboi *et al.*, 2002; Ozden *et al.*, 2004). For TBE, increased serum HGF levels may reflect a response to virus multiplication in peripheral tissues and organs during the first phase of the infection or a response to virus-mediated brain tissue damage; increased HGF levels may be responsible for tissue regeneration.

VEGF is a signal protein that stimulates vasculogenesis and angiogenesis. VEGF overexpression can contribute to the development of encephalitis because VEGF increases the permeability of peripheral and CNS vasculature by permeating endothelial cells in venules and capillaries (Roberts and Palade, 1995; Mayhan, 1999; Ay *et al.*, 2008). VEGF has been shown to enhance MMP-9 activity (Valable *et al.*, 2005). As previously mentioned, serum MMP-9 levels and the ratio of MMP-9/ TIMP-1 were significantly higher in TBE patients than in control subjects (Palus *et al.*, 2014b), as well as in CSF MMP-9 levels in TBE patients were associated with brain inflammatory, disruption of the blood-brain barrier, and disease severity (Kang *et al.*, 2013). The levels of VEGF in TBE patients provide further evidence that injury to the BBB is critical during TBE development.

This study, reports increased serum levels of various cytokines and growth factors, together with decreased serum levels of important monoamine neurotransmitters, in patients with TBE. This investigation also provides the first demonstration that TBE patients show increased serum levels of HGF and VEGF, which may represent novel and mechanistically important inflammatory biomarkers of TBE.

Analysis of Serum Levels of Cytokines, Chemokines, Growth Factors, and Monoamine Neurotransmitters in Patients With Tick-borne Encephalitis: Identification of Novel Inflammatory Markers With Implications for Pathogenesis

Martin Palus,^{1,2,3} Petra Formanová,^{1,4} Jiří Salát,¹ Eva Žampachová,⁵ Jana Elsterová,^{1,2,3} and Daniel Růžek^{1,2,3,4*}

¹Department of Virology, Veterinary Research Institute, Brno, Czech Republic

²Laboratory of Arbovirology, Institute of Parasitology, Biology Centre of the Czech Academy of Sciences, České Budějovice, Czech Republic

³Department of Medical Biology, Faculty of Science, University of South Bohemia, České Budějovice, Czech Republic

⁴Institute of Experimental Biology, Faculty of Science, Masaryk University, Brno, Czech Republic

⁵Laboratory of Virology, Hospital České Budějovice, České Budějovice, Czech Republic

Tick-borne encephalitis (TBE) is a leading human neuroinfection in Europe and northeastern Asia. However, the pathophysiology of TBE is not understood completely. This study sought to determine the specific serum mediators that are associated with acute TBE. The levels of 30 cytokines, chemokines, and growth factors were measured in serum samples from 87 patients with clinically and serologically confirmed acute TBE and from 32 control subjects using the Cytokine Human Magnetic 30-Plex Panel for the Luminex platform. Serum levels of the monoamine neurotransmitters serotonin, dopamine, and noradrenaline were measured via enzyme-linked immunosorbent assay. TBE virus infection elicited increased levels of the pro-inflammatory cytokines interleukin (IL)-6, IL-8, and IL-12. TBE patients had higher IL-12:IL-4 and IL-12:IL-10 ratios than control patients, reflecting the global pro-inflammatory cytokine balance. Serum levels of the monoamine neurotransmitters serotonin, dopamine, and noradrenaline were significantly lower in TBE patients than in the control group. Most interestingly, increased levels of hepatocyte growth factor and vascular endothelial growth factor were observed in TBE patients; these proteins may be novel and mechanistically important inflammatory biomarkers of TBE. **J. Med. Virol.** 87:885–892, 2015. © 2015 Wiley Periodicals, Inc.

KEY WORDS: tick-borne encephalitis virus; neuroinflammation; luminex; neuroinfection

INTRODUCTION

Tick-borne encephalitis (TBE) is one of the most important human viral infections of the central nervous system (CNS) in Eurasia. The etiological agent, TBE virus (TBEV), is a member of the family *Flaviviridae*, genus *Flavivirus*, together with other important human viruses like West Nile virus, Yellow fever virus, Japanese encephalitis virus, Dengue virus, and Omsk hemorrhagic fever virus. Although TBE can be prevented effectively by vaccination, more than 13,000 clinical cases of TBE, including numerous deaths, are reported annually in more than 30 countries in Europe and northeastern Asia [Charrel et al., 2004; Mansfield et al., 2009]. The TBE prevalence is increasing and the virus is spreading to areas that previously were non-endemic. In the years 1974–2003, a continuous increase in TBE morbidity was observed in Europe, and from 2004 to 2006, another considerable increase was seen in the Czech Republic, Germany, Poland, Slovenia, and Switzerland [Suss, 2008].

Grant sponsor: Czech Science Foundation; Grant numbers: P502/11/2116; GA14-29256S.; Grant sponsor: MEYS of the Czech Republic under the NPU I program; Grant number: LO1218.

*Correspondence to: Daniel Růžek, Veterinary Research Institute, Hudcova 70, CZ-62100 Brno, Czech Republic. E-mail: ruzekd@paru.cas.cz

Accepted 2 December 2014

DOI 10.1002/jmv.24140

Published online 11 February 2015 in Wiley Online Library (wileyonlinelibrary.com).

The typical clinical features of TBE caused by European TBEV strains are characterized by a biphasic course. The primary phase includes non-specific symptoms such as fever, muscle pain, headache, and malaise, and the typical secondary phase involves neurological symptoms including meningitis, meningoencephalitis, and meningoencephalomyelitis [Růžek et al., 2010]. There is no specific therapy for TBE other than supportive measures.

The pathophysiology of TBE is unclear [Růžek et al., 2009]. The pathology observed during TBE suggests that some components of the host immune system contribute to disease development and immunopathology [Gelpi et al., 2006; Růžek et al., 2009]. Therefore, the roles of cytokines, chemokines, and growth factors during TBE are among the main key issues that have not been addressed fully to date. Previous reports characterized an acute immune response to TBEV by profiling certain cytokines and chemokines (e.g., tumor necrosis factor alpha (TNF- α), interleukin (IL)-1 β , IL-6, CXCL10, CXCL11, CXCL12, CXCL13) in the sera or cerebrospinal fluid of TBE patients [Kondrusik et al., 2001; Atrasheuskaya et al., 2003; Zajkowska et al., 2011]. However, limited sample sizes often restricted the analysis of multiple cytokines of interest via traditional methodologies.

In this study, acute immune response to TBEV was characterized by measuring a panel of 30 cytokines, chemokines, and growth factors, including molecules that have been never or rarely studied in TBE patients; the method employed a fluorescent bead-based technology in a multiplex array system. In addition, the levels of monoamine neurotransmitters were measured in TBE patients and in control subjects via enzyme-linked immunosorbent assay (ELISA), since it was suggested recently that decreased levels of monoamine neurotransmitters such as serotonin may correlate with TBE severity [Sumliyaya et al., 2013]. Here, the serum levels of pro-inflammatory cytokines IL-6, IL-8, and IL-12 were increased and the levels of monoamine neurotransmitters were decreased in TBE patients compared to control subjects. This investigation also provides the first demonstration that TBE patients harbor increased serum levels of hepatocyte growth factor (HGF) and vascular endothelial growth factor (VEGF), which may represent novel and mechanistically important inflammatory biomarkers of TBE.

MATERIALS AND METHODS

Serum samples were obtained from 87 patients (53 males and 33 females, aged 4–80 years; median, 47 years) with acute TBE that was confirmed via serology (clinically manifest TBE and ELISA-based detection of specific anti-TBEV IgM and IgG antibodies [Test-Line, Brno, Czech Republic]). The control subjects for measurements of serum cytokine/chemokine/growth factors/neurotransmitters were 32

healthy individuals comprising a matched-age group (13 males and 19 females; aged 4–77 years; median, 35.5 years). Samples were collected from patients and control subjects in 2012 in South Bohemia, Czech Republic; aliquots of all serum samples were stored at -80°C . The work described in this study was carried out in accordance with the Declaration of Helsinki. Patients and control subjects (or their parents) provided informed consent before sample collection. Samples were investigated anonymously. The study protocol was approved by the Institutional Ethical Committee (PARU AVCR No. 01/11).

Concentrations of 30 cytokines, chemokines, and growth factors were measured in serum samples using the Human Cytokine Magnetic 30-Plex Panel for the Luminex platform (Life Technologies, Frederick, MD) using a MAGPIX instrument (Luminex, Austin, TX). All procedures were performed according to the manufacturer's instructions. The immunoassay detects IL-1 β , IL-1 receptor antagonist (IL-1RA), IL-2, IL-2 receptor (IL-2R), IL-4, IL-5, IL-6, IL-7, IL-8, IL-10, IL-12 (p40/p70), IL-13, IL-15, IL-17, TNF- α , interferon alpha (IFN- α), interferon gamma (INF- γ), granulocyte colony stimulating factor (G-CSF), granulocyte macrophage colony stimulating factor (GM-CSF), eotaxin (CCL11), inducible protein (IP)-10 (CXCL10), macrophage chemotactic protein (MCP)-1, monokine induced by gamma interferon (MIG; CXCL9), macrophage inflammatory protein (MIP)-1 α (CCL3), MIP-1 β (CCL4), regulated upon expression normal T-cell expressed and secreted (RANTES; CCL5), and the growth factors epidermal growth factor, basic fibroblast growth factor, HGF, and VEGF.

Concentrations of serum monoamine neurotransmitters were measured with the Serotonin ELISA Fast Track kit (LDN, Nordhorn, Germany), the Noradrenaline Sensitive ELISA kit (DLD Diagnostika, Hamburg, Germany), and the Dopamine Sensitive ELISA kit (DLD Diagnostika, Hamburg, Germany). Concentrations of all analyzed mediators are reported as pg per ml of serum.

Statistical significance in the between-group differences in the concentration of inflammatory mediators in sera was analyzed using the Mann–Whitney test (*P*). Identification of outliers was performed with Dixon's Q test. Correction for multiple hypothesis testing used Benjamini and Hochberg's false discovery rate adjustment (*q*). The Kruskal–Wallis test and Dun's multiple comparison test were used to determine differences among groups in age and sex comparisons. Differences with $P < 0.05$ and $q < 0.05$ were considered significant. Analyses and calculations were performed using GraphPad Prism 5.04 (GraphPad Software, La Jolla, CA).

RESULTS

Soluble factor concentrations were measured in 87 patients during the acute phase of TBE and in

32 uninfected and healthy control subjects who were selected randomly. Relative to controls, TBE patients had significantly elevated levels of cytokines IL-6 ($P < 0.0001$; $q < 0.01$), IL-8 ($P < 0.01$; $q < 0.01$), and IL-12 ($P < 0.01$; $q < 0.05$) (Fig. 1; Supplemental Table 1). Serum samples from TBE patients contained significantly higher concentrations of growth factors HGF ($P < 0.001$; $q < 0.01$) and VEGF ($P < 0.01$; $q < 0.05$) than serum samples from uninfected control subjects (Fig. 1). The concentration of VEGF in TBE patients was at the level of detection, but most control subjects had VEGF levels under the detection limit. Concentrations of IL-5 ($P < 0.05$; $q < 0.05$), GM-CSF ($P < 0.05$; $q < 0.05$), and MCP-1 ($P < 0.0001$; $q < 0.01$) were lower in sera from TBE patients than in sera from control subjects (Fig. 1). TBE patients had noticeably lower serum levels of serotonin ($P < 0.05$; $q < 0.05$), dopamine ($P < 0.0001$; $q < 0.01$), and noradrenaline ($P < 0.0001$; $q < 0.01$) than uninfected control subjects (Fig. 2). In addition, the Mann-Whitney test identified significantly increased concentrations of G-CSF and epidermal growth factor ($P < 0.05$) in the sera of TBE patients, but these differences were insignificant after correction for multiple-hypothesis testing ($q > 0.05$) (Supplemental Table 1).

There were no significant differences ($P > 0.05$) between patients and control subjects in terms of the concentrations of cytokines/chemokines TNF- α , IL-1 β , IL-1RA, IL-2, IL-2R IL-4, IL-7, IL-10, IL-13, IL-15, IL-17, IP-10, IFN- α , IFN- γ , MIP-1 α , MIP-1 β , eotaxin/CCL11, MIG, RANTES, and fibroblast growth factor (Supplemental Table 1). The levels of IL-2, IL-7, IL-17, and TNF- α were at or below the limit of detection. There was no difference in the IL-2:IL-2R and IL-1 β :IL-1RA ratios between TBE patients and control subjects ($P > 0.05$) (data not shown).

Pro/anti-inflammatory immune system balance was analyzed by comparing the ratios of pro/anti-inflammatory cytokines. Patients with TBE infection had significantly higher ($P < 0.05$) IL-12:IL-4 and IL-12:IL-10 ratios than control subjects (Fig. 3). No significant difference was detected in other comparisons (IFN- γ :IL-10, IFN- γ :IL-4, IL-2:IL-4, IL-2:IL-10) (data not shown).

When patients and control subjects were divided into two groups according to age (<50 years and ≥ 50 years), significant differences between groups were observed only in the levels of GM-CSF ($P < 0.05$) and MCP-1 ($P < 0.05$); TBE patients <50 years had significantly ($P < 0.05$) lower levels of GM-CSF and MCP-1 than patients ≥ 50 years (Fig. 4). No differences were seen between controls younger and older than 50 years of age (Fig. 4).

No significant differences in the levels of any analyzed cytokine/chemokine/growth factor were detected between male and female TBE patients, or between male and female control subjects (data not shown).

DISCUSSION

The role of cytokines, chemokines, growth factors, and other soluble mediators during TBE is a major issue that has not been addressed fully to date. In this study, an acute immune response to TBEV was subjected to a multiplex analysis of 30 cytokines, chemokines, and growth factors in sera from TBE patients and control subjects. In addition, ELISA was used to measure the levels of three monoamine neurotransmitters in TBE patients and control subjects. Due to the unavailability of clinical data for the TBE patients included in this study, the overall immune response during TBE was characterized independent of disease severity and the timing of sample collection.

TBE patients had significantly elevated levels of proinflammatory cytokines IL-6, IL-8, and IL-12 (Fig. 1). In addition to its proinflammatory role, the anti-inflammatory properties of IL-6 have been described. Moreover, IL-6 plays important roles in regulatory and inflammatory processes within the CNS [März et al., 1999; Atrasheuskaya et al., 2003]. In most cases, IL-6 production is associated with a protective immune response, but unregulated overproduction can be harmful to the host. A previous study reported high concentrations of serum IL-6 in TBE patients during the first week of hospitalization, but these levels decreased in parallel with increased levels of their soluble receptors [Atrasheuskaya et al., 2003]. This decrease in cytokine levels was accompanied by an increase in the levels of IL-10, an immunoregulatory cytokine with anti-inflammatory properties [Atrasheuskaya et al., 2003]. Interestingly, pediatric TBE patients displayed the highest levels of serum IL-6 at admission, but did not manifest symptoms of meningitis or meningoencephalitis, as the adults did [Atrasheuskaya et al., 2003]. Another study demonstrated that only some TBE patients harbored elevated serum levels of IL-6; these levels correlated with age, but not with gender or disease outcome [Toporkova et al., 2008]. No correlation between serum IL-6 levels and age was detected in the present study.

IL-8 plays a crucial role in the recruitment of neutrophils and T cells into the CNS and is associated with blood-brain barrier dysfunction. IL-8 is also known to induce the expression of matrix metalloproteinase (MMP)-9, which was shown to be increased in serum [Palus et al., 2014] and cerebrospinal fluid [Kang et al., 2013] in patients with TBE. Higher concentrations of IL-8 in sera from TBE patients indicate this molecule's possible role in immunopathology in the CNS.

IL-12 makes important contributions to the primary activation of cell-mediated specific immunity, a critical part of the immune response to viral infections. IL-12 activates natural killer cells and T lymphocytes and mediates enhancement of the cytotoxic activity of natural killer cells and CD8⁺ T cells

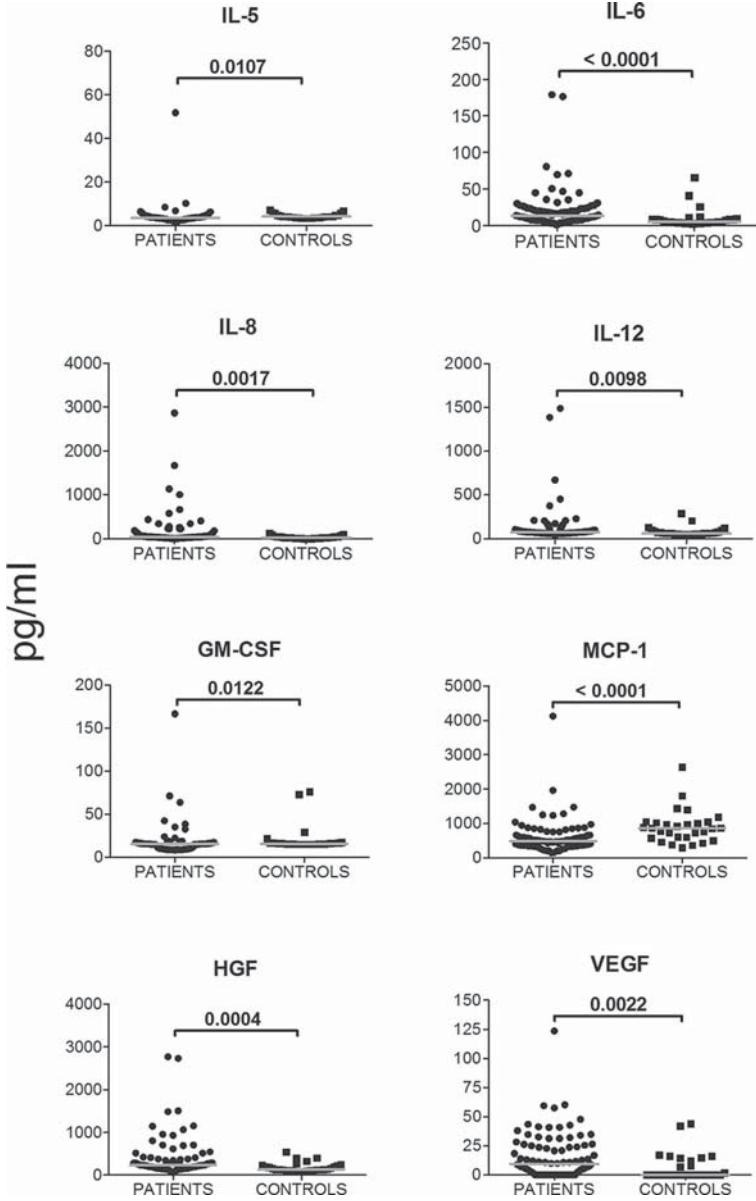


Fig. 1. Serum concentrations of IL-5, IL-6, IL-8, IL-12, GM-CSF, MCP-1, HGF, and VEGF in TB patients and control subjects evaluated by the multiplex system described in Materials and Methods. Horizontal lines indicate median values.

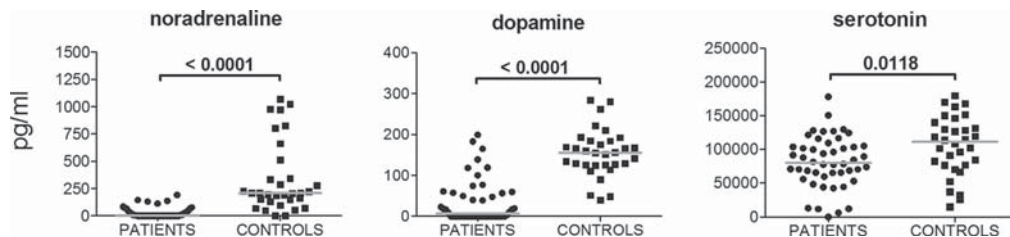


Fig. 2. Serum concentrations of serotonin, dopamine, and noradrenaline in TBE patients and control subjects. Horizontal lines indicate median values.

[Trinchieri, 2003]. Here, IL-12 levels were higher in TBE patients than in control subjects. Moreover, significantly higher IL-12:IL-4 and IL-12:IL-10 ratios were detected in sera from TBE patients, reflecting the global proinflammatory cytokine balance in infected human hosts.

The levels of IL-5, GM-CSF, and MCP-1 were lower in sera from TBE patients than in sera from control subjects. IL-5 is a typical cytokine produced by Th2 cells, playing a central role in differentiation and in the activation of eosinophils. Further, IL-5 triggers B-cell differentiation into antibody-producing plasma cells [Kouro and Takatsu, 2009]. During the acute phase, suppression of IL-5 production below control levels indicates the existence of Th1 (cell-mediated) proinflammatory polarization of the host immune response during TBE neuroinfection.

GM-CSF and macrophage colony-stimulating factor are principal microglial growth factors; their expression (along with that of their cognate receptors) is upregulated in the injured or diseased CNS [Giulian and Ingeman, 1988; Raivich et al., 1991; Lee et al., 1994; Cosenza-Nashat et al., 2007]. Here, GM-CSF levels were slightly lower in sera from TBE patients than in that from control subjects, which is puzzling and requires further study.

MCP-1 plays an essential role in several peripheral and CNS inflammatory disorders characterized by mononuclear cell infiltrates. However, MCP-1 may

also perform several vital functions in addition to its participation in cell recruitment, and may have either a protective or detrimental role depending on the inflammatory stimulus, cell type, or disease state [Thompson et al., 2008]. Interestingly, significantly lower levels of MCP-1 in sera from TBE patients than in sera from control subjects were detected in the present investigation. A previous study reported a clear correlation between MCP-1 mRNA production in TBEV-infected mice and disease severity [Palus et al., 2013]. The observed lower serum levels of MCP-1 in TBE patients require further confirmation in a future study.

There were no significant differences between TBE patients and control subjects in terms of the serum concentrations of cytokines/chemokines TNF- α , IL-1 β , IL-1RA, IL-2, IL-2R, IL-4, IL-7, IL-10, IL-13, IL-15, IL-17, IP-10, IFN- α , IFN- γ , MIP-1 α , MIP-1 β , G-CSF, eotaxin/CCL11, MIG, RANTES, epidermal growth factor, or fibroblast growth factor (Supplemental Table 1); the levels of IL-2, IL-7, IL-17, and TNF- α were at or below the limit of detection. Decreased concentrations could be caused by analyte instability during storage of the serum samples. Consistent with previous studies, the concentrations of circulating IL-1RA were higher than the corresponding levels of IL-1 β [Dinarello, 1998; Atrasheuskaya et al., 2003]. The ratio of IL-1 β to IL-1RA is considered to be more important for the outcome of the infection than the

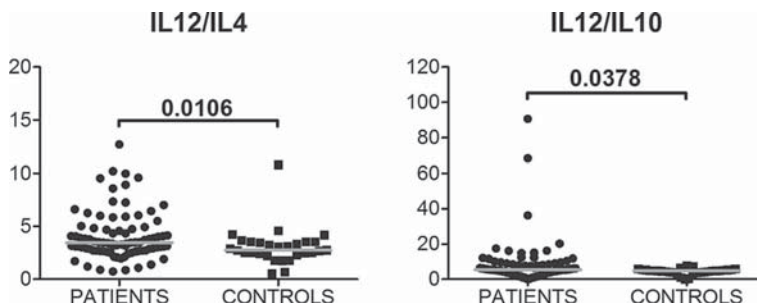


Fig. 3. Ratios of serum levels of IL-12:IL-4 and IL-12:IL-10 in TBE patients and control subjects. Horizontal lines indicate median values.

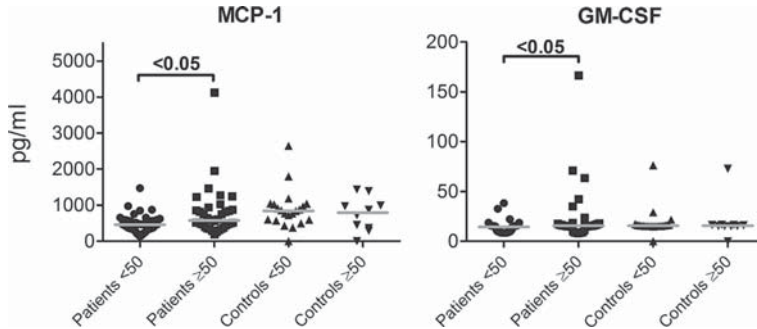


Fig. 4. Serum concentrations of MCP-1 and GM-CSF in TBE patients and in control subjects aged <50 years and ≥ 50 years. Horizontal lines indicate mean values.

concentration of IL-1 β itself; this ratio can serve as a good prognostic marker [Atrasheuskaya et al., 2003]. However, in the present study, no significant difference was observed between the IL-1 β :IL-1RA ratios in TBE patients and control subjects. This lack suggests differences in IL-1 β :IL-1RA ratios between European TBE cases that are usually mild and Russian TBE, which is frequently severe. Previous reports of increased serum levels of IP-10 and TNF- α in TBE patients [Kondrusik et al., 2001; Zajkowska et al., 2011] were not confirmed in this study, probably due to high variation in the data caused by inconsistent timing of sample collection.

Generally, TBE patients older than 50 years have significantly more sequelae and a higher fatality rate [Haglund et al., 1996]. In this study, patients <50 years had significantly lower levels of GM-CSF and MCP-1 than patients ≥ 50 years, suggesting stronger down-regulation of the innate immune response in the case of these markers in younger patients. However, there were no differences in the other analytes between TBE patients <50 years and ≥ 50 years of age.

The serum levels of the monoamine neurotransmitters serotonin, dopamine, and noradrenaline during acute TBE infection were also determined (Fig. 2). Sumlivaya et al. [2013] demonstrated that during the acute peak period of TBE, serum serotonin levels were significantly lower in TBE patients than in healthy controls. In the paralytic form of TBE, the levels of serum serotonin were noticeably lower than in the nonparalytic form [Sumlivaya et al., 2013]. Based on these data, the authors concluded that serum serotonin levels can serve as a marker of CNS damage during TBE and that they predict the development of severe forms of TBE [Sumlivaya et al., 2013]. The present study confirmed the lower levels of serotonin in TBE patients versus levels in control subjects, but the serum levels of catecholamines (dopamine and noradrenaline) were decreased in TBE patients as well. Catecholamines are known to

be decreased in the cerebrospinal fluid of Japanese encephalitis patients [Misra et al., 2005]. The lower levels of monoamine neurotransmitters detected in sera from TBE patients may be association with neuropsychological complications observed frequently during or after TBE [Juchnowicz et al., 2002; Schmolck et al., 2005].

Among the prominent findings of this study was the novel observation that serum concentrations of HGF and VEGF were increased in TBE patients in comparison to control subjects (Fig. 1). HGF, also known as hepatopoietin A or scatter factor, serves as a mitogen (stimulating growth and enhancing the cell motility of various epithelial cells) and as a morphogen [Matsumoto and Nakamura, 1991; Ozden et al., 2004]. Increased amounts of HGF have been observed in sera from patients after acute injuries, especially to the liver, kidneys, and lungs, where HGF serves as a regeneration factor. HGF is produced by mesenchymal cells in response to injuries to a distant organ [Kono et al., 1992]. Increased levels of HGF were reported in the cerebrospinal fluid of patients with various diseases affecting brain tissue [Yamada et al., 1994; Fenton et al., 1998; Tsuboi et al., 2002; Ozden et al., 2004]. In TBE, increased serum HGF levels may reflect a response to virus multiplication in peripheral tissues and organs during the first phase of the infection or a response to virus-mediated brain tissue damage; increased HGF levels may be responsible for tissue regeneration. The specific role of HGF production during TBE remains to be defined.

Here, the serum levels of VEGF were mostly under the detection limit in control subjects, but were detectable in TBE patients. VEGF is a signal protein that stimulates vasculogenesis and angiogenesis. VEGF overexpression can contribute to the development of encephalitis because VEGF increases the permeability of peripheral and CNS vasculature by permeating endothelial cells in venules and capillaries [Roberts and Palade, 1995; Mayhan, 1999; Ay et al.,

2008]. VEGF has been shown to enhance MMP-9 activity [Valable et al., 2005]. A previous study demonstrated that serum MMP-9 levels and the ratio of MMP-9 to tissue inhibitor of metalloproteinase-1 were significantly higher in TBE patients than in control subjects [Palus et al., 2014]. Another study showed that elevated CSF MMP-9 levels in TBE patients were associated with brain inflammatory reactions, disruption of the blood-brain barrier, and disease severity [Kang et al., 2013]. Measuring the levels of VEGF in TBE patients yielded further evidence that injury to the blood-brain barrier is critical during the development of TBE.

In summary, the present study is the first report of increased serum levels of various cytokines and growth factors, as well as decreased serum levels of important monoamine neurotransmitters, in patients with TBE. The growth factors HGF and VEGF represent new inflammatory biomarkers of TBE with potentially important biological functions, findings worthy of further investigation. Increased knowledge of inflammatory mediators activated during TBE may provide a basis for the design and development of new pharmacological approaches to treat this important neuroinfection.

ACKNOWLEDGMENTS

The authors are greatly indebted to Professor Jan Kopecký for general support of our work. The funders had no role in the study design, data collection and analysis, decision to publish, or preparation of the manuscript.

REFERENCES

- Atrasheuskaya AV, Fredeking TM, Ignatyev GM. 2003. Changes in immune parameters and their correction in human cases of tick-borne encephalitis. *Clin Exp Immunol* 131:148–154.
- Ay I, Francis JW, Brown RH, Jr. 2008. VEGF increases blood-brain barrier permeability to Evans blue dye and tetanus toxin fragment C but not adeno-associated virus in ALS mice. *Brain Res* 1234:198–205.
- Charrel RN, Attoui H, Butenko AM, Clegg JC, Deubel V, Frolova TV, Gould EA, Gritsun TS, Heinz FX, Labuda M, Lashkevich VA, Loktev V, Lundkvist A, Lvov DV, Mandl CW, Niedrig M, Papa A, Petrov VS, Plyusnin A, Randolph S, Süs J, Zlobin VI, de Lamballerie X. 2004. Tick-borne virus diseases of human interest in Europe. *Clin Microbiol Infect* 10:1040–1055.
- Cosenza-Nashat M, Zhao ML, Marshall HD, Si Q, Morgello S, Lee SC. 2007. Human immunodeficiency virus infection inhibits granulocyte-macrophage colony-stimulating factor-induced microglial proliferation. *J Neurovirol* 13:536–548.
- Dinarello CA. 1998. Interleukin-1, interleukin-1 receptors and interleukin-1 receptor antagonist. *Int Rev Immunol* 16:457–499.
- Fenton H, Finch PW, Rubin JS, Rosenberg JM, Taylor WG, Kuo-Leblanc V, Rodriguez-Wolf M, Baird A, Schipper HM, Stopa EG. 1998. Hepatocyte growth factor (HGF/SF) in Alzheimer's disease. *Brain Res* 779:262–270.
- Gelpei E, Preusser M, Laggner U, Garzuly F, Holzmann H, Heinz FX, Budka H. 2006. Inflammatory response in human tick-borne encephalitis: Analysis of postmortem brain tissue. *J Neurovirol* 12:322–327.
- Giuliani D, Ingeman JE. 1988. Colony-stimulating factors as promoters of amoeboid microglia. *J Neurosci* 8:4707–4717.
- Haglund M, Forsgren M, Lindh G, Lindquist L. 1996. A 10-year follow-up study of tick-borne encephalitis in the Stockholm area and a review of the literature: Need for a vaccination strategy. *Scand J Infect Dis* 28:217–224.
- Juchnowicz D, Rudnik I, Czernikiewicz A, Zajkowska J, Pancewicz SA. 2002. [Mental disorders in the course of Lyme borreliosis and tick borne encephalitis]. *Przegl Epidemiol* 56:37–50.
- Kang X, Li Y, Wei J, Zhang Y, Bian C, Wang K, Wu X, Hu Y, Li J, Yang Y. 2013. Elevation of matrix metalloproteinase-9 level in cerebrospinal fluid of tick-borne encephalitis patients is associated with IgG extravasation and disease severity. *PLoS ONE* 8:e77427.
- Kondrusik M, Pancewicz S, Zajkowska J, Hermanowska-Szpakowicz T. 2001. Tumor necrosis factor alpha and interleukin 1-beta in serum of patients with tick-borne encephalitis. *Pol Merkuri Lekarski* 11:26–28.
- Kono S, Nagaïke M, Matsumoto K, Nakamura T. 1992. Marked induction of hepatocyte growth factor mRNA in intact kidney and spleen in response to injury of distant organs. *Biochem Biophys Res Commun* 186:991–998.
- Kouro T, Takatsu K. 2009. IL-5- and eosinophil-mediated inflammation: From discovery to therapy. *Int Immunol* 21:1303–1309.
- Lee SC, Liu W, Brosnan CF, Dickson DW. 1994. GM-CSF promotes proliferation of human fetal and adult microglia in primary cultures. *Glia* 12:309–318.
- März P, Otten U, Rose-John S. 1999. Neural activities of IL-6-type cytokines often depend on soluble cytokine receptors. *Eur J Neurosci* 11:2995–3004.
- Mansfield KL, Johnson N, Phipps LP, Stephenson JR, Fooks AR, Solomon T. 2009. Tick-borne encephalitis virus – A review of an emerging zoonosis. *J Gen Virol* 90:1781–1794.
- Matsumoto K, Nakamura T. 1991. Hepatocyte growth factor: Molecular structure and implications for a central role in liver regeneration. *J Gastroenterol Hepatol* 6:509–519.
- Mayhan WG. 1999. VEGF increases permeability of the blood-brain barrier via a nitric oxide synthase/cGMP-dependent pathway. *Am J Physiol* 276:C1148–C1153.
- Misra UK, Kalita J, Pandey S, Khanna VK, Babu GN. 2005. Cerebrospinal fluid catecholamine levels in Japanese encephalitis patients with movement disorders. *Neurochem Res* 30:1075–1078.
- Ozden M, Kalkan A, Demirdag K, Denk A, Kilic SS. 2004. Hepatocyte growth factor (HGF) in patients with hepatitis B and meningitis. *J Infect* 49:229–235.
- Palus M, Vojtíšková J, Salát J, Kopecký J, Grubhoffer L, Lipoldová M, Demant P, Růžek D. 2013. Mice with different susceptibility to tick-borne encephalitis virus infection show selective neutralizing antibody response and inflammatory reaction in the central nervous system. *J Neuroinflammation* 10:77.
- Palus M, Zampachová E, Elsterová J, Růžek D. 2014. Serum matrix metalloproteinase-9 and tissue inhibitor of metalloproteinase-1 levels in patients with tick-borne encephalitis. *J Infect* 68:165–169.
- Raivich G, Gehrman J, Kreutzberg GW. 1991. Increase of macrophage colony-stimulating factor and granulocyte-macrophage colony-stimulating factor receptors in the regenerating rat facial nucleus. *J Neurosci Res* 30:682–686.
- Roberts WG, Palade GE. 1995. Increased microvascular permeability and endothelial fenestration induced by vascular endothelial growth factor. *J Cell Sci* 108:2369–2379.
- Růžek D, Dohler G, Donoso Mantke O. 2010. Tick-borne encephalitis: Pathogenesis and clinical implications. *Travel Med Infect Dis* 8:223–232.
- Růžek D, Salát J, Palus M, Gritsun TS, Gould EA, Dyková I, Skallová A, Jelínek J, Kopecký J, Grubhoffer L. 2009. CD8+ T-cells mediate immunopathology in tick-borne encephalitis. *Virology* 384:1–6.
- Schmolck H, Maritz E, Kletzin I, Korinthenberg R. 2005. Neurologic, neuropsychologic, and electroencephalographic findings after European tick-borne encephalitis in children. *J Child Neurol* 20:500–508.
- Sumlivaya ON, Vorobyeva NN, Karakulova YuV. 2013. State of humoral part of the serotonergic system in patients with tick-borne encephalitis. Abstract. Proceedings of Russian Scientific Conference with International Participation “Up-to-date Problems of Tick-borne Encephalitis.” October 8–10, 2013. Chumakov Institute of Poliomyelitis and Viral Encephalitis, Moscow, Russia, p 45.

- Suss J. 2008. Tick-borne encephalitis in Europe and beyond-the epidemiological situation as of 2007. *Euro Surveill* 13:18916.
- Thompson WL, Karpus WJ, Van Eldik LJ. 2008. MCP-1-deficient mice show reduced neuroinflammatory responses and increased peripheral inflammatory responses to peripheral endotoxin insult. *J Neuroinflammation* 5:35.
- Toporkova MG, Aleshin SE, Ozherelkov SV, Nadezhdina MV, Stephenson JR, Timofeev AV. 2008. Serum levels of interleukin 6 in recently hospitalized tick-borne encephalitis patients correlate with age, but not with disease outcome. *Clin Exp Immunol* 152:517–521.
- Trinchieri G. 2003. Interleukin-12 and the regulation of innate resistance and adaptive immunity. *Nat Rev Immunol* 3:133–146.
- Tsuboi Y, Kakimoto K, Akatsu H, Daikuhara Y, Yamada T. 2002. Hepatocyte growth factor in cerebrospinal fluid in neurologic disease. *Acta Neurol Scand* 106:99–103.
- Valable S, Montaner J, Bellail A, Berezowski V, Brillault J, Cecchelli R, Divoux D, Mackenzie ET, Bernaudin M, Roussel S, Petit E. 2005. VEGF-induced BBB permeability is associated with an MMP-9 activity increase in cerebral ischemia: Both effects decreased by Ang-1. *J Cereb Blood Flow Metab* 25:1491–1504.
- Yamada T, Tsubouchi H, Daikuhara Y, Prat M, Comoglio PM, McGeer PL, McGeer EG. 1994. Immunohistochemistry with antibodies to hepatocyte growth factor and its receptor protein (c-MET) in human brain tissues. *Brain Res* 637:308–312.
- Zajkowska J, Moniuszko-Malinowska A, Pancewicz SA, Muszyńska-Mazur A, Kondrusik M, Grygorczuk S, Swierzbńska-Pijanowska R, Dunaj J, Czupryna P. 2011. Evaluation of CXCL10, CXCL11, CXCL12 and CXCL13 chemokines in serum and cerebrospinal fluid in patients with tick borne encephalitis (TBE). *Adv Med Sci* 56:311–317.

SUPPORTING INFORMATION

Additional supporting information may be found in the online version of this article at the publisher's web-site.

CHAPTER VII

Tick-borne encephalitis virus neutralization by high dose intravenous immunoglobulin

Jana Elsterová, Martin Palus, Jana Širmarová, Jan Kopecký, Hans Helmut Niller, Daniel Růžek

Ticks and Tick-borne Diseases 2016 (in press)

DOI: 10.1016/j.ttbdis.2016.11.007

<http://dx.doi.org/10.1016/j.ttbdis.2016.11.007>

Tick-borne encephalitis virus neutralization by high dose intravenous immunoglobulin (IVIG)

(summary)

The mechanisms by which TBEV causes encephalitis are not completely revealed, but direct viral cytolytic damage and already mentioned immune pathology are likely. There is no specific treatment currently available for TBE disease. However, vaccination remains the most reliable prophylaxis. The mouse experiments indicate that an immunomodulatory treatment that reduce the inflammatory immune response, while not disabling it, may help restrict flaviviral CNS pathology. Since immune modulation by tetracycline was helpful, immunomodulatory therapy may be the way to go (Atrasheuskaya *et al.*, 2003). The most suitable therapy would lead to stimulation of protective immune reactions, normalization of immune regulation, and restriction of the immune response mechanisms that are associated with tissue damage.

There is a sizable number of case reports describing successfully treated arboviral encephalitis with high doses of intravenous immunoglobulins. Passive transfer of IVIG is already a well-established and clinically validated procedure. IVIG preparations are successfully used for treatment of patients suffering from a variety of diseases (Ben-Nathan *et al.*, 2003) including viral encephalitis, like Japanese encephalitis (Caramello *et al.*, 2006, 2007), West Nile virus encephalitis (Makhoul *et al.*, 2009; Ben-Nathan *et al.*, 2003), herpes simplex encephalitis (Erlich *et al.*, 1987), etc. Nevertheless, only very few reports of severe TBE cases that substantially improved after application of IVIG (Kleiter *et al.*, 2007) are available. The protective effect of passively administered IVIG has been attributed to the ability of the specific antibodies to neutralize the virus. We determined the titers of TBEV-neutralizing antibodies in two IVIG lots originating from the same manufacturer, and tested their ability to treat a lethal TBEV-infection in a mouse model.

More than 100-fold difference in TBEV-neutralizing capacity was demonstrated between the two individual IVIG lots. High TBEV-neutralizing activity of IVIG containing TBEV-specific antibody was confirmed in two different human neural cell lines, but IVIG without TBEV-specific antibodies had no or little effect on virus titers in cultures. In TBEV-infected mice, 90 % of protection was achieved when treated with IVIG containing high titers of TBEV-specific antibodies, whereas no immunotherapeutic effect was seen after administration of IVIG without TBEV-specific antibodies. We did not observe any indications for antibody dependent enhancement (Kopecky *et al.*, 1991) caused by IVIG containing TBEV-specific antibodies at neutralizing or sub-neutralizing levels nor in human neural cells *in vitro* neither in TBE murine models *in vivo*.

We can conclude that IVIG lots with high TBEV-specific antibody titers might represent a useful post-exposure prophylaxis or first-line effective therapy in TBE. These findings are particularly important for patients with high risk of severe TBE, including those with primary immunodeficiency or those with failed anti-TBEV vaccination, who depend on the presence of protective levels of antibodies present in IVIG preparations.

Tick-borne encephalitis virus neutralization by high dose intravenous immunoglobulin

Running title: TBEV neutralization by IVIG

Jana Elsterova,^{1,2,3} Martin Palus,^{1,2,3} Jana Sirmarova,¹ Jan Kopecky,³ Hans Helmut Niller,⁴ and Daniel Ruzek^{1,2*}

- (1) Department of Virology, Veterinary Research Institute, Hudcova 70, CZ-62100 Brno, Czech Republic
- (2) Institute of Parasitology, Biology Centre of the Czech Academy of Sciences, Branisovska 31, CZ-37005 Ceske Budejovice, Czech Republic
- (3) Faculty of Science, University of South Bohemia, Branisovska 31, CZ-37005 Ceske Budejovice, Czech Republic
- (4) Institute for Medical Microbiology and Hygiene, University of Regensburg, Franz-Josef-Strauss Allee: 11, 93053 Regensburg, Germany

*Author for Correspondence: Daniel Ruzek, Veterinary Research Institute, Hudcova 70, CZ-62100 Brno, Czech Republic, e-mail: ruzekd@paru.cas.cz, phone: +420-728-216-958, fax: +420-5-4121-1229

Abstract

Tick-borne encephalitis (TBE) is a potentially lethal neuroinfection in humans, caused by TBE virus (TBEV). Currently, there are no approved therapeutic agents to treat TBE. Previously, it was suggested that application of high dose intravenous immunoglobulin (IVIG) may pose potentially successful treatment for severe cases of TBE. In this study, we determined the titers of TBEV-neutralizing antibodies in two IVIG lots originating from the same manufacturer, and tested their ability to treat a lethal TBEV-infection in a mouse model. Using an *in vitro* assay, more than 100-fold difference in TBEV-neutralizing capacity was demonstrated between the two individual IVIG lots. High TBEV-neutralizing activity of IVIG containing TBEV-specific antibody was confirmed in two different human neural cell lines, but

IVIG without TBEV-specific antibodies had no or little effect on virus titers in the culture. In TBEV-infected mice, 90 % of protection was achieved when the mice were treated with IVIG containing higher titers of TBEV-specific antibodies, whereas no immunotherapeutic effect was seen when mice were treated with IVIG without TBEV-specific antibodies. No antibody-dependent enhancement of TBEV infectivity induced by cross-reactive antibodies or by virus-specific antibodies at neutralizing or sub-neutralizing levels was observed either in cell culture or in TBEV-infected mice treated with any of the IVIG preparations. The results indicate that IVIG lots with high TBEV antibody titers might represent a post-exposure prophylaxis or first-line effective therapy of patients with a severe form of TBE.

Key words: flavivirus; ticks; neutralizing antibodies; IVIG; antibody-dependent enhancement; immunotherapy

Introduction

Tick-borne encephalitis virus (TBEV) (family *Flaviviridae*, genus *Flavivirus*) is a causative agent of tick-borne encephalitis (TBE), a severe human neuroinfection manifesting as meningitis, meningoencephalitis, meningoencephalomyelitis or meningoencephalomyelorradiculitis. The infection is fatal in approximately 1 % of cases, but in up to 46 % of cases it may result in long-lasting or permanent neurological damage, known as post-encephalitic syndrome. This include neuropsychiatric problems, balance disorders, headache, dysphasia, hearing defects, spinal paralysis, tremor, etc. (Haglund and Günther, 2003). The most severe cases are reported in elder (Jelenik et al., 2010) or immunocompromised patients (Chmelik et al., 2016). However, severe courses of TBE with accompanying post-encephalitis syndrome do also occur in children (von Stülpnagel et al., 2016) Although an effective vaccine against TBEV is available, a vaccination coverage remains still low in several endemic countries (Süss et al., 2010). During the last 30 years, there has been a continuous increase in the numbers of human cases of TBE in Europe. Currently, between 10,000 and 15,000 TBE cases per year are reported in Europe and Asia (Süss, 2008; Bogovic and Strle, 2015). There are no approved therapeutic agents to treat TBE. The use of specific anti-TBEV immunoglobulins for TBE therapy was

discontinued in Europe due to the concerns of antibody-dependent enhancement (ADE) of the infectivity after post-exposure prophylaxis in children (Kluger et al., 1995; Waldvogel et al., 1996). However, ADE was not confirmed in TBEV-infected mice after passive pre- or post-exposure prophylactic administration of the specific anti-TBEV antibodies (Kreil and Eibl, 1997). Moreover, specific anti-TBEV immunoglobulins are still in use in Russia, where a single post-exposure administration an anti-TBEV immunoglobulin in a dose of 0.05 ml/kg body weight ensures protection on average in 79 % of TBE cases (Pen'evskaia and Rudakov, 2010). Based on an increasing number of case reports on the successful treatment of other arboviral infections, including Japanese encephalitis, Eastern equine encephalitis, West Nile fever, or chikungunya, with high dose intravenous immunoglobulins (IVIG) (Ben-Nathan et al., 2003; 2009; Srivastava et al., 2015; Planitzer et al., 2007; Caramello et al., 2006; 2007; Rajapakse, 2009; Golomb et al., 2001; Chusri et al., 2011; Hamdan et al., 2002; Shimoni et al., 2001), we suggested using IVIG also for the treatment of severe cases of TBE (Růžek et al., 2013). IVIG is a commercial preparation of purified human IgG manufactured from pooled plasma from thousands of healthy donors and is approved for clinical use (Rhoades et al., 2000). IVIG has a broad repertoire of antibodies neutralizing various pathogens and neutralization is commonly assumed to be the main mechanism of action. Moreover, IVIG has important immunomodulatory effects, which include activation/blockade of Fc receptors, attenuation of complement-mediated damage, induction of anti-inflammatory cytokines, anti-inflammatory effect by cytokine-specific, or CD4 and MHC class I-specific autoantibodies, autoantibodies against the Fas receptor, etc. (Boros et al., 2005).

In this study, the potency of IVIG for TBEV neutralization was tested *in vitro* in two human neural cell lines, and *in vivo* using a lethal mouse model mimicking severe cases of TBE in humans. Our results demonstrate that individual IVIG lots even from the same manufacturer can differ significantly in the titers of TBEV-neutralizing antibodies. The passive administration of IVIG containing sub-neutralizing levels of TBEV-specific antibodies has no effect on the survival of TBEV-infected mice, but IVIG containing anti-TBEV antibodies can effectively prevent or ameliorate the development of the disease.

Material and Methods

Human serum and IVIG preparations

Pooled human serum was obtained from Sigma-Aldrich (St. Louis, MO, USA). Two lots of OCTAGAM® 10% [100 mg/ml] (Octapharma, Manchester, UK) were used; i.e., lot No. A125C8534 (further referred as IVIG1), and lot No. C343A8541 (further referred as IVIG2). The IVIG1 and IVIG2 preparations represented a pooled material from more than 3,500 donors, and contained human normal IgG > 95%, with a broad spectrum of antibodies against various infectious agents. IgA content was ≤ 0.2 mg/ml (http://www.octapharma.com.au/fileadmin/user_upload/octapharma.au/product_docs/octagam_10__PI.pdf).

Cell cultures

Human neuroblastoma cells and human glioblastoma cells (kindly provided by Professor T. Eckschlager, 2nd Faculty of Medicine, Charles University in Prague) were grown at 37 °C/5% CO₂ in Iscove's modified Dulbecco's medium (IMDM) supplemented with 10 % fetal calf serum (FCS) and 1 % mixture of antibiotics/antimycotics (penicillin, streptomycin; Biosera). Porcine kidney stable (PS) cells (Kořuch and Mayer, 1975) were grown at 37 °C in Leibovitz's L-15 medium supplemented with 3 % newborn calf serum and 1 % mixture of antibiotics/antimycotics (penicillin, streptomycin; Biosera).

ELISA and plaque reduction neutralization test

Specific anti-TBEV antibodies in the pooled human serum, IVIG1 and IVIG2 were determined by sandwich-type ELISA (IMMUNOZYM FSME (TBE) IgG; PROGEN Biotechnik, Germany). The assay was performed according to the instruction of the manufacturer. The IgG antibody titer was expressed in Vienna Units per ml (VIEU/ml).

Presence of specific neutralizing anti-TBEV antibodies in IVIG preparations and pooled human serum was determined by plaque reduction

neutralization test (PRNT) as described previously (Bárdoš et al., 1983), with slight modifications. Ten mg/ml of protein content of the IVIG1, IVIG2, and pooled human serum were used for PRNT. Inactivation of complement was done by incubation at 56 °C for 30 min. Two fold serial dilutions of the samples were incubated with 1×10^3 pfu of TBEV strain Hypr for 90 min at 37 °C. After that, 5×10^4 of PS cells was added to the wells of 96-well plate and the suspension was overlaid with carboxymethylcellulose. After incubation for 5 days, the cells were fixed and stained as described previously (De Madrid and Porterfield, 1969). The last dilution of the sample that caused 80-100 % reduction of cytolysis was regarded as the endpoint titer.

Virus stocks, infection of cell cultures, and virus titrations

Low-passage TBEV strains Neudoerfl (kindly provided by Professor F. X. Heinz, Medical University in Vienna; passaged four times in brains of suckling mice) and Hypr (passaged six times in brains of suckling mice) were used in the study. TBEV strain Neudoerfl was isolated in 1971 from an *Ixodes ricinus* tick in Burgenland, Austria; Hypr strain was isolated in 1953 from the blood of a deceased child in Moravia, Czech Republic.

Human neuroblastoma or human glioblastoma cells were seeded in 96-well plates at concentration of 1×10^4 cells/well and cultured overnight. The other day, the cells were infected with TBEV strain Neudoerfl at a multiplicity of infection (m.o.i.)=5. The cells were treated with either IVIG1 or IVIG2 under three regimens. One group was pretreated with 10 mg/ml of either IVIG1 or IVIG2 for 4 hours before the infection. The second group was treated with the same concentrations of the preparations after the infection throughout the whole experiment. The third group represented a combination of both; i.e., combined pretreatment as well as treatment post-infection. A control group represented TBEV-infected cells without any treatment. Cell supernatants were collected daily from day 1 to day 4 (neuroblastoma), and 1 to day 4 and on day 6 (glioblastoma) post-inoculation, and subjected to a plaque assay.

The titer of the virus was assayed on PS cell monolayers based on a modified protocol by De Madrid and Porterfield (1969). Briefly, tenfold dilutions of

the virus suspension were placed in 96-well plates and 1×10^4 of PS cells per well was added. After 4 hour incubation at 37 °C and 0.5 % CO₂, a carboxymethylcellulose (1.5% in L-15 medium) overlay was added to each well. Following 5 day incubation at 37 °C and 0.5 % CO₂, the cells were stained with naphtalene black. Infectivity was expressed as pfu/ml.

Viral RNA was isolated from cell culture supernatants by QIAamp Viral RNA Mini Kit (Qiagen), and viral genome copies were quantified using RT-qPCR for TBEV (Path-TBEV-EASY; Primerdesign) on a Rotor Gene-3000 (Corbett Research).

Cell cytotoxicity of both IVIG preparations was tested by Annexin V Apoptosis Detection Kit FITC (eBioscience, CA, USA). Briefly, human neuroblastoma or glioblastoma cells were seeded in 24-well plates in concentration of 3×10^5 of cells/ml. The cells were subsequently incubated in the presence of IVIG preparations or the pooled human serum at concentrations 0 mg/ml, 0.1 mg/ml, 1 mg/ml, and 10 mg/ml for 24 hours. Cell viability was tested 72 hours after the IVIG/pooled human serum addition according to the instructions in the kit manual. The analysis was performed using BD FACS Canto II flow cytometer with BD FACS Diva Software.

Mice and virus Inoculation

Female BALB/c mice of 5 to 6 weeks of age were obtained from Harlan Laboratories, Inc. (Indiana, USA). The mice were housed in plastic cages with sterilized wood-chip bedding in a specific-pathogen free room under constant temperature of 22 °C and relative humidity of 65 %. Sterilized pellet diet and water was provided *ad libitum*. Ten mice per group were used in the experiments.

The mice were inoculated subcutaneously with 10^3 pfu of TBEV Hypr strain. Hypr strain was selected because of its high virulence for laboratory mice. The recipient group of mice was administered with 0.5 ml either human sera or IVIG1 or IVIG2 (50 mg/ml) intraperitoneally daily from 1 to 5 days post-

infection (p.i.). Control mice received PBS at the same time intervals. The mice were monitored daily for 28 days p.i.

The research complied with all relevant European Union guidelines for work with animals and was in accordance with the Czech national law guidelines on the use of experimental animals and protection of animals against cruelty (animal Welfare Act No. 246/1992 Coll.). The protocol was approved by the Committee on the Ethics of Animal Experimentation of the Institute of Parasitology and of the Departmental Expert Committee for the Approval of Projects of Experiments on Animals of the Czech Academy of Sciences (permit No. 165/2010).

Statistical analysis

Kruskal-Wallis test and Dunn's Multiple comparison test was used for comparisons of the concentrations of TBEV-neutralizing antibodies in the individual preparations by PRNT, as well for comparisons of viral titers in cell culture. Results from ELISA were analyzed by two-way ANOVA-Bonferroni multiple comparison. Cell viability after treatment with individual preparations was analyzed by Bartlett's test for equal variances and Dunn's Multiple comparison test. Survival rates were analyzed by log-rank Mantel-Cox test. All tests were performed using GraphPad Prism 5.00 (GraphPad Software, Inc., USA). *P*-values <0.05 were considered to be statistically significant.

Results

Detection of anti-TBEV antibodies in the investigated preparations

To investigate the titer of antibodies against TBEV in the pooled human serum and both IVIG preparations, the samples were analyzed by ELISA and PRNT. No anti-TBEV antibodies were detected in the pooled human serum. IVIG1 contained detectable titers of anti-TBEV antibodies (approx. 250 VIEU/ml) only when the lowest dilution (i.e., 10 mg/ml) was tested. On the other hand, IVIG2 contained high titers of anti-TBEV antibodies within high

range of dilutions from 10 mg/ml (approx. 1,250 VIEU/ml) to 0.1 mg/ml (approx. 120 VIEU/ml) (Fig. 1A).

Pooled human serum did not contain any TBEV-neutralizing antibodies as determined by PRNT. The titers of TBEV-neutralizing antibodies in IVIG1 were at the borderline level. IVIG2 contained high levels of TBEV-neutralizing antibodies reaching titers 1:125, which is approximately 100-fold higher titer when compared to IVIG1 (Fig. 1B).

Reduction of TBEV-growth in human neural cell lines

IVIG1 and IVIG2 were tested for their ability to inhibit TBEV growth *in vitro* in two human neural cell types; i.e., human neuroblastoma, and human glioblastoma cells. Previously, both these cell types were shown to be highly sensitive to TBEV and to produce high virus titers (Ruzek et al., 2009). To exclude any false-positive effect caused by potential cytotoxicity of the preparations tested, the toxicity of both IVIG preparations was first examined in both cell systems by detecting apoptotic cells based on the detection of phosphatidylserine on the cell membrane, and necrotic cells by labeling nuclear proteins. No toxicity was observed when the cells were incubated in the presence of preparations at the concentrations ranging from 0.1 to 10 mg/ml (data not shown).

The cells were infected with TBEV strain Neudoerfl at a multiplicity of infection (m.o.i.)=5. The cells were treated with either IVIG1 or IVIG2 under three regimens as described in Material and Methods. Cell supernatants were collected and subjected to a plaque assay.

TBEV titers reached approximately 10^7 pfu/ml, and 10^6 pfu/ml in untreated neuroblastoma and glioblastoma cells, respectively. Pretreatment or treatment with IVIG1, or combination of both, had no effect on TBEV titer in neuroblastoma cells at any time point investigated with the exception of day 1 p.i. (Fig. 2A). In human glioblastoma cells, a slight decrease in virus titer was seen only in cells treated with IVIG1 at day 4 p.i. (Fig. 2C). On the other hand, IVIG2 had a strong inhibitory effect on virus growth in cell culture (Fig. 2B, D). In human neuroblastoma cells, pretreatment with IVIG2 had no

significant effect on virus growth, but when the pretreatment was combined with post-infection treatment, virus titers were significantly reduced up to 10^4 -fold compared to the untreated TBEV-infected cells. Treatment with IVIG2 post-infection reduced virus titers in the culture approximately 10^2 fold compared to the untreated cells (Fig. 2B). Similar effect was seen in case of TBEV-infected glioblastoma cells, where the treatment post-infection or combination of the pretreatment and posttreatment resulted in significant reduction of virus titer compared to untreated TBEV-infected cells, reaching a maximum of 10^3 -to- 10^4 -fold reduction on days 2 and 3 (Fig. 2D). Combined pre- and posttreatment of glioblastoma and neuroblastoma cells with IVIG2 reduced also the number of TBEV RNA copies in cell culture supernatant, as measured by RT-qPCR. There was approximately 1.5-2 \log_{10} difference in the number of viral genomic copies in the supernatant of the treated and control cultures on day 3 p.i. (data not shown).

Protection of mice from a lethal TBEV infection by IVIG

Infection of mice is a well-established model to investigate the mechanism and the efficacy of treatment interventions or immune protection against TBEV infection. In our experiments, mice were infected with 10^3 pfu of TBEV Hypr strain, which is a dose causing 100% mortality. The infection in mice was associated with classical signs of neuroinfection; i.e., ruffled fur, hunched posture, paresis, etc. Due to ethical reasons, mice in a terminal stage of the neuroinfection were euthanized. Groups of 10 TBEV-infected mice were given daily intraperitoneal injections of 50 mg of either IVIG1 or IVIG2 from day 1 to day 5 p.i. Control groups contained TBEV-infected mice that were treated intraperitoneally at the same intervals with 0.8 ml PBS or pooled human serum.

The results summarized in Fig. 3, show that passively transferred IVIG2 conferred 90% survival of this otherwise lethal challenge, whereas no therapeutic efficacy was achieved using IVIG1. Similarly, no mice treated with pooled human serum or PBS survived. All mice treated with IVIG1/pooled human serum/PBS died within 12 days after virus inoculation and no differences were seen in the mean survival time between these groups ($p>0.05$). The results clearly show that IVIG2 containing high levels of

TBEV-neutralizing antibodies had high antiviral effect in TBEV-infected mice ($p < 0.0001$), while IVIG1 had no therapeutic activity.

Discussion

Passive transfer of IVIG is a well-established and extensively clinically used procedure. IVIG preparations are successfully used for treatment of patients suffering from a variety of diseases, including myasthenia gravis, idiopathic thrombocytopenia purpura, inflammatory demyelinating polyneuropathy (Ben-Nathan et al., 2003), but also various viral encephalitides (Caramello et al., 2006, 2007; Makhoul et al., 2009; Ben-Nathan et al., 2003; Golomb et al., 2001; Erlich et al., 1987). In most of these cases, the protective effect of passively administered IVIG has been attributed to the ability of the specific antibodies to neutralize the virus. Based on these data, we suggested to treat severe cases of TBE with IVIG as early in the course of the disease as possible, and proposed to conduct a randomized controlled treatment study focused on IVIG treatment of the severe TBE cases (Růžek et al., 2013). However, there are still only few reports of cases of severe TBE that substantially improved after application of IVIG (Kleiter et al., 2007).

As demonstrated in the present study, the efficiency of the protection by passive antibodies was directly related to the amount of specific antibodies present in the IVIG preparation. In this study, we investigated the titers of antibodies against TBEV in two IVIG lots from the same manufacturer. The levels of anti-TBEV antibodies were at the borderline level in one IVIG lot, but the second lot investigated contained high levels of TBEV-specific antibodies, as demonstrated by ELISA as well as by PRNT. A variability in TBEV-specific antibodies content in IVIG preparations from different geographic origins was shown previously by Rabel et al. (2012) and Goldacker et al. (2015). IVIG preparations originating in Europe had much higher titers than IVIG from Russia, and IVIG from the US contained no detectable titers of TBEV-specific antibodies. It was suggested that the fractionation of IVIG from plasma donations collected around the world would produce IVIG with universal content of antibodies against a broad range of pathogens (Bayry et al., 2003), which is, unfortunately, not feasible at present. The US represent the most important source of human plasma

for IVIG production, and the IVIG manufacture in Europe largely depends on plasma donations from the US (Rabel et al., 2012). With respect to differences in the specific antibody content between individual IVIG lots, each lot should be marked with the details on the geographical origin of the plasma or this information should be available on request from the respective manufacturer. A preparation of a “tailor-made” pathogen-specific IVIG enriched with antibodies against specific infectious agents was also suggested (Bayry et al., 2003). In case of TBE, IVIG preparations not containing specific anti-TBEV antibodies might be spiked with chimeric/humanized anti-TBEV monoclonals (Baykov et al., 2014).

Inhibition of TBEV growth by the two IVIG lots was investigated *in vitro* in two human neural cell lines; i.e., human neuroblastoma and human glioblastoma cells. In both cell lines, a significant reduction of TBEV growth was seen when the cells were treated with the higher TBEV neutralization titer IVIG lot, while treatment with IVIG lacking neutralizing levels of TBEV-specific antibodies had no or little effect on virus growth. IVIG2 probably neutralized virus particles released from the infected cells; however, the growth of the virus in the culture was inhibited as well, as demonstrated by the reduced numbers of viral RNA copies in the culture supernatant.

A more convincing evidence for a potentially beneficial clinical effect of IVIG for the therapy of TBE needs to be provided by the direct demonstration of the efficacy *in vivo* (Planitzer et al., 2007). In our experiments, mice were inoculated with a lethal dose of TBEV. No control mice or mice treated with IVIG lacking neutralizing levels of TBEV-specific antibodies survived the virus challenge. By contrast, 90% of TBEV-infected mice treated with the higher TBEV neutralization titer IVIG lot survived the otherwise lethal TBEV challenge. These results demonstrated a good correlation between the *in vitro* and *in vivo* IVIG neutralization activity. Similarly to our study, Planitzer et al. (2007) showed a good correlation between WNV neutralization as measured by a functional *in vitro* assay and protection against an otherwise lethal WNV infection *in vivo* and suggested that the *in vitro* assays can be useful in revealing important functional parameters of individual IVIG lots.

To enter the brain, immunoglobulins must cross the blood-brain barrier (BBB). Using mouse model, it was demonstrated that a significant fraction of

systemically administered IVIG enters the brain through a saturable transport across the BBB. This suggests that therapeutically relevant IVIG concentrations can be reached in cerebral tissues even in the absence of BBB disruption (St-Amour et al., 2013). It was found that TBEV infection induces considerable breakdown of the BBB in mice (Růžek et al., 2011), and the integrity of the BBB is also damaged in severe cases of TBE in humans (Palus et al., 2014; Chekhonin et al., 2002; Kang et al., 2013). Breakdown of the blood–brain barrier thus allows increased access of IVIG into the brain.

The use of specific anti-TBEV immunoglobulins for TBE therapy was discontinued in Europe due to ADE concerns. However, in Russia, specific immunoglobulins are still in use and the immunotherapy ensures high level of protection (Pen'evskaia and Rudakov, 2010). ADE of flavivirus infection, with an exception for dengue (Pinto et al., 2015), is still without a clear proof *in vivo*, and a subject to debate (Kreil and Eibl, 1997). For TBEV, ADE has been demonstrated *in vitro* in infected macrophages (Kopecky et al., 1991; Phillipotts et al., 1985). However, it was demonstrated that the same antibodies that were able to enhance TBEV replication in mouse peritoneal macrophages *in vitro* were protective against lethal TBEV infection in mice (Kreil and Eibl, 1997). Neither sublethal TBEV challenges nor suboptimal dilutions of the immunoglobulins, even if applied together, could provide any indication of ADE occurring *in vivo* (Kreil and Eibl, 1997). In the present study, we did not see any indications for ADE caused by IVIG containing TBEV-specific antibodies at neutralizing or sub-neutralizing levels in both human neural cells *in vitro* as well as in TBE murine models *in vivo*. Even if the ADE phenomenon might occur in rare cases due to the exclusive administration of specific anti-TBEV immunoglobulins, it is likely that the ADE effect may be suppressed by the immunomodulatory effects of the high amounts of generic immunoglobulins contained in the IVIG preparations.

In summary, this study shows that (i) individual IVIG lots, even from the same manufacturer, have significantly different content of TBEV-specific antibodies, (ii) IVIG lots containing TBEV-specific antibodies effectively neutralize the virus *in vitro* as well as in mice, while IVIG lots without TBEV-specific antibodies have no TBEV-neutralizing activity (iii) IVIG lots lacking TBEV-specific antibodies exhibit no immunomodulatory effect leading to improved survival of TBEV-infected mice, and (iv) no ADE of TBEV infectivity

was observed after treatment with IVIG, regardless on the amount of TBEV-specific antibodies present in the preparation.

Based on the results of the present study, we can conclude that IVIG lots with high TBEV-specific antibody titers might represent a useful post-exposure prophylaxis or first-line effective therapy in TBE. These findings are particularly important for patients with high risk of severe TBE, including those with primary immunodeficiency or those with failed anti-TBEV vaccination, who depend on the presence of protective levels of antibodies present in IVIG preparations.

Acknowledgements

This study was supported by Czech Science Foundation projects 14-29256S and 16-20054S, Ministry of Health of the Czech Republic, grant No. 16-34238A, and by project LO1218 with financial support from the Ministry of Education, Youth and Sports of the Czech Republic under the NPU I program. We acknowledge a grant for the development of research organization (RVO: RO0516).

Conflict of Interest

None.

References

- Bárdos, V., Sixl, W., Wisidagama, C.L., Halouzka, J., Stünzner, D., Hubálek, Z., Withalm, H. 1983. Prevalence of arbovirus antibodies in sera of animals in Sri Lanka. *Bull. World Health Organ.* 61(6), 987-90.
- Baykov, I.K., Matveev, A.L., Stronin, O.V., Ryzhikov, A.B., Matveev, L.E., Kasakin, M.F., Richter, V.A., Tikunova, N.V. 2014. A protective chimeric antibody to tick-borne encephalitis virus. *Vaccine* 32(29), 3589-94.
- Bayry, J., Lacroix-Desmazes, S., Kazatchkine, M.D., Kaveri, S.V. 2003. Intravenous immunoglobulin for infectious diseases: tailor-made or universal? *J. Infect. Dis.* 188(10), 1610.

- Ben-Nathan, D., Lustig, S., Tam, G., Robinzon, S., Segal, S., Rager-Zisman, B. 2003. Prophylactic and therapeutic efficacy of human intravenous immunoglobulin in treating West Nile virus infection in mice. *J. Infect. Dis.* 188(1), 5-12.
- Ben-Nathan, D., Gershoni-Yahalom, O., Samina, I., Khinich, Y., Nur, I., Laub, O., Gottreich, A., Simanov, M., Porgador, A., Rager-Zisman, B., Orr, N. 2009. Using high titer West Nile intravenous immunoglobulin from selected Israeli donors for treatment of West Nile virus infection. *BMC Infect. Dis.* 9, 18.
- Bogovic P, Strle F. 2015. Tick-borne encephalitis: A review of epidemiology, clinical characteristics, and management. *World J Clin Cases.* 3(5), 430-41.
- Boros, P., Gondolesi, G., Bromberg, J.S. 2005. High dose intravenous immunoglobulin treatment: mechanisms of action. *Liver Transpl.* 11(12), 1469-80.
- Caramello, P., Canta, F., Balbiano, R., Lipani, F., Ariaudo, S., De Agostini, M., Calleri, G., Boglione, L., Di Caro, A. 2006. Role of intravenous immunoglobulin administration in Japanese encephalitis. *Clin. Infect. Dis.* 43(12), 1620-1.
- Chekhonin VP, Zhirkov YA, Belyaeva IA, Ryabukhin IA, Gurina OI, Dmitriyeva TB. 2002. Serum time course of two brain-specific proteins, alpha(1) brain globulin and neuron-specific enolase, in tick-born encephalitis and Lyme disease. *Clin Chim Acta.* 320(1-2):117-25.
- Chmelík, V., Chrdele, A., Růžek, D. 2016. Fatal tick-borne encephalitis in an immunosuppressed 12-year-old patient. *J. Clin. Virol.* 74, 73-4.
- Chusri, S., Siripaitoon, P., Hirunpat, S., Silpapojakul, K. 2011. Case reports of neuro-Chikungunya in southern Thailand. *Am. J. Trop. Med. Hyg.* 85(2), 386-9.
- De Madrid, A.T., Porterfield, J.S. 1969. A simple micro-culture method for the study of group B arboviruses. *Bull. World Health Organ.* 40(1), 113-21.
- Erllich, K.S., Dix, R.D., Mills, J. 1987. Prevention and treatment of experimental herpes simplex virus encephalitis with human immune serum globulin. *Antimicrob. Agents Chemother.* 31(7), 1006-9.
- Goldacker, S., Witte, T., Huzly, D., Schlesier, M., Peter, H.H., Warnatz, K. 2015. Analysis of specific IgG titers against tick-borne encephalitis in patients with primary antibody deficiency under immunoglobulin substitution therapy: impact of plasma donor origin. *Front. Immunol.* 5, 675.
- Golomb, M.R., Durand, M.L., Schaefer, P.W., McDonald, C.T., Maia, M., Schwamm, L.H. 2001. A case of immunotherapy-responsive eastern equine encephalitis with diffusion-weighted imaging. *Neurology* 56(3), 420-1.
- Haglund, M., Günther, G. 2003. Tick-borne encephalitis--pathogenesis, clinical course and long-term follow-up. *Vaccine* 21 Suppl 1, S11-8.
- Hamdan, A., Green, P., Mendelson, E., Kramer, M.R., Pitlik, S., Weinberger, M. 2002. Possible benefit of intravenous immunoglobulin therapy in a lung transplant recipient with West Nile virus encephalitis. *Transpl. Infect. Dis.* 4(3), 160-2.
- Jelenik, Z., Keller, M., Briggs, B., Günther, G., Haglund, M., Hudeckova, H., Jilkova, E., Mickiene, A., Sandell, B., Steffen, R., Strle, F. 2010. Tick-borne encephalitis and golden agers: position paper of the International Scientific Working Group on Tick-borne encephalitis (ISW-TBE). *Wien. Med. Wochenschr.* 160(9-10), 247-51.

- Kang X, Li Y, Wei J, Zhang Y, Bian C, Wang K, Wu X, Hu Y, Li J, Yang Y. 2013. Elevation of matrix metalloproteinase-9 level in cerebrospinal fluid of tick-borne encephalitis patients is associated with IgG extravasation and disease severity. *PLoS One*. 8(11):e77427.
- Kleiter, I., Jilg, W., Bogdahn, U., Steinbrecher, A. 2007. Delayed humoral immunity in a patient with severe tick-borne encephalitis after complete active vaccination. *Infection* 35(1), 26-9.
- Kluger, G., Schöttler, A., Waldvogel, K., Nadal, D., Hinrichs, W., Wündisch, G.F., Laub, M.C. 1995. Tickborne encephalitis despite specific immunoglobulin prophylaxis. *Lancet* 346(8988), 1502.
- Kopecký, J., Grubhoffer, L., Tomková, E. 1991. Interaction of tick/borne encephalitis virus with mouse peritoneal macrophages. The effect of antiviral antibody and lectin. *Acta Virol.* 35(3), 218-25.
- Kozuch, O., Mayer, V. 1975. Pig kidney epithelial (PS) cells: a perfect tool for the study of flaviviruses and some other arboviruses. *Acta Virol.* 19(6), 498.
- Kreil, T.R., Eibl, M.M. 1997. Pre- and postexposure protection by passive immunoglobulin but no enhancement of infection with a flavivirus in a mouse model. *J. Virol.* 71(4), 2921-7.
- Makhoul, B., Braun, E., Herskovitz, M., Ramadan, R., Hadad, S., Norberto, K. 2009. Hyperimmune gammaglobulin for the treatment of West Nile virus encephalitis. *Isr. Med. Assoc. J.* 11(3), 151-3.
- Palus M, Zampachová E, Elsterová J, Růžek D. 2014. Serum matrix metalloproteinase-9 and tissue inhibitor of metalloproteinase-1 levels in patients with tick-borne encephalitis. *J Infect.* 68(2):165-9.
- Pen'evskaia, N.A., Rudakov, N.V. 2010. [Efficiency of use of immunoglobulin preparations for the postexposure prevention of tick-borne encephalitis in Russia (a review of semi-centennial experience)]. *Med. Parazitol. (Mosk)* (1), 53-9.
- Phillipotts, R.J., Stephenson, J.R., Porterfield, J.S. 1985. Antibody-dependent enhancement of tick-borne encephalitis virus infectivity. *J. Gen. Virol.* 66 (Pt 8), 1831-7.
- Pinto AK, Brien JD, Lam CY, Johnson S, Chiang C, Hiscott J, Sarathy VV, Barrett AD, Shresta S, Diamond MS. 2015. Defining New Therapeutics Using a More Immunocompetent Mouse Model of Antibody-Enhanced Dengue Virus Infection. *MBio.* 6(5):e01316-15.
- Planitzer, C.B., Modrof, J., Kreil, T.R. 2007. West Nile virus neutralization by US plasma-derived immunoglobulin products. *J. Infect. Dis.* 196(3), 435-40.
- Rabel, P.O., Planitzer, C.B., Farcet, M.R., Kreil, T.R. 2012. Tick-borne encephalitis virus-neutralizing antibodies in different immunoglobulin preparations. *Clin. Vaccine Immunol.* 19(4), 623-5.
- Rajapakse, S. 2009. Intravenous immunoglobulins in the treatment of dengue illness. *Trans. R. Soc. Trop. Med. Hyg.* 103(9), 867-70.
- Rhoades, C.J., Williams, M.A., Kelsey, S.M., Newland, A.C. 2000. Monocyte-macrophage system as targets for immunomodulation by intravenous immunoglobulin. *Blood Rev.* 14(1), 14-30.

- Růžek, D., Vancová, M., Tesarová, M., Ahantarig, A., Kopecký, J., Grubhoffer, L. 2009. Morphological changes in human neural cells following tick-borne encephalitis virus infection. *J. Gen. Virol.* 90(Pt 7), 1649-58.
- Růžek, D., Dobler, G., Niller, H.H. 2013. May early intervention with high dose intravenous immunoglobulin pose a potentially successful treatment for severe cases of tick-borne encephalitis? *BMC Infect. Dis.* 13, 306.
- Shimoni, Z., Niven, M.J., Pitlick, S., Bulvik, S. 2001. Treatment of West Nile virus encephalitis with intravenous immunoglobulin. *Emerg. Infect. Dis.* 7(4), 759.
- Srivastava, R., Ramakrishna, C., Cantin, E. 2015. Anti-inflammatory activity of intravenous immunoglobulins protects against West Nile virus encephalitis. *J. Gen. Virol.* 96(Pt 6), 1347-57.
- St-Amour I, Paré I, Alata W, Coulombe K, Ringuette-Goulet C, Drouin-Ouellet J, Vandal M, Soulet D, Bazin R, Calon F. 2013. Brain bioavailability of human intravenous immunoglobulin and its transport through the murine blood-brain barrier. *J Cereb Blood Flow Metab.* 33(12):1983-92.
- Suss, J. 2008. Tick-borne encephalitis in Europe and beyond--the epidemiological situation as of 2007. *Euro Surveill.* 13(26).
- Süss, J., Kahl, O., Aspöck, H., Hartelt, K., Vaheri, A., Oehme, R., Hasle, G., Dautel, H., Kunz, C., Kupreviciene, N., Zimmermann, H.P., Atkinson, B., Dobler, G., Kutsar, K., Heinz, F.X. 2010. Tick-borne encephalitis in the age of general mobility. *Wien. Med. Wochenschr.* 160(3-4), 94-100.
- von Stülpnagel, C., Winkler, P., Koch, J., Zeches-Kansy, C., Schöttler-Glas, A., Wolf, G., Niller, H.H., Staudt, M., Kluger, G., Rostasy, K. 2016. MRI-imaging and clinical findings of eleven children with tick-borne encephalitis and review of the literature. *Eur. J. Paediatr. Neurol.* 20(1), 45-52.
- Waldvogel, K., Bossart, W., Huisman, T., Boltshauser, E., Nadal, D. 1996. Severe tick-borne encephalitis following passive immunization. *Eur. J. Pediatr.* 155(9), 775-9.

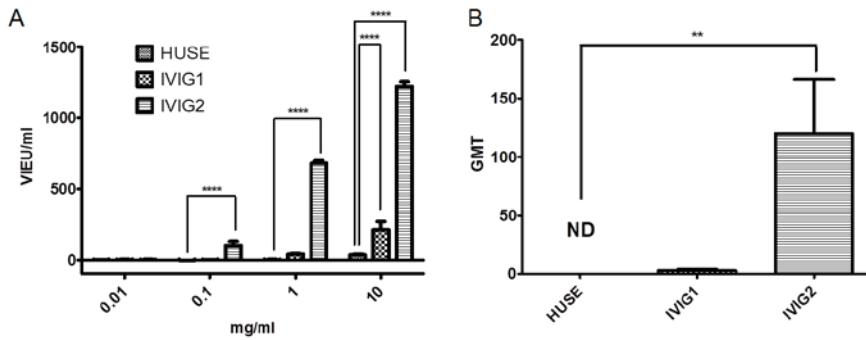


Fig. 1 Specific anti-TBEV antibodies in the pooled human serum (HUSE), IVIG1 and IVIG2 were determined by sandwich-type ELISA **(A)** and by PRNT **(B)**. For ELISA, the concentrations of HUSE, IVIG1 and IVIG2 of 0.01 mg/ml, 0.1 mg/ml, 1 mg/ml and 10 mg/ml were used. A two way ANOVA-Bonferroni multiple comparison was used for the analysis; the error bars represent standard deviations (****, $p < 0.0001$) **(A)**. PRNT was performed on PS cells with 10 mg/ml of IVIG1, IVIG2 and HUSE, and 1×10^3 pfu of TBEV. The level of TBEV-neutralizing antibodies is expressed as geometric mean titer (GMT) with standard deviation. A Kruskal-Wallis statistics and Dunn's Multiple comparison test was used for the analysis (**, $p < 0.01$; ND, not detected) **(B)**.

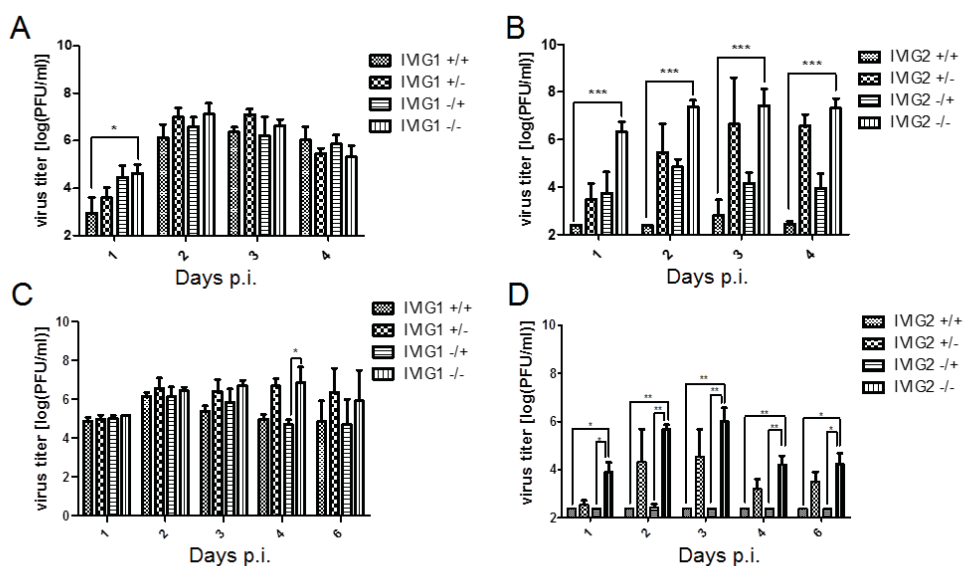


Fig. 2 IVIG1 and IVIG2 were tested for their ability to inhibit TBEV growth *in vitro* in two human neural cell types; i.e., human neuroblastoma (**A-B**), and human glioblastoma cells (**C-D**). The experiment was performed with 10 mg/ml of either IVIG1 or IVIG2 and the viral titer was determined by plaque assay as described in Material and Methods. The detection threshold was 2.3794 log₁₀ PFU/ml. The experiments were repeated three times and tested in duplicates. A Kruskal-Wallis statistics and Dunn's Multiple comparison test was used for the analysis (*, $p < 0.05$; **, $p < 0.01$; ***, $p < 0.001$).

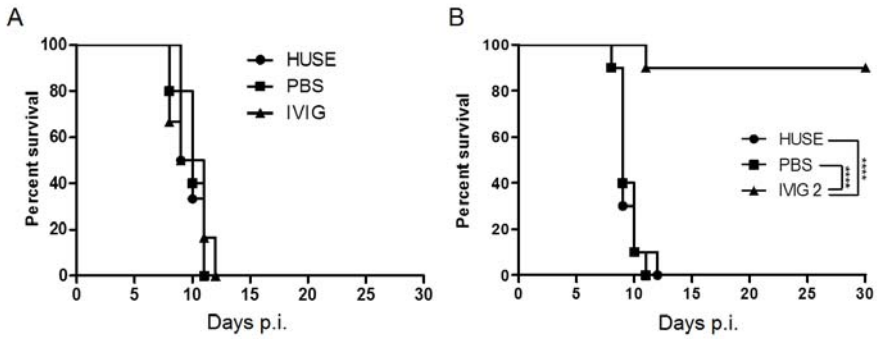


Fig. 3 Survival curve of mice infected with a lethal dose of TBEV. The recipient group of mice was administered with 0.5 ml either HUSE or 50 mg/ml of IVIG1 (**A**) or IVIG2 (**B**) intraperitoneally daily from 1 to 5 days p.i. Control mice received PBS at the same time intervals. The mice were monitored daily for 28 days p.i. A log-rank test was used for the analysis (****, $p < 0.0001$).

CHAPTER VIII

Nucleoside inhibitors of tick-borne encephalitis virus

Luděk Eyer, James J. Valdés, Victor A. Gil, Radim Nencka, Hubert Hřebabecký, Michal Šála, Jiří Salát, Jiří Černý, Martin Palus, Erik De Clercq, Daniel Růžek

Antimicrobial Agents and Chemotherapy 2015, 59:5483–5493

DOI: 10.1128/AAC.00807-15

<http://aac.asm.org/content/59/9/5483.short>

Nucleoside inhibitors of tick-borne encephalitis virus (summary)

Due to the dual role of the immune system during TBE and delicate border between, the inhibition of virus replication should be first choice option in anti-TBE medical treatment development. The use of nucleoside analogues is generally safe and well tolerated by the host body since they target viral but not cellular polymerases and cause premature termination of viral nucleic acid synthesis (de Clercq and Neyts, 2009).

A series of nucleoside analogues was tested for their ability to inhibit the TBEV replication in porcine kidney cells and human neuroblastoma cells. The nucleoside analogues 7-deaza-2'-C-methyladenosine (7-deaza-2'-CMA), 2'-C-methyladenosine (2'-CMA), and 2'-C-methylcytidine (2'-CMC) inhibited TBEV replication. These compounds showed dose-dependent inhibition of TBEV-induced cytopathic effects, TBEV replication (50% inhibition concentrations [IC50] of $5.1 \pm 0.4 \mu\text{M}$ for 7-deaza-2'-CMA, $7.1 \pm 1.2 \mu\text{M}$ for 2'-CMA, and $14.2 \pm 1.9 \mu\text{M}$ for 2'-CMC) and viral antigen production. Notably, 2'-CMC was relatively cytotoxic to porcine kidney cells (50% cytotoxic concentration [CC50] of $\sim 50 \mu\text{M}$). The anti-TBEV effect of 2'-CMA in cell culture diminished gradually after day 3 posttreatment. 7-Deaza-2'-CMA showed no detectable cellular toxicity ($\text{CC}_{50} > 50 \mu\text{M}$), and the antiviral effect in culture was stable for >6 days posttreatment. Computational molecular analyses revealed that compared to the other two compounds, 7-deaza-2'-CMA formed a large cluster near the active site of the TBEV polymerase. High antiviral activity and low cytotoxicity suggest that 7-deaza-2'-CMA is a promising candidate for further investigation as a potential therapeutic agent in treating TBEV infection.

The compounds will be tested further in a mouse model of TBEV infection. These compounds, even if they are not clinically effective, may be useful research tools or starting points for drug development efforts against TBEV. Because of its high antiviral activity and low cytotoxicity, 7-Deaza-2'-CMA is an attractive candidate for further investigation as a potential therapeutic

agent not only for TBE treatment but also for treating other flaviviral neuroinfections.

Nucleoside Inhibitors of Tick-Borne Encephalitis Virus

Luděk Eyer,^a James J. Valdés,^b Víctor A. Gil,^c Radim Nencka,^d Hubert Hřebabecký,^d Michal Šála,^d Jiří Salát,^a Jiří Černý,^{a,b,e} Martin Palus,^{a,b,e} Erik De Clercq,^f Daniel Růžek^{a,b,e}

Department of Virology, Veterinary Research Institute, Brno, Czech Republic^a; Institute of Parasitology, Biology Centre of the Czech Academy of Sciences, České Budějovice, Czech Republic^b; Joint BSC-CRG-IRB Research Program in Computational Biology, Barcelona Supercomputing Center, Barcelona, Spain^c; Institute of Organic Chemistry and Biochemistry, The Czech Academy of Sciences, Prague, Czech Republic^d; Faculty of Science, University of South Bohemia, České Budějovice, Czech Republic^e; Rega Institute for Medical Research, Leuven, Belgium^f

Tick-borne encephalitis virus (TBEV) is a leading cause of human neuroinfections in Europe and Northeast Asia. There are no antiviral therapies for treating TBEV infection. A series of nucleoside analogues was tested for the ability to inhibit the replication of TBEV in porcine kidney cells and human neuroblastoma cells. The interactions of three nucleoside analogues with viral polymerase were simulated using advanced computational methods. The nucleoside analogues 7-deaza-2'-C-methyladenosine (7-deaza-2'-CMA), 2'-C-methyladenosine (2'-CMA), and 2'-C-methylcytidine (2'-CMC) inhibited TBEV replication. These compounds showed dose-dependent inhibition of TBEV-induced cytopathic effects, TBEV replication (50% effective concentrations [EC₅₀] of 5.1 ± 0.4 μM for 7-deaza-2'-CMA, 7.1 ± 1.2 μM for 2'-CMA, and 14.2 ± 1.9 μM for 2'-CMC) and viral antigen production. Notably, 2'-CMC was relatively cytotoxic to porcine kidney cells (50% cytotoxic concentration [CC₅₀] of ~50 μM). The anti-TBEV effect of 2'-CMA in cell culture diminished gradually after day 3 posttreatment. 7-Deaza-2'-CMA showed no detectable cellular toxicity (CC₅₀ > 50 μM), and the antiviral effect in culture was stable for >6 days posttreatment. Computational molecular analyses revealed that compared to the other two compounds, 7-deaza-2'-CMA formed a large cluster near the active site of the TBEV polymerase. High antiviral activity and low cytotoxicity suggest that 7-deaza-2'-CMA is a promising candidate for further investigation as a potential therapeutic agent in treating TBEV infection.

Tick-borne encephalitis virus (TBEV) belongs to the *Flaviviridae* family, which includes other human- and animal-pathogenic viruses of global importance, such as West Nile virus (WNV), dengue virus (DENV), Japanese encephalitis virus (JEV), yellow fever virus (YFV), and hepatitis C virus (HCV) (1). TBEV virions are approximately 50 nm in diameter and are composed of a spherical nucleocapsid surrounded by a host-derived lipid bilayer. The TBEV genome is a single-stranded, plus-sense RNA about 11 kb in length that encodes a single polyprotein; this polyprotein is co- and posttranslationally processed into 3 structural and 7 nonstructural proteins (2).

In Europe and Northeast Asia, tick-borne encephalitis (TBE) represents one of the most important and serious neuroviral infections. More than 13,000 clinical cases of TBE, including numerous deaths, are reported annually worldwide (3, 4). The considerable increase in TBE incidence in countries where it is endemic and the emergence of the disease in several Western and Northern European countries have made TBE an increasing public health risk. In Europe, the most affected areas are southern Germany, Switzerland, Austria, the Czech Republic, Slovakia, Hungary, Slovenia, the Baltic states, Poland, parts of Scandinavia, and European Russia (5). The disease is usually biphasic: the first stage is febrile with flu-like symptoms, while the second phase manifests most often as meningitis, encephalitis, meningoencephalitis, meningoencephalomyelitis, and radiculitis. There are long-lasting or permanent neuropsychiatric sequelae in 10 to 20% of the infected patients (6). Although human vaccines against TBEV are currently available, the vaccination coverage remains quite low in several of the countries where TBEV is endemic (7). No specific antiviral therapy has been developed for TBE, and patient treatment is limited to supportive care (8). There is thus an urgent need for an effective approach to treatment that is based on specific inhibitors of TBEV replication.

Chemically modified nucleosides, also called nucleoside analogues or nucleoside inhibitors, represent the largest class of antiviral drugs. These compounds generally act via DNA or RNA chain termination with the potential exception of ribavirin, for which the mechanism may depend upon the virus and experimental system (9). Nucleoside analogues have been widely used as inhibitors of numerous medically important viruses, including HIV, herpesvirus, and hepatitis B virus (10, 11). Regarding flaviviruses, nucleoside analogues have been demonstrated to be efficacious in HCV replicon assays (12–16) and also against DENV (17–21), WNV (22), and YFV (23). Some of them were described as broad-spectrum inhibitors of various RNA viruses (24–27). 2'-Modified nucleoside analogues exhibit a high antiflavivirus activity and good pharmacokinetic properties (9). For TBEV inhibition, however, these compounds have not been tested thoroughly, if they have been tested at all. The high degree of homology between the polymerases of TBEV and other flaviviruses (28) suggests, however, that an investigation of nucleoside analogues as inhibitors of TBEV would be worthwhile.

Received 4 April 2015 Returned for modification 28 April 2015

Accepted 18 June 2015

Accepted manuscript posted online 29 June 2015

Citation Eyer L, Valdés JJ, Gil VA, Nencka R, Hřebabecký H, Šála M, Salát J, Černý J, Palus M, De Clercq E, Růžek D. 2015. Nucleoside inhibitors of tick-borne encephalitis virus. *Antimicrob Agents Chemother* 59:5483–5493. doi:10.1128/AAC.00807-15.

Address correspondence to Daniel Růžek, ruzekd@paru.cas.cz.

Supplemental material for this article may be found at <http://dx.doi.org/10.1128/AAC.00807-15>.

Copyright © 2015, American Society for Microbiology. All Rights Reserved.

doi:10.1128/AAC.00807-15

In the present study, a series of nucleoside analogues were tested for the ability to inhibit TBEV replication in cell culture. Particular attention was paid to chemically modified nucleosides that have reported antiviral activity against other flaviviruses, especially HCV (14) or hemorrhagic fever-associated flaviviruses (i.e., Alkhurma hemorrhagic fever virus, Omsk hemorrhagic fever virus, and Kyasanur Forest disease virus) (29). Compounds with favorable inhibitory profiles in the virus titer reduction assays were further assayed for the ability to inhibit virus-induced cytopathic effects and to suppress viral antigen expression in infected cell cultures. The lead compounds were subsequently evaluated for dose-response inhibition of TBEV replication and for potential cytotoxic effects on host cells. Based on these screens, we identified three compounds with strong anti-TBEV activity. The favorable characteristics of one of these compounds, 7-deaza-2'-C-methyladenosine (7-deaza-2'-CMA), indicate that it merits further investigation as a therapeutic agent for treating TBEV infections.

MATERIALS AND METHODS

Cell cultures, virus strains, and antiviral compounds. Porcine kidney stable (PS) cells were cultured at 37°C in Leibovitz (L-15) medium supplemented with 3% precolostral calf serum and a 1% mixture of penicillin and glutamine (Sigma-Aldrich, Prague, Czech Republic) (30). Human neuroblastoma UKF-NB-4 cells were cultured at 37°C in 5% CO₂ in Iscove's modified Dulbecco's medium (IMDM) supplemented with 10% fetal bovine serum and a 1% mixture of penicillin and streptomycin (Sigma-Aldrich) (31). All experiments were performed with TBEV strains Hypr and Neudoerfl, which are representatives of the West European TBEV subtype. Ribavirin and 2'-C-methyladenosine (2'-CMA) were synthesized at the Institute of Organic Chemistry and Biochemistry (Prague, Czech Republic). 7-deaza-2'-C-methyladenosine (7-deaza-2'-CMA), 2'-C-methylcytidine (2'-CMC), and 6-azauridine were purchased from Carbosynth (Compton, United Kingdom). Mericitabine was purchased from ChemScene (Monmouth Junction, NJ). The test compounds were solubilized in 100% (vol/vol) dimethyl sulfoxide (DMSO) to yield 10 mM stock solutions.

Viral titer reduction assay. PS or UKF-NB-4 cells were seeded in 96-well plates (approximately 2×10^5 cells per well) and incubated for 24 h to form a confluent monolayer. Following incubation, the medium was aspirated from the wells and replaced with 200 μ l of fresh medium containing a 50 μ M concentration of the test compound (three wells per compound). The cells were immediately infected with the Hypr or Neudoerfl TBEV strain at a multiplicity of infection (MOI) of 0.1. As a negative control, DMSO was added to virus- and mock-infected cells at a final concentration of 0.5% (vol/vol). After 72 h of incubation, the medium was collected and immediately frozen at -80°C . Viral titers were determined by plaque assay.

Plaque assay. Virus titers were assayed using PS cell monolayers as described previously (32). Briefly, 10-fold dilutions of TBEV were prepared in 24-well tissue culture plates, and PS cells were added in suspension (0.6×10^5 to 1.5×10^5 cells per well). After a 4-h incubation, the suspension was overlaid with 1.5% (wt/vol) carboxymethylcellulose in L-15 medium. Following a 5-day incubation at 37°C, the infected plates were washed with phosphate-buffered saline (PBS) and the cell monolayers were stained with naphthalene black. The virus titer was expressed as PFU per milliliter.

CPE inhibition assay and CPE quantification. The PS cells were seeded in 96-well plates, the test compounds were added, and the cells were infected with TBEV as described for the viral titer reduction assay. Culture medium was collected 3 to 4 days postinfection (p.i.) to yield a 40 to 50% cytopathic effect (CPE) in virus control wells. The CPE was monitored visually using an Olympus BX-5 microscope equipped with an Olympus DP-70 charge-coupled-device (CCD) camera. To quantify the

CPE, both cell death and viability were determined using commercially available colorimetric *in vitro* assays. Cell death was evaluated using the CytoTox 96 nonradioactive cytotoxicity assay (Promega, WI) by following the manufacturer's instructions. This assay is based on quantitative measurement of lactate dehydrogenase, a stable cytosolic enzyme that is released upon cell lysis. Cell death was estimated as the percentage of colorimetric absorbance at 490 nm by the compound-treated cells relative to the absorbance by chemically lysed cells. Cell viability was evaluated by determining formazan exclusion in confluent cell cultures in a colorimetric assay utilizing Dojindo's highly water-soluble tetrazolium salt (Cell Counting Kit-8; Dojindo Molecular Technologies, MD). Cell viability was expressed as the percentage of absorbance at 450 nm by compound-treated cells relative to the absorbance by DMSO-treated cells.

Immunofluorescence staining. PS cells were cultured on slides treated with the test compound (0 to 50 μ M) and infected with the TBEV Hypr strain at an MOI of 0.1. At day 4 postinfection, the cells were subjected to cold acetone-methanol (1:1) fixation for 10 min, rinsed in saline, and blocked with 10% fetal bovine serum. Cells were labeled with a mouse monoclonal antibody that recognizes the flavivirus group surface antigen (1:250; Sigma-Aldrich, Prague, Czech Republic) by incubation for 1 h at 37°C. After a washing with saline-Tween 20 (0.05% [vol/vol]), the cells were labeled with an anti-mouse goat secondary antibody conjugated with fluorescein isothiocyanate (FITC) (1:500) by incubation for 1 h at 37°C. The cells were counterstained with 4',6-diamidino-2-phenylindole (DAPI) (1 μ g ml⁻¹; Sigma-Aldrich) for 30 min at 37°C and mounted in 2.5% 1,4-diazabicyclo[2.2.2]octane (DABCO; Sigma-Aldrich). The images were acquired with an Olympus IX71 epifluorescence microscope equipped with a Hammamatsu OrcaR2 camera and controlled using Xcellence software. The images were processed using Fiji software (33).

Cytotoxicity assays. PS cell monolayers in 96-well plates were treated with test compounds at a concentration range of 0 to 50 μ M (2-fold dilutions, three wells per concentration). At 4 days p.i., the potential cytotoxicity of test compounds was determined in terms of cell viability and death using Cell Counting Kit-8 (Dojindo Molecular Technologies) and the CytoTox 96 nonradioactive cytotoxicity assay (Promega, WI), respectively, as described for CPE quantification. The concentration of compound that reduced cell viability by 50% was considered the 50% cytotoxic concentration (CC₅₀).

Dose-response studies with 2'-CMA, 7-deaza-2'-CMA, and 2'-CMC. PS cell monolayers that were cultured for 24 h in 96-well plates were treated with 200 μ l of medium containing the test compounds (2'-CMA, 7-deaza-2'-CMA, and 2'-CMC) at concentrations from 0 to 50 μ M (2-fold dilution, three wells per concentration) and infected with the TBEV Hypr strain at an MOI of 0.1. The medium was collected from the wells at 1-day intervals (postinfection days 1 to 6), and the viral titers were determined by plaque assays. The obtained virus titers were utilized to construct TBEV growth curves and dose-response curves for selected nucleoside inhibitors. The dose-response curves on postinfection days 3 and 4 were used to estimate the most widely used measures of drug potency: the 50% effective concentration (EC₅₀), the concentration of compound required to inhibit the viral titer by 50% compared to the control value), the selectivity index (SI = CC₅₀/EC₅₀), and the slope value (Hill coefficient). The EC₅₀s were calculated as follows: a dose-response inhibition curve was fitted to a four parameter logistic curve using Prism 5.04 software (GraphPad, Inc., CA) according to the equation $Y = \text{Bottom} + (\text{Top} - \text{Bottom}) / [1 + 10^{\text{Hill coefficient}(\log \text{EC}_{50} - X)}]$. In this equation, X is the logarithm of the concentration, Y is the logarithm of the titer, bottom and top correspond to the asymptotes of the sigmoidal curve, Hill coefficient corresponds to the slope at the inflection point of the curve, and log EC₅₀ is the calculated midpoint of the curve. The EC₅₀ was calculated as $10^{\log \text{EC}_{50}}$. The standard errors of the EC₅₀s were estimated by the delta method.

Computer-aided protein modeling and preparation, and protein-ligand exploration and clustering. The crystal structures of viral polymerases from HCV (PDB codes 1nb4 and 1nb6), WNV (PDB code 2hfz),

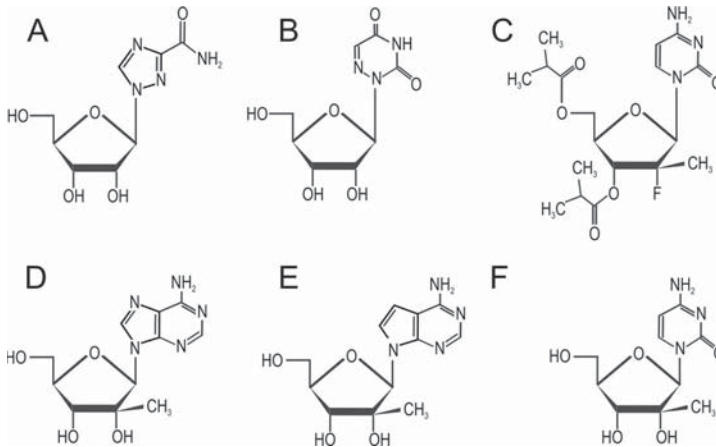


FIG 1 The structures of the nucleoside analogues tested in this study. (A) Ribavirin; (B) 6-azauridine; (C) mercitabine; (D) 2'-CMA; (E) 7-deaza-2'-CMA; (F) 2'-CMC.

and JEV (PDB code 4k6m) were used for computer simulations that would complement the experimental results from this study. The TBEV structure was modeled using Modeler (34). The models were evaluated using the protein model-qualifying servers ModFOLD, QMEAN, and RESPROX (35–37). Based on a consensus, the best-ranked TBEV model was then selected for subsequent *in silico* experiments. Since X-ray crystallography methods do not resolve hydrogen atoms, Schrödinger's Maestro Protein Preparation Wizard was used for each viral polymerase structure to assign hydrogen atoms and to optimize the assigned hydrogen-bond network (38). The respective ligands for each protein structure were removed prior to preparation. After protein preparation, an energy minimization (using the default conditions in Schrödinger's Maestro package) (39) was performed for each crystal structure, including the modeled TBEV polymerase structure, to alter the initial conformation and to remove any steric clashes prior to simulations. In addition, the HCV-UTP bound structure (PDB code 1nb6) has two Mn^{2+} ions as co-factors, with several water molecules surrounding the nucleoside. These were also added to all structures and remained constrained for all subsequent simulations.

We used the Protein Energy Landscape Explorer (PELE) algorithm to perform protein-ligand simulations of the three nucleoside triphosphate analogues identified in this study and the aforementioned viral polymerases. For the simulations, we used the triphosphate form of the nucleoside analogues (2'-CMA-TP, 2'-CMC-TP, and 7-deaza-2'-CMA-TP) since they are phosphorylated *in vivo*. A detailed explanation of the PELE algorithm can be found in references (40 and 41), and its many uses can be seen at <https://pele.bsc.es/>. Briefly, PELE performs three steps. First, localized ligand perturbations and protein perturbations are performed using an anisotropic network model (ANM) (42) to move the alpha-carbon backbone toward a new position after minimization. Second, PELE optimizes amino acid side chains in proximity of the ligand using steric filters and a rotamer library (43). Finally, PELE uses a truncated Newton minimizer and a surface generalized implicit solvent for minimization, achieving a local minimum after the initial perturbation (44). These steps are repeated for a desired number of iterations and are performed in parallel using several computer-processing units (CPUs). The output is a series of trajectories that represent conformational changes of the side chains and ligand exploration. A Monte Carlo Metropolis criterion is implemented in the PELE algorithm that accepts or rejects these trajectories based on their calculated energies: if they are equal to or less than (accepts) or greater

than (rejects) the initial calculated energy (45). To calculate the energy, the PELE algorithm uses a standard force field that describes the potential energy of a molecular system, known as optimized potentials for liquid simulations (OPLS-2005) (46). The only parameters that were altered from the unconstrained ligand migration ready-made script provided by the PELE server were the ANM type, which was set to 4, and the addition of ANM mode 6 for favorable protein perturbations. The number of iterations was increased to 2,000 for increased sampling.

Cluster analysis was performed for the TBEV PELE simulations using pyProCT (47), a Python cluster analysis tool specifically adapted for biomolecules. Regular cluster analysis methods require a deep understanding of the data set and the algorithm. In addition, these methods are sensitive to small changes in its parameters. Instead of forcing users to perform a blind analysis, pyProCT implements a hypothesis-driven protocol. First, the user employs domain knowledge to characterize the desired result in terms of measurable clustering attributes (e.g., maximum and minimum number of clusters, size, noise, cluster separation, etc.) Second, the software searches the clustering space to obtain the clusters that best fit the hypothesis. The same script was used for each nucleoside triphosphate analogue in the PELE protein-ligand exploration simulations of the TBEV-modeled polymerase. The script instructs pyProCT to calculate the distances of each nucleoside using (i) an iterative superposition of the protein backbone and (ii) the calculated distances between the heavy atoms and the geometrical center of the ligand. The K-medoids, DBSCAN, spectral clustering, hierarchical (single-linkage), and GROMOS clustering algorithms were used, with up to 50 parameterizations for each one. The allowed clusterings had to have 3 to 20 clusters with a minimum of 300 elements. No more than 20% of the elements could be tagged as noise. The evaluation function that chose the best clustering was a combination of the silhouette index and a naive cohesion measure. This choice of evaluation functions favors results in which the clusters are well separated with a special emphasis on their compactness. Finally, the "atomic_distances" postprocessing option was used in order to obtain a human-readable file with the per-element distances between serine 331 (Ser331) of the TBEV modeled polymerase and the ligand as well as the per-cluster statistics.

RESULTS

Inhibition of TBEV growth, TBEV-induced CPE, and viral antigen expression. Six nucleoside analogues with chemical modifi-

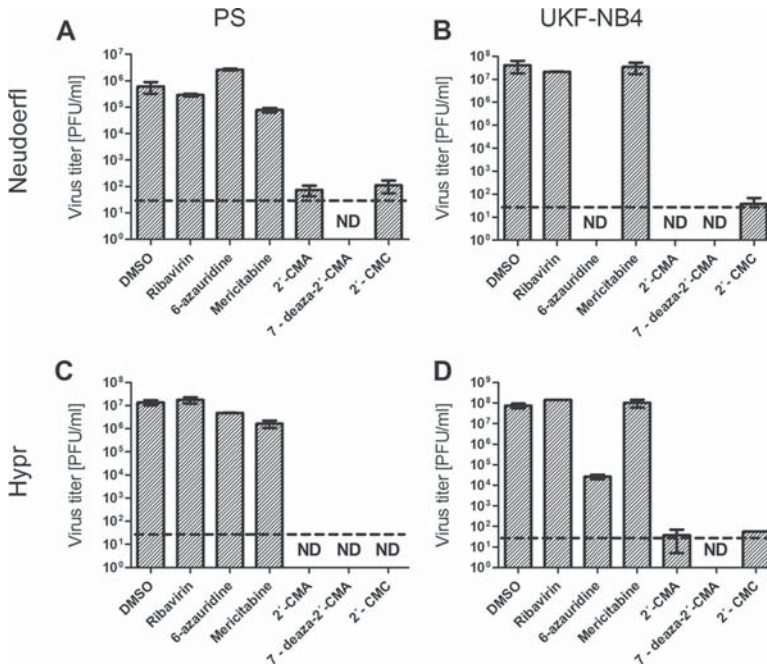


FIG 2 Reduction of TBEV titers by the indicated nucleoside analogues. PS or UKF-NB-4 cells were infected with TBEV (Hypr or Neudoerfl strain) at a multiplicity of infection of 0.1 and treated with nucleoside analogues at 50 μ M. The TBEV titers were determined by the plaque assay 3 days postinfection. DMSO-treated cells were used as a negative control. Bars show the mean values from three biological replicate wells, and the error bars indicate the standard errors of the means ($n = 3$). ND, not detected (below the detection limit). Horizontal dashed lines indicate the minimum detectable threshold of 1.44 \log_{10} PFU ml^{-1} .

cations of the ribose or purine/pyrimidine moiety (Fig. 1) were tested for the ability to inhibit the growth of the Hypr and Neudoerfl TBEV strains *in vitro* in PS cells and human neuroblastoma cells. The compounds were tested at a concentration of 50 μ M, and the inhibition of TBEV growth was investigated in the culture supernatants 3 days p.i. using a plaque assay.

The Hypr and Neudoerfl TBEV strains (MOI of 0.1) reached mean peak titers of 10^7 and 10^6 PFU/ml, respectively, in PS cells at 3 days p.i. In human neuroblastoma cells, both TBEV strains reached a viral titer of approximately 10^8 PFU/ml at 3 days p.i. Three of the nucleoside analogues tested, 7-deaza-2'-CMA, 2'-CMA, and 2'-CMC, inhibited the growth of both TBEV strains in PS cells and in human neuroblastoma cells. In PS cells, treatment with 50 μ M each compound reduced virus titers 10^4 - to 10^7 -fold compared to that in a mock-treated culture (Fig. 2A and B). Even greater viral titer reduction (10^6 - to 10^8 -fold) was observed in TBEV-infected human neuroblastoma cells (Fig. 2C and D).

Ribavirin and mericitabine showed weak or no anti-TBEV effects in PS cells and human neuroblastoma cells. 6-Azauridine showed no antiviral effect in PS cells; however, this compound significantly reduced the viral titer (10^3 -fold for Hypr and 10^6 -fold for Neudoerfl) in human neuroblastoma cells (Fig. 2B and D).

To verify the primary screening results, we next investigated the compounds using the CPE inhibition assay. Inhibition of TBEV-induced CPE in PS cells in the presence of the test com-

pounds was monitored using light microscopy 3 to 4 days p.i. The TBEV Hypr strain had a strong CPE on the target PS cells on day 3 p.i. in the absence of nucleoside inhibitors (Fig. 3A). A strong CPE was also observed in PS cell cultures treated with ribavirin (Fig. 3A), mericitabine, and 6-azauridine (see Fig. S1B and C in the supplemental material), indicating that these compounds had no protective effects on the survival and growth of PS cells exposed to TBEV. 6-Azauridine was highly cytotoxic, causing cell death and morphological changes in PS cells. Both adenosine derivatives, i.e., 7-deaza-2'-CMA and 2'-CMA, completely inhibited the CPE at concentrations of 50 μ M and had no adverse morphological effects on growing cells. However, a relatively strong CPE was observed in 2'-CMC-treated PS cell monolayers (Fig. 3A).

The CPE of 7-deaza-2'-CMA, 2'-CMA, and 2'-CMC on TBEV-infected PS cells was evaluated quantitatively in terms of cell viability and death using two independent colorimetric *in vitro* assays. Mock-treated TBEV-infected PS cells showed a high rate of cell death, i.e., 46% dead cells, at day 4 p.i. (Fig. 3B; see Fig. S2 in the supplemental material). TBEV-infected PS cells treated with either 7-deaza-2'-CMA or 2'-CMA showed a low rate of cell death (11 to 15%) and high viability (95 to 105%). The measured values were close to the cell death and viability values determined for mock-treated uninfected PS cells (11% and 100%, respectively) that were used as negative controls (Fig. 3B; see also Fig. S2 in the supplemental material). The results strongly indicate that

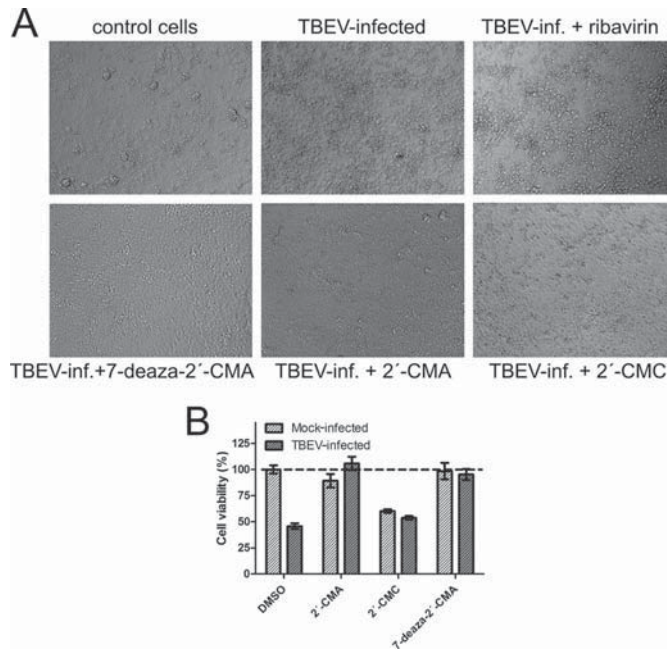


FIG 3 Inhibition of the TBEV-induced cytopathic effect by the indicated nucleoside analogues. PS cells were infected with TBEV strain Hypr at a multiplicity of infection of 0.1 and were left untreated (DMSO) or treated with 50 μ M ribavirin, 7-deaza-2'-CMA, 2'-CMA, or 2'-CMC. Inhibition of the CPE was monitored on day 3 or 4 postinfection (A). (B) Quantification of the CPE in TBEV-infected and mock-infected cells treated with 50 μ M 2'-CMA, 2'-CMC, or 7-deaza-2'-CMC. The CPE was expressed as the percentage of cell viability at day 4 postinfection. The horizontal dashed line indicates cell viability and cell death in DMSO-treated uninfected cells (control). The bars indicate the means, and error bars indicate SEMs ($n = 3$).

7-deaza-2'-CMA and 2'-CMA at concentrations of 50 μ M completely protected PS cells from TBEV, allowing them to survive in the presence of TBEV with no apparent cytotoxicity. For 2'-CMC, development of the CPE was marked by increased cell death (26 to 28%) and decreased cell viability (54 to 60%) (Fig. 3B; see also Fig. S2).

The antiviral effect of 7-deaza-2'-CMA, 2'-CMA and 2'-CMC was further confirmed by immunofluorescence staining, which was used to assess the expression of the TBEV surface E antigen in PS cells as an index of viral infectivity and replication *in vitro*. The TBEV surface E antigen was strongly expressed in TBEV-infected mock-treated cells (Fig. 4), and no virus antigen was detected in mock-infected PS cells (data not shown). Immunofluorescence staining revealed that 7-deaza-2'-CMA, 2'-CMA, and 2'-CMC at concentrations of 50 μ M completely inhibited the expression of the TBEV surface E antigen in virus-infected PS cells (Fig. 4). These results correlated with the strong suppression of TBEV growth in the 7-deaza-2'-CMA-, 2'-CMA-, and 2'-CMC-treated cell cultures (Fig. 2A and C).

Cytotoxicities of TBEV inhibitors. The cytotoxicities of 7-deaza-2'-CMA, 2'-CMA, and 2'-CMC were evaluated in PS cells using a cell viability assay (Fig. 5) and subsequently confirmed by a cell death assay (see Fig. S3 in the supplemental material). No cellular toxicity was seen in cultures of PS cells treated with 7-deaza-2'-CMA at concentrations ranging from 0 to 50 μ M ($CC_{50} > 50 \mu$ M) 4 days posttreatment (Fig. 5C and Table 1; see

also Fig. S3C). A cell viability assay showed similar results with 2'-CMA ($CC_{50} > 50 \mu$ M). However, 50 μ M 2'-CMA moderately increased cell death, by \sim 22%, at 4 days after drug administration (Fig. 5A and Table 1; see also Fig. S3A) compared to the rate for mock-treated cells (\sim 15%). For both adenosine derivatives, the concentration of 50 μ M had no detectable effect on cell proliferation. 2'-CMC showed a dose-dependent cytotoxic effect on PS cell cultures 4 days posttreatment. Based on a cell viability assay, the CC_{50} of 2'-CMC was determined to be \sim 50 μ M (Fig. 5B and Table 1; see also Fig. S3B).

Dose-response antiviral activities of the TBEV inhibitors.

The compounds that showed TBEV inhibitory effects in the initial experiments, i.e., 7-deaza-2'-CMA, 2'-CMA, and 2'-CMC, were further evaluated to determine their dose-dependent antiviral activities. PS cells were infected with the Hypr strain (MOI of 0.1) and immediately treated with each compound at a concentration range of 0 to 50 μ M. The culture supernatants were then subjected to the plaque assay. TBEV titers in the culture supernatants were assayed daily on days 1 to 6 p.i. The dose-response curves on postinfection days 3 and 4 were used to estimate the EC_{50} , SI, and slope value.

All three compounds reduced the viral titer in a dose-dependent manner (Fig. 6; see also Fig. S4 in the supplemental material). The shape of the dose-response curves for 7-deaza-2'-CMA changed over time from a flat curve on day 1 p.i. to typical sigmoidal curves with relatively steep slopes on days 2 to 6 p.i. (Fig. 6A).

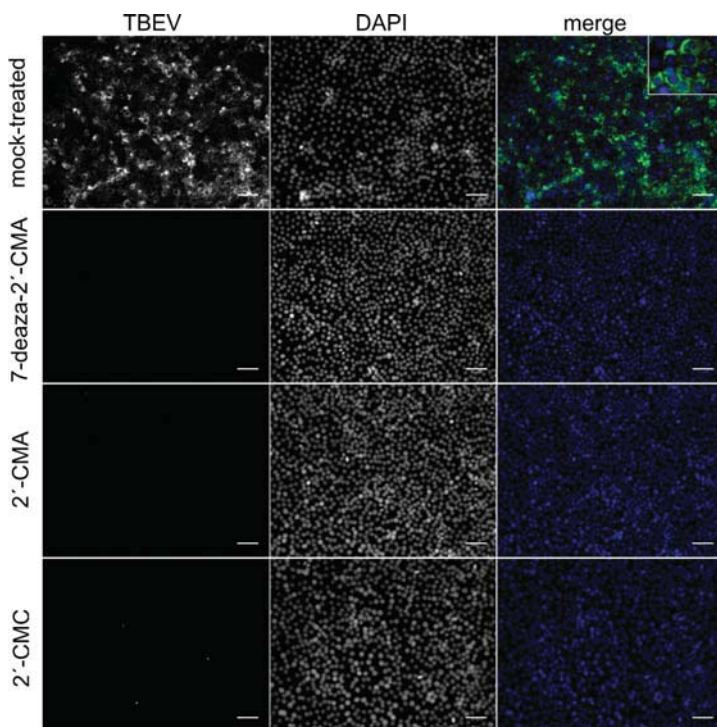


FIG 4 Inhibition of TBEV viral antigen expression by the indicated nucleoside inhibitors. PS cells were infected with TBEV and treated with 0.5% DMSO or with 50 μM 7-deaza-2'-CMA, 2'-CMA, or 2'-CMC. PS cells were fixed on slides at day 4 postinfection and stained with flavivirus-specific antibody labeled with FITC (green) and then counterstained with DAPI (blue). Scale bars, 50 μm .

7-Deaza-2'-CMA reduced the viral titer, showing an EC_{50} of $5.1 \pm 0.4 \mu\text{M}$ and a selectivity index (SI) of >9.8 (Table 1). 7-Deaza-2'-CMA was ineffective in terms of reducing the viral titer at concentrations of 0.1 and 0.5 μM , and the TBEV growth curves were indistinguishable from the TBEV growth curve for mock-treated cells (see Fig. S4A). At a concentration of 3.1 μM , the TBEV inhibitory effect of 7-deaza-2'-CMA became more evident, resulting in $\sim 10^2$ -fold reduction in the titer relative to that in mock-treated cells. Marked inhibitory effects on TBEV replication were observed at concentrations of 7-deaza-2'-CMA at or above 6.2 μM . When the compound was added at concentrations of 12.5, 25, and 50 μM , there was a significant and steady reduction in viral titer (a 10^6 - to 10^7 -fold reduction). At these concentrations, 7-deaza-2'-CMA reduced the mean TBEV titers to below the limit of detection ($1.44 \log_{10}$ PFU ml^{-1}) between p.i. days 4 and 6.

A cytidine derivative, 2'-CMC, also showed marked dose-dependent inhibition of TBEV titers. The shape and particularly the slope of the 2'-CMC dose-response curve were similar to those of 7-deaza-2'-CMA (Fig. 6B). However, 2'-CMC was approximately 3-fold less potent in terms of inhibiting TBEV than was 7-deaza-2'-CMA (EC_{50} of $14.2 \pm 1.9 \mu\text{M}$) (Table 1). The relatively low SI value of ~ 3.5 was due to the considerable cytotoxicity of the compound for PS cells, as described above. At 0.1, 0.5, and 3.1 μM , 2'-CMC inhibited virus replication weakly or not at all. The in-

hibitory effects of 2'-CMC became more evident at concentrations of 6.2 to 12.5 μM , with virus titer reduction of about 10^2 at 6 days p.i. 2'-CMC completely suppressed TBEV replication at concentrations of 25 and 50 μM ; there was a 10^4 - to 10^6 -fold reduction in viral titer during the experimental period (see Fig. S4B in the supplemental material).

2'-CMA showed a significant dose-dependent antiviral effect only at day 3 p.i. (Fig. 6C). The 2'-CMA dose-response curve was characterized by an EC_{50} of $7.1 \pm 1.2 \mu\text{M}$ (SI of about 7) and by a relatively low Hill coefficient (0.7 for 2'-CMA versus 2.7 for 7-deaza-2'-CMA and 2.2 for 2'-CMC [Table 1]). At day 3 p.i., 2'-CMA strongly reduced TBEV titers at concentrations of 20 and 50 μM , resulting in $>10^5$ -fold viral titer inhibition relative to that in mock-treated TBEV-infected cells. Although the initial decrease in viral titers was very strong, the inhibitory effects of 2'-CMA diminished gradually after day 3 p.i., regardless of concentration. The decrease in the antiviral effect of 2'-CMA over time allowed the virus titers in 50 μM 2'-CMA-treated cells to rebound to 1.7×10^6 PFU/ml at day 6 p.i. (see Fig. S4C).

Exploration of NS5B with nucleoside analogues using PELE. Selection and characterization of drug-resistant HCV replicons revealed that serine 282 (Ser282) determines the efficacy of the inhibitory nucleoside 2'-CMA (13). Figure S5 in the supplemental material illustrates the proof of principle for our PELE-based ex-

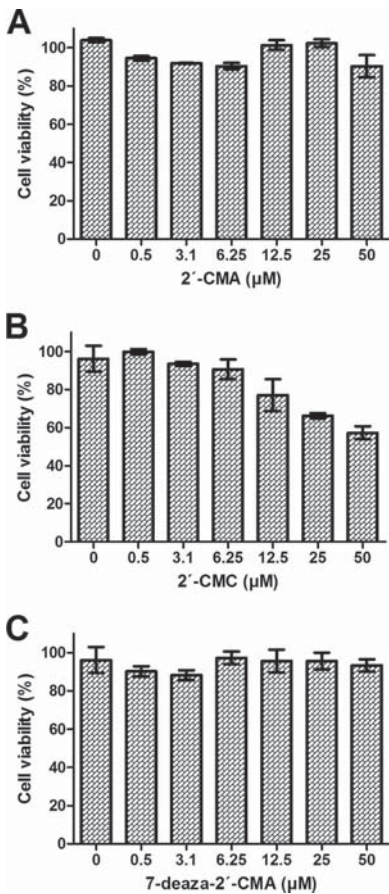


FIG 5 Cytotoxicity of the indicated nucleoside inhibitors. Cytotoxicity was determined by incubating PS cells with the indicated concentrations of 2'-CMA (A), 2'-CMC (B), or 7-deaza-2'-CMA (C) and is expressed in terms of cell viability and cell death at day 4 postinfection. The bars indicate the mean values from three replicate wells, and the error bars indicate the SEMs.

ploration of nucleoside triphosphate analogues with viral polymerases. In the bound crystal structure of HCV (PDB code 1nb6), the distance between the alpha carbon of Ser282 and the geometric center of the heavy atoms of UTP is 9.3 Å as measured using the Maestro package (39). Figure S5 shows that for the most part, UTP explores ~20 to 70 Å away from the Ser282 in both the bound and unbound (or apoenzyme) crystal structures of the HCV polymerase. In both cases, however, there was UTP exploration <20 Å away from the Ser282 (encircled in Fig. S5), and this separate cluster approaches the native position of the bound HCV-UTP complex (*y* axes in Fig. S5; i.e., the geometric center position of all heavy atoms of UTP in PDB code 1nb6).

To further validate the results of the nucleoside triphosphate analogue exploration, we simulated the experimental results reported by Migliaccio et al. (13), who investigated the inhibitory

effect of 2'-CMA using HCV and other phylogenetically related viruses *in vitro*. Figure S6A in the supplemental material shows the exploration of 2'-CMA-triphosphate (2'-CMA-TP) in proximity to the homologous serine residue of the viral polymerases of the HCV (PDB code 1nb6), WNV (PDB code 2hfh), and JEV (PDB code 4k6m) crystal structures. This analysis showed that 2'-CMA-TP spent the majority of the exploration away from the homologous serine residue. Further investigation of whether 2'-CMA is an effective inhibitor of JEV is needed since no such experiments have been reported. Figure S6B shows that the three effective nucleoside triphosphate analogues used in the current study, i.e., 2'-CMA-TP, 2'-CMC-TP, and 7-deaza-2'-CMA-TP, also explored in proximity to the Ser331 of the modeled tertiary structure of TBEV NS5B (the residue homologous to HCV Ser282).

The results from the clustering analysis are summarized in Table S1 in the supplemental material. Visual inspection of all three nucleoside triphosphate analogue clusters for the TBEV polymerase showed two types of clusters. The first type was generated by a partition of the space sampled in the exploration of each nucleoside. Since this zone was densely populated, it was difficult to find a good balance between cluster compactness and separation (which would penalize the silhouette index). The second type of cluster had better-defined boundaries since these clusters formed "natural" aggregates that were created as the nucleoside explored the protein surface in proximity to Ser331 of the TBEV polymerase. From this second group or second type of cluster, we selected those that were <18 Å from the alpha carbon of Ser331 (green areas in Fig. 7A). The logic behind this cutoff criterion is depicted graphically in Fig. S5 in the supplemental material, i.e., the encircled cluster. During the exploration of the HCV polymerase, UTP approaches the binding site (*y* axes in Fig. S5; 2 to 12 Å from its native position) as it "cuts off" from the majority of the modeling for exploration (18 to 20 Å from Ser282; *x* axes in Fig. S5).

All three simulations showed a large cluster (colored the same shade of green in Fig. 7B) with more than half of its elements in proximity to Ser 331 (especially for 7-deaza-2'-CMA-TP). For 2'-CMA-TP and 2'-CMC-TP, there were elements of other clusters (colored different shades of green in Fig. 7B) that also seemed to be in proximity to Ser331 of the TBEV polymerase. Assuming that phylogenetically related viral polymerases have similar binding sites, we used the central position of UTP bound to HCV (PDB code 1nb6) to geometrically determine the pathway toward the predicted binding site of TBEV. The scatter plots in Fig. 7C show that the majority of modeling for the exploration is away from Ser331 (i.e., the first type of cluster; >20 Å). Each scatter plot, however, has a linear correlation (r^2) of >0.9, approaching the predicted binding site of the TBEV polymerase, which is clearly shown by the large single cluster of 7-deaza-2'-CMA-TP (Fig. 7).

TABLE 1 Characteristics of selected TBEV-inhibiting nucleosides

Compound	EC ₅₀ ^a μM ^a	Hill coefficient ^a	CC ₅₀ μM ^a (viability assay)	SI (CC ₅₀ /EC ₅₀)
7-deaza-2'-CMA	5.1 ± 0.4	2.7 ± 0.5	>50	>9.8
2'-CMA	7.1 ± 1.2	0.7 ± 0.1	>50	>7.0
2'-CMC	14.2 ± 1.9	2.2 ± 0.5	~50	~3.5

^a Determined from three independent experiments.

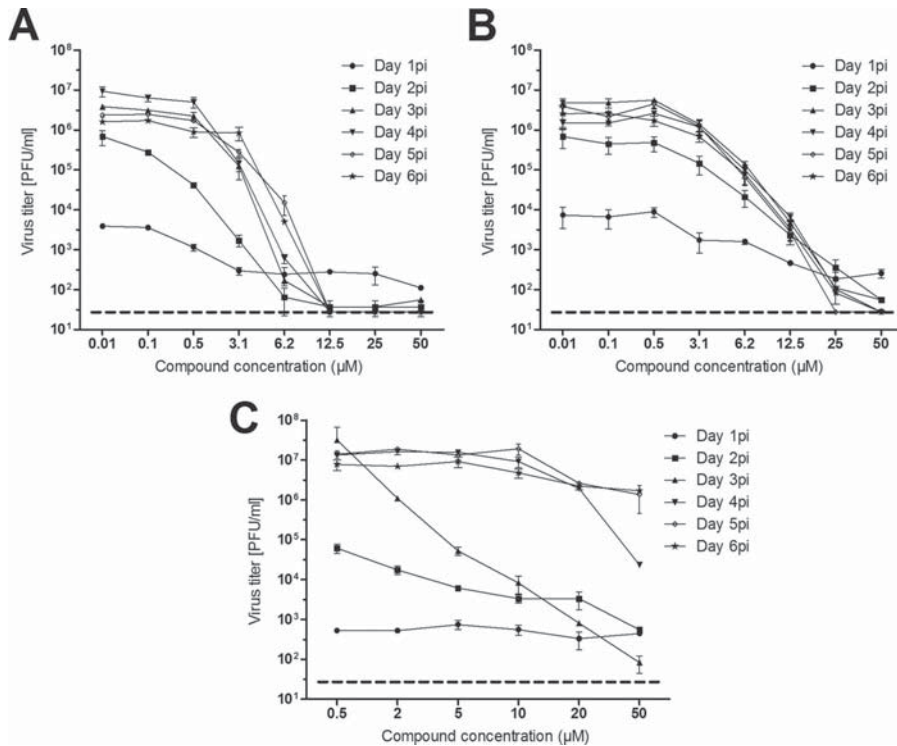


FIG 6 Dose-dependent effect of the indicated TBEV inhibitors on virus titers. PS cells were infected with TBEV at a multiplicity of infection of 0.1 and treated with 7-deaza-2'-CMA (A), 2'-CMC (B), or 2'-CMA (C) at the indicated concentrations. TBEV titers were monitored at days 1 to 6 postinfection. The mean titers from three biological replicates are shown, and error bars indicate SEMs ($n = 3$). The horizontal dashed line indicates the minimum detectable threshold of $1.44 \log_{10} \text{PFU ml}^{-1}$.

DISCUSSION

TBE is a substantial public health problem in some parts of Europe and Asia. At present, there is no specific treatment for TBE other than supportive care. Few studies have tested potential TBEV inhibitors (48), and there is an urgent need for safe, efficient drugs for treating patients with TBE. In this study, a series of nucleoside analogues that were previously reported to inhibit members of the *Flaviviridae* family were tested for the ability to suppress TBEV replication. We could not determine the structure-activity relationship for all of the compounds in this study, although this will be the subject of a future investigation.

The anti-TBEV activity of the compounds was determined in PS cells and in human neuroblastoma cells. PS cells are widely used for TBEV isolation and for multiplication and plaque assays (30). Human neuroblastoma cells are highly sensitive to TBEV infection and represent a valuable model for neuropathogenesis studies of TBEV as well as for studies of several other neurotropic viruses (31). The initial screening was performed using two TBEV strains, Neudoerfl and Hypr, which represent two virulence models. Neudoerfl, the European prototype TBEV strain, exhibits medium virulence, while the Hypr strain is highly virulent (49). Although ribavirin, 6-azauridine, and mericitabine

have been described as potent inhibitors of several flaviviruses (29, 41, 50), these compounds did not reproducibly inhibit TBEV *in vitro* at concentrations of 50 µM. 6-Azauridine has been reported in the literature to be relatively well tolerated by several host cell lines as well as being well tolerated *in vivo* (29). However, in our experiments, this compound had a strong cytotoxic effect on both PS cells (see Fig. S1C in the supplemental material) and human neuroblastoma cells (data not shown), resulting in significantly reduced viral titers in 6-azauridine-treated human neuroblasts (Fig. 2B and D).

Three 2'-C-methyl-substituted nucleosides, 2'-CMC, 2'-CMA, and 7-deaza-2'-CMA, strongly inhibited the *in vitro* growth of TBEV in both cell lines and were selected as lead candidate compounds for further testing. 2'-CMC was recently tested for its ability to inhibit replication of yellow fever virus (23), Alkhurma hemorrhagic fever virus, Kyasanur Forest disease virus, and Omsk hemorrhagic fever virus (29). Moreover, the 3'-valyl ester of 2'-CMC, valopicitabine, showed viral load reductions in patients infected with genotype 1 HCV in clinical trials, although it was subsequently discontinued for the treatment of hepatitis C (55, 56). Our results indicate that 2'-CMC had strong antiviral activity against both the Hypr and Neudoerfl TBEV strains; however, this

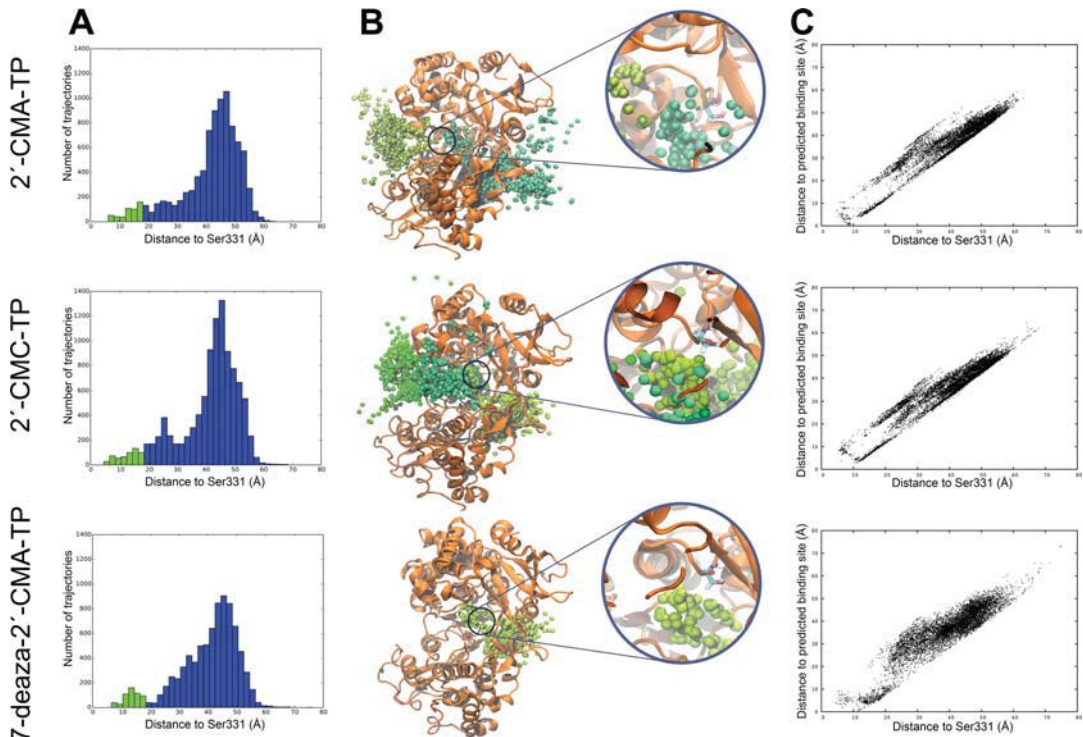


FIG 7 Cluster analyses of nucleoside triphosphate analogue exploration of the TBEV polymerase. (A) The distance for each of the studied nucleoside triphosphate analogues (2'-CMA-TP, 2'-CMC-TP, and 7-deaza-2'-CMA-TP) are shown in the histograms. The 0- to 18-Å range, which denotes the proximity toward Ser331 (x axes), is colored light green. (B) Tertiary representations of the selected clusters for each system. Each nucleoside is represented by its C-7 atom. (C) Scatter plots depict the approach of each nucleoside toward the predicted binding site of TBEV.

compound was cytotoxic for PS cells (CC_{50} of about $50 \mu\text{M}$). The substitution of cytosine for adenine in 2'-CMA, a compound that has recently been used for experimental therapy of HCV and DENV infections (18, 51), significantly reduced the cytotoxicity for both cell lines and increased the anti-TBEV inhibitory effect of the compound. However, viral replication gradually rebounded after 3 days in the treated cultures (Fig. 6C). The observed decrease in antiviral activity of 2'-CMA and the rebound in viral titer were probably related to the rapid deamination of 2'-CMA by cellular adenosine deaminase to the inactive inosine derivative (52). Such an intracellular deamination is described as an undesirable effect in the inhibitory activity of 2'-CMA against HCV replication, resulting in poor bioavailability and rapid clearance of 2'-CMA in plasma (14). 2'-CMA could be also inactivated by cellular phosphorylases, which are enzymes that catalyze phosphorylase of the purine glycosidic bond (12). Alternatively, the evolution of 2'-CMA-resistant TBEV mutants could explain the observed viral titer rebound (53).

The incorporation of the 7-deaza moiety into the 2'-CMA molecule eliminated cytotoxicity in both PS cells and human neuroblastoma cells. The potency of 7-deaza-2'-CMA to inhibit TBEV replication was comparable to that of 2'-CMA and was

approximately 3-fold higher than that of 2'-CMC. The inhibitory effect of 7-deaza-2'-CMA was stable over the 6-day experimental period, and there was no rebound in viral titer during this period. The 7-deaza-purine substitution is described as an important modification of the nucleobase that strongly affects the biological properties of the nucleoside analogue. The 7-deaza modification alters the glycosyl torsion angle, which may change the glycosyl bond length. This could lead to a rearrangement in the general electronic character of the purine base and, in particular, to disruption of the alignment of the 3'-hydroxyl function for nucleophilic attack on the alpha phosphorus of the next incoming NTP. The 7-deaza modification may, therefore, result in enhanced potency of the nucleoside analogue in terms of terminating viral RNA synthesis (9, 14). Due to the antiviral activity and low cytotoxicity of 7-deaza-2'-CMA, this nucleoside derivative has been widely tested to determine whether it inhibits the RNA replication of other medically important flaviviruses. For example, 7-deaza-2'-CMA inhibits HCV replication with an EC_{50} of $0.3 \mu\text{M}$ with no apparent cytotoxicity and shows promising pharmacokinetic properties in several animal species, including primates (14, 54). Similar antiviral properties have been demonstrated for the 7-deaza-substituted derivative of 2'-C-acetylene-adenosine

sine, which was recently reported to suppress DENV replication in the transient-replicon assay and in a mouse model (18).

To understand the efficacies of 2'-CMA, 2'-CMC, and 7-deaza-2'-CMA for inhibiting TBEV, we simulated the exploration of the TBEV polymerase by the triphosphate form of each nucleoside analogue (Fig. 7). The computational simulations showed that these inhibitors sampled toward the binding site of the TBEV polymerase. There are a couple of other clusters that aggregate toward the TBEV binding site for 2'-CMA-TP and 2'-CMC-TP. Based on our experimental results, we infer that the pathway is represented by the single cluster of 7-deaza-2'-CMA-TP in Fig. 7, but a more robust analysis must be performed to confirm this hypothesis. Takhampunya et al. (41) developed a method for calculating the ligand/drug binding free energy during its exploration toward the active site of a protein. Their results showed strong correlations with experimental data. We are currently using such methods to determine the viral polymerase binding pathways of 2'-CMA, 2'-CMC, and 7-deaza-2'-CMA and their binding free energies.

In conclusion, we identified three compounds with activity against TBEV *in vitro*. These compounds will be tested further in a mouse model of TBEV infection. These compounds, even if they are not clinically effective, may be useful research tools or starting points for drug development efforts against TBEV. Because of its high antiviral activity and low cytotoxicity, 7-deaza-2'-CMA is an attractive candidate for further investigation as a potential therapeutic agent not only for TBE treatment but also for treating other flaviviral neuroinfections.

ACKNOWLEDGMENTS

We are greatly indebted to Jan Kopecký and Libor Grubhoffer for general support of our work, to Ivana Huvarová for excellent technical assistance, to Vladimír Babák for statistical data processing, and to Jiří Volf for preparation of the immunofluorescence images.

This study was supported by Czech Science Foundation projects P502/11/2116 and GA14-29256S and by project LO1218 from the Ministry of Education, Youth and Sports of the Czech Republic under the NPU I program and by AdmireVet project no. CZ.1.05/2.1.00/01.0006-ED/0006/01/01. We acknowledge a grant for the development of research organization (RVO: 61388963). J.J.V. was supported by project CZ.1.07/2.3.00/30.0032, which is cofinanced by the European Social Fund and the state budget of the Czech Republic. V.A.G. was sponsored by the European project PELE (ERC-2009-Adg 25027).

The funders played no role in study design, data collection and analysis, the decision to publish, or the preparation of the manuscript.

REFERENCES

- Baier A. 2011. Flaviviral infections and potential targets for antiviral therapy, p 89–104. In Ruzek D (ed), *Flavivirus encephalitis*. InTech, Rijeka, Croatia.
- Chambers TJ, Hahn CS, Galler R, Rice CM. 1990. Flavivirus genome organization, expression, and replication. *Annu Rev Microbiol* 44:649–688. <http://dx.doi.org/10.1146/annurev.mi.44.100190.003245>.
- Dumpis U, Crook D, Oksi J. 1999. Tick-borne encephalitis. *Clin Infect Dis* 28:882–890. <http://dx.doi.org/10.1086/515195>.
- Heinz FX, Mandl CW. 1993. The molecular biology of tick-borne encephalitis virus. *APMIS* 101:735–745. <http://dx.doi.org/10.1111/j.1699-0463.1993.tb00174.x>.
- Heinz FX, Stiasny K, Holzmann H, Grgic-Vitek M, Kriz B, Essl A, Kundi M. 2013. Vaccination and tick-borne encephalitis, Central Europe. *Emerg Infect Dis* 19:69–76. <http://dx.doi.org/10.3201/eid1901.120458>.
- Ruzek D, Dobler G, Mantke OD. 2010. Tick-borne encephalitis: pathogenesis and clinical implications. *Travel Med Infect Dis* 8:223–232. <http://dx.doi.org/10.1016/j.tmaid.2010.06.004>.
- Zavadská D, Anca I, Andre F, Bakir M, Chlibek R, Cizman M, Ivaskeviciene I, Mangarov A, Meszner Z, Pokorn M, Prymula R, Richter D, Salman N, Simurka P, Tamm E, Tesovic G, Urbancikova I, Usonis V. 2013. Recommendations for tick-borne encephalitis vaccination from the Central European Vaccination Awareness Group (CEVAG). *Hum Vaccin Immunother* 9:362–374. <http://dx.doi.org/10.4161/hv.22766>.
- Puig-Basagoiti F, Tilgner M, Forshey BM, Philpott SM, Espina NG, Wentworth DE, Goebel SJ, Masters PS, Falgout B, Ren P, Ferguson DM, Shi PY. 2006. Triaryl pyrazoline compound inhibits flavivirus RNA replication. *Antimicrob Agents Chemother* 50:1320–1329. <http://dx.doi.org/10.1128/AAC.50.4.1320-1329.2006>.
- De Clercq E, Neyts J. 2009. Antiviral agents acting as DNA or RNA chain terminators. *Handb Exp Pharmacol* 189:53–84. http://dx.doi.org/10.1007/978-3-540-79086-0_3.
- De Clercq E. 2004. Antivirals and antiviral strategies. *Nat Rev Microbiol* 2:704–720. <http://dx.doi.org/10.1038/nrmicro975>.
- De Clercq E. 2011. A 40-year journey in search of selective antiviral chemotherapy. *Annu Rev Pharmacol Toxicol* 51:1–24. <http://dx.doi.org/10.1146/annurev-pharmtox-010510-100228>.
- Eldrup AB, Allerson CR, Bennett CF, Bera S, Bhat B, Bhat N, Bosserman MR, Brooks J, Burlein C, Carroll SS, Cook PD, Getty KL, MacCoss M, McMasters DR, Olsen DB, Prakash TP, Prhavc M, Song QL, Tomassini JE, Xia J. 2004. Structure-activity relationship of purine ribonucleosides for inhibition of hepatitis C virus RNA-dependent RNA polymerase. *J Med Chem* 47:2283–2295. <http://dx.doi.org/10.1021/jm030424e>.
- Migliaccio G, Tomassini JE, Carroll SS, Tomei L, Altamura S, Bhat B, Bartholomew L, Bosserman MR, Ceccacci A, Colwell LF, Cortese R, De Francesco R, Eldrup AB, Getty KL, Hou XS, LaFemina RL, Ludmerer SW, MacCoss M, McMasters DR, Stahlhut MW, Olsen DB, Hazuda DJ, Flores OA. 2003. Characterization of resistance to non-obligate chain-terminating ribonucleoside analogs that inhibit hepatitis C virus replication *in vitro*. *J Biol Chem* 278:49164–49170. <http://dx.doi.org/10.1074/jbc.M305041200>.
- Olsen DB, Eldrup AB, Bartholomew L, Bhat B, Bosserman MR, Ceccacci A, Colwell LF, Fay JF, Flores OA, Getty KL, Grobler JA, LaFemina RL, Markel EJ, Migliaccio G, Prhavc M, Stahlhut MW, Tomassini JE, MacCoss M, Hazuda DJ, Carroll SS. 2004. A 7-deaza-adenosine analog is a potent and selective inhibitor of hepatitis C virus replication with excellent pharmacokinetic properties. *Antimicrob Agents Chemother* 48:3944–3953. <http://dx.doi.org/10.1128/AAC.48.10.3944-3953.2004>.
- Klumpp K, Leveque V, Le Pogam S, Ma H, Jiang WR, Kang HS, Granycome C, Singer M, Laxton C, Hang JQ, Sarma K, Smith DB, Heindl D, Hobbs CJ, Merrett JH, Symons J, Cammack N, Martin JA, Devos R, Najera I. 2006. The novel nucleoside analog R1479 (4'-azidocytidine) is a potent inhibitor of NS5B-dependent RNA synthesis and hepatitis C virus replication in cell culture. *J Biol Chem* 281:3793–3799. <http://dx.doi.org/10.1074/jbc.M510195200>.
- Klumpp K, Kalayanov G, Ma H, Le Pogam S, Leveque V, Jiang WR, Inocencio N, De Witte A, Rajyaguru S, Tai E, Chanda S, Irwin MR, Sund C, Winquist A, Maltseva T, Eriksson S, Usova E, Smith M, Alker A, Najera I, Cammack N, Martin JA, Johansson NG, Smith DB. 2008. 2'-Deoxy-4'-azido nucleoside analogs are highly potent inhibitors of hepatitis C virus replication despite the lack of 2'-alpha-hydroxyl groups. *J Biol Chem* 283:2167–2175. <http://dx.doi.org/10.1074/jbc.M708929200>.
- Yin Z, Chen YL, Schul W, Wang QY, Gu F, Duraiswamy J, Kondreddi RR, Niyomrattanakit P, Lakshminarayana SB, Goh A, Xu HY, Liu W, Liu B, Lim JY, Ng CY, Qing M, Lim CC, Yip A, Wang G, Chan WL, Tan HP, Lin K, Zhang B, Zou G, Bernard KA, Garrett C, Beltz K, Dong M, Weaver M, He H, Pichota A, Dartois V, Keller Thomas H, Shi PY. 2009. An adenosine nucleoside inhibitor of dengue virus. *Proc Natl Acad Sci U S A* 106:20435–20439. <http://dx.doi.org/10.1073/pnas.0907101106>.
- Chen YL, Yin Z, Duraiswamy J, Schul W, Lim CC, Liu B, Xu HY, Qing M, Yip A, Wang G, Chan WL, Tan HP, Lo M, Liung S, Kondreddi RR, Rao R, Gu H, He H, Keller TH, Shi PY. 2010. Inhibition of dengue virus RNA synthesis by an adenosine nucleoside. *Antimicrob Agents Chemother* 54:2932–2939. <http://dx.doi.org/10.1128/AAC.00140-10>.
- Chen YL, Yin Z, Lakshminarayana SB, Qing M, Schul W, Duraiswamy J, Kondreddi RR, Goh A, Xu HY, Yip A, Liu B, Weaver M, Dartois V, Keller TH, Shi PY. 2010. Inhibition of dengue virus by an ester prodrug of an adenosine analog. *Antimicrob Agents Chemother* 54:3255–3261. <http://dx.doi.org/10.1128/AAC.00397-10>.
- Latour DR, Jekle A, Javanbakht H, Henningsen R, Gee P, Lee I, Tran P, Ren S, Kutach AK, Harris SF, Wang SM, Lok SJ, Shaw D, Li J, Heilek

- G, Klumpp K, Swinney DC, Deval J. 2010. Biochemical characterization of the inhibition of the dengue virus RNA polymerase by beta-D-2'-ethynyl-7-deaza-adenosine triphosphate. *Antiviral Res* 87:213–222. <http://dx.doi.org/10.1016/j.antiviral.2010.05.003>.
21. Lee JC, Tseng CK, Wu YH, Kaushik-Basu N, Lin CK, Chen WC, Wu HN. 2015. Characterization of the activity of 2'-C-methylcytidine against dengue virus replication. *Antiviral Res* 116:1–9. <http://dx.doi.org/10.1016/j.antiviral.2015.01.002>.
 22. Chen H, Liu L, Jones SA, Banavali N, Kass J, Li Z, Zhang J, Kramer LD, Ghosh AK, Li H. 2013. Selective inhibition of the West Nile virus methyltransferase by nucleoside analogs. *Antiviral Res* 97:232–239. <http://dx.doi.org/10.1016/j.antiviral.2012.12.012>.
 23. Julander JG, Jha AK, Choi JA, Jung KH, Smee DF, Morrey JD, Chu CK. 2010. Efficacy of 2'-C-methylcytidine against yellow fever virus in cell culture and in a hamster model. *Antiviral Res* 86:261–267. <http://dx.doi.org/10.1016/j.antiviral.2010.03.004>.
 24. Smee DF, Morris JLB, Barnard DL, Vanaerschot A. 1992. Selective inhibition of arthropod-borne and arenaviruses in vitro by 3'-fluoro-3'-deoxyadenosine. *Antiviral Res* 18:151–162. [http://dx.doi.org/10.1016/0166-3542\(92\)90035-4](http://dx.doi.org/10.1016/0166-3542(92)90035-4).
 25. Smee DF, Alaghamandan HA, Ramasamy K, Revankar GR. 1995. Broad-spectrum activity of 8-chloro-7-deazaguanosine against RNA virus infections in mice and rats. *Antiviral Res* 26:203–209. [http://dx.doi.org/10.1016/0166-3542\(94\)00084-L](http://dx.doi.org/10.1016/0166-3542(94)00084-L).
 26. Ojwang JO, Ali S, Smee DF, Morrey JD, Shimasaki CD, Sidwell RW. 2005. Broad-spectrum inhibitor of viruses in the Flaviviridae family. *Antiviral Res* 68:49–55. <http://dx.doi.org/10.1016/j.antiviral.2005.06.002>.
 27. Chatelain G, Debing Y, De Burghgraeve T, Zmurko J, Saudi M, RozenSKI J, Neyts J, Van Aerschot A. 2013. In search of flavivirus inhibitors: evaluation of different tritylated nucleoside analogues. *Eur J Med Chem* 65:249–255. <http://dx.doi.org/10.1016/j.ejmech.2013.04.034>.
 28. Koonin EV, Dolja VV. 1993. Evolution and taxonomy of positive-strand RNA viruses—implications of comparative analysis of amino acid sequences. *Crit Rev Biochem Mol Biol* 28:375–430. <http://dx.doi.org/10.3109/10409239309078440>.
 29. Flint M, McMullan LK, Dodd KA, Bird BH, Khristova ML, Nichol ST, Spiropoulou CF. 2014. Inhibitors of the tick-borne, hemorrhagic fever-associated flaviviruses. *Antimicrob Agents Chemother* 58:3206–3216. <http://dx.doi.org/10.1128/AAC.02393-14>.
 30. Kozuch O, Mayer V. 1975. Pig kidney epithelial (ps) cells—perfect tool for study of flavi-viruses and some other arboviruses. *Acta Virol* 19:498.
 31. Růžek D, Vancova M, Tesarova M, Ahantari G, Kopecky J, Grubhoffer L. 2009. Morphological changes in human neural cells following tick-borne encephalitis virus infection. *J Gen Virol* 90:1649–1658. <http://dx.doi.org/10.1099/vir.0.010058-0>.
 32. De Madrid AT, Porterfield JS. 1969. A simple micro-culture method for study of group B arboviruses. *Bull World Health Organ* 40:113–121.
 33. Schindelin J, Arganda-Carreras I, Frise E, Kaynig V, Longair M, Pietzsch T, Preibisch S, Rueden C, Saalfeld S, Schmid B, Tinevez JY, White DJ, Hartenstein V, Eliceiri K, Tomancak P, Cardona A. 2012. Fiji: an open-source platform for biological-image analysis. *Nat Methods* 9:676–682. <http://dx.doi.org/10.1038/nmeth.2019>.
 34. Sali A, Blundell TL. 1993. Comparative protein modeling by satisfaction of spatial restraints. *J Mol Biol* 234:779–815. <http://dx.doi.org/10.1006/jmbi.1993.1626>.
 35. McGuffin LJ, Buenavista MT, Roche DB. 2013. The ModFOLD4 server for the quality assessment of 3D protein models. *Nucleic Acids Res* 41:W368–W372. <http://dx.doi.org/10.1093/nar/gkt294>.
 36. Benkert P, Kuenzli M, Schwede T. 2009. QMEAN server for protein model quality estimation. *Nucleic Acids Res* 37:W510–W514. <http://dx.doi.org/10.1093/nar/gkp322>.
 37. Berjanskii M, Zhou J, Liang Y, Lin G, Wishart DS. 2012. Resolution-by-proxy: a simple measure for assessing and comparing the overall quality of NMR protein structures. *J Biomol NMR* 53:167–180. <http://dx.doi.org/10.1007/s10858-012-9637-2>.
 38. Li X, Jacobson MP, Zhu K, Zhao S, Friesner RA. 2007. Assignment of polar states for protein amino acid residues using an interaction cluster decomposition algorithm and its application to high resolution protein structure modeling. *Proteins* 66:824–837.
 39. Schrödinger LLC. 2010. Maestro version 9.1. Schrödinger LLC, New York, NY.
 40. Madadkar-Sobhani A, Guallar V. 2013. PELE web server: atomistic study of biomolecular systems at your fingertips. *Nucleic Acids Res* 41:W322–W328. <http://dx.doi.org/10.1093/nar/gkt454>.
 41. Takhampunya R, Ubol S, Houng HS, Cameron CE, Padmanabhan R. 2006. Inhibition of dengue virus replication by mycophenolic acid and ribavirin. *J Gen Virol* 87:1947–1952. <http://dx.doi.org/10.1099/vir.0.81655-0>.
 42. Atilgan AR, Durell SR, Jernigan RL, Demirel MC, Keskin O, Bahar I. 2001. Anisotropy of fluctuation dynamics of proteins with an elastic network model. *Biophys J* 80:505–515. [http://dx.doi.org/10.1016/S0006-3495\(01\)76033-X](http://dx.doi.org/10.1016/S0006-3495(01)76033-X).
 43. Jacobson MP, Friesner RA, Xiang ZX, Honig B. 2002. On the role of the crystal environment in determining protein side-chain conformations. *J Mol Biol* 320:597–608. [http://dx.doi.org/10.1016/S0022-2836\(02\)00470-9](http://dx.doi.org/10.1016/S0022-2836(02)00470-9).
 44. Still WC, Tempczyk A, Hawley RC, Hendrickson T. 1990. Semianalytical treatment of solvation for molecular mechanics and dynamics. *J Am Chem Soc* 112:6127–6129. <http://dx.doi.org/10.1021/ja00172a038>.
 45. Borrelli KW, Vitalis A, Alcantara R, Guallar V. 2005. PELE: protein energy landscape exploration. A novel Monte Carlo based technique. *J Chem Theory Comput* 1:1304–1311.
 46. Jorgensen WL, Tiradorives J. 1988. The Opls potential functions for proteins—energy minimizations for crystals of cyclic peptides and crambin. *J Am Chem Soc* 110:1657–1666. <http://dx.doi.org/10.1021/ja00214a001>.
 47. Gil VA, Guallar V. 2014. pyProCT: automated cluster analysis for structural bioinformatics. *J Chem Theory Comput* 10:3236–3243. <http://dx.doi.org/10.1021/ct500306s>.
 48. Osolodkin DI, Kozlovskaya LI, Dueva EV, Dotsenko VV, Rogova YV, Frolov KA, Krivoklysko SG, Romanova EG, Morozov AS, Karganova GG, Palyulin VA, Pentkovski VM, Zefirov NS. 2013. Inhibitors of tick-borne flavivirus reproduction from structure-based virtual screening. *ACS Med Chem Lett* 4:869–874. <http://dx.doi.org/10.1021/ml400226s>.
 49. Wallner G, Mandl CW, Ecker M, Holzmann H, Stiasny K, Kunz C, Heinz FX. 1996. Characterisation and complete gene sequences of high- and low-virulence variants of tick-borne encephalitis virus. *J Gen Virol* 77:1035–1042. <http://dx.doi.org/10.1099/0022-1317-77-5-1035>.
 50. Crance JM, Scaramozzino N, Jouan A, Garin D. 2003. Interferon, ribavirin, 6-azauridine and glycyrrhizin: antiviral compounds active against pathogenic flaviviruses. *Antiviral Res* 58:73–79. [http://dx.doi.org/10.1016/S0166-3542\(02\)00185-7](http://dx.doi.org/10.1016/S0166-3542(02)00185-7).
 51. Carroll SS, Tomassini JE, Bosserman M, Getty K, Stahlhut MW, Eldrup AB, Bhat B, Hall D, Simcoe AL, LaFemina R, Rutkowski CA, Wolanski B, Yang ZC, Migliaccio G, De Francesco R, Kuo LC, MacCoss M, Olsen DB. 2003. Inhibition of hepatitis C virus RNA replication by 2'-modified nucleoside analogs. *J Biol Chem* 278:11979–11984. <http://dx.doi.org/10.1074/jbc.M210914200>.
 52. Cristalli G, Costanzi S, Lambertucci C, Lupidi G, Vittori S, Volpini R, Camaioni E. 2001. Adenosine deaminase: functional implications and different classes of inhibitors. *Med Res Rev* 21:105–128. [http://dx.doi.org/10.1002/1098-1128\(200103\)21:2<105::AID-MED1002>3.0.CO;2-U](http://dx.doi.org/10.1002/1098-1128(200103)21:2<105::AID-MED1002>3.0.CO;2-U).
 53. Kinney RM, Huang CYH, Rose BC, Kroeker AD, Dreher TW, Iversen PL, Stein DA. 2005. Inhibition of dengue virus serotypes 1 to 4 in Vero cell cultures with morpholino oligomers. *J Virol* 79:5116–5128. <http://dx.doi.org/10.1128/JVI.79.8.5116-5128.2005>.
 54. Carroll SS, Ludmerer S, Handt L, Koepfingler K, Zhang NR, Graham D, Davies ME, MacCoss M, Hazuda D, Olsen DB. 2009. Robust antiviral efficacy upon administration of a nucleoside analog to hepatitis C virus-infected chimpanzees. *Antimicrob Agents Chemother* 53:926–934. <http://dx.doi.org/10.1128/AAC.01032-08>.
 55. Carroll SS, Koepfingler K, Vavrek M, Zhang NR, Handt L, MacCoss M, Olsen DB, Reddy KR, Sun ZL, van Poelje PD, Fujitaki JM, Boyer SH, Linemeyer DL, Hecker SJ, Erion MD. 2011. Antiviral efficacy upon administration of a HepDirect prodrug of 2'-C-methylcytidine to hepatitis C virus-infected chimpanzees. *Antimicrob Agents Chemother* 55:3854–3860. <http://dx.doi.org/10.1128/AAC.01152-10>.
 56. Sofia MJ, Chang W, Furman PA, Mosley RT, Ross BS. 2012. Nucleoside, nucleotide, and non-nucleoside inhibitors of hepatitis C virus NS5B RNA-dependent RNA polymerase. *J Med Chem* 55:2481–2531. <http://dx.doi.org/10.1021/jm201384j>.

CHAPTER IX

Structure-activity relationships of nucleoside analogues for inhibition of tick-borne encephalitis virus

Luděk Eyer, Markéta Šmídková, Radim Nencka, Jiří Neča, Tomáš Kastl, Martin Palus, Erik De Clercq, Daniel Růžek

Antiviral Research 2016, 133:119-129

DOI: 10.1016/j.antiviral.2016.07.018

<http://dx.doi.org/10.1016/j.antiviral.2016.07.018>

Nucleoside Inhibitors of Zika Virus

Luděk Eyer, Radim Nencka, Ivana Huvarová, Martin Palus, Maria Joao Alves, Ernest A. Gould, Erik De Clercq, Daniel Růžek

The Journal of Infectious Disease 2016, 214 (5): 707-711.

DOI: 10.1093/infdis/jiw226

<http://jid.oxfordjournals.org/content/early/2016/05/26/infdis.jiw226.abstract>

Structure-activity relationships of nucleoside analogues for inhibition of tick-borne encephalitis virus

(summary)

In connection, we identified three 2'-C-methylated nucleoside analogues (i.e., 2'-C-methyladenosine, 2'-C-methylcytidine and 7-deaza-2'-C-methyladenosine) as effective inhibitors of TBEV replication *in vitro* (Eyer *et al.*, 2015), we report here a structure-activity relationship study based on the antiviral/cytotoxicity profile of 29 nucleoside derivatives, each differing in chemical substituents on the ribose ring and in the type and chemical modifications of the heterobase. We evaluated the series of nucleoside derivatives using two standardized *in vitro* assay systems, for their ability to inhibit TBEV replication in cell lines of neuronal as well as extraneural origin. Also the effect on replication of another medically important flavivirus, Zika virus (ZIKV) was tested in VERO cell culture. The growing evidence that ZIKV causes devastating infant brain defects and other neurological disorders in humans and no specific antiviral therapy is available at present underline the demand of seeking effective medical intervention.

The series of tested compounds included 2'-C- or 2'-O-methyl substituted nucleosides, 2'-C-fluoro-2'-C-methyl substituted nucleosides, 3'-O-methyl substituted nucleosides, 3'-deoxynucleosides, derivatives with 4'-C-azido substitution, heterobase modified nucleosides and neplanocins. Our data demonstrate a relatively stringent structure-activity relationship for modifications at the 2', 3', and 4' nucleoside positions. Modifications, such as introduction of 2'- α -fluoro-2'- β -methyl moiety into the C2' position or various substitutions of the O2' and O3' positions, led to a complete loss of anti-TBEV activity ($IC_{50} > 50 \mu M$). Similarly, structural modifications of the hydrogen-bonding capacity of the purine/pyrimidine heterobase were accompanied by either inefficacy against TBEV or highly increased cytotoxicity. Finally, promising results were achieved for some nucleosides, exhibiting cell-type dependent anti-TBEV effect (C4' azido substituted pharmacophores failed in inhibition in human neuroblastoma cells only), which can be explained by metabolic differences in diverse cell populations.

Our results indicate that under *in vitro* conditions C2' methylation exerted activity against TBEV (IC₅₀ from 0.3 to 11.1 μM) and ZIKV (IC₅₀ from 5.26 to 45.45 μM). Whereas C4' azido substituted pharmacophores were ineffective against ZIKV replication, on the other hand inhibition of TBEV replication was achieved at least in PS cell culture (IC₅₀ of 2.7 and 0.3 μM).

These compounds, even if they are not clinically effective, may represent useful research tools or promising starting point for specific antiviral drug development efforts against TBEV and ZIKV infections.



Contents lists available at ScienceDirect

Antiviral Research

journal homepage: www.elsevier.com/locate/antiviral

Structure-activity relationships of nucleoside analogues for inhibition of tick-borne encephalitis virus



Luděk Eyer^a, Markéta Šmídková^b, Radim Nencka^b, Jiří Neča^a, Tomáš Kastl^a, Martin Palus^{a,d}, Erik De Clercq^c, Daniel Růžek^{a,d,*}

^a Department of Virology, Veterinary Research Institute, Hudcova 70, CZ-62100 Brno, Czech Republic

^b Institute of Organic Chemistry and Biochemistry, The Czech Academy of Sciences, Fleming Sq. 2, CZ-16610 Prague, Czech Republic

^c Rega Institute for Medical Research, KU Leuven, Minderbroedersstraat 10, B-3000 Leuven, Belgium

^d Institute of Parasitology, Biology Centre of the Czech Academy of Sciences, and Faculty of Science, University of South Bohemia, Branišovská 31, CZ-37005 České Budějovice, Czech Republic

ARTICLE INFO

Article history:

Received 10 February 2016

Received in revised form

5 July 2016

Accepted 24 July 2016

Available online 28 July 2016

Keywords:

Structure-activity relationship

Tick-borne encephalitis

Nucleoside inhibitor

Antiviral activity

Cytotoxicity

ABSTRACT

Tick-borne encephalitis (TBE) represents one of the most serious arboviral neuro-infections in Europe and northern Asia. As no specific antiviral therapy is available at present, there is an urgent need for efficient drugs to treat patients with TBE virus (TBEV) infection. Using two standardised *in vitro* assay systems, we evaluated a series of 29 nucleoside derivatives for their ability to inhibit TBEV replication in cell lines of neuronal as well as extraneural origin. The series of tested compounds included 2'-C- or 2'-O-methyl substituted nucleosides, 2'-C-fluoro-2'-C-methyl substituted nucleosides, 3'-O-methyl substituted nucleosides, 3'-deoxynucleosides, derivatives with 4'-C-azido substitution, heterobase modified nucleosides and neplanocins. Our data demonstrate a relatively stringent structure-activity relationship for modifications at the 2', 3', and 4' nucleoside positions. Whereas nucleoside derivatives with the methylation at the C2' position or azido modification at the C4' position exerted a strong TBEV inhibition activity (EC₅₀ from 0.3 to 11.1 μM) and low cytotoxicity *in vitro*, substitutions of the O2' and O3' positions led to a complete loss of anti-TBEV activity (EC₅₀ > 50 μM). Moreover, some structural modifications of the heterobase moiety resulted in a high increase of cytotoxicity *in vitro*. High antiviral activity and low cytotoxicity of C2' methylated or C4' azido substituted pharmacophores suggest that such compounds might represent promising candidates for further development of potential therapeutic agents in treating TBEV infection.

© 2016 Elsevier B.V. All rights reserved.

1. Introduction

Tick-borne encephalitis virus (TBEV), a causative agent of tick-borne encephalitis (TBE), is a member of the *Flaviviridae* family, which includes many medically important viruses, such as hepatitis C virus (HCV), West Nile virus, Zika virus, dengue virus, Japanese encephalitis virus, yellow fever virus, and several haemorrhagic fever-associated flaviviruses (Baier, 2011). TBE represents one of the most serious arboviral neuro-infections in Europe and northern Asia with thousands of TBEV-infected people and many reported deaths annually (Dumpis et al., 1999; Heinz and Mandl, 1993). The

characteristic clinical symptoms of acute TBE range from a mild meningitis to severe meningoencephalitis/myelitis with the risk of temporary or permanent neurologic sequelae after TBE infection (Růžek et al., 2010). Although safe and efficient vaccines against TBEV are available, the number of TBE patients in the endemic regions of Europe continuously increases (Heinz et al., 2013; Zavadská et al., 2013). As no specific antiviral therapy is available at present, there is an urgent need for efficient drugs to treat patients with TBEV infection (Puig-Basagoiti et al., 2006).

Inhibitors of viral polymerases are the largest class of approved antiviral drugs, of which the largest number is represented by nucleoside analogue inhibitors (De Clercq, 2011). Mode of action of nucleoside inhibitors is based on the premature termination of viral RNA synthesis (De Clercq and Neyts, 2009). Following intracellular phosphorylation, the 5'-triphosphate metabolites are competitively incorporated into the viral RNA nascent chains, which

* Corresponding author. Veterinary Research Institute, Hudcova 70, CZ-62100 Brno, Czech Republic.

E-mail address: ruzekd@paru.cas.cz (D. Růžek).

<http://dx.doi.org/10.1016/j.antiviral.2016.07.018>

0166-3542/© 2016 Elsevier B.V. All rights reserved.

prevents further extension of the incorporated analogue by addition of the next nucleoside triphosphate resulting in formation of incomplete (non-functional) viral RNA chains. In general, the antiviral activity of nucleoside inhibitors is predominantly determined by steric interference (hydrogen bonding capability) between the nucleoside triphosphate and the viral polymerase active site. Moreover, the effect of the absence, conformational constraints, or steric/electronic hindrance of the nucleoside 3'-hydroxyl function on formation of a phosphodiester linkage with the incoming nucleoside triphosphate could also play an important role in the efficient termination of viral RNA synthesis (De Clercq, 2004; De Clercq and Neyts, 2009). Cellular uptake and intracellular metabolism (such as deamination, phosphorolysis or phosphorylation) can also considerably influence the antiviral activity of a nucleoside analogue (Eldrup et al., 2004; Tomassini et al., 2005; Ma et al., 2007).

Previously, we identified three 2'-C-methylated nucleoside analogues (i.e., 2'-C-methyladenosine, 2'-C-methylcytidine and 7-deaza-2'-C-methyladenosine) as effective inhibitors of TBEV replication *in vitro* (Eyer et al., 2015). In connection with these results, we report here a structure-activity relationship study based on the antiviral/cytotoxicity profile of 29 nucleoside derivatives, each differing in chemical substituents on the ribose ring and in the type and chemical modifications of the heterobase. We focused our attention on the evaluation of 2', 3', and 4'-modified nucleosides, for which antiviral activity was previously reported for other viruses, especially HCV (Eldrup et al., 2004; Klumpp et al., 2008; Sofia et al., 2012), Zika (Eyer et al., 2016), dengue (Lee et al., 2015), yellow fever (Julander et al., 2010), and haemorrhagic fever-associated flaviviruses (Flint et al., 2014). The tested compounds were characterized using standardised *in vitro* assay systems in terms of inhibition of TBEV replication, inhibition of virus-induced cytopathic effect (CPE) formation, suppression of viral antigen expression in TBEV-infected cell cultures, and evaluation of viability on compound-treated host cells. Based on these screens, we identified the 2'-C-methyl or 4'-C-azido substituents as important for a selective TBEV inhibition and a low cytotoxicity *in vitro*.

2. Material and methods

2.1. Cell cultures, virus strains and antiviral compounds

Porcine kidney stable (PS) cells, a cell line widely used for TBEV isolation, multiplication, and for conducting plaque assays (Kozuch and Mayer, 1975), were cultured at 37 °C in Leibovitz (L-15) medium supplemented with 3% precolostral calf serum and a 1% mixture of penicillin and glutamine (Sigma-Aldrich, Prague, Czech Republic). Human neuroblastoma UKF-NB-4 cells, a valuable model for neuropathogenesis studies of TBEV (Ruzek et al., 2009), were cultured at 37 °C in 5% CO₂ in Iscove's modified Dulbecco's medium (IMDM) with 10% foetal bovine serum and a 1% mixture of antibiotics (Sigma-Aldrich, Prague, Czech Republic). Hypr and Neudoerfl TBEV strains, typical representatives of the West European TBEV subtype, were used for evaluation of the antiviral activity of the test compounds. Nucleoside analogues were purchased as follows: 2'-C-methyl, 2'-O-methyl, and 3'-O-methyl substituted nucleosides, 3'-deoxynucleosides, sofosbuvir, and 6-azauridine from Carbonsynth (Compton, UK), 4'-azidocytidine, balapiravir and RO-9187 from Medchemexpress (Stockholm, Sweden), nplanocin A from Cayman Chemical Company (Ann Arbor, Michigan), 3-deazaneplanocin A from Selleckchem (Munich, Germany), mercitabine from ChemScene (Monmouth Junction, NJ), PSI-6206 from ApexBio (Boston, MA), tubercidin, toyocamycin, sangivamycin, ribavirin and 2'-deoxynucleosides from Sigma-Aldrich (Prague, Czech Republic). Nucleotide triphosphate standards for HPLC

analysis were purchased from TriLink Biotechnologies (San Diego, CA). The test compounds were solubilised in 100% DMSO to yield 10 mM stock solutions.

2.2. *In vitro* antiviral assays

A viral titre inhibition assay was performed to measure the antiviral efficacy of nucleoside analogues in cell culture. PS or UKF-NB-4 cells were seeded in 96-well plates (approximately 2×10^4 cells per well) and incubated for 24 h to form a confluent monolayer. Following incubation, the medium was aspirated from the wells and replaced with 200 µl of fresh medium containing 50 µM of the test compound (three wells per compound), which was inoculated with the Hypr or Neudoerfl TBEV strain at a multiplicity of infection (MOI) of 0.1. As a negative control, DMSO was added to virus- and mock-infected cells at a final concentration of 0.5% (v/v). Culture medium was collected 3 days postinfection (p.i.) to yield a 40–50% CPE in virus control wells. The CPE was monitored visually using the Olympus BX-5 microscope equipped with an Olympus DP-70 CCD camera. Viral titres were determined by plaque assays and expressed as PFU ml⁻¹ (De Madrid and Porterfield, 1969). For dose-response studies, PS cell monolayers were cultured with 200 µl of medium containing the test compounds over the concentration range of 0–50 µM and TBEV (Hypr strain) at an MOI of 0.1. The medium was collected from the wells at 2-day intervals (post-infection days 1, 3 and 5), the viral titres were determined by plaque assays and used to construct TBEV dose-response curves. The dose-response curves on post-infection days 3 were used to estimate the 50% effective concentration (EC₅₀).

2.3. Immunofluorescence staining

To measure the compound-induced inhibition of viral surface antigen expression, a cell-based flavivirus immunostaining assay was performed as previously described (Eyer et al., 2015). Briefly, PS cells were seeded on slides, infected with the TBEV Hypr strain at an MOI of 0.1, treated with the test compound (50 µM) and cultured for 4 days at 37 °C. After a cold acetone-methanol (1:1) fixation and blocking with 10% foetal bovine serum, the cells were incubated with a mouse monoclonal antibody recognising the flavivirus group surface antigen (1:250, Sigma-Aldrich, Prague, Czech Republic) and subsequently labelled with an anti-mouse goat secondary antibody conjugated with FITC (1:500) by incubation for 1 h at 37 °C. The cells were counterstained with DAPI (1 µg ml⁻¹) to visualise the cell nuclei. Finally, the cells were mounted in 2.5% DABCO (Sigma-Aldrich, Czech Republic) and the fluorescence signal was recorded with an Olympus IX71 epifluorescence microscope.

2.4. Cytotoxicity assays

PS cells were grown in 96-well plates overnight to form a confluent monolayer and subsequently treated with test compounds over the concentration range of 0–50 µM. At day 3 p.i., the medium was collected and the potential cytotoxicity of test compounds was determined in terms of cell viability using the Cell Counting Kit-8 (Dojindo Molecular Technologies, Munich, Germany) according to the manufacturer's instructions. The concentration of compound that reduced cell viability by 50% was considered the 50% cytotoxic concentration (CC₅₀).

2.5. Quantification of 2'-C-methylated nucleosides in compound-treated cells

The UKF-NB4 cells were plated at a density of 2×10^5 cells/ml in 6-well plates for 48 h and subsequently exposed to tested

compounds at concentration of 10 or 50 μM . After 0, 2, 4, and 8-h intervals, the cells were rinsed with PBS, harvested by scraping and centrifuged at 2800 rpm for 2 min. The pellet was resuspended in 500 μl methanol and sonicated for 1 min. The obtained suspension (50 μl) was used for protein quantification (BCA method – Pierce BCA Protein Assay Kit, Thermo Scientific, San Jose, CA). After centrifugation, the supernatant was used for quantitative determination of 2'-C-methylated nucleosides using liquid chromatography-tandem mass spectrometry (LC-MS/MS) (Zouharova et al., 2016). An Agilent 1200 chromatographic system (Agilent Technologies, Germany), consisted of binary pump, vacuum degasser, autosampler, and thermostatted column compartment, was used. Separation of modified nucleosides was carried out using a Zorbax Eclipse Plus C18, 2.1 \times 150 mm, 3.5 μm particle size

column (Agilent, USA) under isocratic conditions. Mobile phase contained methanol according to the analyzed nucleoside and 0.1% of formic acid in water. The flow rate of the mobile phase was 0.25 ml/min, the column temperature was set at 40 $^{\circ}\text{C}$. A triple quadrupole mass spectrometer Agilent 6410 Triple Quad LC/MS (Agilent Technologies, USA) with an electrospray interface (ESI) was used for detection of nucleosides in cells. The mass spectrometer was operated in the positive mode and selected ion monitoring (SIM) was used for quantification.

2.6. Crude cellular extract preparation

PS and UKF-NB4 cells (5×10^6) were washed with PBS, resuspended in 2 ml of 50 mM Tris-HCl buffer (pH 7.4) containing 1 mM

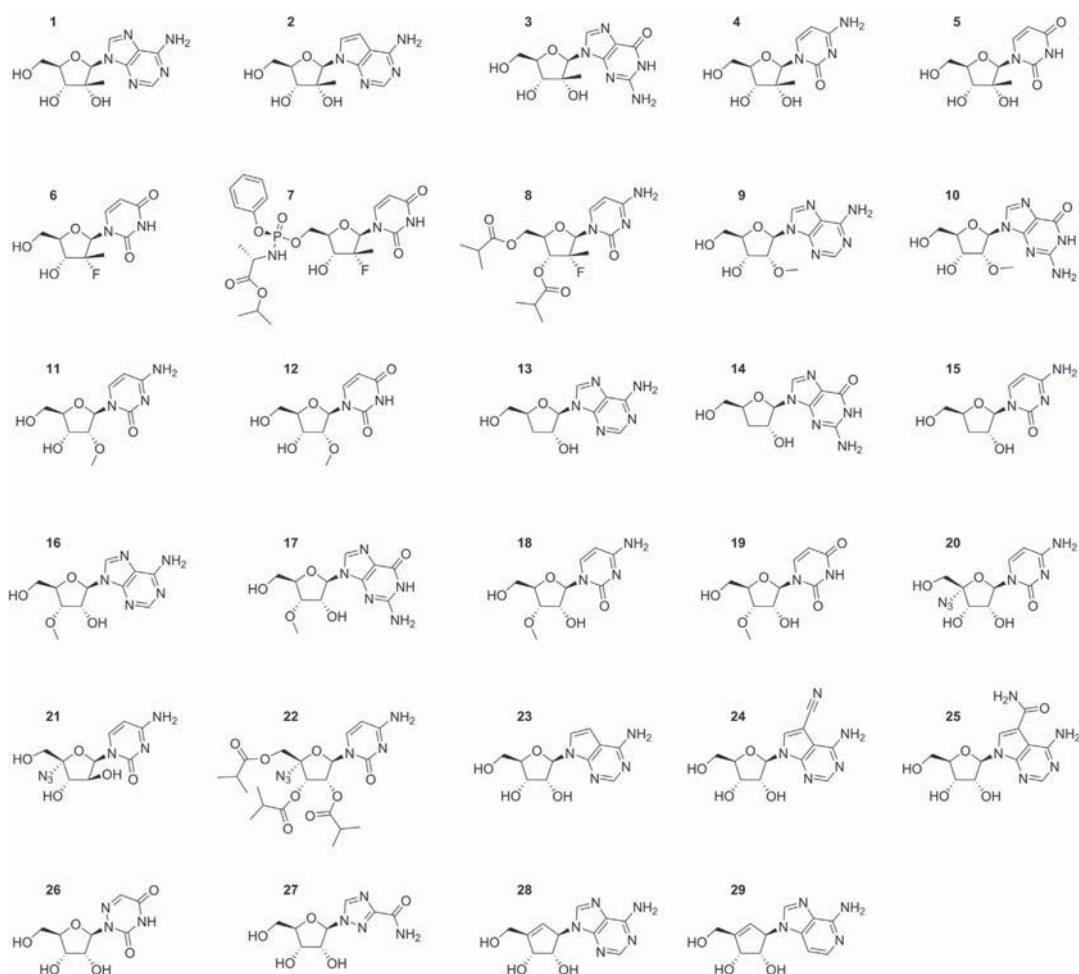


Fig. 1. The structures of the nucleoside analogues tested in this study. (1) 2'-C-methyladenosine, (2) 7-deaza-2'-C-methyladenosine, (3) 2'-C-methylguanosine, (4) 2'-C-methylcytidine, (5) 2'-C-methyluridine, (6) PSI-6206, (7) sofosbuvir, (8) mericitabine, (9) 2'-O-methyladenosine, (10) 2'-O-methylguanosine, (11) 2'-O-methylcytidine, (12) 2'-O-methyluridine, (13) 3'-deoxyadenosine, (14) 3'-deoxyguanosine, (15) 3'-deoxycytidine, (16) 3'-O-methyladenosine, (17) 3'-O-methylguanosine, (18) 3'-O-methylcytidine, (19) 3'-O-methyluridine, (20) 4'-azidocytidine, (21) RO-9187, (22) balapiravir, (23) 7-deazaadenosine (tubercidin), (24) 7-deaza-7-cyanoadenosine (toyocamycin), (25) 7-deaza-7-carbamoyladenosine (sangivamycin), (26) 6-azauridine, (27) ribavirin, (28) neplanocin A, (29) 3-deazaneplanocin A.

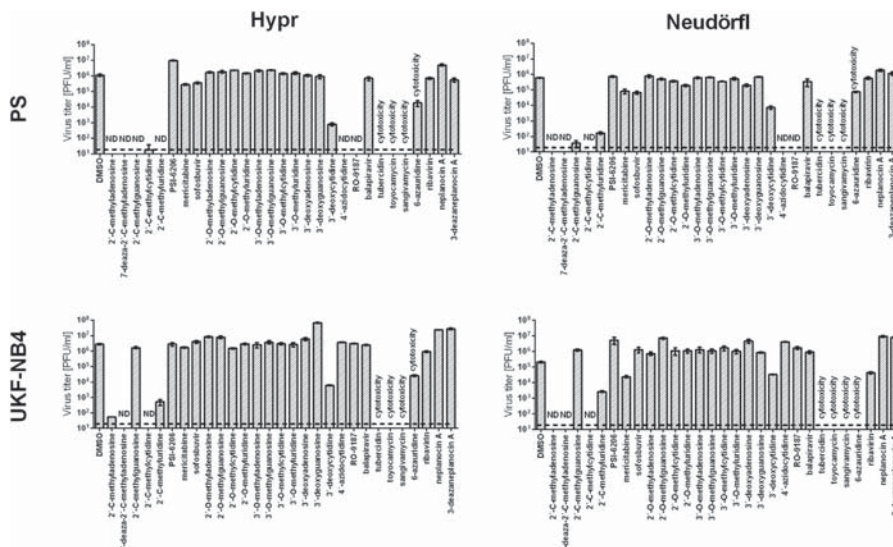


Fig. 2. Reduction of TBEV titres by the indicated nucleoside analogues. PS or UKF-NB-4 cells were infected with TBEV (Hypr or Neudorfli strain) at a multiplicity of infection (MOI) of 0.1 and then treated with 50 μ M nucleoside analogues. The TBEV titres were determined by the plaque assay 3 days p.i. Viral titres are expressed as PFU mL⁻¹. Bars show the mean values from three biological replicate wells, and the error bars indicate the standard errors of the means (n = 3). ND, not detected (below the detection limit). The horizontal dashed line indicates the minimum detectable threshold of 1.44 log₁₀ PFU mL⁻¹.

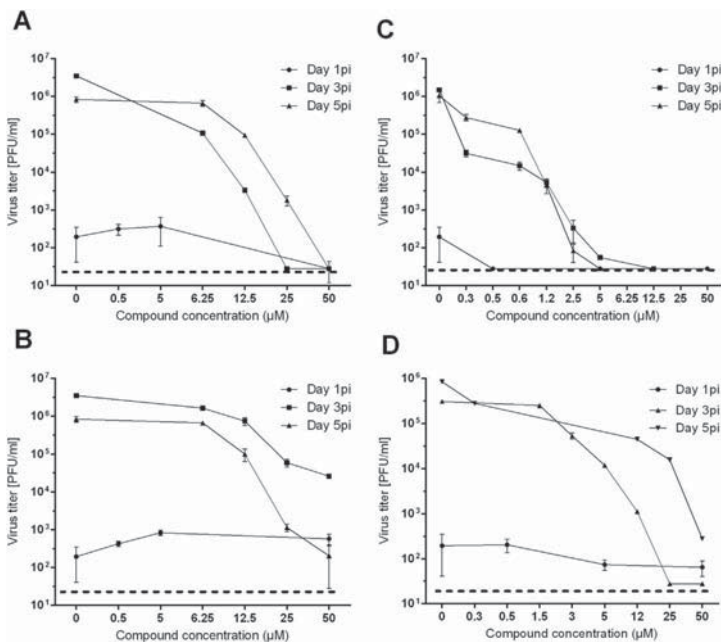


Fig. 3. Dose-dependent effects of the indicated TBEV inhibitors on virus titres. PS cells were infected with TBEV at a multiplicity of infection (MOI) of 0.1 and treated with 2'-C-methylguanosine (A), 2'-C-methyluridine (B), RO-9187 (C) and (D) 4'-azidocytidine at the indicated concentrations. TBEV titres were monitored at days 1, 3, and 5 p.i. The mean titres from three biological replicates are shown, and error bars indicate standard errors of the mean (n = 3). The horizontal dashed line indicates the minimum detectable threshold of 1.44 log₁₀ PFU mL⁻¹.

dithiothreitol, 5 mM MgCl₂, and protease inhibitor and phosphatase inhibitor cocktail (Sigma Aldrich, Prague, Czech Republic) and homogenized using sonication. After that, the homogenate was centrifuged at 30,000g for 30 min. Aliquots (100 µl) were stored at –80 °C until use.

2.7. Metabolism of compounds in crude extract

The tested compounds (2'-C-methylguanosine, 2'-O-methylcytidine, 4'-azidocytidine and RO-9187) at concentration of 100 µM were added to 100 µl of crude extract and incubated at 37 °C for 0, 0.5, 2, 4, and 8 h. The samples were deproteinized by methanol precipitation (400 µl of methanol to 100 µl of sample), centrifuged at 14,000g for 10 min and subsequently used for HPLC analysis.

2.8. HPLC analysis

The samples (50 µl) were injected onto the Supelcosil LC-18-T HPLC column (150 mm × 3 mm I. D., 3 µm). Mobile phase A corresponded to 50 mM KH₂PO₄ (pH 3.1) with 10 mM tetrabutylammonium hydrogensulphate, mobile phase B to 50 mM KH₂PO₄ (pH 3.1) with 10 mM tetrabutylammonium hydrogen sulphate and 30% acetonitrile (v/v) in HPLC-grade water and mobile phase C to 50 mM KH₂PO₄ (pH 3.1) with 10 mM tetrabutylammonium hydrogen sulphate. The gradient started with 100% mobile phase A going isocratically in 5 min, followed by steep change from C to B in 6 min, ongoing nonlinearly to 75% B in 30 min and then going

linearly to 100% mobile phase A in 35 min. The flow rate was 0.75 ml/min. The absorption spectra of the eluate were recorded by a PDA detector. The concentrations of intact compounds and their phosphates in crude extract were calculated from the peak areas by using calibration curves made up from their standards, which are characterized in terms of retention times (Rt) and absorption maxima in [Supplementary Table 1](#).

3. Results

3.1. Modifications of the ribose 2'-position

We described previously that 2'-C-methyladenosine, 2'-C-methylcytidine, and 7-deaza-2'-C-methyladenosine are effective inhibitors of TBEV replication *in vitro* (Eyer et al., 2015). In order to further investigate the structure-activity relationships for the ribose 2'-modifications, we tested a large group of 2'-C- or 2'-O-substituted nucleosides (Fig. 1, structures 1–12) for their anti-TBEV activity and cytotoxicity using standardised *in vitro* assays.

As expected, 2'-C-methylguanosine and 2'-C-methyluridine displayed an inhibitory effect on TBEV replication in PS cells (Fig. 2). Both derivatives reduced the viral titre in a dose-dependent manner (EC₅₀ of 1.4 µM (2'-C-methylguanosine) and 11.1 µM (2'-C-methyluridine)) and the antiviral effect appeared to be stable throughout the five-day experimental period (Fig. 3A,B, Table 1). Surprisingly, 2'-C-methylguanosine failed to inhibit TBEV when applied to human neuroblastoma cells (Fig. 2). 2'-C-

Table 1
TBEV-inhibition and cytotoxicity characteristics of the studied nucleoside analogues.

Structure number ^a	Compound	EC ₅₀ ^{b, c} (µM)	App.EC ₅₀ ^{b, d} (µM)	CC ₅₀ ^b (µM)	SI ^e
(1)	2'-C-methyladenosine	1.4 ± 0.01	7.1 ± 1.2 ^f	>50.0 ^g	>37.03
(2)	7-deaza-2'-C-methyladenosine	1.1 ± 0.03	5.1 ± 0.4 ^f	>50.0 ^g	>46.7
(3)	2'-C-methylguanosine	1.4 ± 0.01	13.5 ± 0.8	>50.0	>35.7
(4)	2'-C-methylcytidine	1.8 ± 0.4	14.2 ± 0.4 ^f	~50.0 ^g	~28.4
(5)	2'-C-methyluridine	11.1 ± 0.4	25.1 ± 7.2	>50.0	>4.5
(6)	PSI-6206	>50.0	>50.0	>50.0	1.0
(7)	sofosbuvir	>50.0	>50.0	>50.0	1.0
(8)	mericitabine	>50.0	>50.0 ^g	>50.0 ^g	1.0
(9)	2'-O-methyladenosine	>50.0	>50.0	>50.0	1.0
(10)	2'-O-methylguanosine	>50.0	>50.0	>50.0 ^f	1.0
(11)	2'-O-methylcytidine	>50.0	>50.0	>50.0	1.0
(12)	2'-O-methyluridine	>50.0	>50.0	>50.0	1.0
(13)	3'-deoxyadenosine	>50.0	>50.0	>50.0	1.0
(14)	3'-deoxyguanosine	>50.0	>50.0	>50.0	1.0
(15)	3'-deoxycytidine ^h	41.2 ± 0.01	79.4 ± 2.3	80.2 ± 0.01	1.9
(16)	3'-O-methyladenosine	>50.0	>50.0	>50.0	1.0
(17)	3'-O-methylguanosine	>50.0	>50.0	>50.0	1.0
(18)	3'-O-methylcytidine	>50.0	>50.0	>50.0	1.0
(19)	3'-O-methyluridine	>50.0	>50.0	>50.0	1.0
(20)	4'-azidocytidine	2.7 ± 0.1	9.3 ± 0.3	>50.0	>18.6
(21)	RO-9187	0.3 ± 0.01	1.5 ± 0.2	>50.0 ^f	>192.3
(22)	balapiravir	>50.0	>50.0	>50.0	1.0
(23)	7-deazaadenosine (tubercidin)	ND ^f	ND ^f	2.1 ± 0.2	–
(24)	7-deaza-7-cyanoadenosine (toyocamycin)	ND ^f	ND ^f	0.1 ± 0.01	–
(25)	7-deaza-7-carbamoylguanosine (sangivamycin)	ND ^f	ND ^f	0.8 ± 0.1	–
(26)	6-azauridine	ND ^f	ND ^f	7.0 ± 0.5	–
(27)	ribavirin	> 50.0	> 50.0	> 50.0	1.0
(28)	neplanocin A	> 50.0	> 50.0	> 50.0 ^f	1.0
(29)	3-deazaneplanocin A	> 50.0	> 50.0	> 50.0	1.0

^a See Fig. 1.

^b Determined from three independent experiments.

^c Calculated as a 50% reduction of viral titers using the Reed-Muench method.

^d Calculated as a point of inflection from dose-response curves using log-transformed viral titers.

^e SI = CC₅₀/EC₅₀.

^f ND, not determined. As TBEV replication is dependent on cell proliferation, the EC₅₀ values of cytotoxic compounds cannot be assessed.

^g Values reported previously by Eyer et al., 2015.

^h Dose-response experiment for 3'-deoxycytidine including the cytotoxicity assay was performed in the concentration range from 0 to 400 µM.

ⁱ Treatment the cell culture with 2'-O-methylguanosine, RO-9187, and neplanocin A at concentration of 50 µM led to a reduction in the cell viability to 84.4, 86.9 and 83.6%, respectively.

Methylguanosine and 2'-C-methyluridine inhibited the expression of the TBEV surface E antigen in PS cells (Fig. 4B, C) and showed no cytotoxic effects at the highest tested concentration of 50 μ M with no detectable effect on cell proliferation (Fig. 5A).

Replacement of the 2'-C-methyl group by the 2'- α -fluoro-2'- β -methyl moiety led to a loss in antiviral activity, as observed in PSI-6206, sofosbuvir and mericitabine ($EC_{50} > 50 \mu$ M). Similarly, 2'-O-methyl substituted nucleosides caused no or negligible activity against both TBEV strains (Fig. 2). A moderate decline of cell viability (to 84.4%) was seen in PS cell cultures treated with 50 μ M of 2'-O-methylguanosine (Fig. 5A).

3.2. Modifications of the ribose 3'-position

Of all 3'-deoxynucleosides tested (Fig. 1, structures 13–15), only 3'-deoxycytidine showed a moderate inhibitory activity (EC_{50} of 41.2 μ M) (Fig. 2). The anti-TBEV activity of 3'-deoxycytidine was accompanied by a slight cytotoxic effect on PS cell monolayers

(Fig. 5A, Table 1). In contrast, 3'-deoxyadenosine and 3'-deoxyguanosine exhibited no detectable inhibitory effect on TBEV replication ($EC_{50} > 50 \mu$ M) (Fig. 2) and were well tolerated by the cultured PS cells (Fig. 5A). Methylation of the 3'-hydroxyl group to generate the corresponding 3'-O-methyl modified structures (Fig. 1, structures 16–19) also resulted in a complete loss in antiviral activity, regardless of the purine/pyrimidine heterobase identity (Fig. 2). 3'-O-Methyl modified derivatives exerted no cytotoxic effects and caused no morphological changes in the PS cell cultures (Fig. 5A).

3.3. Modifications of the ribose 4'-position

4'-Azidocytidine and its arabino-counterpart 2'- α -deoxy-2'- β -hydroxy-4'-azidocytidine, termed RO-9187 (Fig. 1, structures 20 and 21), exhibited a dose-dependent anti-TBEV effect in PS cell cultures (EC_{50} of 2.7 and 0.3 μ M, respectively) (Fig. 3C,D; Table 1). These compounds, however, failed to inhibit TBEV when applied on

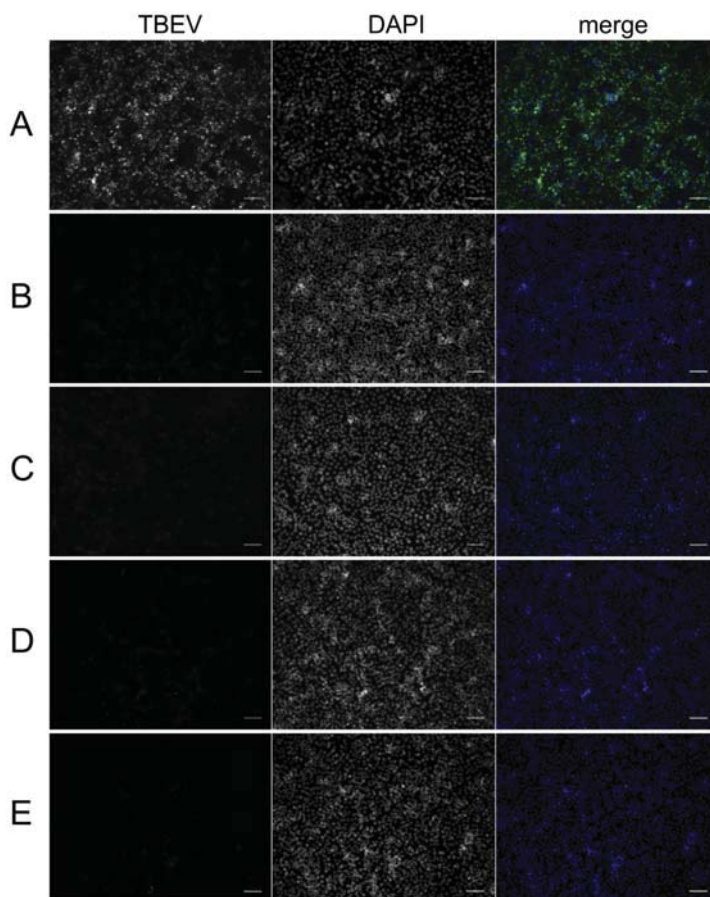


Fig. 4. Inhibition of TBEV viral antigen expression by nucleoside inhibitors. PS cells were infected with TBEV and treated with 0.5% DMSO (A) or with 50 μ M 2'-C-methylguanosine (B), 2'-C-methyluridine (C), RO-9187 (D), and 4'-azidocytidine (E). PS cells were fixed on slides at day 3 postinfection and stained with flavivirus-specific antibody labelled with FITC (green) and counterstained with DAPI (blue). Scale bars, 50 μ m. (For interpretation of the references to colour in this figure legend, the reader is referred to the web version of this article.)

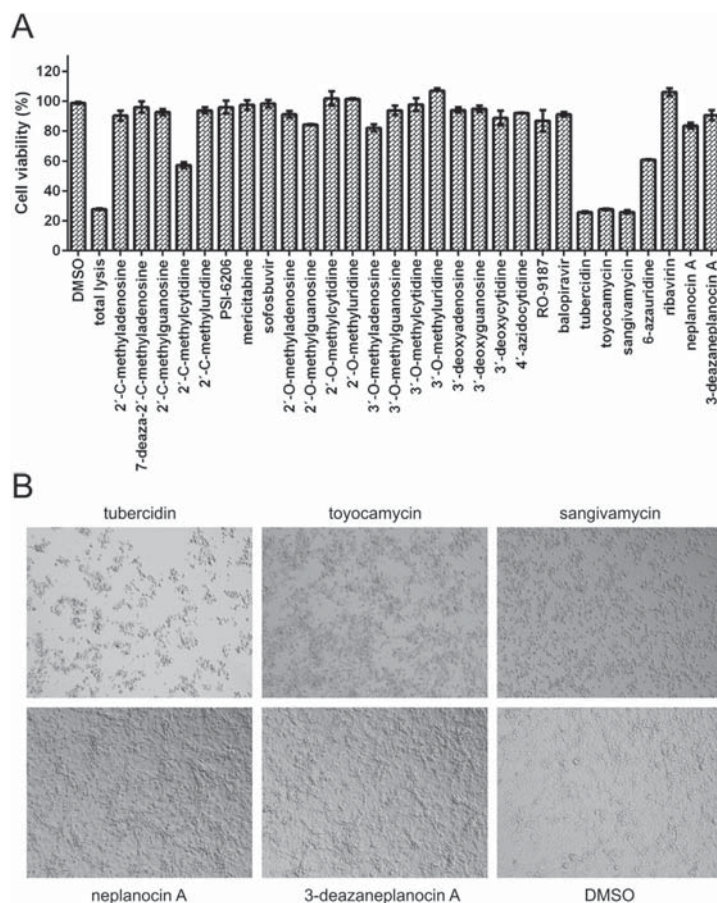


Fig. 5. Cytotoxicity of nucleoside inhibitors. Cytotoxicity was determined by treatment PS cells with the 50 μ M of indicated nucleoside analogues and was expressed in terms of cell viability at day 3 postinfection. The bars indicate the mean values from three replicate wells, and the error bars indicate the standard errors of the mean (A). Cytotoxic effects and morphological changes of PS cells induced by the indicated nucleoside analogues (50 μ M) at day 3 after treatment (B).

human neuroblastoma cells (Fig. 2). 4'-Azidocytidine and RO-9187 at the concentration of 50 μ M showed a significant inhibition of the viral protein E expression in TBEV-infected compound-treated PS cells (Fig. 4D,E). On the other hand, balopiravir (Fig. 1, structure 22), an ester prodrug of 4'-azidocytidine, was found to be completely inactive in inhibiting TBEV *in vitro*. Whereas 4'-azidocytidine and balopiravir exerted no cytotoxic effects on the PS cell cultures, RO-9187 (at 50 μ M) showed a slight decrease of the cell viability (to 86.9%) (Fig. 5A).

3.4. Modification of the purine/pyrimidine heterobase

The combination of the 7-deaza modification of adenosine and the 2'-C-methyl-ribose substitution has created a strong TBEV inhibitor, 7-deaza-2'-C-methyladenosine (EC₅₀ of 1.1 μ M), showing no cytotoxic effect on either PS or UKF-NB4 cells (Table 1). Based on these results, we further tested several heterobase-modified nucleosides in which hydrogen bond donors or acceptors were either

omitted or added, mainly at the heterobase 7-position (Fig. 1, structures 23–27). 7-Deazaadenosine (tubercidin) displayed a strong cytotoxicity on PS cell monolayers (CC₅₀ of 2.1 μ M) (Fig. 5, Table 1). As TBEV replication is dependent on cell proliferation, the antiviral effect of tubercidin and other cytotoxic compounds could not be assessed (Fig. 2). Similarly, 7-deaza-7-cyano- and 7-deaza-7-carbamoyl substituted derivatives of tubercidin (i.e., toyocamycin and sangivamycin) exerted demonstrable toxicity when dosed at a concentration of 50 μ M (CC₅₀ values of 0.1 and 0.8 μ M, respectively) (Table 1). Ribavirin and 6-azauridine had no protective effects on the survival and growth of PS cells exposed to TBEV (Fig. 2).

3.5. Other nucleoside modifications

Neplanocin A and 3-deazaneplanocin A (Fig. 1, structures 28 and 29), in which the ribofuranose ring is replaced by the cyclopentenyl moiety, exhibited no antiviral activity *in vitro* using both Hypr and Neudoerfl strains and in both the PS and UKF-NB4 cell lines

($EC_{50} > 50 \mu\text{M}$) (Fig. 2). Moreover, neplanocin A exerted a detectable cytotoxic effect on compound-treated PS cells; Treatment the cell culture with compound concentration of $50 \mu\text{M}$ led to a reduction in the cell viability to 83.6%. Morphological changes observed on neplanocin-treated cultures (Fig. 5B) have been probably attributed to an alteration in cellular transmethylation mediated through an effect on *S*-adenosylhomocysteine hydrolase (Borchardt et al., 1984).

3.6. The kinetics of 2'-C-methylated nucleoside uptake

The kinetics of 2'-C-methylguanosine and 2'-C-methyluridine uptake were studied in UKF-NB4 cells using a rapid and sensitive LC-MS/MS based approach. The highest intracellular amounts of individual compounds were detected at the 2nd h after treatment (Fig. 6). Between posttreatment hours 4 and 8, the intracellular amount of 2'-C-methylated compounds markedly decreased as compared to the 2nd h of the experiment. This phenomenon was probably related to the activation of intracellular phosphorylation pathways and to the intensive conversion of intact nucleoside molecules to their corresponding triphosphate forms (Eldrup et al., 2004). A relatively high amount of intracellular 2'-C-methyluridine was detected in cell cultures treated with $50 \mu\text{M}$ of the compound at 4–8 h after treatment (Fig. 6D). This result is in agreement with a lower anti-TBEV activity of 2'-C-methyluridine (EC_{50} of $11.1 \mu\text{M}$) and could be explained by a reduced intracellular phosphorylation efficiency of the compound.

3.7. Intracellular metabolism of selected nucleosides in PS and UKF-NB4 cells

In order to explain the biological activity of the tested nucleoside analogues in terms of metabolic activation, we performed analysis of metabolic conversion of selected nucleosides to their active triphosphate forms using two distinct cell lines. Cellular

extracts from PS or UKF-NB4 cells were incubated with 2'-C-methylguanosine, 2'-O-methylcytidine, 4'-azidocytidine or RO-9187 ($100 \mu\text{M}$) for 0, 0.5, 2, 4, and 8 h and subsequently analyzed by HPLC.

In PS cells, nucleoside conversion to the corresponding triphosphates was observed in 2'-C-methylguanosine (at 4 and 8 h after treatment) and RO-9187 (at hour 8) (Supplementary Table 2). Triphosphate conversion of 4'-azidocytidine was not observed within 8 h interval. As expected, 2'-O-methylcytidine (showing no anti-TBEV effect) exerted no intracellular conversion to triphosphates in PS cells. No deamination/demethylation of the compounds was observed during the incubation for 8 h in PS cellular extract.

In UKF-NB4 cells, no detachable phosphorylation products were identified in all nucleosides tested (Supplementary Table 2). Our results indicate, that the depletion of 2'-O-methylcytidine, 4'-azidocytidine and RO-9187 in time could be a result of their extensive deamination. As absorption maxima of metabolic products of both azido-derivatives (236.7 nm) were distinct from that of uridine (262.5 nm), it can be expected that no cleavage of azido-group (and no conversion to uridine) occurs in UKF-NB4 cellular extracts. The absorption maximum of 2'-O-methylcytidine metabolic product (262.5 nm) indicates also possible demethylation processes resulting in the extensive conversion of the compound to uridine after the incubation (data not shown).

A detailed study of metabolic activation of TBEV inhibitors in both PS and UKF-NB4 cells goes beyond the scope of this report and will be a subject of a future article.

4. Discussion

Based on the high degree of homology between the TBEV and HCV genomes and similarities at the protein levels (Koonin and Dolja, 1993), we can expect that the mode of TBEV inhibition mediated by 2', 3' and 4'-modified nucleosides is similar to that of

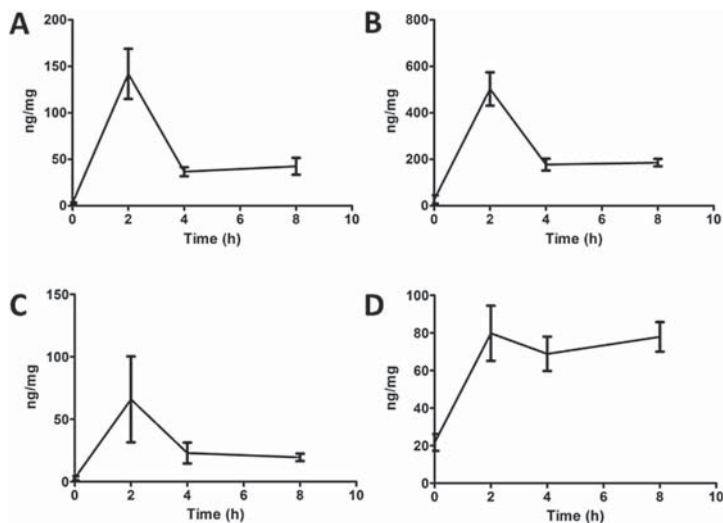


Fig. 6. The kinetics of 2'-C-methylated nucleoside uptake. The UKF-NB4 cells were grown for 48 h and subsequently exposed to 2'-C-methylguanosine at concentration of $10 \mu\text{M}$ (A) or $50 \mu\text{M}$ (B) or 2'-C-methyluridine at concentration of $10 \mu\text{M}$ (C) or $50 \mu\text{M}$ (D). After 0, 2, 4, and 8-h intervals the cells were harvested by scraping and used for quantitative determination of 2'-C-methylated nucleosides by LC-MS/MS. The intracellular amounts of the individual compounds are expressed in ng of compound per mg of cellular proteins. The mean values from three replicate wells are indicated, and the error bars indicate the standard errors of the mean.

HCV, for which the nucleoside activities and interactions with viral polymerase were studied in detail using *in vitro* (Carroll et al., 2003; Klumpp et al., 2006, 2008; Migliaccio et al., 2003; Olsen et al., 2004) and *in vivo* systems (Carroll et al. 2009, 2011). The interactions of three 2'-C-methylated nucleosides with the TBEV-polymerase active site were simulated using advanced computational methods (Eyer et al., 2015).

Evaluation of various modifications at the nucleoside 2'-position revealed, that the introduction of the 2'-C-methyl substituent to the nucleoside β -face resulted in a strong inhibition of TBEV replication *in vitro*. Based on the EC₅₀ values for individual 2'-C-methylated nucleosides tested (ranging from 1.1 to 11.1 μ M), it is obvious that their antiviral activities were slightly affected by the identity of the heterobase. Similarly, the heterobase type can influence the metabolic stability of the 2'-C-methylated nucleoside. Whereas 2'-C-methyladenosine was metabolized rapidly, which was manifested by a gradual disappearance of the compound's antiviral effect (Cristalli et al., 2001; Eyer et al., 2015), the other tested 2'-C-methylated derivatives were characterized by an increased metabolic stability *in vitro*. The cytotoxicity of the 2'-C-methylated nucleosides was observed to be none or negligible, except for 2'-C-methylcytidine (CC₅₀ of 50 μ M) (Eyer et al., 2015). In contrast, tubercidin, toyocamycin and sangivamycin, devoid of the 2'-C-methyl group, were observed to be highly cytotoxic for PS cells at submicromolar concentrations. The cytotoxicity of tubercidin was ascribed to its incorporation into cellular nucleic acids by cellular enzymes, whereas 2'-C-methyl substituted nucleosides were described as poor substrates for human DNA polymerases (Olsen et al., 2004). Taken together, the 2'-C-methyl substituent appeared to be an important structural element for a highly selective TBEV inhibition and a reduced cytotoxicity *in vitro*. It is likely that the 2'-C-methyl substituent does not adversely affect the binding of a nucleoside to the viral polymerase active site; this binding is probably made possible by the presence of some additional steric space in the vicinity of the 2'-carbon, allowing the polymerase active site to accommodate the 2'-C-methyl substituent. After incorporation, such a substituent is probably responsible for efficient termination of viral RNA chain elongation (Carroll et al., 2003).

Interestingly, no or negligible anti-TBEV activity was observed for 2'- α -fluoro-2'- β -methyl or 2'-O-methyl substituted nucleosides. We can speculate that the introduction of the fluoro moiety into the C2' position or the methyl moiety into the O2' position eliminates the 2'- α -hydroxy hydrogen bond donor/acceptor, which results in the complete abrogation of the nucleoside inhibitory activity. The ability of flaviviral polymerases to discriminate against nucleoside triphosphates modified at the 2'-position on the ribose α -face is probably related to the need of the polymerase to avoid the incorporation of 2'- α -deoxynucleoside monophosphates into the viral nascent RNA chain (Eldrup et al., 2004). In case of the NS5B polymerase of HCV, such discrimination against 2'- α -deoxynucleosides was described to be mediated by several conserved amino acid residues (most probably by Asp-225) in the polymerase active site, which are crucial for hydrogen bond formation with the 2'- α -hydroxy group (Bressanelli et al. 2002). Ineffectiveness of 2'- α -deoxynucleosides for TBEV inhibition was also demonstrated in our *in vitro* antiviral assays (data not shown). No anti-TBEV activity of 2'-O-methylcytidine could be also ascribed to its inefficient intracellular conversion to corresponding triphosphate and, moreover, to an extensive deamination/demethylation resulting in a conversion to uridine.

2'- α -Deoxy-2'- β -hydroxy-4'-azidocytidine (RO-9187, an arabinoside stereoisomer of 4'-azidocytidine) is a compound structurally related to 2'-deoxyribonucleosides, particularly due to the absence of the 2'- α -hydroxy substituent on the ribose ring. Moreover, RO-

9187, similarly to 2'-deoxyribonucleosides and other arabinonucleosides, was described to occupy preferentially the 2'-endo conformation, which is typical for the B-form DNA (Klumpp et al., 2008). This makes RO-9187 significantly different from nucleosides possessing the 2'- α -hydroxy substituent (e.g., natural ribonucleoside substrates or 2'-C-methyl substituted nucleosides), which are characterized by the 3'-endo conformation, typical for the A-form RNA (Eldrup et al., 2004; Klumpp et al., 2008). In sharp contrast to 2'-deoxyribonucleosides, which showed no activity against TBEV in PS cell cultures, RO-9187 was demonstrated to be the strongest TBEV inhibitor of the entire test series (EC₅₀ of 0.3 μ M). Based on this finding, we can assume that some additional hydrogen bonding interactions of the polymerase active site with both the 2'- β -hydroxy substituent and the 4'-azido substituent could compensate for the loss of 2'- α -hydroxy interaction, resulting

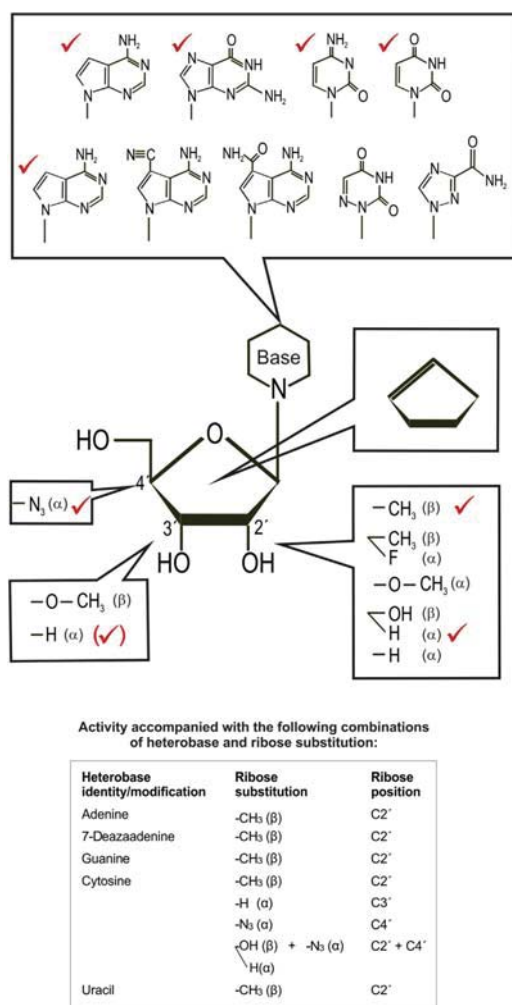


Fig. 7. Structure-activity relationships for substitutions at the 2', 3', and 4' nucleoside positions and for purine/pyrimidine heterobase identity/modifications.

in the strong and selective anti-TBEV activity of RO-9187 (Klumpff et al., 2008). Anti-TBEV activity of RO-9187 was strongly cell line-dependent and was observed only in TBEV-infected PS cell cultures. The same phenomenon was demonstrated also in 4'-azido-cytidine and, surprisingly, in 2'-C-methylguanosine, suggesting possible metabolic differences between PS and human neuroblastoma cell lines. In PS cells, phosphorylation processes were detected and no deamination/demethylation was observed. This is in a sharp contrast with UKF-NB4 cells, where no conversion to triphosphate forms was observed, and extensive deamination or demethylation of the compounds was indicated in this cell line.

3'-Deoxyadenosine, 3'-deoxyguanosine and all tested 3'-O-methylated nucleosides caused no significant inhibition of TBEV replication *in vitro*. Thus, the observed inactivity of 3'-modified nucleosides might be interpreted as the requirement of the TBEV NS5 polymerase active site for a 3'-hydroxyl group to form the appropriate hydrogen bonding interaction with the nucleoside triphosphate molecule. However, 3'-deoxycytidine exerted a moderate anti-TBEV effect (EC₅₀ of 75.9 μM) despite the lack of the 3'-hydroxyl moiety, which indicated that TBEV NS5 polymerase is probably able to bind 3'-deoxynucleoside triphosphates and that the observed inactivity of 3'-modified nucleosides could instead be related to inefficient cellular uptake and metabolism to convert the nucleoside molecule into the corresponding triphosphate form (Eldrup et al., 2004).

In conclusion, our data demonstrate a relatively stringent structure-activity relationship for modifications at the 2', 3', and 4' nucleoside positions (Fig. 7). Of all structural modifications tested, only the methylation of the C2' nucleoside position or the azido modification of the C4' position resulted in an inhibition of TBEV replication and a low cytotoxicity *in vitro*. Other structural modifications, such as introduction of 2'-α-fluoro-2'-β-methyl moiety into the C2' position or various substitutions of the O2' and O3' positions, led to a complete loss of anti-TBEV activity. On the other hand, some structure-activity relationship flexibility was found for change of the purine/pyrimidine heterobase identity; replacement of adenine to guanine, cytosine or uracil appeared to have only a limited effect on the antiviral activity and cytotoxicity of the nucleoside analogue. However, structural modifications of the hydrogen-bonding capacity of the heterobase were strongly accompanied by either an inefficacy against TBEV or a highly increased cytotoxicity. Finally, we identified, that some nucleosides exhibit cell-type dependent anti-TBEV effect, which can be explained by metabolic differences in diverse cell populations. Our results indicate that C2' methylated and C4' azido substituted pharmacophores, even if they are not clinically effective, may represent useful research tools or starting points for antiviral drug development efforts against TBEV infection.

Acknowledgements

The authors are greatly indebted to Dr. Ivana Huvarová for excellent technical assistance and to Dr. Vladimír Babák for computational data processing. This study was supported by Czech Science Foundation project GA14-29256S and 16-20054S, Ministry of Health of the Czech Republic (grant No. 16–34238A), and by project LO1218 with financial support from the Ministry of Education, Youth and Sports of the Czech Republic under the NPU I program. We acknowledge a grant for the development of research organization (RVO: 61388963).

Appendix A. Supplementary data

Supplementary data related to this article can be found at <http://dx.doi.org/10.1016/j.antiviral.2016.07.018>.

References

- Baier, A., 2011. Flavivirus infections and potential targets for antiviral therapy. In: Ruzek, D. (Ed.), *Flavivirus Encephalitis*. InTech, Rijeka, Croatia.
- Borchardt, R.T., Keller, B.T., Patelthombre, U., 1984. Neplanocin-a – a potent inhibitor of S-Adenosylhomocysteine hydrolase and of vaccinia virus multiplication in mouse L929 cells. *J. Biol. Chem.* 259, 4353–4358.
- Bressanelli, S., Tomei, L., Rey, F.A., De Francesco, R., 2002. Structural analysis of the hepatitis C virus RNA polymerase in complex with Ribonucleotides. *J. Virol.* 76, 3482–3492. <http://dx.doi.org/10.1128/JVI.76.7.3482-3492.2002>.
- Carroll, S.S., Koepflinger, K., Vavrek, M., Zhang, N.R., Handt, L., MacCoss, M., Olsen, D.B., Reddy, K.R., Sun, Z.L., van Poelje, P.D., Fujitaki, J.M., Boyer, S.H., Linemeyer, D.L., Hecker, S.J., Erion, M.D., 2011. Antiviral efficacy upon administration of a HepDirect prodrug of 2'-C-Methylcytidine to hepatitis C virus-infected chimpanzees. *Antimicrob. Agents Chemother.* 55, 3854–3860. <http://dx.doi.org/10.1128/AAC.01152-10>.
- Carroll, S.S., Tomassini, J.E., Bosserman, M., Getty, K., Stahlhut, M.W., Eldrup, A.B., Bhat, B., Hall, D., Simcoe, A.L., LaFemina, R., Rutkowski, C.A., Wolanski, B., Yang, Z.C., Migliaccio, G., De Francesco, R., Kuo, L.C., MacCoss, M., Olsen, D.B., 2003. Inhibition of hepatitis C virus RNA replication by 2'-modified nucleoside analogs. *J. Biol. Chem.* 278, 11979–11984. <http://dx.doi.org/10.1074/jbc.M210914200>.
- Carroll, S.S., Ludmerer, S., Handt, L., Koepflinger, K., Zhang, N.R., Graham, D., Davies, M.E., MacCoss, M., Hazuda, D., Olsen, B.D., 2009. Robust antiviral efficacy upon administration of a nucleoside analog to hepatitis C virus-infected chimpanzees. *Antimicrob. Agents Chemother.* 53, 926–934. <http://dx.doi.org/10.1128/AAC.01032-08>.
- Cristalli, G., Costanzi, S., Lambertucci, C., Lupidi, G., Vittori, S., Volpini, R., Camaioni, E., 2001. Adenosine deaminase: functional implications and different classes of inhibitors. *Med. Res. Rev.* 21, 105–128. DOI: 10.1002/1098-1128(200103)21:2<105::AID-MED1002>3.0.CO;2-U.
- De Clercq, E., 2004. Antivirals and antiviral strategies. *Nat. Rev. Microbiol.* 2, 704–720. <http://dx.doi.org/10.1038/nrmicro975>.
- De Clercq, E., 2011. A 40-year journey in search of selective antiviral chemotherapy. *Annu. Rev. Pharmacol. Toxicol.* 51, 1–24. <http://dx.doi.org/10.1146/annurev-pharmtox.010510-100228>.
- De Clercq, E., Neyts, J., 2009. Antiviral agents acting as DNA or RNA chain terminators. In: *Handbook of Experimental Pharmacology*, 189, pp. 53–84. http://dx.doi.org/10.1007/978-3-540-79086-0_3.
- De Madrid, A.T., Porterfield, J.S., 1969. A simple micro-counting method for study of group B arboviruses. *Bull. World Health Organ.* 40, 113–121.
- Dumpis, U., Crook, D., Oksi, J., 1999. Tick-borne encephalitis. *Clin. Infect. Dis.* 28, 882–890. <http://dx.doi.org/10.1086/515195>.
- Eldrup, A.B., Allerson, C.R., Bennett, C.F., Bera, S., Bhat, B., Bhat, N., Bosserman, M.R., Brooks, J., Burlein, C., Carroll, S.S., Cook, P.D., Getty, K.L., MacCoss, M., McMasters, D.R., Olsen, D.B., Prakash, T.P., Prhavc, M., Song, Q.L., Tomassini, J.E., Xia, J., 2004. Structure-activity relationship of purine ribonucleosides for inhibition of hepatitis C virus RNA-dependent RNA polymerase. *J. Med. Chem.* 47, 2283–2295. <http://dx.doi.org/10.1021/jm030424e>.
- Eyer, L., Valdes, J.J., Gil, V.A., Nencka, R., Hrebabecky, H., Sala, M., Salat, J., Cerny, J., Palus, M., De Clercq, E., Ruzek, D., 2015. Nucleoside inhibitors of tick-borne encephalitis virus. *Antimicrob. Agents Chemother.* 59, 5483–5493. <http://dx.doi.org/10.1128/AAC.00807-15>.
- Eyer, L., Nencka, R., Huvarová, I., Palus, M., Joao Alves, M., Gould, E.A., De Clercq, E., Ruzek, D., 2016. Nucleoside inhibitors of Zika virus. *J. Infect. Dis.* <http://dx.doi.org/10.1093/infdis/jiw226>. [Epub ahead of print].
- Flint, M., McMullan, L.K., Dodd, K.A., Bird, B.H., Khristova, M.L., Nichol, S.T., Spiropoulou, C.F., 2014. Inhibitors of the tick-borne, hemorrhagic fever-associated flaviviruses. *Antimicrob. Agents Chemother.* 58, 3206–3216. <http://dx.doi.org/10.1128/AAC.02393-14>.
- Heinz, F.X., Mandl, C.W., 1993. The molecular-biology of tick-borne encephalitis-virus. *Apmis* 101, 735–745. <http://dx.doi.org/10.1111/j.1699-0463.1993.tb00174.x>.
- Heinz, F.X., Stiasny, K., Holzmann, H., Grgic-Vitek, M., Kriz, B., Essl, A., Kundi, M., 2013. Vaccination and tick-borne encephalitis, central Europe. *Emerg. Infect. Dis.* 19, 69–76. <http://dx.doi.org/10.3201/eid1901.120458>.
- Julander, J.G., Jha, A.K., Choi, J.A., Jung, K.H., Smeed, D.F., Morrey, J.D., Chu, C.K., 2010. Efficacy of 2'-C-methylcytidine against yellow fever virus in cell culture and in a hamster model. *Antivir. Res.* 86, 261–267. <http://dx.doi.org/10.1016/j.antiviral.2010.03.004>.
- Klumpff, K., Leveque, V., Le Pogam, S., Ma, H., Jiang, W.R., Kang, H.S., Granycome, C., Singer, M., Laxton, C., Hang, J.Q., Sama, K., Smith, D.B., Heindl, D., Hobbs, C.J., Merrett, J.H., Symons, J., Cammack, N., Martin, J.A., Devos, R., Najera, I., 2006. The novel nucleoside analog R1479 (4'-azido-cytidine) is a potent inhibitor of NS5B-dependent RNA synthesis and hepatitis C virus replication in cell culture. *J. Biol. Chem.* 281, 3793–3799. <http://dx.doi.org/10.1074/jbc.M510195200>.
- Klumpff, K., Kalayanov, G., Ma, H., Le Pogam, S., Leveque, V., Jiang, W.R., Inocencio, N., De Witte, A., Rajiyaguru, S., Tai, E., Chanda, S., Irwin, M.R., Sund, C., Winquist, A., Maltseva, T., Eriksson, S., Usova, E., Smith, M., Alker, A., Najera, I., Cammack, N., Martin, J.A., Johansson, N.G., Smith, D.B., 2008. 2'-deoxy-4'-azido nucleoside analogs are highly potent inhibitors of hepatitis C virus replication despite the lack of 2'-alpha-hydroxyl groups. *J. Biol. Chem.* 283, 2167–2175. <http://dx.doi.org/10.1074/jbc.M708929200>.
- Koonin, E.V., Dolja, V.V., 1993. Evolution and taxonomy of positive-strand RNA

- viruses – implications of comparative-analysis of amino-acid-sequences. *Crit. Rev. Biochem. Mol. Biol.* 28, 375–430. <http://dx.doi.org/10.3109/10409239309078440>.
- Kozuch, O., Mayer, V., 1975. Pig kidney epithelial (ps) cells – perfect tool for study of flavi-viruses and some other arboviruses. *Acta Virol.* 19, 498.
- Lee, J.C., Tseng, C.K., Wu, Y.H., Kaushik-Basu, N., Lin, C.K., Chen, W.C., Wu, H.N., 2015. Characterization of the activity of 2'-C-methylcytidine against dengue virus replication. *Antivir. Res.* 116, 1–9. <http://dx.doi.org/10.1016/j.antiviral.2015.01.002>.
- Ma, H., Jiang, W.R., Robledo, N., Leveque, V., Ali, S., Lara-Jaime, T., Masjedizadeh, M., Smith, D.B., Cammack, N., Klumpp, K., Symons, J., 2007. Characterization of the metabolic activation of hepatitis C virus nucleoside inhibitor beta-D-2'-Deoxy-2'-fluoro-2'-C-methylcytidine (PSI-6130) and identification of a novel active 5'-triphosphate species. *J. Biol. Chem.* 282, 29812–29820. <http://dx.doi.org/10.1074/jbc.M705274200>.
- Migliaccio, G., Tomassini, J.E., Carroll, S.S., Tomei, L., Altamura, S., Bhat, B., Bartholomew, L., Bosserman, M.R., Ceccacci, A., Colwell, L.F., Cortese, R., De Francesco, R., Eldrup, A.B., Getty, K.L., Hou, X.S., LaFemina, R.L., Ludmerer, S.W., MacCoss, M., McMaster, D.R., Stahlhut, M.W., Olsen, D.B., Hazuda, D.J., Flores, O.A., 2003. Characterization of resistance to non-obligate chain-terminating ribonucleoside analogs that inhibit hepatitis C virus replication in vitro. *J. Biol. Chem.* 278, 49164–49170. <http://dx.doi.org/10.1074/jbc.M305041200>.
- Olsen, D.B., Eldrup, A.B., Bartholomew, L., Bhat, B., Bosserman, M.R., Ceccacci, A., Colwell, L.F., Fay, J.F., Flores, O.A., Getty, K.L., Grobler, J.A., LaFemina, R.L., Markel, E.J., Migliaccio, G., Prhac, M., Stahlhut, M.W., Tomassini, J.E., MacCoss, M., Hazuda, D.J., Carroll, S.S., 2004. A 7-deaza-adenosine analog is a potent and selective inhibitor of hepatitis C virus replication with excellent pharmacokinetic properties. *Antimicrob. Agents Chemother.* 48, 3944–3953. <http://dx.doi.org/10.1128/AAC.48.10.3944-3953.2004>.
- Puig-Basagoiti, F., Tilgner, M., Forshey, B.M., Philpott, S.M., Espina, N.G., Wentworth, D.E., Goebel, S.J., Masters, P.S., Falgout, B., Ren, P., Ferguson, D.M., Shi, P.Y., 2006. Triaryl pyrazoline compound inhibits flavivirus RNA replication. *Antimicrob. Agents Chemother.* 50, 1320–1329. <http://dx.doi.org/10.1128/AAC.50.4.1320-1329.2006>.
- Ruzek, D., Dobler, G., Donoso Mantke, O., 2010. Tick-borne encephalitis: pathogenesis and clinical implications. *Travel Med. Infect. Dis.* 8, 223–232. <http://dx.doi.org/10.1016/j.tmaid.2010.06.004>.
- Ruzek, D., Vancova, M., Tesarova, M., Achantarig, A., Kopecky, J., Grubhoffer, L., 2009. Morphological changes in human neural cells following tick-borne encephalitis virus infection. *J. General Virol.* 90, 1649–1658. <http://dx.doi.org/10.1099/vir.0.010058-0>.
- Sofia, M.J., Chang, W., Furman, P.A., Mosley, R.T., Ross, B.S., 2012. Nucleoside, nucleotide, and non-nucleoside inhibitors of hepatitis C virus NS5B RNA-dependent RNA-polymerase. *J. Med. Chem.* 55, 2481–2531. <http://dx.doi.org/10.1021/jm201384j>.
- Tomassini, J.E., Getty, K., Stahlhut, M.W., Shim, S., Bhat, B., Eldrup, A.B., Prakash, T.P., Carroll, S.S., Flores, O., MacCoss, M., McMaster, D.R., Migliaccio, G., Olsen, D.B., 2005. Inhibitory effect of 2'-substituted nucleosides on hepatitis C virus replication correlates with metabolic properties in replicon cells. *Antimicrob. Agents Chemother.* 49, 2050–2058. <http://dx.doi.org/10.1128/AAC.49.5.2050-2058.2005>.
- Zavadská, D., Anca, I., Andre, F., Bakir, M., Chlibek, R., Cizman, M., Ivaskeviciene, I., Mangarov, A., Meszner, Z., Pokorn, M., Prymula, R., Richter, D., Salman, N., Simurka, P., Tamm, E., Tesovic, G., Urbancikova, I., Usonis, V., 2013. Recommendations for tick-borne encephalitis vaccination from the central european vaccination awareness group (CEVAG). *Hum. Vaccines Immunother.* 9, 362–374. <http://dx.doi.org/10.4161/hv.22766>.
- Zouharova, D., Lipenska, I., Fojtikova, M., Kulich, P., Neca, J., Slany, M., Kovarcik, K., Turanek-Knotigova, P., Hubatka, F., Celechovska, H., Masek, J., Koudelka, S., Prochazka, L., Eyer, L., Plockova, J., Bartheldyova, E., Miller, A.D., Ruzek, D., Raska, M., Janeba, Z., Turanek, J., 2016. Antiviral activities of 2,6-diaminopurine-based acyclic nucleoside phosphonates against herpesviruses: *In vitro* study results with pseudorabies virus (PrV, SuHV-1). *Veterinary Microbiol.* 184, 84–93. <http://dx.doi.org/10.1016/j.vetmic.2016.01.010>.

Nucleoside Inhibitors of Zika Virus

Luděk Eyer,¹ Radim Nencka,² Ivana Huvarová,¹ Martin Palus,^{1,3,4} Maria Joao Alves,⁵ Ernest A. Gould,⁶ Erik De Clercq,⁷ and Daniel Růžek^{1,3,4}

¹Department of Virology, Veterinary Research Institute, Brno, ²Institute of Organic Chemistry and Biochemistry, Czech Academy of Sciences, Prague, ³Institute of Parasitology, Biology Center of the Czech Academy of Sciences, and ⁴Faculty of Science, University of South Bohemia, České Budějovice, Czech Republic; ⁵National Institute of Health Dr Ricardo Jorge–CEVDI/INSA, Águas de Moura, Portugal; ⁶Aix Marseille Université, IRD French Institute of Research for Development, EHESP French School of Public Health, EPV UMR_D 190 Emergence des Pathologies Virales, France; and ⁷Rega Institute for Medical Research, KU Leuven, Belgium

There is growing evidence that Zika virus (ZIKV) can cause devastating infant brain defects and other neurological disorders in humans. However, no specific antiviral therapy is available at present. We tested a series of 2'-C- or 2'-O-methyl-substituted nucleosides, 2'-C-fluoro-2'-C-methyl-substituted nucleosides, 3'-O-methyl-substituted nucleosides, 3'-deoxynucleosides, derivatives with 4'-C-azido substitution, heterobase-modified nucleosides, and neplanocins for their ability to inhibit ZIKV replication in cell culture. Antiviral activity was identified when 2'-C-methylated nucleosides were tested, suggesting that these compounds might represent promising lead candidates for further development of specific antivirals against ZIKV.

Keywords. Zika virus; flavivirus; nucleoside analogue; antiviral; therapy.

On 1 February 2016, the World Health Organization declared a public health emergency of international concern regarding neurological disorders associated with the rapid emergence of Zika virus (ZIKV) in Oceania and the Americas [1]. Previously, ZIKV was a relatively neglected mosquito-borne arbovirus in the genus *Flavivirus*, family *Flaviviridae*. ZIKV infections have been known in Africa and Asia since the 1940s. During the last years, the virus caused several outbreaks of infection across Oceania [2]. In May 2015, a ZIKV outbreak was first reported in Brazil, and within months most countries in Latin America and the Caribbean had reported local transmission of the virus [1, 3]. Until recently, ZIKV was associated with benign infection in humans, with common symptoms that include fever, rash, joint pain, and conjunctivitis. The illness was usually mild, with symptoms lasting for several days. However, there is growing evidence in Oceania and the Americas that ZIKV can cause devastating brain birth defects, most prominently

microcephaly [4], and neurological disorders in adults, including Guillain-Barré syndrome, meningoencephalitis [5], and myelitis [6]. At present, neither vaccination nor specific antiviral therapies are available to prevent or treat ZIKV infections, making a search for effective viral inhibitors an international research priority.

Nucleoside analogues are an important class of antiviral agents now commonly used as therapeutics for human viral infections, including AIDS and hepatitis B virus, cytomegalovirus, and herpes simplex virus infections [7]. These agents are generally safe and well tolerated since they target viral but not cellular polymerases and cause premature termination of viral nucleic acid synthesis [7]. In the present study, we evaluated 2'-C- and 2'-O-methyl-substituted nucleosides, 2'-C-fluoro-2'-C-methyl-substituted nucleosides, 3'-O-methyl-substituted nucleosides, 3'-deoxynucleosides, derivatives with a 4'-C-azido substitution, heterobase-modified nucleosides, and neplanocins for their ability to inhibit ZIKV replication in cell culture, with the objective of identifying promising lead candidates for further development of specific antivirals against ZIKV.

METHODS

Vero cells (ATCC CCL-81, African Green Monkey, adult kidney, epithelial) were used for determining ZIKV multiplication, for antiviral assays, and for conducting plaque assays. The cells were cultured at 37°C in 5% CO₂ in Dulbecco's modified Eagle's medium supplemented with 10% fetal bovine serum and a 1% mixture of antibiotics (Sigma-Aldrich, Prague, Czech Republic).

ZIKV strain MR766 (prototype strain, isolated from blood from experimental forest sentinel rhesus monkey, Uganda, 1947; GenBank accession no. AY632535) from the collection of the National Institute of Health Dr Ricardo Jorge–CEVDI/INSA (Águas de Moura, Portugal) and from the European Virus Archive was used for evaluation of the antiviral activity of the test compounds. The virus was passaged >100 times in suckling mice and/or in Vero cells prior to this study.

The following nucleoside analogues were purchased: 2'-C-methyl-, 2'-O-methyl-, and 3'-O-methyl-substituted nucleosides, 3'-deoxynucleosides, sofosbuvir, and 6-azauridine from Carboxynth (Compton, United Kingdom); 4'-azidocytidine, balapiravir, and RO-9187 from Medchemexpress (Stockholm, Sweden); neplanocin A from Cayman Chemical (Ann Arbor, Michigan); 3-deazaneplanocin A from Selleckchem (Munich, Germany); mericitabine from ChemScene (Monmouth Junction, New Jersey); PSI-6206 from ApexBio (Boston, Massachusetts); and tubercidin, toyocamycin, sangivamycin, ribavirin, and 2'-deoxynucleosides from Sigma-Aldrich (Prague, Czech Republic); rigid amphipathic. The test compounds were solubilized

Received 7 April 2016; accepted 24 May 2016; published online 27 May 2016.

Correspondence: D. Růžek, Veterinary Research Institute, Hudcova 70, Brno CZ-62100, Czech Republic (ruzekd@paru.cas.cz).

The Journal of Infectious Diseases® 2016;214:707–11

© The Author 2016. Published by Oxford University Press for the Infectious Diseases Society of America. All rights reserved. For permissions, e-mail journals.permissions@oup.com. DOI: 10.1093/infdis/jiw226

in 100% dimethyl sulfoxide (DMSO) to yield 10 mM stock solutions.

A viral infectivity inhibition assay was performed to measure the antiviral efficacy of nucleoside analogues in cell culture. Vero cells were seeded in 96-well plates (approximately 2×10^4 cells/well) and incubated without the presence of the drug for 24 hours, to form a confluent monolayer. Following incubation, the medium was aspirated from the wells and replaced with 200 μ L of fresh medium containing 50 μ M of the test compound (3 wells/compound), which was inoculated with ZIKV at a multiplicity of infection (MOI) of 0.1 plaque-forming units (PFU) at the same time as the test compound were added. As a negative control, DMSO was added to virus- and mock-infected cells at a final concentration of 0.5% (v/v). Culture medium was monitored for 5 days after infection to yield a 70%–90% cytopathic effect (CPE) in virus control wells, using the Olympus BX-5 microscope equipped with an Olympus DP-70 CCD camera. To quantify the CPE, culture media were collected at the end of the experiment (ie, day 5 after infection), and cell death was determined using the CytoTox 96 Non-Radioactive Cytotoxicity Assay (Promega; Madison, Wisconsin) according to the manufacturer's instructions as described previously [8]. Viral titers were determined by plaque assay and expressed as PFU/milliliter [9]. For dose-response studies, Vero cell monolayers were cultured with 200 μ L of medium containing the test compounds over the concentration range of 0–100 μ M and ZIKV at a MOI of 0.1. Drug addition and virus infection was done at the same time. The medium was collected from the wells at 2 and 3 days after infection, and the viral titers were determined by plaque assay and used to construct ZIKV dose-response curves. The dose-response curves on day 2 after infection were used to estimate the 50% effective concentration (EC_{50}). To measure the compound-induced inhibition of viral surface antigen expression, a cell-based flavivirus immunostaining assay was performed as previously described [8]. For determination of nucleoside analogue cytotoxicity, a colorimetric assay using Dojindo's highly water-soluble tetrazolium salt (Cell Counting Kit-8, Dojindo Molecular Technologies; Rockville, Maryland) and the CytoTox 96 Non-Radioactive Cytotoxicity Assay (Promega; Madison, Wisconsin) were used. The concentration of compound that reduced cell viability by 50% was considered as the 50% cytotoxic concentration (CC_{50}).

RESULTS

A series of 29 nucleoside analogues (Supplementary Figure 1) was tested at a concentration of 50 μ M for their ability to inhibit CPE mediated by ZIKV infection on Vero cells. Inhibition of ZIKV-induced CPE was monitored by light microscopy from days 1 to 5 after infection and quantified at the end of the experiment, using the colorimetric cell death in an in vitro assay. Five of the nucleoside analogues, 7-deaza-2'-C-methyladenosine (7-deaza-2'-CMA), 2'-C-methyladenosine (2'-CMA), 2'-

C-methylcytidine (2'-CMC), 2'-C-methylguanosine (2'-CMG), and 2'-C-methyluridine (2'-CMU), were found to inhibit ZIKV-mediated CPE in cell culture at a concentration of 50 μ M and to reduce significantly the cell death ratio in the test wells when compared with mock-treated ZIKV-infected cells ($P < .05$, by a 2-tailed Student *t* test). All other compounds had no or little effect on ZIKV-induced CPE and cell death. Tubercidin, toyocamycin, and sangivamycin were found to be cytotoxic, causing cell death in all cells at micromolar concentrations. On the basis of these preliminary results, nucleosides with a methyl moiety at the 2'-C position of the ribose ring (7-deaza-2'-CMA, 2'-CMA, 2'-CMC, 2'-CMG, and 2'-CMU) were selected for further testing.

2'-C-methylated derivatives reduced the viral titer in a dose-dependent manner (mean EC_{50} [\pm SD] of 5.26 ± 0.12 μ M for 2'-CMA, 8.92 ± 3.32 μ M for 7-deaza-2'-CMA, 22.25 ± 0.03 μ M for 2'-CMG, 10.51 ± 0.02 μ M for 2'-CMC, and 45.45 ± 0.64 μ M for 2'-CMU; Figure 1A and Table 1). Dose-response curves for the 2'-C-methylated nucleosides were characterized by a typical sigmoidal shape with relatively steep slopes both on days 2 and 3 after infection (Supplementary Figure 2). Interestingly, 2'-CMU exhibited a relatively weak anti-ZIKV effect, treatment with 100 μ M of the compound reduced virus titers 10^2 -fold as compared to a mock-treated culture. The anti-ZIKV activity of 2'-C-methylated nucleosides was further confirmed by a cell-based flavivirus immunostaining assay. 2'-C-methylated nucleosides exhibited a dose-dependent inhibition of the expression of ZIKV surface E antigen in Vero cells at day 2 after infection (Figure 1C). A strong inhibition of ZIKV antigen expression was observed in 2'-CMA, 7-deaza-2'-CMA, and 2'-CMC as compared to 2'-CMG and 2'-CMU, for which relatively high EC_{50} values were calculated.

The cytotoxicity of 2'-C-methylated nucleosides was assessed in Vero cells. Except for 2'-CMC, which exerted a weak cytotoxic effect on Vero cells (treatment of the cell culture at a compound concentration of 100 μ M led to a reduction in cell viability to 69.3%), all 2'-C-methylated nucleosides tested showed no cytotoxic effects at the highest tested concentration of 100 μ M with no detectable effect on cell proliferation (Table 1 and Figure 1B).

DISCUSSION

ZIKV, a previously neglected mosquito-borne virus, is prompting worldwide concern because of its alarming connection to a neurological birth disorder. In most cases, ZIKV causes a benign disease, but in some patients the infection can manifest as myelitis or meningoencephalitis, or it can trigger Guillain-Barré syndrome, a severe neurological disorder characterized by progressive muscle weakness that can result in respiratory failure [1, 3–6]. No effective therapy for ZIKV infection is available at present; therefore, research on possible antiviral compounds active against ZIKV has become an international priority. Because human cells lack RNA-dependent RNA polymerase (RdRp), this

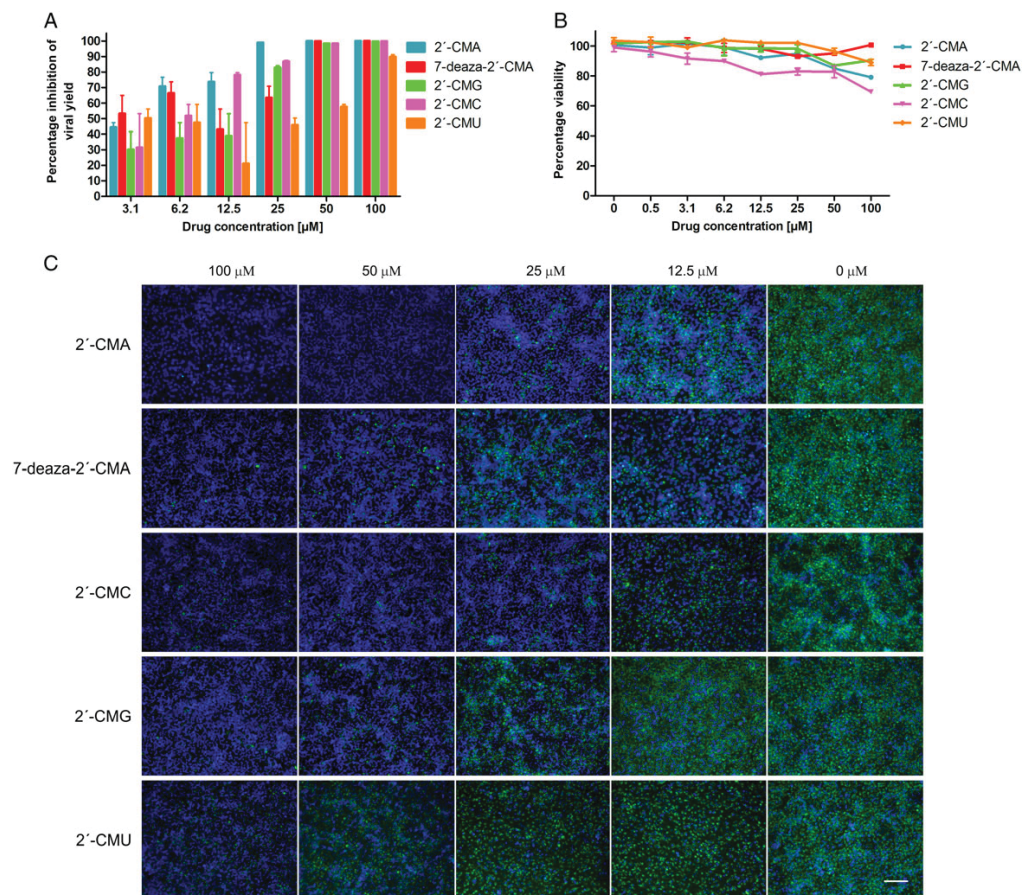


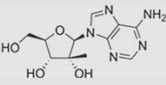
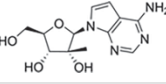
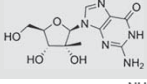
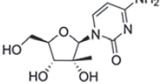
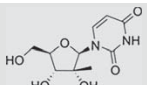
Figure 1. A, Dose-dependent inhibition of Zika virus (ZIKV) replication by 2'-C-methylated nucleosides in Vero cells. Vero cells were treated with different concentrations of 2'-C-methylated nucleosides and at the same time infected with ZIKV. Culture supernatants were collected at 48 hours after infection and analyzed for ZIKV infectivity by plaque assay. B, Viability of Vero cells treated by 2'-C-methylated nucleosides at a range of concentrations of 0–100 μM. Vero cells were exposed to the tested compounds for 72 hours. Viability was measured by a colorimetric assay, using Dojindo's highly water-soluble tetrazolium salt test (triplicate setting) and confirmed by optical microscopy. C, Inhibition of ZIKV antigen expression by nucleoside inhibitors. ZIKV-infected Vero cells were fixed on slides at 48 hours after infection and stained with flavivirus-specific antibody labeled with FITC (green) and counterstained with DAPI (blue). Scale bar, 50 μm.

class of enzymes appears to be one of the most promising targets for antivirals against flaviviruses that use RdRp for replication. Nucleoside analogs can target viral RdRp to terminate viral RNA replication after incorporation into the viral nascent RNA chain [10–12]. Here, we analyzed a library of nucleoside analogues for their in vitro activity against ZIKV.

Evaluation of various modifications at the nucleoside 2'-position revealed that the introduction of the 2'-C-methyl substituent to the nucleoside β-face resulted in inhibition of ZIKV replication in vitro. Different EC_{50} values for individual 2'-C-methylated nucleosides (ranging from 5.26 to 45.45 μM)

indicate that their antiviral activities were substantially affected also by the identity of the heterocyclic base moiety. Introduction of guanine or especially uridine into the nucleoside molecule considerably reduced the anti-ZIKV activity in vitro. The cytotoxicity of the 2'-C-methylated nucleosides was observed to be either zero or negligible, except for 2'-CMC. The cytotoxicity of the studied compounds was assessed also in human neuroblastoma cells UKF-NB-4 (data not shown) and in porcine kidney cells (PS) [8] with results comparable to those for Vero cells. This is in a sharp contrast with high (submicromolar) cytotoxicity of tubercidin, toyocamycin, and sangivamycin, chemically

Table 1. ZIKV Inhibition and Cytotoxicity Characteristics of Selected Nucleoside Analogues

Compound	Structure	EC ₅₀ , μM, Mean ± SD ^{a,b}	Apparent EC ₅₀ , μM, Mean ± SD ^{a,c}	CC ₅₀ , μM ^a	SI ^d
2'-C-methyladenosine		5.26 ± 0.12	26.41 ± 1.14	>100 ^f	>19.01
7-deaza-2'-C-methyladenosine		8.92 ± 3.32	42.87 ± 1.88	>100	>11.21
2'-C-methylguanosine		22.25 ± 0.03	71.23 ± 4.11	>100	>4.49
2'-C-methylcytidine		10.51 ± 0.02	61.93 ± 3.76	>100 ^g	>9.51
2'-C-methyluridine		45.45 ± 0.64	>100 ^h	>100	>2.20

Abbreviations: CC₅₀, 50% cytotoxic concentration; EC₅₀, 50% effective concentration; SD, standard deviation; ZIKV, Zika virus.

^a Determined from 3 independent experiments.

^b Calculated as a 50% reduction of virus titers, using the Reed-Muench method.

^c Calculated as a point of inflection from dose-response curves, using log-transformed viral titers.

^d The selectivity index (SI) is calculated as CC₅₀/EC₅₀.

^e Treatment with 100 μM of 2'-CMU reduced virus titers 10²-fold compared to a mock-treated culture.

^f Treatment of cell culture with 2'-CMA at a concentration of 100 μM led to a reduction in cell viability to 79.1%.

^g Treatment of cell culture with 2'-CMC at concentration of 100 μM led to a reduction in cell viability to 69.3%.

related structures devoid of the 2'-C-methyl group. Taken together, the 2'-C-methyl substituent appeared to be an important structural element for highly selective ZIKV inhibition and reduced cytotoxicity. We can speculate that the 2'-C-methyl substituent does not prevent binding to the ZIKV RdRp active site and allows the viral RNA chain termination. During the peer review of this manuscript, another group published further evidence that 7-deaza-2'-CMA exhibits anti-ZIKV activity [13].

Interestingly, no or negligible anti-ZIKV activity was observed for 2'-α-fluoro-2'-β-methyl- or 2'-O-methyl-substituted nucleosides, as well as for 3'-O-modified nucleosides. The introduction of the fluoro- moiety into the C2' position or the methyl moiety into the O2' or O3' position probably eliminates the 2'-α-hydroxy or 3'-α-hydroxy hydrogen bond donor/acceptor, which could result in complete abrogation of the nucleoside inhibitory activity. The observed inactivity could be also explained by inefficient cellular uptake and metabolism to convert the nucleoside molecule to the corresponding triphosphate form [14]. A detailed study of the compound uptake and metabolic conversion goes beyond the scope of this brief report and will be a subject of a future report. Neither nucleosides with 4'-azido modification nor nucleosides with chemically modified hetero-base moiety exerted anti-ZIKV activity.

In conclusion, we have demonstrated that 2'-C-methylated nucleosides exerted activity against ZIKV under in vitro conditions. These compounds provide a basis for structure-based optimization and rational design of effective prodrugs, which will be further tested in rodent models for therapy of ZIKV infection.

Supplementary Data

Supplementary materials are available at <http://jid.oxfordjournals.org>. Consisting of data provided by the author to benefit the reader, the posted materials are not copyedited and are the sole responsibility of the author, so questions or comments should be addressed to the author.

Notes

Financial support. This work was supported by the Czech Science Foundation (grantGA14-29256S); the Ministry of Education, Youth, and Sports of the Czech Republic, under the NPU I program (grant LO1218); the National Subvention for the Development of Research Organizations (grant RVO:61388963); the European Virus Archive Goes Global project, which has received funding from the European Union's Horizon 2020 research and innovation program (grant 653316).

Potential conflicts of interest. All authors: No reported conflicts. All authors have submitted the ICMJE Form for Disclosure of Potential Conflicts of Interest. Conflicts that the editors consider relevant to the content of the manuscript have been disclosed.

References

1. Lazear HM, Stringer EM, de Silva AM. The emerging Zika virus epidemic in the Americas: research priorities. *JAMA* 2016; 315:1945-6.

2. Roth A, Mercier A, Lepers C, et al. Concurrent outbreaks of dengue, chikungunya and Zika virus infections - an unprecedented epidemic wave of mosquito-borne viruses in the Pacific 2012–2014. *Euro Surveill* **2014**; 19.
3. Broutet N, Krauer F, Riesen M, et al. Zika virus as a cause of neurologic disorders. *N Engl J Med* **2016**; 374:1506–9.
4. Mlakar J, Korva M, Tul N, et al. Zika virus associated with microcephaly. *N Engl J Med* **2016**; 374:951–8.
5. Carteau G, Maquart M, Bedet A, et al. Zika virus associated with meningoencephalitis. *N Engl J Med* **2016**; 374:1595–6.
6. Mécharles S, Herrmann C, Poullain P, et al. Acute myelitis due to Zika virus infection. *Lancet* **2016**; 387:1481.
7. De Clercq E, Neyts J. Antiviral agents acting as DNA or RNA chain terminators. *Handb Exp Pharmacol* **2009**; 189:53–84.
8. Eyer L, Valdés JJ, Gil VA, et al. Nucleoside inhibitors of tick-borne encephalitis virus. *Antimicrob Agents Chemother* **2015**; 59:5483–93.
9. De Madrid AT, Porterfield JS. A simple micro-culture method for the study of group B arboviruses. *Bull World Health Organ* **1969**; 40:113–21.
10. Sampath A, Padmanabhan R. Molecular targets for flavivirus drug discovery. *Antiviral Res* **2009**; 81:6–15.
11. Botting C, Kuhn RJ. Novel approaches to flavivirus drug discovery. *Expert Opin Drug Discov* **2012**; 7:417–28.
12. Kok WM. New developments in flavivirus drug discovery. *Expert Opin Drug Discov* **2016**; 11:433–45.
13. Zmurko J, Marques RE, Schols D, et al. The viral polymerase inhibitor 7-deaza-2'-C-methyladenosine is a potent inhibitor of in vitro Zika virus replication and delays disease progression in a robust mouse infection model. *PLoS Negl Trop Dis* **2016**; 10:e0004695.
14. Eldrup AB, Allerson CR, Bennett CF, et al. Structure-activity relationship of purine ribonucleosides for inhibition of hepatitis C virus RNA-dependent RNA polymerase. *J Med Chem* **2004**; 47:2283–95.

Discussion/Summary

Emerging arthropod-borne viral encephalitis of diverse origins represent an immense global health problem. There is no specific therapy available and vaccination remains the best prophylaxis against some of them. TBE represents major public health risk, with more than 13 thousands cases per year. Its endemic distribution range from central Europe to Northern Asia.

Hosts get infected mainly via feeding of infected tick. TBEV replicates in the site of tick attachment, reaches draining lymph node followed by viremia and distribution of the virus to peripheral organs. During second viremic phase the virus crosses the BBB and reaches the CNS. TBE development is strongly associated with neuronal injury in CNS. CNS pathology following TBEV infection is the consequence of both, viral infection and inflammatory response. Post mortem studies of human patients revealed apparent changes in formation of perivascular infiltration, foci of damaged/degenerated or necrotic neurons (Gelpi *et al.*, 2005; 2006). Direct viral infection of neurons is considered to be the major cause of neurological symptoms of TBE because of physiological dysfunction of the infected cells (Hayasaka *et al.*, 2010).

Infected neurons undergo massive ultrastructural changes, including highly reorganized and proliferated Endoplasmic reticulum, redistributions in Golgi apparatus, viral protein accumulation in dendrites etc. (CHAPTER III; Hirano *et al.*, 2014; Bily *et al.*, 2015). Infected neurons activate antiviral status including autophagy mechanisms, which surprisingly cause enhancement in virus replication (CHAPTER III; Bily *et al.*, 2015). Another antiviral defense of infected neurons is represented by antiviral molecules expression enhancement, that might initialize necrotic or apoptotic cellular death (CHAPTER I; Ruzek *et al.*, 2009). Cellular death by this etiology promotes CNS dysfunction as well as indirectly induced death of other cells by cytotoxic mediators released by infected cells of neural and non-neural origin (CHAPTER IV, V; Lindquist *et al.*, 2013; Ruzek *et al.*, 2010; Palus *et al.*, 2014a; Palus *et al.*, 2013).

Such important non-neural cell population in CNS represent astrocytes. Astrocytes are not the primary target cells for TBEV infection, but some portion of this cell type is sensitive to infection (CHAPTER IV; Palus *et al.*, 2014a). Although viral infection is not generally as robust in human glial cells as in neurons, they produce considerably higher levels of immune mediators, such as cytokines and chemokines (CHAPTER IV; Palus *et al.*, 2014a). Astrocytes and other glial cells highly influence the balance between host protection and neurotoxicity. Especially, mediators such as IP-10/CXCL10, MIP-1 β /CCL4, IL-1 β , IL-6, IL-8, TNF- α etc. have neurotoxic potential (CHAPTER IV; Palus *et al.*, 2014a). Similarly, in a mouse study we showed that high expression of various cytokines/chemokines during TBE is able to mediate immunopathology, and might be associated with a more severe course of infection and increased fatality (CHAPTER II; Palus *et al.*, 2013). Research based on laboratory mouse model and histopathology of patients brains that died because of TBE imply to key role of CD8⁺T-cells in the immunopathology of TBE (Gelpi *et al.*, 2005; 2006). Our research was one of the first that experimentally demonstrated CD8⁺ dependent mechanism of immunopathology in CNS during TBE (CHAPTER I; Ruzek *et al.*, 2009). It was presented by prolonged survival of SCID or CD8^{-/-} mice following infection compared with immunocompetent mice or mice with adoptively transferred CD8⁺ T-cells. Experiments based on adoptive transfer of CD8⁺ or CD4⁺ T-cells revealed that whilst CD8⁺ T-cells mediate immunopathology, CD4⁺ T-cells confine the development of TBE. The helper CD4⁺ T-cells play a protective role although the mechanism for this is not clear; probably by stimulation of macrophage-like cells (CHAPTER I; Ruzek *et al.*, 2009). CD4⁺ T-cells are believed to control viral infections through the activation of B- and CD8⁺ T-cell responses, production of inflammatory and antiviral cytokines, direct cytotoxic effects on infected cells and promotion of memory response (Sitati and Diamond, 2006). On the other hand, the role of CD8⁺ T-cells can be dual; in the absence of immune response infection even by a less virulent strain of the virus on its own is also capable of causing encephalitis followed by death (CHAPTER I;

Ruzek *et al.*, 2009). These findings confirm the hypothesis that TBE development is tightly dependent on neuronal damage caused by virus itself and by tissue destruction caused by immune overreaction as well.

The mechanism of TBE development and brain damage is far more complex. Serological surveys suggest that only a small portion of TBEV human infection will developed clinical manifestation of TBE. The majority of human cases (70-95% of for European subtype and 98% for Siberia TBEV subtype) are asymptomatic or subclinical (Ruzek *et al.*, 2010). Impact factors influencing TBE development are defined to the same extent by host and by virus properties. Biological virus properties differ strain to strain. TBEV is not a uniform virus, natural isolates show numerous variants differing in virulence and neuroinvasiveness (Ruzek *et al.*, 2008; Mayer *et al.*, 1969). Virus properties such as virulence, tissue tropism, etc., may potentiate immunopathology during the infection.

Nevertheless, biological properties of the host play important role too. Morbidity of TBE is age-dependent and is the highest in elderly (Lindquist and Vapalahti, 2008; Gritsun *et al.*, 2003). Not only age, but also severity of illness in the acute stage and low neutralising antibody titres at onset are associated with severe forms of the disease (Lindquist and Vapalahti, 2008). Our study on mouse genetic model experimentally underline the importance of neutralising antibody titres during disease development. We compared two parental mice strains and one recombinant strain (CcS-11). The most sensitive strain (CcS-11) failed in production of neutralizing antibodies, but exhibited strong cytokine/chemokine mRNA production in the brain resulting in shortest survival time and highest susceptibility among studied mouse strains (CHAPTER II; Palus *et al.*, 2013). In addition, the genotype of the patient has been shown to influence TBE development. Such an example is a specific gene polymorphism for chemokine receptor CCR5, which is important for leukocytes transportation across BBB and is associated with higher risk of TBE development (Kindberg *et al.*, 2008). Furthermore, single nucleotide polymorphism in the promoter region of the CD209 gene is associated with human predisposition to severe forms of tick-

borne encephalitis (Barkhash *et al.*, 2012). Moreover, study based on single nucleotide polymorphisms located within the *OAS1*, *OAS2*, *OAS3*, and *OASL* genes analyzed in 142 patients with Russian TBE suggests a possible association between these 5 *OAS* single nucleotide polymorphisms and the outcome of TBEV infection in Russian population (Barkhash *et al.*, 2010). Also, single nucleotide deletion in coding region of chemokine receptor CCR5 and single nucleotide polymorphism rs3775291 in TLR3 gene seem to be predispositions to TBE in a Russian population (Barkhash *et al.*, 2013) etc.

One of the crucial steps during TBE development is crossing the BBB, which is formed by endothelial cells, pericytes and astrocytes. The BBB is formed along microcapillaries inside the CNS that separates from blood by tight net of endothelial cells stitched together by tight junctions that do not occur elsewhere in circulation. During TBE increased levels of neurospecific proteins are detected in patient's sera (Chekhonin *et al.*, 2002) indicating increased BBB permeability. We have shown that also higher levels of MMP-9 occur in the sera of patients with TBE (CHAPTER V; Palus *et al.*, 2014b). Various experimental studies demonstrated that MMP-9 might be a potential mediator of BBB disruption (Ruzek *et al.*, 2011; Paul *et al.*, 1998). MMP-9 is capable of degrading a major component of the basement membrane of the cerebral endothelium, collagen IV, and promotes the migration of cells through tissues or across the BBB (Ichiyama *et al.*, 2007; 2008). To investigate the function of the BBB during TBE, the levels of MMP-9 and its common tissue inhibitor, TIMP-1, were measured in serum from patients with acute phase of TBE. In our study, serum MMP-9 levels and MMP-9/TIMP-1 ratios in TBE patients were significantly higher than in controls (CHAPTER V; Palus *et al.*, 2014b). According to the results of our another study, infected astrocytes are the key producers of MMP-9 (CHAPTER IV; Palus *et al.*, 2014a). To investigate TBEV entry into CNS, we prepared a BBB model based on human brain endothelial cells and examined replication kinetics and virus ability of BBB disruption. No changes in the integrity of BBB were observed during the infection comparing to controls employing FITC-dextran transmigration assay and transendothelial

electrical resistance measurement. However, high viral load was found on the luminal (brain side) of the BBB model suggesting the cell-free entry into CNS without compromising the integrity of BBB (Palus *et al.*, in prep). These findings are further supported by the results obtained in mouse experimental model, where the BBB disruption occurred after TBEV entered the brain (Ruzek *et al.*, 2011). Therefore, we conclude that the BBB disruption is than a result of brain proinflammatory mediators overexpression rather than a result of the virus infection itself.

There is a sizable number of case reports of successfully treated arboviral encephalitis with high doses of unspecific intravenous immunoglobulins (IVIG). Passive transfer of IVIG is already a well-established and clinically used procedure. The IVIG effector functions include modulation of expression and function of Fc receptors, complement activation, complement binding, anti-inflammatory effects ensuing from interference with the cytokine network, provision of anti-idiotypic antibodies, and modulation of T- and B-cell activation (Boros *et al.*, 2005). IVIG preparations are successfully used for treatment of patients suffering from a variety of diseases (Ben-Nathan *et al.*, 2003), including various viral encephalitides, like Japanese encephalitis (Caramello *et al.*, 2006, 2007), West Nile virus encephalitis (Makhoul *et al.*, 2009; Ben-Nathan *et al.*, 2003), herpes simplex encephalitis (Erlich *et al.*, 1987), etc. Only few reports of cases of severe TBE that substantially improved after application of IVIG (Kleiter *et al.*, 2007), though. The protective effect of passively administered IVIG has been attributed to the ability of the specific antibodies to neutralize the virus.

Unfortunately, passive post-exposure prophylaxis for non-vaccinated persons was discontinued as a cautionary measure and never re-introduced again due to a couple of severe childhood TBE cases observed after administering specific hyperimmune serum to non-vaccinated children after tick bites (Kluger *et al.*, 1995; Waldvogel *et al.*, 1996). Moreover, antibody-dependent enhancement (ADE) was observed in *in vitro* studies with human monocytic cell culture and TBEV infection (Ozherelkov *et al.*, 2008) as well as

in infected macrophages (Kopecky *et al.*, 1991; Phillipotts *et al.*, 1985). On the other hand, the same antibodies causing ADE *in vitro* showed protective effect against lethal TBEV infection in mice (Kreil and Eibl, 1997). So far, occurrence of ADE during TBEV infection has no clear systematic *in vivo* proof and needs to be clearly addressed in randomized study (Ruzek *et al.*, 2013).

In our study we revealed more than 100-fold difference in TBEV-neutralizing capacity in two IVIG lots originating from the same manufacturer (CHAPTER VII; Elsterová *et al.*, 2016 accepted). High TBEV-neutralizing activity of IVIG containing TBEV-specific antibody was confirmed in two different human neural cell lines, but IVIG without TBEV-specific antibodies had no or little effect on virus titers in the culture. In TBEV-infected mice, 90 % of protection was achieved in mice treated with IVIG containing higher titers of TBEV-specific antibodies, whereas no immunotherapeutic effect was seen in mice treated with IVIG without TBEV-specific antibodies. We did not observe any indications for ADE caused by IVIG containing TBEV-specific antibodies at neutralizing or sub-neutralizing levels in both human neural cells *in vitro* as well as in TBE murine models *in vivo*. Based on these results we conclude that IVIG lots with high TBEV-specific antibody titers might represent a useful post-exposure prophylaxis or first-line effective therapy in TBE (CHAPTER VII; Elsterová *et al.*, 2016 accepted). These findings are particularly important for patients with high risk of severe TBE, including those with primary immunodeficiency or those with failed anti-TBEV vaccination, who depend on the presence of protective levels of antibodies present in IVIG preparations.

An alternative treatment option, currently under discussion, is corticosteroids administration. It was demonstrated that corticoids have a favorable effect during the acute stage of this disease (Dunyewicz *et al.*, 1981). It can be speculated that the effect of corticosteroids in TBE may be explained by the down-regulation of MMP-9 activity, since corticosteroid improve capillary functions by reducing activity of MMP-9 and increasing

levels of TIMPs (Rosenberg *et al.*, 1996). MMP-9 levels were shown to be significantly increased in TBE patients (CHAPTER V; Palus *et al.*, 2014b). However, the use of corticosteroids may be questioned, as corticosteroid treatment did not seem to improve the outcome of the disease (Mickiene *et al.* 2002).

According to our results, the role of the immune system in case of TBEV infection is dual i.e. protective and immunopathological. Unfortunately, it is not obvious where the edge line is. The most problematic part during immunosuppressive therapy is the extent and timing of the immunosuppression. The reaction might be insufficient and thus suppress the protective role of immune system resulting in higher CNS damage caused by extensive replication of the virus. Therefore, our first effort should be targeted to effective inhibition of the virus replication which will be followed by administration of immunomodulators resulting in immunopathology inhibition.

Therefore, nucleoside analogues as anti-viral inhibitor present an suitable option. Application of nucleoside analogues is generally safe and well tolerated since they target viral but not cellular polymerases and cause premature termination of viral nucleic acid synthesis (de Clercq and Neyts, 2009) and represent the most successful and widely used antiviral therapy.

In our laboratory a series of nucleoside analogues was tested for the ability to inhibit TBEV replication in porcine kidney cells and human neuroblastoma cells. The nucleoside analogues 7-deaza-2'-C-methyladenosine (7-deaza-2'-CMA), 2'-C-methyladenosine (2'-CMA), and 2'-C-methylcytidine (2'-CMC) inhibited TBEV replication (CHAPTER VIII; Eyer *et al.*, 2015). Since, 7-Deaza-2'-CMA show high antiviral activity and low cytotoxicity, is an attractive candidate for further investigation as a potential therapeutic agent not only for TBE treatment but also for therapy of other flaviviral neuroinfections (CHAPTER VIII; Eyer *et al.*, 2015).

Moreover, in other studies we reported a structure-activity relationship based on the antiviral/cytotoxicity profile of 29 nucleoside derivatives, each differing in chemical substituents and in chemical modifications of heterobases. Using *in vitro* assay systems, the series of nucleoside derivatives was evaluated for their ability to inhibit TBEV replication (CHAPTER IX; Eyer *et al.*, 2016a) and Zika virus (ZIKV) replication (CHAPTER IX; Eyer *et al.*, 2016b). The results indicate that C2' methylated substituents exerted activity against TBEV and ZIKV. Whereas C4' azido substituted pharmacophores were ineffective against ZIKV replication, on the other hand inhibition of TBEV replication was achieved at least in one of the used cell cultures. The differences among the cell lines can be explained by metabolic differences.

These promising compounds, even if they are not clinically effective, may be useful research tools or starting points for anti-flaviviral drug development.

In conclusion, dual role of the immune system, direct viral damage in CNS and their functional interactions, play crucial role during TBE. Anti-viral inhibition of virus replication followed by immunomodulatory application should resemble ideal therapeutical strategy in a way to reduce viral replication and prevent immunopathological reactions.

4.1 Some of proposed future plans

Comparison of TBEV replication cycle in vertebrate and tick cells

For better understanding of TBEV life cycle and to reveal how viruses hijack cellular pathways, we plan to compare replication in human neuroblastoma cell line with replication in vector tick cell line. Detailed information about TBEV replication steps in tick cells is needed. Moreover, tick cell lines represent an excellent tool for research on interactions between TBEV and its tick vector at the cellular and molecular level (Ruzek *et al.*, 2008).

Identify the function and basis of tubule-like structures / fibrillary structures

With confocal or fluorescent microscopy, we observed fibrillary structures composed of viral E protein in cisterns of the ER in infected astrocytes (Palus *et al.*, 2014a), neurons (Bily *et al.*, 2015) and neuroblastoma cells. These structures resemble by its shape the tubule-like structures that we observed in mentioned cells using electron tomography. Our observations imply that E protein is present in these structures. Therefore, to answer this question we plan to perform more experiments using immunolabeling of E protein and nonstructural TBEV protein together with electron tomography.

NS1 protein during TBEV infection as potential diagnostic factor

TBEV NS1 protein is a highly immunogenic protein that provides full protection against infection in immunized animals and raises antibody response in infected people (Jacobs *et al.*, 1992). However, the biological function of this protein is still not clear.

We are planning to quantify NS1 antibody response in patients with acute TBEV and compare NS1 antibody response to anti-E protein antibody response. And perform *in vitro* and *in vivo* experiments that provide data on dynamics of NS1 protein secretion.

Development of a multicellular BBB model and identification of cellular interactions during TBEV infection

In our studies we identified basic interaction of TBEV with human primary neurovascular unit cells: astrocytes (Palus *et al.*, 2014a), neurons (Bily *et al.* 2015), pericytes and brain microvascular endothelial cells (unpublished data). Our data suggest that TBEV itself does not cause BBB disruption. All mentioned cells are sensitive to infection, however, non-neural cells are characterized by low infection rate, 2-17 %, and no visible CPE in infected samples even after long lasting cultivation. Infected astrocytes are a source of high levels of cytokine/chemokine mediators, brain microvascular cells do not express any change in cell adhesion molecules and tight junction proteins after infection etc. We plan to test the interaction of activated/infected cell types and its secreted molecules upon the infection, with other cell types within neurovascular unit cells. We hypothesized that cytokines released by infected neurons will activate astrocytes/microglia, which will be followed by extensive cytokine signal amplification.

And finally, we plan to measure the effect of cytokines/chemokines secreted by infected/activated pericytes/astrocytes on the integrity of the blood-brain barrier. Our hypothesis is that treatment of human endothelial cells with cytokines/chemokines produced by infected/activated pericytes/astrocytes/microglia will increase trans-endothelial permeability that will be associated with decreased electrical resistance and changes in the expression of tight junction molecules.

4.2 References

- Atrasheuskaya, A.V., Fredeking, T.M., Ignatyev, G.M., 2003. Changes in immune parameters and their correction in human cases of tick-borne encephalitis. *Clinical and experimental immunology* 131, 148-154.
- Ay, I., Francis, J.W., Brown, R.H., 2008. VEGF increases blood–brain barrier permeability to Evans blue dye and tetanus toxin fragment C but not adeno-associated virus in ALS mice. *Brain research* 1234, 198-205.
- Barkhash, A.V., Perelygin, A.A., Babenko, V.N., Brinton, M.A., Voevoda, M.I., 2012. Single nucleotide polymorphism in the promoter region of the CD209 gene is associated with human predisposition to severe forms of tick-borne encephalitis. *Antiviral research* 93, 64-68.
- Barkhash, A.V., Perelygin, A.A., Babenko, V.N., Myasnikova, N.G., Pilipenko, P.I., Romaschenko, A.G., Voevoda, M.I., Brinton, M.A., 2010. Variability in the 2'-5'-oligoadenylate synthetase gene cluster is associated with human predisposition to tick-borne encephalitis virus-induced disease. *The Journal of infectious diseases* 202, 1813-1818.
- Barkhash, A.V., Voevoda, M.I., Romaschenko, A.G., 2013. Association of single nucleotide polymorphism rs3775291 in the coding region of the TLR3 gene with predisposition to tick-borne encephalitis in a Russian population. *Antiviral research* 99, 136-138.
- Ben-Nathan, D., Lustig, S., Tam, G., Robinzon, S., Segal, S., Rager-Zisman, B., 2003. Prophylactic and therapeutic efficacy of human intravenous immunoglobulin in treating West Nile virus infection in mice. *Journal of Infectious Diseases* 188, 5-12.
- Bily, T., Palus, M., Eyer, L., Elsterova, J., Vancova, M., Ruzek, D., 2015. Electron tomography analysis of tick-borne encephalitis virus infection in human neurons. *Scientific reports* 5.
- Boros, P., Gondolesi, G., Bromberg, J.S., 2005. High dose intravenous immunoglobulin treatment: mechanisms of action. *Liver transplantation* 11, 1469-1480.
- Caramello, P., Canta, F., Balbiano, R., Lipani, F., Ariaudo, S., De Agostini, M., Calleri, G., Boglione, L., Di Caro, A., 2006. Role of intravenous immunoglobulin administration in Japanese encephalitis. *Clinical infectious diseases* 43, 1620-1621.
- Caramello, P., Canta, F., Balbiano, R., Lipani, F., Ariaudo, S., De Agostini, M., Calleri, G., Boglione, L., Di Caro, A., 2007. A case of imported JE acquired during short travel in Vietnam. Are current recommendations about vaccination broader? *Journal of travel medicine* 14, 346-348.
- De Clercq, E., Neyts, J., 2009. Antiviral agents acting as DNA or RNA chain terminators, In: *Antiviral Strategies*. Springer, pp. 53-84.
- Del Zoppo, G.J., 2010. The neurovascular unit, matrix proteases, and innate inflammation. *Annals of the New York Academy of Sciences* 1207, 46-49.

- Dunyewicz, M., Mertenova, J., Moravcova, E., Kulkova, H., 1981. Corticoids in the therapy of TBE and other viral encephalitides. C. Kunz (Ed.), Tick-borne encephalitis, Facultas-Verlag pp. 36–44.
- Elsterova, J., Palus, M., Kopecky, J., Niller, H.H., Ruzek, D. 2016. Tick-borne encephalitis virus neutralization by high dose intravenous immunoglobulin (IVIG). *Ticks Tick-Borne Diseases*. (accepted)
- Erlich, K., Dix, R., Mills, J., 1987. Prevention and treatment of experimental herpes simplex virus encephalitis with human immune serum globulin. *Antimicrobial agents and chemotherapy* 31, 1006-1009.
- Eyer, L., Nencka, R., Huvarova, I., Palus, M., Alves, M.J., Gould, E.A., De Clercq, E., Ruzek, D. 2016b. Nucleoside inhibitors of Zika virus. *Journal of Infectious Diseases*, 214(5):707-11.
- Eyer, L., Smidkova, M., Nencka, R., Neca, J., Kastl, T., Palus, M., De Clercq, E., Růžek, D., 2016a. Structure-activity relationships of nucleoside analogues for inhibition of tick-borne encephalitis virus. *Antiviral research* 133, 119-129.
- Eyer, L., Valdes, J.J., Gil, V.A., Nencka, R., Hrebabecky, H., Sala, M., Salat, J., Cerny, J., Palus, M., De Clercq, E., 2015. Nucleoside inhibitors of tick-borne encephalitis virus. *Antimicrobial agents and chemotherapy* 59, 5483-5493.
- Gelpi, E., Preusser, M., Garzuly, F., Holzmann, H., Heinz, F.X., Budka, H., 2005. Visualization of Central European tick-borne encephalitis infection in fatal human cases. *Journal of neuropathology and experimental neurology* 64, 506-512.
- Gelpi, E., Preusser, M., Laggner, U., Garzuly, F., Holzmann, H., Heinz, F.X., Budka, H., 2006. Inflammatory response in human tick-borne encephalitis: analysis of postmortem brain tissue. *Journal of neurovirology* 12, 322-327.
- Gritsun, T.S., Frolova, T.V., Zhankov, A.I., Armesto, M., Turner, S.L., Frolova, M.P., Pogodina, V.V., Lashkevich, V.A., Gould, E.A., 2003a. Characterization of a siberian virus isolated from a patient with progressive chronic tick-borne encephalitis. *Journal of virology* 77, 25-36.
- Gritsun, T.S., Lashkevich, V.A., Gould, E.A., 2003b. Tick-borne encephalitis. *Antiviral research* 57, 129-146.
- Hayasaka, D., Nagata, N., Hasegawa, H., Sata, T., Takashima, I., Koike, S., 2010. Early mortality following intracerebral infection with the Oshima strain of tick-borne encephalitis virus in a mouse model. *The Journal of veterinary medical science / the Japanese Society of Veterinary Science* 72, 391-396.
- Hirano, M., Yoshii, K., Sakai, M., Hasebe, R., Ichii, O., Kariwa, H., 2014. Tick-borne flaviviruses alter membrane structure and replicate in dendrites of primary mouse neuronal cultures. *The Journal of general virology* 95, 849-861.
- Hussmann, K.L., Samuel, M.A., Kim, K.S., Diamond, M.S., Fredericksen, B.L., 2013. Differential replication of pathogenic and nonpathogenic strains of West Nile virus within astrocytes. *Journal of virology* 87, 2814-2822.
- Chambers, T.J., Diamond, M.S., 2003. Pathogenesis of flavivirus encephalitis. *Advances in virus research* 60, 273-342.
- Chekhonin, V.P., Zhirkov, Y.A., Belyaeva, I.A., Ryabukhin, I.A., Gurina, O.I., Dmitriyeva, T.B., 2002. Serum time course of two brain-specific proteins, alpha(1) brain globulin and neuron-specific enolase, in tick-born

- encephalitis and Lyme disease. *Clinica chimica acta; international journal of clinical chemistry* 320, 117-125.
- Ichiyama, T., Matsushige, T., Siba, P., Suarkia, D., Takasu, T., Miki, K., Furukawa, S., 2008. Cerebrospinal fluid levels of matrix metalloproteinase-9 and tissue inhibitor of metalloproteinase-1 in subacute sclerosing panencephalitis. *Journal of Infection* 56, 376-380.
- Ichiyama, T., Siba, P., Suarkia, D., Takasu, T., Miki, K., Kira, R., Kusuhara, K., Hara, T., Toyama, J., Furukawa, S., 2007. Serum levels of matrix metalloproteinase-9 and tissue inhibitors of metalloproteinases 1 in subacute sclerosing panencephalitis. *Journal of the neurological sciences* 252, 45-48.
- Jacobs, S.C., Stephenson, J.R., Wilkinson, G.W., 1992. High-level expression of the tick-borne encephalitis virus NS1 protein by using an adenovirus-based vector: protection elicited in a murine model. *Journal of virology* 66, 2086-2095.
- Juchnowicz, D., Rudnik, I., Czernikiewicz, A., Zajkowska, J., Pancewicz, S.A., 2002. [Mental disorders in the course of lyme borreliosis and tick borne encephalitis]. *Przegląd epidemiologiczny* 56 Suppl 1, 37-50.
- Kang, X., Li, Y., Wei, J., Zhang, Y., Bian, C., Wang, K., Wu, X., Hu, Y., Li, J., Yang, Y., 2013. Elevation of matrix metalloproteinase-9 level in cerebrospinal fluid of tick-borne encephalitis patients is associated with IgG extravasation and disease severity. *PloS one* 8, e77427.
- Kindberg, E., Mickiene, A., Ax, C., Akerlind, B., Vene, S., Lindquist, L., Lundkvist, A., Svensson, L., 2008. A deletion in the chemokine receptor 5 (CCR5) gene is associated with tickborne encephalitis. *The Journal of infectious diseases* 197, 266-269.
- King, N.J., Getts, D.R., Getts, M.T., Rana, S., Shrestha, B., Kesson, A.M., 2007. Immunopathology of flavivirus infections. *Immunology and cell biology* 85, 33-42.
- Kleiter, I., Jilg, W., Bogdahn, U., Steinbrecher, A., 2007. Delayed humoral immunity in a patient with severe tick-borne encephalitis after complete active vaccination. *Infection* 35, 26-29.
- Kluger, G., Schöttler, A., Waldvogel, K., Nadal, D., Hinrichs, W., Wündisch, G., Laub, M., 1995. Tickborne encephalitis despite specific immunoglobulin prophylaxis. *The Lancet* 346, 1502.
- Kono, S., Nagaike, M., Matsumoto, K., Nakamura, T., 1992. Marked induction of hepatocyte growth factor mRNA in intact kidney and spleen in response to injury of distant organs. *Biochemical and biophysical research communications* 186, 991-998.
- Kopecky, J., Grubhoffer, L., Tomkova, E., 1991. Interaction of tick/borne encephalitis virus with mouse peritoneal macrophages. The effect of antiviral antibody and lectin. *Acta virologica* 35, 218-225.
- Kornyei, S., 1978. Contribution to the histology of tick-borne encephalitis. *Acta neuropathologica* 43, 179-183.
- Kreil, T.R., Eibl, M.M., 1997. Pre- and postexposure protection by passive immunoglobulin but no enhancement of infection with a flavivirus in a mouse model. *Journal of virology* 71, 2921-2927.

- Kumar, M., Verma, S., Nerurkar, V.R., 2010. Pro-inflammatory cytokines derived from West Nile virus (WNV)-infected SK-N-SH cells mediate neuroinflammatory markers and neuronal death. *Journal of neuroinflammation* 7, 73.
- Lindquist, L., Vapalahti, O., 2008. Tick-borne encephalitis. *Lancet* 371, 1861-1871.
- Liuzzi, G.M., Mastroianni, C.M., Santacroce, M.P., Fanelli, M., D'agostino, C., Vullo, V., Riccio, P., 2000. Increased activity of matrix metalloproteinases in the cerebrospinal fluid of patients with HIV-associated neurological diseases. *Journal of neurovirology* 6, 156-163.
- Makhoul, B., Braun, E., Herskovitz, M., Ramadan, R., Hadad, S., Norberto, K., 2009. Hyperimmune gammaglobulin for the treatment of West Nile virus encephalitis. *The Israel Medical Association journal: IMAJ* 11, 151-153.
- Martínez-Torres, F.J., Wagner, S., Haas, J., Kehm, R., Sellner, J., Hacke, W., Meyding-Lamadé, U., 2004. Increased presence of matrix metalloproteinases 2 and 9 in short-and long-term experimental herpes simplex virus encephalitis. *Neuroscience letters* 368, 274-278.
- Matsumoto, K., Nakamura, T., 1991. Hepatocyte growth factor: molecular structure, roles in liver regeneration, and other biological functions. *Critical reviews in oncogenesis* 3, 27-54.
- Mayer, V., Dobrocka, E., 1969. Propagation of tick-borne encephalitis virus variants in short-term cultures of normal human leukocytes. *Acta virologica* 13, 435-438.
- Mayhan, W.G., 1999. VEGF increases permeability of the blood-brain barrier via a nitric oxide synthase/cGMP-dependent pathway. *American Journal of Physiology-Cell Physiology* 276, C1148-C1153.
- Mickiene, A., Laiskonis, A., Gunther, G., Vene, S., Lundkvist, A., Lindquist, L., 2002. Tickborne encephalitis in an area of high endemicity in lithuania: disease severity and long-term prognosis. *Clinical infectious diseases : an official publication of the Infectious Diseases Society of America* 35, 650-658.
- Offerdahl, D.K., Dorward, D.W., Hansen, B.T., Bloom, M.E., 2012. A three-dimensional comparison of tick-borne flavivirus infection in mammalian and tick cell lines. *PloS one* 7, e47912.
- Ozden, M., Kalkan, A., Demirdag, K., Denk, A., Kilic, S.S., 2004. Hepatocyte growth factor (HGF) in patients with hepatitis B and meningitis. *Journal of Infection* 49, 229-235.
- Ozherelkov, S.V., Kalinina, E.S., Kozhevnikova, T.N., Sanin, A.V., Timofeeva, T., Timofeev, A.V., Stivensov, D.R., 2008. [Experimental study of the phenomenon of antibody dependent tick-borne encephalitis virus infectivity enhancement in vitro]. *Zhurnal mikrobiologii, epidemiologii, i immunobiologii*, 39-43.
- Palus, M., Bily, T., Elsterova, J., Langhansova, H., Salat, J., Vancova, M., Ruzek, D., 2014a. Infection and injury of human astrocytes by tick-borne encephalitis virus. *The Journal of general virology* 95, 2411-2426.
- Palus, M., Vojtiskova, J., Salat, J., Kopecky, J., Grubhoffer, L., Lipoldova, M., Demant, P., Ruzek, D., 2013. Mice with different susceptibility to tick-borne encephalitis virus infection show selective neutralizing antibody response

- and inflammatory reaction in the central nervous system. *Journal of neuroinflammation* 10, 77.
- Palus, M., Zampachova, E., Elsterova, J., Ruzek, D., 2014b. Serum matrix metalloproteinase-9 and tissue inhibitor of metalloproteinase-1 levels in patients with tick-borne encephalitis. *The Journal of infection* 68, 165-169.
- Paul, R., Lorenzl, S., Koedel, U., Sporer, B., Vogel, U., Frosch, M., Pfister, H.W., 1998. Matrix metalloproteinases contribute to the blood—brain barrier disruption during bacterial meningitis. *Annals of neurology* 44, 592-600.
- Pekny, M., Wilhelmsson, U., Pekna, M., 2014. The dual role of astrocyte activation and reactive gliosis. *Neuroscience letters* 565, 30-38.
- Phillipotts, R.J., Stephenson, J.R., Porterfield, J.S., 1985. Antibody-dependent enhancement of tick-borne encephalitis virus infectivity. *The Journal of general virology* 66 (Pt 8), 1831-1837.
- Potokar, M., Korva, M., Jorgacevski, J., Avsic-Zupanc, T., Zorec, R., 2014. Tick-borne encephalitis virus infects rat astrocytes but does not affect their viability. *PLoS one* 9, e86219.
- Ramesh, G., MacLean, A.G., Philipp, M.T., 2013. Cytokines and chemokines at the crossroads of neuroinflammation, neurodegeneration, and neuropathic pain. *Mediators of inflammation* 2013, 480739.
- Roberts, W.G., Palade, G.E., 1995. Increased microvascular permeability and endothelial fenestration induced by vascular endothelial growth factor. *Journal of cell science* 108, 2369-2379.
- Rosenberg, G., Dencoff, J., Correa, N., Reiners, M., Ford, C., 1996. Effect of steroids on CSF matrix metalloproteinases in multiple sclerosis Relation to blood-brain barrier injury. *Neurology* 46, 1626-1632.
- Ruzek, D., Bell-Sakyi, L., Kopecky, J., Grubhoffer, L., 2008. Growth of tick-borne encephalitis virus (European subtype) in cell lines from vector and non-vector ticks. *Virus research* 137, 142-146.
- Ruzek, D., Dobler, G., Donoso Mantke, O., 2010. Tick-borne encephalitis: pathogenesis and clinical implications. *Travel medicine and infectious disease* 8, 223-232.
- Ruzek, D., Dobler, G., Niller, H.H., 2013. May early intervention with high dose intravenous immunoglobulin pose a potentially successful treatment for severe cases of tick-borne encephalitis? *BMC infectious diseases* 13, 306.
- Ruzek, D., Salat, J., Palus, M., Gritsun, T.S., Gould, E.A., Dykova, I., Skalova, A., Jelinek, J., Kopecky, J., Grubhoffer, L., 2009. CD8+ T-cells mediate immunopathology in tick-borne encephalitis. *Virology* 384, 1-6.
- Ruzek, D., Salat, J., Singh, S.K., Kopecky, J., 2011. Breakdown of the blood-brain barrier during tick-borne encephalitis in mice is not dependent on CD8+ T-cells. *PLoS one* 6, e20472.
- Samuel, M.A., Morrey, J.D., Diamond, M.S., 2007. Caspase 3-dependent cell death of neurons contributes to the pathogenesis of West Nile virus encephalitis. *Journal of virology* 81, 2614-2623.
- Sasseville, V.G., Smith, M.M., Mackay, C.R., Pauley, D.R., Mansfield, K.G., Ringler, D.J., Lackner, A.A., 1996. Chemokine expression in simian

- immunodeficiency virus-induced AIDS encephalitis. *The American journal of pathology* 149, 1459.
- Schmolck, H., Maritz, E., Kletzin, I., Korinthenberg, R., 2005. Neurologic, neuropsychologic, and electroencephalographic findings after European tick-borne encephalitis in children. *Journal of child neurology* 20, 500-508.
- Sitati, E.M., Diamond, M.S., 2006. CD4+ T-cell responses are required for clearance of West Nile virus from the central nervous system. *Journal of virology* 80, 12060-12069.
- Sui, Y., Stehno-Bittel, L., Li, S., Loganathan, R., Dhillon, N.K., Pinson, D., Nath, A., Kolson, D., Narayan, O., Buch, S., 2006. CXCL10-induced cell death in neurons: role of calcium dysregulation. *European Journal of Neuroscience* 23, 957-964.
- Sumlivaya, O.N., Vorobyeva, N.N., Karakulova, Yu.V., 2013. State of humoral part of the serotonergic system in patients with tickborne encephalitis. Abstract. Proceedings of Russian Scientific Conference with International Participation "Up-to-date Problems of Tick-borne Encephalitis." October 8–10, 2013. Chumakov Institute of Poliomyelitis and Viral Encephalitides, Moscow, Russia, p 45.
- Tsuboi, Y., Kakimoto, K., Akatsu, H., Daikuhara, Y., Yamada, T., 2002. Hepatocyte growth factor in cerebrospinal fluid in neurologic disease. *Acta neurologica Scandinavica* 106, 99-103.
- Valable, S., Montaner, J., Bellail, A., Berezowski, V., Brillault, J., Cecchelli, R., Divoux, D., MacKenzie, E.T., Bernaudin, M., Rousset, S., 2005. VEGF-induced BBB permeability is associated with an MMP-9 activity increase in cerebral ischemia: both effects decreased by Ang-1. *Journal of Cerebral Blood Flow & Metabolism* 25, 1491-1504.
- Verma, S., Kumar, M., Nerurkar, V.R., 2011. Cyclooxygenase-2 inhibitor blocks the production of West Nile virus-induced neuroinflammatory markers in astrocytes. *The Journal of general virology* 92, 507-515.
- Waldvogel, K., Bossart, W., Huisman, T., Boltshauser, E., Nadal, D., 1996. Severe tick-borne encephalitis following passive immunization. *European journal of pediatrics* 155, 775-779.
- Wang, P., Dai, J., Bai, F., Kong, K.-F., Wong, S.J., Montgomery, R.R., Madri, J.A., Fikrig, E., 2008. Matrix metalloproteinase 9 facilitates West Nile virus entry into the brain. *Journal of virology* 82, 8978-8985.
- Wang, Y., Lobigs, M., Lee, E., Müllbacher, A., 2003. CD8+ T cells mediate recovery and immunopathology in West Nile virus encephalitis. *Journal of virology* 77, 13323-13334.
- Yamada, T., Tsubouchi, H., Daikuhara, Y., Prat, M., Comoglio, P., McGeer, P., McGeer, E., 1994. Immunohistochemistry with antibodies to hepatocyte growth factor and its receptor protein (c-MET) in human brain tissues. *Brain research* 637, 308-312.
- Yang, C.M., Lin, C.C., Lee, I.T., Lin, Y.H., Yang, C.M., Chen, W.J., Jou, M.J., Hsiao, L.D., 2012. Japanese encephalitis virus induces matrix metalloproteinase-9 expression via a ROS/c-Src/PDGFR/PI3K/Akt/MAPKs-dependent AP-1 pathway in rat brain astrocytes. *Journal of neuroinflammation* 9, 12.

CURRICULUM VITAE

Martin Palus

*23.3.1987 (Příbram, Czech Republic)

palus@paru.cas.cz; MartinPalus(at)seznam.cz

Educational background

Faculty of Science, University of South Bohemia in České Budějovice

2012- (present): Ph.D. (Infectious Biology); PhD thesis:

Tick-borne encephalitis - from pathogenesis to therapy

2015:

RNDr. (Advanced Master's degree: "Rerum Naturalium Doctor"=Doctor of Natural Sciences; Clinical Biology)

2009-2012:

MSc. (Clinical Biology); Master thesis:

The role of the host genetic background on the pathogenesis of tick-borne encephalitis

2007-2009:

BSc. (Biology-Biomedical Laboratory Techniques);

Bachelor thesis: Study of the pathogenesis of tick-borne encephalitis in hosts with different genetic and immunological background (graduated with honors)

2006-2009:

BSc. (Biology) Bachelor thesis:

Study of the pathogenesis of tick-borne encephalitis in hosts with different genetic and immunological background (graduated with honors)

Employment

2014-present: Research Assistant **Emerging Viral Diseases**, Veterinary Research Institute, Brno, Czech Republic

2011-present: Research Assistant **Laboratory of Arbovirology** Institute of Parasitology, Biology Centre, Academy of the Sciences of the Czech Republic

2011-2012: Assistant, **Laboratory of Biological Monitoring and Protection**, The National Institute for Nuclear, Chemical and Biological Protection, Czech Republic

2009: Assistant **Dept. of Parasite Immunology**, Biology Centre, Academy of the Sciences of the Czech Republic, Institute of Parasitology

Research Funding (Principal Investigator)

2015: Role of the human brain microvascular endothelial cells during tick-borne encephalitis virus infection in the central nervous system (one-year individual grant project) **Grant Agency of the University of South Bohemia**

2014: Role of the human non-neural cells in the neuronal injury during tick-borne encephalitis (one-year individual grant project) **Grant Agency of the University of South Bohemia**

Postgraduate Courses

2014: PREDEMICS, National Institute for Infectious Diseases “L. Spallanzani”– Rome: **Workshop on zoonotic features of viral infections from the animal reservoir to pandemic emergence**

2012: Institute of Postgraduate Education in Medicine in Prague: **Methods in Laboratory Medicine** (accredited qualification course)

Research Internships

2011: (4 months) Erasmus Programme: **Arbovirus Pathogenesis Group**, The Roslin Institute and Royal (Dick) School of Veterinary Studies, The University of Edinburgh

Publications

With Impact Factor

Elsterova J., **Palus M.**, Kopecky J., Niller H.H., Ruzek D. 2016. Tick-borne encephalitis virus neutralization by high dose intravenous immunoglobulin (IVIg). *Ticks Tick-Borne Dis.* (accepted) **[IF=2.690]**

Eyer L., Šmídková M., Nencka R., Neča J., Kastl T., **Palus M.**, De Clercq E., Růžek D. (2016) Structure-activity relationships of nucleoside analogues for inhibition of tick-borne encephalitis virus. **Antiviral Res.** 133:119-129. **[IF=4.909]**

Eyer L., Nencka R., Huvarová I., **Palus M.**, Joao Alves M., Gould E.A., De Clercq E., Růžek D. (2016) Nucleoside Inhibitors of Zika Virus. **J Infect Dis.** 214(5):707-11. **[IF=6.344]**

Černý J., Selinger M., **Palus M.**, Vavrušková Z., Tykalová H., Bell-Sakyi L., Štěrba J., Grubhoffer L., Růžek D. (2016) Expression of a second open reading frame present in the genome of tick-borne encephalitis virus strain Neudoerfl is not detectable in infected cells. **Virus Genes** 52(3):309-16. **[IF=1.285]**

- Eyer L., Valdés J.J., Gil V.A., Nencka R., Hřebabecký H., Šála M., Salát J., Černý J., **Palus M.**, De Clercq E., Růžek D. (2015) Nucleoside inhibitors of tick-borne encephalitis virus. **Antimicrob Agents Chemother.** 59: 5483-5493. [IF=4.415]
- Bílý T., **Palus M.**, Eyer L., Elsterová J., Vancová M., Růžek D. (2015) Electron tomography analysis of tick-borne encephalitis virus infection in human neurons. **Scientific Reports** 5: 10745. [IF=5.228]
- Palus M.**, Formanová P., Salát J., Žampachová E., Elsterová J., Růžek D. (2015) Analysis of serum levels of cytokines, chemokines, growth factors and monoamine neurotransmitters in patients with tick-borne encephalitis: identification of novel inflammatory markers with implications to pathogenesis. **Journal of Medical Virology** 87: 885-892. [IF=1.998]
- Palus M.**, Bílý T., Elsterová J., Langhansová H., Salát J., Vancová M., Růžek D. (2014) Infection and injury of human astrocytes by tick-borne encephalitis virus. **J Gen Virol.** Nov; 952411-26. [IF=3.192]
- Palus M.**, Žampachová E., Elsterová J., Růžek D. (2014) Serum matrix metalloproteinase-9 and tissue inhibitor of metalloproteinase-1 levels in patients with tick-borne encephalitis. **J. Infect.** Feb;68(2):165-9. [IF=4.382]
- Palus M.**, Vojtíšková J., Salát J., Kopecký J., Grubhoffer L., Lipoldová M., Demant P., Růžek D. (2013) Mice with different susceptibility to tick-borne encephalitis virus infection show selective neutralizing antibody response and inflammatory reaction in the central nervous system. **J. Neuroinflamm.** Jun 27;10:77. [IF=4.667]
- Růžek D., Salát J., **Palus M.**, Gritsun T.S., Gould E.A., Dyková I., Skallová A., Jelínek J., Kopecký J., Grubhoffer L. (2009) CD8+ T-cells mediate immunopathology in tick-borne encephalitis. **Virology.** Feb 5;384(1):1-6. [IF=3.200]

Without Impact Factor

- Palus M.**, Růžek D. (2013) Tick-borne encephalitis: still more questions than answers (in Czech). **Vakcinologie** 7(4), 158-164.

Conferences: Martin Palus also actively presented his results at numerous Czech and international conferences.

Awards and general informations

2015: Award for the best Czech and Slovak young microbiologist of the year (Czechoslovak Society for Microbiology; XXIV. Tomasek Days of young microbiologists, Brno)

2013: Best poster award (Moscow, “ Chumakov IPVE” RAMS,
Up-to-date problems of tick-borne encephalitis)

June 2010 – English certificate - TOEFL ITP

Basic knowledge of German

Computer skills: basic knowledge of bioinformatics, statistics

© for non-published parts Martin Palus
palus@paru.cas.cz

Tick-borne encephalitis - from pathogenesis to therapy
Ph.D Thesis Series, 2016, No. 17

All rights reserved
For non-commercial use only

Printed in the Czech Republic by Typodesign
Edition of 20 copies

University of south Bohemia in České Budějovice
Faculty of Science
Branišovská 1760
CZ-37005 České Budějovice, Czech Republic

Phone: +420 387 776 201
www.prf.jcu, e-mail: secret-fpr@prf.jcu.cz